



The
University
Of
Sheffield.

Regulation and function of a novel gene cluster in
Campylobacter jejuni

A thesis submitted in part fulfilment for the degree of
Doctor of Philosophy.

Department of Molecular Biology and Biotechnology.

The University of Sheffield

Michael A White

BSc (Hons) The University of Nottingham

MRes The University of Nottingham

September 2016

Abstract

The genome of *Campylobacter jejuni* NCTC 11168 contains a small three gene operon encoding a series of seemingly un-related proteins not typically found in bacteria. Immediately upstream of this operon are two genes encoding a small DNA-binding protein and a membrane bound cytoplasmic protein, proposed to act as a sensor-regulator system. The DNA-binding protein tightly represses the expression of the structural operon under normal growth conditions and its removal results in a strong (>100-fold) up-regulation of the operon. The operon contains 3 structural genes which encode for proteins not typically found in microbial genomes, *cj0423* encodes a small membrane protein, *cj0424* encodes a periplasmic lipid binding MORN domain protein (Membrane Occupation and Recognition Nexus) and *cj0425* encodes for a periplasmic cystatin like protein (cysteine protease inhibitor).

Bioinformatic analysis revealed that the structural genes within this cluster are highly variable between *Campylobacter jejuni* and *Campylobacter coli* strains yet the regulatory mechanisms appear highly conserved. The only structural gene which appears conserved between *Campylobacter* strains is *cj0423*, which shows architectural similarity to phage derived holin proteins.

Initially the project focused on the hypothesis that the genes were responsible for defending against cationic antimicrobial peptides (CAMPs). This however proved to be incorrect and a series of mutant and complementation constructs were produced in a newly genome sequenced laboratory variant of *C. jejuni* (designated NCTC 11168-DJK for this study). To assay for the roles of the genes, a series of LacZ reporter constructs were produced to screen for potential inducers of the operon. The Biolog® phenotype microarray system was also adapted for use as a high throughput screening system using the LacZ reporter.

During the course of this work the cystatin like protein Cj0425 was shown to not inhibit the activity of the archetypal cysteine protease papain. Both bioinformatic analysis and *in-vitro* pulldown assays were unable to locate a native binding partner for the protein, implying its role may be targeted to foreign proteins or perhaps unrelated to protease inhibition.

A series of novel assays were developed to examine the possibility that the operon may be involved in defending against foreign derived periplasmic-acting toxins such as those secreted by the type VI secretion system from other Gram-negative bacteria.

Acknowledgements

I would firstly like to thank Professor Dave Kelly for his continuous support and guidance throughout the PhD and for the number of heavily subsidized Friday afternoon beverages purchased for me over the last 4 years. To everyone I have had the pleasure of meeting in Sheffield over the last 4 years, they have been some of the best in my life and I wish you all the very best in the future.

I would like to thank the members of lab F1 past and present, in particular Dr John Kendal, Dr Rick Salmon, Dr Shadi Zakai, Dr Abrar Akbar, Reem Farsi, Dr Jonathan Butler, Aidan Taylor, Calum Patrick, Leonardo Rosa, Nitanshu Garg, Tom Puttick and Dr Jon Smart. I would also like to thank our various collaborators, in particular Dr John Rafferty for help with the crystallography and Dr Sarah Coulthurst for help with the type VI secretion.

I would also like to thank my parents and grandma for their support throughout this project and in particular for their support in getting to the ~~holiday~~ conference in New Zealand.

Lastly a huge thank you to Victoria for keeping me (relatively) sane over the past 4 years.

M.A.W

2016

[Publications and presentations](#)

[Publications:](#)

H. Al-Haideri, **M. A. White**, D. J. Kelly, Major contribution of the type II beta carbonic anhydrase CanB (Cj0237) to the capnophilic growth phenotype of *Campylobacter jejuni*. Environ Microbiol 18, 721-735 (2016).

[Presentations:](#)

Shadi Zakai, **Michael White**, Dave Kelly. The role of lipid asymmetry in maintaining the integrity of the outer membrane of *Campylobacter jejuni*. CHRO, Aberdeen UK, September 2013, poster presentation.

Michael White, Dave Kelly. Regulation of the Resistance to Innate Defences system in *Campylobacter jejuni*. CampyUK, Liverpool UK, September 2014, poster presentation.

Michael White, Jonathan Butler, Ed Guccione, Andy Hitchcock, Dave Kelly. A novel regulatory system controlling genes for cell envelope function in *C. jejuni*. CHRO, Rotorua New Zealand, November 2015, poster presentation.

Abbreviations

Abs _{xxx}	absorbance at xxx nm
aa	amino acid
Å	Angstroms
Amp	ampicillin
APS	ammonium persulphate
ATP	adenine triphosphate
BHI	brain heart infusion
bp	base pair
BSA	bovine serum albumin
°C	degrees Celsius
cat	chloramphenicol acetyl transferase
Cia	<i>Campylobacter</i> invasion antigens
CCV	<i>Campylobacter</i> containing vesicle
cDNA	complementary DNA
CDT	cytotoxic distending toxin
CFE	cell free extract
Cft	<i>Campylobacter</i> ferritin
c-di-GMP	bis-(3'-5')-cyclic di-guanosine monophosphate
Cj	<i>Campylobacter jejuni</i>
cm	centimetre
Cm	chloramphenicol
CM	cytoplasmic membrane
CO ₂	carbon dioxide
cv	column volume
Da	Dalton
DEPC	diethylpyrocarbonate
dH ₂ O	distilled water
DMF	dimethyl formamide
DMSO	dimethyl sulphoxide
DNA	deoxyribonucleic acid
DNase	deoxyribonuclease
DTT	dithiothreitol
Ec	<i>Escherichia coli</i>
EDTA	ethylenediamine tetra-acetic acid
EMSA	electrophoretic mobility shift assay
ETC	electron transport chain
Fe-S	iron sulphur
fla	flagellin
Fur	ferric uptake regulator
g	gram
HEPES	4-(2-hydroxyethyl)-1-piperazineethanesulfonic acid
HIC	hydrophobic interaction chromatography
HO·	hydroxyl radical
H ₂ O	water
H ₂ O ₂	hydrogen peroxide
Hyd	hydrogenase
Hp	<i>Helicobacter pylori</i>
HPLC	high performance liquid chromatography
hr	hour
Hz	hertz
IM	inner membrane

IPTG	isopropyl β -D-1-thiogalactopyranoside
ISA	isothermal assembly
kan	kanamycin
kb	kilobase
kDa	kiloDalton
kV	kilovolt
l	litre
LacZ	β -galactosidase
LB	Luria-Bertani
LOS	lipooligosaccharide
LPS	lipopolysaccharide
M	Molar
MB	metal binding
MCP	methyl-accepting chemotaxis proteins
mg	milligram
MH	Muller-Hinton
MHS	Muller-Hinton with 20 mM serine
mm	millimetre
mM	millimolar
MOMP	major outer membrane protein
MOPS	3-(N-morpholino)propanesulfonic acid
MORN	membrane occupation and recognition nexus
mRNA	messenger ribonucleic acid
ms	millisecond
mV	millivolts
MW	molecular weight
MWCO	molecular weight cut off
μ g	microgram
μ l	microlitre
μ M	micromoles
NAD(P)	Nicotinamide adenine dinucleotide (phosphate)
NAD(P)H	Nicotinamide adenine dinucleotide (phosphate) reduced
ng	nanogram
nm	nanometer
nM	nanomolar
NMR	nuclear magnetic resonance
NO	nitric oxide
nt	nucleotide
O_2^-	superoxide
OD _{xxx}	optical density at XXX nm
OE-PCR	overlap extension PCR
OM	outer membrane
ORF	open reading frame
Oor	2-oxoglutarate : acceptor oxidoreductase
Osp	outer surface protein
PAGE	polyacrylamide gel electrophoresis
PBS	phosphate buffered saline
PCR	polymerase chain reaction
pH	hydrogen potential
Pi	isoelectric point
PMF	proton motif force
Por	pyruvate:acceptor oxidoreductase
QH ₂ O	milli-Q water
qRT-PCR	quantitative reverse transcriptase PCR

ROS	reactive oxygen species
RNA	ribonucleic acid
RNAse	ribonuclease
RNR	ribonucleotide reductase
RPM	revolutions per minute
RT	room temperature
s	second
SDM	site directed mutagenesis
SDS	sodium dodecyl sulphate
SDW	sterile distilled water
Sec	general secretory pathway
SMA	<i>Serratia marcescens</i>
T6SS	type VI secretion system
TAE	tris acetate EDTA solution
Tat	twin-arginine translocase
TBS(-T)	tris-buffered saline(with 0.1 % tween-20)
TCA	tricarboxylic acid cycle
TCR	two-component regulator
TEMED	N,N,N',N'-tetramethyl- ethane-1,2-diamine
Tris	tris(hydroxymethyl)aminomethane
UV	ultraviolet
v/v	concentration, volume/volume
WT	wild-type
w/v	concentration, weight/volume
x g	multiplied by gravitational force
X-gal	5-bromo-4-chloro-3-indolyl- β -D-galactopyranoside

Contents

Contents	viii
1 Chapter 1 Introduction	1
1.1 Campylobacter jejuni	1
1.1.1 Campylobacter jejuni: discovery	1
1.1.2 The epsilonproteobacteria	3
1.1.3 Features of the Campylobacter genome sequence	4
1.2 Epidemiology and chicken colonisation of Campylobacter jejuni	6
1.3 Iron homeostasis mechanisms of Campylobacter jejuni	7
1.4 Campylobacter jejuni oxygen tolerance	7
1.5 Capnophilic growth of Campylobacter	8
1.6 Pathogenicity and virulence of Campylobacter jejuni	9
1.6.1 Campylobacter jejuni motility	9
1.6.2 Campylobacter jejuni chemotaxis	10
1.6.3 Adhesion and Invasion	10
1.6.4 Toxin production	11
1.6.5 Protein glycosylation	11
1.7 Gram negative peptidoglycan	12
1.8 Campylobacter peptidoglycan	12
1.9 Cationic antimicrobial peptides	13
1.9.1 The model CAMP polymyxin-B	16
1.9.2 Cathelicidins and β -defensins	16
1.10 Mechanisms of antimicrobial peptide activity	17
1.10.1 The barrel-stave model	19
1.10.2 The toroidal model	19
1.10.3 The carpet model	19
1.11 Sensing and defending against CAMPs	20
1.12 CAMP resistance in Campylobacter jejuni	21
1.13 The type VI secretion system	22
1.13.1 The type VI secretion system toxin-antitoxin system	23
1.14 A cluster of genes in Campylobacter jejuni NCTC11168 which may protect against Cationic Antimicrobial Peptides (CAMPs)	25
1.14.1 Previous work on the gene cluster	25
1.14.2 The Rid operon	29
1.14.3 Early characterisation of the rid system	30
1.14.4 How the Rid system may be involved in CAMP defence	31
1.15 Project Aims:	34
2 Chapter 2 Materials and Methods	35
2.1 Materials used in this study	35
2.2 Organisms used in this study	35

2.3	Campylobacter growth Media	35
2.4	E. coli, S. marcescens and P. aeruginosa growth Media	35
2.5	Antibiotics	35
2.6	Growth of C. jejuni	36
2.6.1	Growth of C. jejuni in MCLMAN minimal media	36
2.6.2	Growth of E. coli, S. marcescens and P. aeruginosa	37
2.7	Campylobacter strains used in this study	37
2.8	E. coli strains used in this study	38
2.9	Other strains used in this study	38
2.10	DNA manipulation.....	38
2.10.1	Isolation and purification of DNA.....	38
2.10.2	DNA manipulation techniques	38
2.10.3	Polymerase chain reaction.....	38
2.10.4	PCR primers used in this study.....	39
2.10.5	Agarose gel electrophoresis.....	42
2.10.6	Restriction enzyme digestion of DNA	42
2.10.7	Ligation of DNA	42
2.10.8	Short fragment sequencing of DNA	42
2.11	Isothermal Assembly Cloning.....	42
2.12	Preparation of chemically competent E. coli	44
2.12.1	Transformation of competent E. coli	45
2.13	Plasmids used in this study	45
2.14	Preparation of chemically competent C. jejuni	47
2.14.1	Transformation of competent C. jejuni.....	47
2.15	Whole cell RNA extraction and purification.....	47
2.15.1	Real time quantitative reverse transcriptase PCR	48
2.16	Preparation of C. jejuni cell free extracts	48
2.17	C. jejuni growth curves	48
2.18	Antimicrobial disc diffusion assay.....	49
2.19	Antimicrobial sensitivity microtiter assay.....	49
2.20	LacZ expression (Miller) assays	49
2.20.1	96 well Biolog phenotype microarray Miller assay	50
2.21	Type VI secretion competition assays with S. marcescens	51
2.22	C. jejuni membrane rigidity assays	51
2.23	Outer membrane permeability nitrocefin assay.....	52
2.24	Outer membrane permeability lysozyme assay	53
2.25	Protein manipulations.....	53
2.25.1	Protein concentration determination.....	53
2.25.2	SDS poly acrylamide gel electrophoresis	54

2.25.2.1	Silver staining	54
2.25.2.2	SDS-PAGE tricine gels	55
2.25.3	Preparation of <i>C. jejuni</i> cell free extracts for western blotting	55
2.25.4	Western blotting for detection of Cj0424 from <i>C. jejuni</i> cell free extracts	55
2.26	Protein purification procedures	55
2.26.1	Overexpression of recombinant protein in <i>E. coli</i> BL21 (DE3)	56
2.26.2	Overexpression of selenomethionine incorporated protein	56
2.26.3	Preparation of <i>E. coli</i> cell free extracts	56
2.26.4	Nickel affinity chromatography	56
2.26.5	Ion exchange chromatography	57
2.26.6	Hydrophobic interaction chromatography	57
2.26.7	Gel filtration chromatography	57
2.26.8	Protein dialysis	57
2.27	Recombinant Cj0425 pull down assays	58
2.28	Thermal shift analysis of Cj0421c	58
2.29	DTNB thiol assay	58
2.30	Papain assay	59
2.31	Cathepsin-B assay	59
2.32	Protein crosslinking	60
2.33	Crystallisation screening	60
2.33.1	Crystallisation optimisation	60
2.33.2	Crystal cryoprotectant and X-ray diffraction	60
3	Chapter 3 – The role of the rid system in <i>Campylobacter</i> sub strains and the role of Cj0422c in CAMP defence.	62
3.1	Introduction	62
3.2	Chapter 3 Results	64
3.2.1	Bioinformatic analysis of the rid operon in <i>Campylobacter jejuni</i> sub strains ...	64
3.2.2	Prevalence of the rid operon in <i>Campylobacter</i> strains isolated from animal sources	64
3.2.3	Bioinformatic analysis reveals different sub types of rid system	66
3.2.4	Representation and transcription of the different rid sub-groups	67
3.2.5	Sequence alignments of the rid transmembrane proteins	68
3.2.6	Generation of knockout mutants in <i>C. jejuni</i> 81116 by Isothermal Assembly Cloning (ISA)	70
3.2.7	Sensitivity of wild type <i>C. jejuni</i> strains and 81116 mutants to the CAMP polymyxin-B	74
3.2.8	Sensitivity of the cj0422c mutant to a range of CAMPs	76
3.2.9	The rid operon is not up-regulated by polymyxin-B	78
3.2.10	Western blot analysis suggests Cj0424 is not up-regulated in response to polymyxin-B	79

3.2.11	Quantitative reverse transcriptase PCR (qRT-PCR) analysis suggests cj0423 is not up-regulated in response to polymyxin-B.....	80
3.2.12	Checking the cj0422c mutant strain for changes in gene expression.....	81
3.2.13	Checking the promoter of the cj0422c mutant strain for sequence changes	82
3.2.14	Re-isolation of the cj0422c mutant strain.....	83
3.2.15	Whole genome sequencing (WGS) of <i>C. jejuni</i>	86
3.2.16	Genomic analysis of the cj0422c mutant strains	94
3.3	Chapter 3 Discussion.....	95
3.3.1	Bioinformatic analysis of the rid operon.....	95
3.3.2	Cj0423 and holin like proteins	96
3.3.3	Secondary mutations in the cj0422c mutant and whole genome sequencing...	97
3.3.4	Genomic analysis of the wild type DJK strain	98
3.3.5	Wild type DJK strain intergenic regions and in frame substitutions.....	99
3.3.6	Wild type DJK strain gene deletions	99
3.3.7	Wild type DJK strain pseudogene re-activations	100
3.3.8	Wild type DJK strain other variations.....	100
3.3.9	Genomic analysis of the NCTC 11168-Hypermotile strain.....	101
4	Chapter 4 – Testing the potential roles of the cj0421c-cj0425 cluster by mutagenesis...	102
4.1	Chapter 4 Introduction	102
4.2	Chapter 4 Results	105
4.2.1	Generation of mutant and complementation strains in <i>C. jejuni</i> 11168-DJK...	105
4.2.2	Construction of cj0421c and cj0422c mutants in <i>C. jejuni</i> 11168-DJK.....	105
4.2.3	Construction of cj0423, cj0424 and cj0425 mutants in <i>C. jejuni</i> 11168-DJK	107
4.2.4	Construction of double, triple and quintuple mutants in <i>C. jejuni</i> 11168-DJK.	109
4.2.5	qRT-PCR analysis of the cj0421c and cj0422c mutants.....	111
4.2.6	Construction of complementation constructs by Isothermal Assembly Cloning (ISA)	112
4.2.7	Construction of cj0421c and cj0422c complementation vectors	115
4.2.8	qRT-PCR analysis of the cj0421c and cj0422c complementation strains.....	117
4.2.9	The cj0421c and cj0422c mutant strains do not show any growth defects	120
4.2.10	The cj0421c, cj0422c and cj0424 mutant strains do not show any change in sensitivity to some antibiotics or CAMPs.....	121
4.2.11	Investigating the rigidity of the cell membrane in the cj0422c mutant	124
4.2.12	Investigating the integrity of the cell membrane in the cj0422c mutant	126
4.2.13	Chicken colonisation studies using the cj0423-4 mutant strain in the <i>C. jejuni</i> 11168-Hypermotile wild type.	129
4.2.14	Examining the peptidoglycan structure of the cj0422c mutant strain	131
4.2.15	Examining the potential role of the cj0423-cj0425 operon as a defense against the antibacterial type VI secretion system	133
4.2.16	<i>Campylobacter jejuni</i> is sensitive to the <i>Serratia marcescens</i> type VI secretion system	135

4.2.17	Different <i>C. jejuni</i> wild type strains vary in sensitivity to the <i>Serratia marcescens</i> type VI secretion system.....	137
4.2.18	The cj0423-4-5 genes do not appear to provide resistance to the <i>S. marcescens</i> type VI secretion system.....	139
4.3	Chapter 4 Discussion.....	141
4.3.1	Antimicrobial sensitivity of the mutant strains.....	141
4.3.2	Membrane integrity of the mutant strains.....	141
4.3.3	Chicken colonisation of the mutant strains.....	142
4.3.4	Peptidoglycan structure of the cj0422c mutant.....	142
4.3.5	The potential role of the cj0421c-cj0425 gene cluster in defence against the type VI secretion system.....	143
5	Chapter 5 – Screening for potential inducers of the cj0423-cj0425 operon.....	146
5.1	Introduction.....	146
5.2	Chapter 5 Results.....	147
5.2.1	Construction of the lacZ reporter strains in <i>C. jejuni</i>	147
5.2.2	Confirmation of the lacZ reporter strains.....	150
5.2.3	Assaying antimicrobial compounds for induction of the cj0423-5 operon.....	152
5.2.4	Assaying sera and peptidoglycan fragments for induction of the cj0423-5 operon	156
5.2.5	Assaying environmental stress conditions for induction of the cj0423-5 operon	158
5.2.6	High throughput screening of the lacZ reporter strain using the Biolog Phenotype Microarray system.....	163
5.2.7	Fold change in LacZ expression from the phenotype microarray assays.....	169
5.2.8	Screening for the up-regulation of the cj0423-5 operon when cj0423 is artificially up-regulated.....	170
5.2.9	Construction of the iron inducible cj0423::fdxA construct in 11168.....	171
5.2.10	qRT-PCR analysis of the cj0423FdxA strain.....	172
5.3	Chapter 5 Discussion.....	173
5.3.1	Construction of the lacZ reporter strain using the cj0046 complementation system	173
5.3.2	Screening therapeutic antimicrobial compounds using the lacZ reporter system	173
5.3.3	Screening non-therapeutic antimicrobial compounds using the lacZ reporter system	174
5.3.4	Screening Human and Chicken sera and peptidoglycan fragments using the lacZ reporter system.....	174
5.3.5	Screening oxidative stress, osmotic stress, pH and temperature changes using the lacZ reporter system.....	175
5.3.6	High throughput screening of compounds using phenotype microarray plates with the lacZ reporter system.....	176
5.3.7	Attempted artificial overexpression of cj0423.....	177

6	Chapter 6 – Biochemical and structural characterisation of Cj0421c, Cj0422c and Cj0425	178
6.1	Chapter 6 Introduction	178
6.2	Chapter 6 Results	180
6.2.1	Overexpression of Cj0421c, Cj0422c and Cj0425 in E. coli BL21-DE3	180
6.2.2	Overexpression and purification of the C-terminal of Cj0421c	182
6.2.3	Screening Cj0421c for potential ligands using thermofluor	185
6.2.4	Attempted crystallisation of Cj0421c.....	186
6.2.5	Overexpression and purification of Cj0422c.....	187
6.2.6	Do Cj0421c and Cj0422c interact.....	189
6.2.7	Crystallisation of Cj0422c.....	192
6.2.7.1	Crystallisation of the native C-terminal His tagged Cj0422c protein.....	192
6.2.7.2	Overexpression and purification of selenomethionine incorporated Cj0422c	194
6.2.7.3	Crystallisation of selenomethionine incorporated Cj0422-N	196
6.2.8	Overexpression and purification of Cj0425	197
6.2.9	Checking purified Cj0425 for the formation of a disulfide bond	200
6.2.10	Cysteine protease inhibitory activity of Cj0425	201
6.2.11	Does Cj0425 have any binding partners in C. jejuni	204
6.3	Chapter 6 Discussion.....	209
6.3.1	Metal binding analysis of cj0421c.....	209
6.3.2	Interaction between Cj0421c and Cj0422c	210
6.3.3	Crystallisation of Cj0422c.....	210
6.3.4	Cj0425 does not inhibit the cysteine proteases papain or cathepsin-B	211
6.3.5	Cj0425 pulldown assays could not find any potential binding partners.....	212
7	Chapter 7 general discussion and future work.....	214
7.1	Unravelling the rid system	214
7.2	Bioinformatic analysis of the cj0421c-cj0425 operon.....	215
7.3	The cj0421c-cj0425 mutant strains show no obvious phenotype	216
7.4	Cj0425 and the type VI secretion system	216
7.5	Screening for potential inducers of the cj0423 promoter	217
7.6	Purification of Cj0421c, Cj0422c and Cj0425	217
7.7	Future work.....	217
8	Appendix	220
8.1	Gel electrophoresis size markers.....	220
8.2	Phenotype microarray plates.....	220
9	References	225

1 [Chapter 1 Introduction](#)

1.1 [Campylobacter jejuni](#)

1.1.1 [Campylobacter jejuni: discovery](#)

Campylobacter species and other closely related genera are Gram-negative, motile, spiral shaped, ϵ -proteobacteria which are often found as colonisers of the mammalian and avian gastrointestinal tracts (Blaser, 1997). Initially discovered as a cause of abortive infection in cattle, *Campylobacter* was originally named *Vibrio fetus* based on its morphological similarity to another *Vibrio* species (Smith, 1918). Another species which showed similar pathogenic characteristics but different antigenic properties, also isolated from diseased cattle, was named *Vibrio jejuni* in 1931 (Jones *et al.*, 1931). The authors also noted the difficulty of culturing *V. jejuni* in the laboratory and that it could not utilise common carbohydrates as a growth medium. The first reported human case of *Campylobacter* infection was after a huge outbreak of gastroenteritis at a prison in Illinois involving some 3,500 people. The source was traced to a contaminated milk supply and a spiral shaped bacterium was isolated from many of the patients (Levy, 1946). While the author initially suspected a virus they noted the possibility that *V. jejuni* may have been the causative agent after finding the organism in fecal samples.

Some of the early work on the characterization of *Campylobacter* was carried out by Elizabeth King who began to note that *Vibrio fetus* and *Vibrio jejuni* were commonly occurring in human disease cases as well as farm animal outbreaks (King, 1957, King, 1962). King also importantly noted that these species had an optimum growth temperature of 42°C. The organisms were subsequently re-named as *Campylobacter* after it became apparent that they differed in certain fundamental aspects and sera reactivity from other *Vibrio* species (Sebald and Veron, 1963). It took a further 10 years before it was noticed that this seemingly opportunistic organism was in fact an underreported endemic pathogen (Butzler *et al.*, 1973).

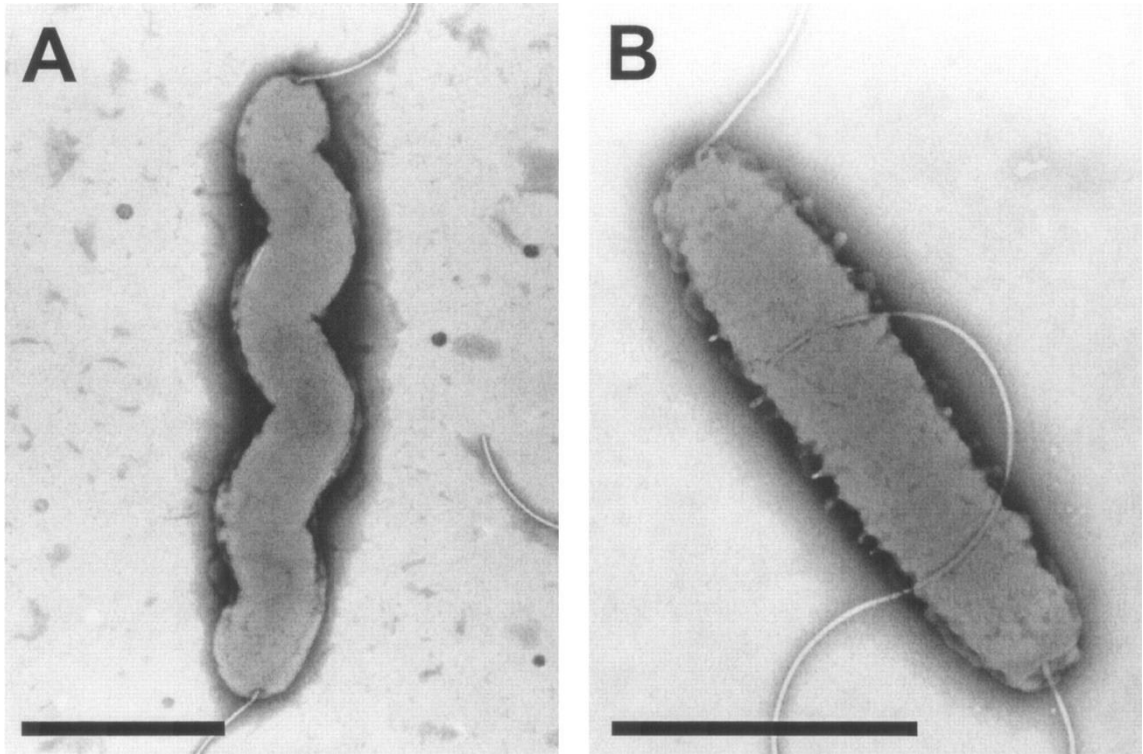


Figure 1: *Campylobacter jejuni* NCTC 11168 cell morphologies. (A) NCTC 11168-O the original clinical isolate of the wild type strain. (B) NCTC 11168-GS, a variant of the 11168-O strain used for producing the original 11168 genome sequence. The cells were negatively stained with 2% (w/v) phosphotungstic acid, the bars are 1 μ M. Image adapted from (Gaynor et al., 2004).

Early attempts to isolate *Campylobacter* from stool samples had proved ineffective due to the presence of large numbers of contaminating coliforms, so the bacterium became associated with infrequent but life threatening systemic blood infections. A *Campylobacter*-selective media was developed containing vancomycin, trimethoprim and the antimicrobial peptide polymyxin-B, which could effectively isolate *Campylobacter* species from stool samples (Skirrow, 1977). Following this improvement in detection methodology, *Campylobacter* outbreaks started to become heavily associated with undercooked chicken meat and *Campylobacter* was frequently isolated from processed chicken at the point of sale. Seasonal variations of *Campylobacter* infections also became apparent with increases in the number of cases during the summer months (Skirrow, 1982). *Campylobacter* has since been shown to be the most common cause of human gastroenteritis in the developed world, outnumbering other gastric pathogens like *Shigella*, *Escherichia coli* and norovirus. The number of reported infections is thought to be an underrepresentation of the true scale of the disease due to the often mild symptoms and the similarity between campylobacteriosis and viral food poisoning (Allos and Blaser, 1995). Taxonomic studies based on 16s rRNA and whole genome sequencing have categorised a number of different bacterial families into the *Campylobacterales* order, including the *Campylobacteraceae*, *Helicobacteraceae*, *Wolinella*, *Sulfurospirillum*, *Thiovulum*

and *Arcobacter* specie (Okoli *et al.*, 2007). The majority of these are microaerophilic to varying degrees. These organisms fall into the epsilon subdivision of the proteobacteria.

1.1.2 *The epsilonproteobacteria*

The ϵ -proteobacteria are better known as colonisers of deep sea thermal vents than chickens, yet *Campylobacter* and *Helicobacter* species are closer relatives of deep sea vent bacteria, which can thrive at 50-60°C than to *E. coli* or *Salmonella* (Campbell *et al.*, 2006). The ϵ -proteobacteria are estimated to have been the second sub-group of proteobacteria to diverge from the original proteobacteria group (after the δ -proteobacteria) (Gilbreath *et al.*, 2011). They are metabolically versatile organisms which play an important role in the Sulphur and Nitrogen cycles around deep sea vents (Nakagawa and Takai, 2008). As such many ϵ -proteobacteria can utilise hydrogen or reduced sulphur compounds as electron donors and nitrate or elemental sulphur as electron acceptors (Takai *et al.*, 2003). Strangely some deep sea vent ϵ -proteobacteria appear to share some virulence factors with their terra bound cousins, including hemolysin, the invasion antigen CiaB and the N-linked glycosylation gene cluster, suggesting that these virulence factors may have originated as survival genes and were adapted as virulence factors by *C. jejuni* and *H. pylori* (Nakagawa *et al.*, 2007).

As well as *Campylobacter* species the other pathogenic members of the *Campylobacterales* are *Helicobacter* species. *Helicobacter pylori* (previously known as *Campylobacter pylori*) is famously associated with duodenal ulcers, causing relapsing infections of the gastric mucosal layer (Marshall *et al.*, 1988). *Helicobacter* species are estimated to infect nearly half the adult human population (Peleteiro *et al.*, 2014), though infection rates vary significantly between countries. *Helicobacter* species possess multiple virulence factors which can severely damage the epithelial layer, including CagA (Cytotoxin associated gene) and VacA (Vacuolating cytotoxin). These toxins are both highly immunogenic with CagA being exported via the Type IV secretion system (along with some peptidoglycan fragments) into the host cell where it interacts with host signaling molecules and VacA, which forms membrane channels in the host cell and can induce apoptosis (Kusters *et al.*, 2006). *Helicobacter* can also use molecular hydrogen as a respiratory substrate (Olson and Maier, 2002), a process which may have evolved in deep sea thermal vents. Another non-pathogenic ϵ -proteobacteria '*Wolinella succinogens*' shares approximately one third of its genes with *Campylobacter* and another third with *Helicobacter* (Baar *et al.*, 2003). Unlike these strains *Wolinella* is able to grow microaerobically and anaerobically using hydrogen or formate as electron donors and a range of organic and inorganic compounds as electron acceptors (Kröger *et al.*, 2002). Like other

non-pathogenic ϵ -proteobacteria *W. succinogens* contains a Nickel-dependent hydrogenase common to anaerobic bacteria.

1.1.3 Features of the *Campylobacter jejuni* genome sequence

The first *Campylobacter jejuni* genome sequence became available in 2000, the NCTC11168 pathogenic human isolated strain was fully sequenced by (Parkhill *et al.*, 2000). The single 1,641,481 base pair chromosome contains 1,654 predicted ORFs with at least 20 probably representing pseudogenes. The genome of *C. jejuni* is comparatively dense with 94.3% of the genome taken up with coding sequences and is relatively AT rich (69.4%). The genome contains 48 distinct poly-G/C tracts which can lead to phase variable switching of genes (Bayliss *et al.*, 2012) (Fouts *et al.*, 2005), these tracts were often found in genes relating to the synthesis or modification of cell surface structures (Parkhill *et al.*, 2000). The 11168 genome predicts only 3 sigma factors, the housekeeping RpoD (σ^{70}), and the motility sigma factors FliA (σ^{28}) and RpoN (σ^{54}) (Jagannathan *et al.*, 2001). The *C. jejuni* NCTC 11168 genome sequence was re-annotated in 2007 by (Gundogdu *et al.*, 2007), the number of complete ORFs was reduced to 1643 and the products from 18.2% of the coding sequence were revised to include more recent discoveries.

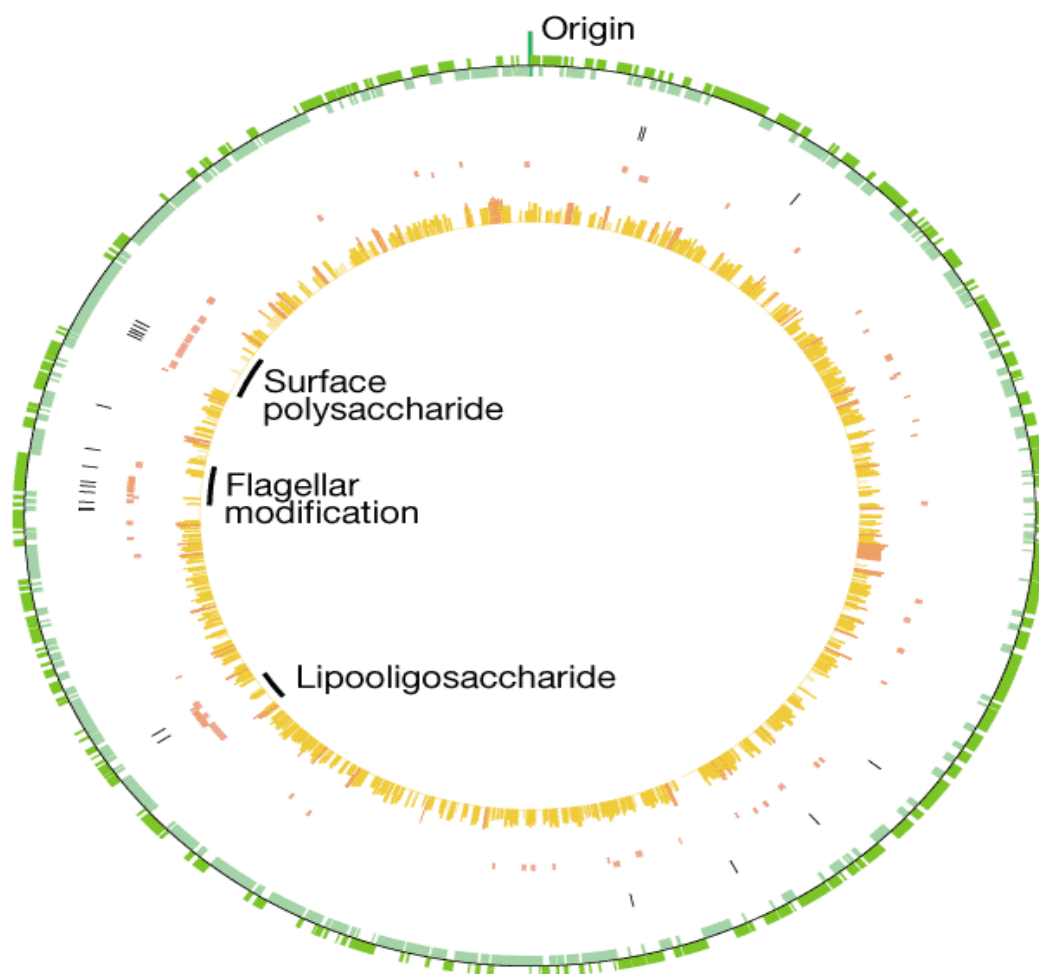


Figure 2: Circular representation of the original *C. jejuni* NCTC 11168 genome sequence. Features of the 1,641,481 bp nucleotide sequence are represented by coloured circles with the putative origin of replication marked. From the outside to the inside, the dark green represents ORFs transcribed in a clockwise orientation, the lighter green represents ORFs transcribed in the anticlockwise orientation. The black lines represent hypervariable sequences and the pink lines represent genes involved in surface polysaccharide, flagellar or lipooligosaccharide production, these clusters are also marked. The inner yellow and orange histogram shows the similarity of each gene to its *Helicobacter pylori* orthologue, the height of the bar and the colour intensity are proportional to the degree of similarity. The image was adapted from (Parkhill et al., 2000).

The genomes of three other commonly used strains of *C. jejuni* were sequenced in 2005 (*C. jejuni* RM 1221), 2006 (*C. jejuni* 81-176) and 2007 (*C. jejuni* 81116) by (Fouts et al., 2005) (Hofreuter et al., 2006) (Pearson et al., 2007) respectively. *C. jejuni* RM1221 contains 1,884 predicted ORFs and a similar CG content and genome length to the 11168 reference strain. The RM1221 strain contains more predicted pseudogenes than 11168 (47 compared to 20) and also contains two non-specific DNA/RNA endonucleases which are thought to inhibit the natural transformation efficiency of RM1221 (Gaasbeek et al., 2010). The *C. jejuni* 81-176 strain is known for its heightened virulence compared to other strains of *C. jejuni*, the strain

contains two plasmids pTet, which contain a tetracycline resistance gene (Batchelor *et al.*, 2004). And pVir which contains components of a Type IV secretion system and has recently been shown to contain a toxin-antitoxin system, where a proteic toxin CjpT is inhibited at the RNA level by a small non-coding RNA *cjpA* (Shen *et al.*, 2016). *C. jejuni* 81116 contains 1,626 predicted ORFs and a similar AT content to 11168. The 81116 genome contains fewer poly-G tracts than 11168 (17 compared to 30 respectively) and has been shown to be both amenable to genetic manipulation while maintaining genome fidelity (Manning *et al.*, 2001). The *C. jejuni* promoter regions differ from other bacteria as instead of a -10 and -35 box region the *C. jejuni* promoters appear to contain only an extended -10 box (Petersen *et al.*, 2003).

1.2 Epidemiology and chicken colonisation of *Campylobacter jejuni*

Campylobacter jejuni is one of the most common causes of food borne illness in the developed world. Its prevalence is largely due to the difficulty in eradicating *C. jejuni* from poultry products and its low infectious dose (>500 cells) (Robinson, 1981). *Campylobacter* infection often leads to bloody diarrhea for a few days and will typically clear up in less than a week without treatment. The most common source of infection is via contaminated poultry meat, or meat contaminated with poultry derived *Campylobacter* such as cross contamination during food preparation. Other sources include contaminated groundwater, cow or pig meat and some unpasteurized milk products as well as domestic pets (Dasti *et al.*, 2010). Poultry birds are the most common hosts for *Campylobacter* probably because of their 42°C body temperature which is the optimum growth temperature for *C. jejuni* and *C. coli*. Typically, *Campylobacter* will colonise chickens between 2-3 weeks old with >90% being colonized by 7 weeks. Colonisation will spread rapidly throughout broiler chicken flocks, becoming almost impossible to eradicate once established in a flock (Evans and Sayers, 2000). This near ubiquity of *Campylobacter* colonisation in chicken production facilities is passed on to the retail market where 60-80% of raw chicken products are contaminated with *Campylobacter* at the point of sale (Müllner *et al.*, 2010).

Campylobacter species take hold in the gastrointestinal tract of chickens and other poultry birds, typically in the caecum and colon. When poultry birds are processed the contents of the caecum and colon can be washed over the skin of the bird where *Campylobacter* will become entrapped in the feather follicles and remain viable at 4°C for over 72 hours (Chantarapanont *et al.*, 2004). The rate of reported *Campylobacter* infections is thought to be considerably lower than the true rate of infection, the infection rate in the United States is estimated to be close to 1 in every 100 every year (Allos and Blaser, 1995). Because *Campylobacter* infection shows similar symptoms to other food-borne pathogens such as *E. coli*, *Salmonella* or

norovirus infection it is probably mistaken for these when in fact *Campylobacter* infection is more common.

1.3 Iron homeostasis mechanisms of *Campylobacter jejuni*

Iron storage and acquisition is essential for microbial survival as iron plays crucial roles in electron transport, gene regulation, the oxidative stress response and metabolic processes. Like most metals, the uptake and storage of iron must be carefully regulated due to the potentially damaging effects of free radical formation (Gilbreath *et al.*, 2011). *Campylobacter jejuni* 11168 encodes homologues of the ferric uptake regulator (Fur) and also contain a separate peroxide stress regulator (PerR) which is a functional analog of a different peroxide stress regulator (OxyR) found in other bacteria (Van Vliet *et al.*, 1999). Unusually the expression of the peroxide stress response in *C. jejuni* is responsive to iron levels rather than reactive oxygen species. Iron can be transported across the outer membrane by porins and dedicated iron specific siderophore uptake mechanisms. *C. jejuni* cannot produce iron chelating siderophores such as enterobactin but is able to scavenge iron from siderophores probably produced by other bacteria. *C. jejuni* possesses a dedicated ferrous enterobactin transporter CfrA which transports iron-bound enterobactin across the inner membrane (Naikare *et al.*, 2013). This transport requires the proton motive force, which is provided by TonB3 which transfers the energy needed for active transport from the inner membrane to the outer membrane (Gresock *et al.*, 2011). The 11168 genome also encodes a FeoB, homologue which is responsible for Fe²⁺ transport across the inner membrane, and is necessary for colonisation and intracellular survival (Naikare *et al.*, 2006). Free iron in the presence of oxygen can lead to reactive oxygen species such as hydroxyl radicals (OH^{*}), peroxides (ROOH) and superoxide (O²⁻) (Storz and Imlay, 1999), which can cause damage to multiple targets within a cell. *C. jejuni* possesses a ferritin-like protein (*Campylobacter* ferritin Cft) which is the main iron storage protein and binds to iron at a 1.5:1 ratio (iron phosphate : ferritin) thereby removing it from circulation (Wai *et al.*, 1995).

1.4 *Campylobacter jejuni* oxygen tolerance

Campylobacter jejuni is a microaerophilic organism which thrives in an oxygen concentration of between 3-10 % and a carbon dioxide concentration of between 5-10 % (Bolton and Coates, 1983). Both atmospheric oxygen and completely anaerobic conditions inhibit growth, though *C. jejuni* does possess mechanisms to cope with oxidative stress. In order to successfully transfer between hosts *Campylobacter* will likely have to persist in atmospheric oxygen and may have to survive sudden oxidative shock when internalised by phagocytes (Wooldridge and Ketley, 1997, Van Vliet *et al.*, 2002). Multiple proteins within *C. jejuni* can be damaged by

oxygen, in particular those containing reactive iron-sulphur clusters. Resisting this damage requires both resistance and repair mechanisms. *C. jejuni* is known for preferential catabolism of L-serine as a primary carbon source, the L-Serine dehydratase SdaA enzyme which catabolises L-serine to pyruvate contains an iron-sulphur cluster and is sensitive to atmospheric oxygen (Velayudhan *et al.*, 2004). The pyruvate and 2-oxoglutarate:acceptor oxidoreductase enzymes (Por and Oor) from the TCA cycle also contain iron Sulphur clusters and homologues from of these enzymes from *H. pylori* have been shown to be damaged by atmospheric oxygen (Hughes *et al.*, 1995). Por and Oor are thought to be protected from oxygen damage by the presence of oxygen binding hemerythrins (Kendall *et al.*, 2014). The *C. jejuni* 11168 genome also encodes two methionine sulphoxide reductases *msrA* and *msrB* which contribute to oxidative stress resistance by repairing methionine residues damaged by oxygen (Atack and Kelly, 2008). It is not known how *C. jejuni* is able to mediate the response to oxidative stress as no direct oxygen sensing mechanism has been found so far. The recently discovered 'Regulator of Response to Peroxide' (RrpA/B) proteins may act as part of a novel oxidative stress response mechanism; both proteins act as DNA-binding regulators. Mutagenesis of RrpB leads to increased sensitivity to oxidative stress and reduced expression of the catalase gene *kataA*, the iron responsive peroxide response regulator *perR* and the heat shock regulator *hspR* (Gundogdu *et al.*, 2011, Gundogdu *et al.*, 2015). While high levels of oxygen can cause considerable damage to *C. jejuni*, the 11168 genome also encodes an oxygen dependent I-type ribonucleotide reductase (RNR) for the production of ribonucleotides (most bacteria contain a class II-type which functions in aerobic and anaerobic environments), the lack of an oxygen independent RNR contributes to the need for low levels of oxygen for growth (Sellars *et al.*, 2002).

1.5 Capnophilic growth of *Campylobacter*

Campylobacter jejuni requires a higher than atmospheric concentration of carbon dioxide for optimal growth (5-10 %) (Bolton and Coates, 1983), the molecular reasons for this unusually high requirement are unclear but it may be due to relatively inefficient enzymes for which CO₂ is a substrate. *Campylobacter jejuni* 11168 encodes an acetyl-CoA carboxylase, essential for fatty acid biosynthesis. This protein has a homologue in *Helicobacter pylori* which shows a low affinity for CO₂ which is considered a reason for the high CO₂ requirement of *H. pylori* (Burns *et al.*, 1995). The *C. jejuni* 11168 genome also encodes 2 carbonic anhydrase enzymes which produce bicarbonate from gaseous CO₂ (Smith and Ferry, 2000). One of these enzymes Cj0237 (CanB) is required for growth in low atmospheric CO₂ concentrations and is only active above pH8 and with a relatively low affinity for CO₂ suggesting inefficient conversion of CO₂ to bicarbonate (Al-Haideri *et al.*, 2016).

1.6 Pathogenicity and virulence of *Campylobacter jejuni*

1.6.1 *Campylobacter jejuni* motility

The best understood virulence factor of *C. jejuni* is probably the flagellar motility apparatus. Knockout deletions of motility genes lead to strains deficient in chicken colonisation and with a reduced ability to cause infection in animal models (Wassenaar *et al.*, 1993, Golden and Acheson, 2002). *Campylobacter* expresses a bipolar unsheathed flagellar composed of FlaA and FlaB oligomers which are close homologues of each other (91.9% sequence identity). *flaA* is regulated by the classical motility sigma factor σ^{28} , while *flaB* is regulated by σ^{54} . Deletion of *flaA* results in the production of a truncated flagellar composed of FlaB, while deletion of FlaB produces only a slight reduction in motility (Guerry *et al.*, 1991). Motility is controlled by the two component FlgS/R sensor regulator system (Wösten *et al.*, 2004), where the production of the major flagellin filament by σ^{28} is induced only after the assembly of the Type III secretion motility apparatus (also known as the flagellin export apparatus) (Joslin and Hendrixson, 2009). This may be because motility is energetically costly and motility mutants in *C. jejuni* are able to grow 3X faster than fully motile strains (Wösten *et al.*, 2004). Flagellar-mediated motility is thought to allow *C. jejuni* to reach certain niches within the host such as passing through the mucosal barrier and to resist expulsion by peristalsis (Szymanski *et al.*, 1995, Hendrixson and DiRita, 2004).

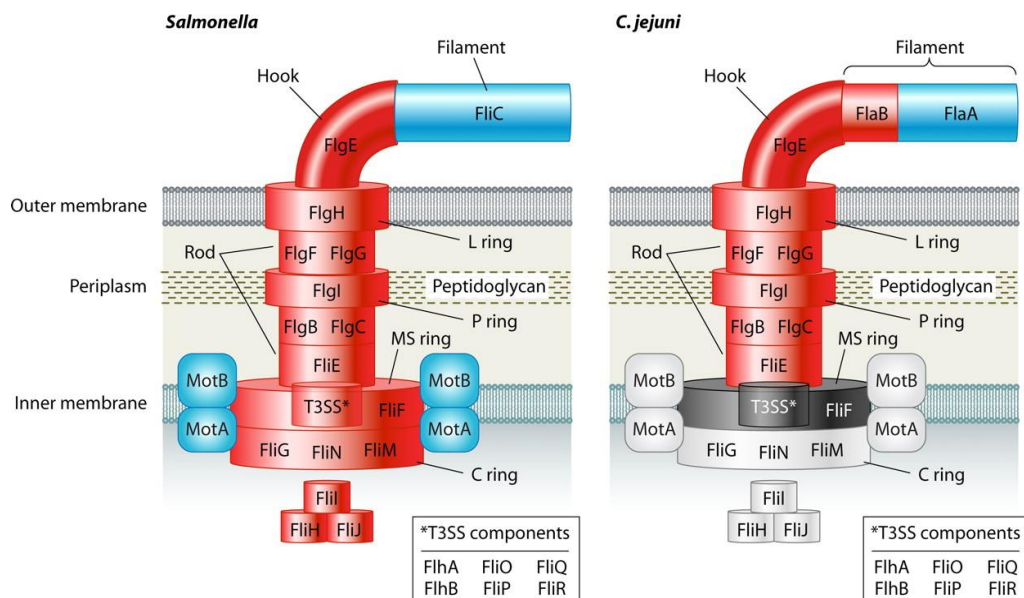


Figure 3: The motility apparatus of *Campylobacter jejuni* and *Helicobacter pylori* compared to *Salmonella* spp and *E. coli*. The protein components of the flagellar apparatus are colour coded to represent alternate transcriptional hierarchies, where the archetypal flagellar apparatus of *E. coli* and *Salmonella* are transcribed in two stages (red then blue). In *C. jejuni* the type III secretion system components shown in black are expressed first which then activates the expression of those in red and then blue. The components shown in grey are transcribed separately to the traditional flagellar hierarchy. Image adapted from (Gilbreath *et al.*, 2011) where some of the proteins required for motility are omitted for simplicity.

1.6.2 *Campylobacter jejuni* chemotaxis

Chemotaxis is the movement towards or away from specific environmental attractants or repellants. The *C. jejuni* 11168 genome predicts 10 methyl-accepting chemotaxis proteins (MCPs) which are involved in sensing extracellular attractants or repellants (Marchant *et al.*, 2002). A 1988 study screening potential chemoattractants and repellants showed that *C. jejuni* demonstrates classical chemotaxis towards L-fucose, L-serine, L-aspartate, L-glutamate, L-cysteine, pyruvate, fumarate, succinate, citrate, malate and ketoglutarate, showing a strong preference for amino acids and metabolic intermediates over carbohydrates. *C. jejuni* also showed chemotactic motility towards mucins which are secreted by epithelial cells. Some types of bile acids were shown to act as chemo-repellants to *C. jejuni* such as cholic acid, deoxycholic acid and taurocholic acid (Hugdahl *et al.*, 1988). *C. jejuni* is also able to respond to localised energy levels and will migrate in response to the redox state of the electron transport chain/proton motive force, this energy-taxis system is mediated by the *Campylobacter* energy taxis proteins CetA and CetB (Elliott and DiRita, 2008).

1.6.3 Adhesion and Invasion

C. jejuni is able to invade intestinal epithelial cells using microtubules rather than the more common actin-cytoskeletal rearrangement internalisation method used by *Salmonella*, *Shigella* or *Yersinia* strains (Oelschlaeger *et al.*, 1993) (Dramsi and Cossart, 1998). The *C. jejuni* genome does not encode for fimbriae or pili, instead attachment to host cells is mediated by adhesins exposed on the cell surface, including the flagellum (Grant *et al.*, 1993). *C. jejuni* produces multiple adhesion and invasion protein including the fibrinonectin binding protein CadF (Konkel *et al.*, 1997), the autotransporter protein CapA (Ashgar *et al.*, 2007) and the outer membrane lipoprotein JlpA (Jin *et al.*, 2001). Intracellular *Campylobacter* is often isolated from patient biopsies and the ability of *C. jejuni* to invade cells has been demonstrated in multiple cell lines (Grant *et al.*, 1993, Dasti *et al.*, 2010). Once internalised within host cells *C. jejuni* is able to resist destruction in the lysosomes by creating its own membrane bound compartment within the host cell termed the *Campylobacter*-containing vacuole or CCV where it undergoes physiological changes in oxygen sensitivity and can persist and divide (Watson and Galán, 2008). When cultured with animal cell cultures *C. jejuni* produces and exports a series of invasion antigens termed *Campylobacter* invasion antigens (Cia) (Rivera-Amill *et al.*, 2001), these are likely secreted by the motility apparatus system due to the lack of any other type III secretion system (Konkel *et al.*, 2004). This indicates that the motility apparatus is involved in both motility and virulence factor secretion which may suggest why the *flaA* flagellin gene is under the control of a different sigma factor to the rest of the motility apparatus, to allow for the export of Cia antigens without assembling the flagellum.

1.6.4 Toxin production

The symptoms of *Campylobacter* infection suggest that toxins play a role in disease progression, the transition from watery to bloody diarrhea suggest that *C. jejuni* is able to actively damage the epithelial lining of the intestines. A variety of different toxins have been associated with *Campylobacter* infection but the best studied are the cytolethal distending toxins *cdtABC* (Dasti *et al.*, 2010). The CdtABC holotoxin is incorporated into the eukaryotic cell by an unknown uptake mechanism where CdtA and CdtC remain at the target cell membrane, these two proteins contain lectin like regions which are structurally similar to the toxin ricin (these domains recognise oligosaccharides) (Heywood *et al.*, 2005) (Young *et al.*, 2007). The exact mechanism for uptake of the Cdt toxins and how they cause cell death are still not fully understood, but it has been demonstrated that toxicity requires all 3 Cdt proteins, the CdtB toxin is thought to be the active component of this system which is exported into the host cell and causes double strand breaks in the host DNA from within the nucleus, eventually leading to pre-programmed cell death (Lara-Tejero and Galán, 2001). The 11168 genome sequence also predicts two haemolysins (*cj0183* and *cj0588*), knockout mutations showed that *Cj0588* is required for invasion but does not show hemolytic activity *in-vitro* and surprisingly removal of *cj0183* does not abolish hemolytic activity (Sałamaszyńska-Guz and Klimuszko, 2008). The study concludes that haemolysis may be mediated by other un-annotated hemolytic proteins. *C. jejuni* also contains a putative phospholipase toxin *pldA*, a deletion mutant of this gene shows impaired colonisation of chickens (Ziprin *et al.*, 2014).

1.6.5 Protein glycosylation

Glycosylation is a common post translational modification system where sugar moieties are covalently bound to proteins. N-linked glycosylation links a glycan to the amide nitrogen of an asparagine residue and O-linked glycosylation links a glycan to the hydroxyl group of serine or threonine residues. *Campylobacter* contains a complex glycosylation pathway which uses both N- and O-linked glycans to modify a range of target proteins. The N-linked glycosylation system in *Campylobacter* is considered the archetypal N-linked glycosylation system, the *pgl* gene cluster is responsible for synthesis of glycans and the attachment of acetylglucosamine-containing heptasaccharide to the asparagine residues of some proteins (Szymanski *et al.*, 1999, Young *et al.*, 2002). The glycan is attached to the conserved residue D/E-X-N-Z-S/T, where N is the glycosylated asparagine and the X and Z are any amino acid (with the exception of proline) (Kowarik *et al.*, 2006). The O-linked glycosylation system is used to heavily modify the flagellar FlaA protein, with up to 19 separate glycans per monomer (McNally *et al.*, 2006). The *pse* gene cluster is responsible for producing pseudaminic acid derivatives which are then attached to the serine or threonine residues. Knockout mutations of some of the *pse* genes

causes a loss of motility implying that glycosylation is essential for motility, and therefore successful colonisation and adherence (McNally *et al.*, 2006, Nothaft and Szymanski, 2010). The biological role of glycosylation is still not clear, mutations within *pgl* genes show decreased colonisation of chickens and a reduction in adherence and invasion of human cells, but why is not fully understood (Karlyshev *et al.*, 2004).

1.7 Gram negative peptidoglycan

Peptidoglycan (also known as murein) is a crucial component of both Gram-positive and Gram-negative bacteria. The peptidoglycan structure is composed of a glycan based backbone composed of repeating residues of N-acetylglucosamine (GlcNAc) and N-acetylmuramic acid (MurNAc). Attached to the GlcNAc residues are short peptide side chains containing both proteinogenic and non-proteinogenic (L and D) amino acids, these peptides are crosslinked forming a rigid net like polymer which is located in the periplasm of Gram-negative bacteria and forms the outer layer of the Gram-positive cell envelope (Vollmer *et al.*, 2004). The peptidoglycan layer is typically anchored to the outer membrane by approximately 10^5 individual lipoproteins (known as Braun's lipoprotein or major outer membrane lipoprotein), which is covalently bound at both ends to the peptidoglycan layer and the outer membrane (Braun, 1975). Synthesis of peptidoglycan begins with the peptide side chains being attached individually to the MurNAc residue using the MurABCDE pathway (Pinho *et al.*, 2013). The GlcNAc residue is then attached and the whole PG monomer is flipped across the inner membrane and attached to the existing peptidoglycan layer by transpeptidase and transglycosylase enzymes. Transpeptidases are also known as penicillin-binding proteins (PBPs) and are common targets for antibiotics (Spratt and Cromie, 1988). The peptidoglycan wall can be repaired and replaced by the action of lytic-transglycosylases, endopeptidases and amidases (Goodell, 1985). Some of the cleaved peptidoglycan fragments are exported outside the cell but many are recycled, in *E. coli* the AmpG (GlcNAc-anhMurNAc) permease transports single peptidoglycan unit from the periplasm to the cytoplasm and the AmpD (anhMurNAc-L-Ala) amidase separate the peptide stem from the glycan dimer (Jacobs *et al.*, 1994). It is estimated that *E. coli* is able to recycle up to 50% of the cleaved peptide stem which can then be re-used without the need to reproduce the peptide (Goodell, 1985).

1.8 *Campylobacter* peptidoglycan

The formation of the *Campylobacter jejuni* cell wall is not particularly well studied, but it appears that the peptidoglycan layer of *C. jejuni* is highly similar in structure to other Gram-negative bacteria. The *C. jejuni* peptidoglycan N-acetylmuramic acid residue can be acetylated by the peptidoglycan O-acetyltransferase PatB and de-acetylated by the O-acetylpeptidoglycan

esterase Ape1. Strangely, the loss of PatB produces no colonisation defect (though the authors note that the acetylation of MurNAc was not abolished suggesting the presence of a PatB analog), while the loss of Ape1 leads to an accumulation of acetylated peptidoglycan residues and reduced chicken colonisation (Ha *et al.*, 2016). Modifications of the *C. jejuni* cell wall have been shown to cause the typical helical shape of *Campylobacter*. The actions of two LD-endopeptidases in *C. jejuni* termed Pgp1 and Pgp2 (peptidoglycan peptidases 1 and 2) cleave specific sites in the peptide stem of the peptidoglycan layer. Removal of these genes results in a non-helical cell, the localisation and expression of these genes is thought to be important as expression of both genes in the periplasm of *E. coli* does not cause the cells to become spiral (Firdich *et al.*, 2012, Firdich *et al.*, 2014). Strangely, the 11168 genome does not appear to encode a homologue of Braun's lipoprotein, the relatively high abundance and small size (8 kDa) of Braun's lipoprotein in the Gram-negative periplasm is usually visible on SDS-PAGE gels and is notably absent from *C. jejuni* (Logan and Trust, 1982). *C. jejuni* does encode a potential substitute protein termed Omp18 (outer membrane protein 18) which may act as an alternative to Braun's lipoprotein, but has not been well studied (Burnens *et al.*, 1995, Konkel *et al.*, 1996). The peptidoglycan recycling system of *E. coli* appears to have no homologues in the *C. jejuni* 11168 genome, the AmpG permease is not found and neither are any of the enzymes involved in degrading and re-forming the peptidoglycan unit after transport into the cytoplasm. Whether *C. jejuni* is able to recycle peptidoglycan is unknown (Parkhill *et al.*, 2000).

1.9 Cationic antimicrobial peptides

Cationic antimicrobial peptides (CAMPs) are an ancient component of the eukaryotic immune system; these simple oligopeptide structures are highly conserved between eukaryotes and are produced to defend against a broad spectrum of potential pathogens including bacteria, fungi, viruses and in some cases tumors. While they do not offer the same flexibility as the adaptive immune system, they play a crucial role within the innate immune system (Hancock and Sahl, 2006). Antimicrobial molecules containing primarily amino acids are produced by all 3 domains of life (Parisien *et al.*, 2008). When synthesised by microbes, AMPs can be produced either ribosomally or via multi-enzyme pathways, which allows for the inclusion of non-proteinogenic amino acids and the formation of cyclic structures (Wiesner and Vilcinskas, 2010). Examples of these include the polymyxins, bacitracins, gramicidins, nisin and the lantibiotics, some of which are used as antimicrobials in the food industry (Guinane *et al.*, 2005). Antimicrobial peptides produced by bacteria are typically referred to as bacteriocins while those produced by higher eukaryotes are referred to as antimicrobial peptides; these tend to be ribosomally produced and are classed into three major families based on secondary structure. (1) The α -helical cathelicidins, which form simple helical structures, (2) the β -sheet

defensins characterised by conserved cysteine residues forming β -sheet ladders. (3) Linear peptides, which tend to show a strong, bias for certain amino acids such as tryptophan, proline, arginine or histidine (Boman, 2003, Gruenheid and Le Moual, 2012). All three families of antimicrobial peptides are largely characterised by their net positive charge and amphipathic properties and are thus named cationic antimicrobial peptides (CAMPs). The peptide sequences of many CAMPs are not highly conserved between eukaryotes yet the structures and positively charged residues are, implying that the mechanism of action and microbial target is highly conserved between bacteria (Matsuzaki, 1999). Almost any type of mammalian cell can produce CAMPs though they are most often associated with areas particularly at risk of infection such as the skin, intestinal lining, eyes and mouth (Gruenheid and Le Moual, 2012).

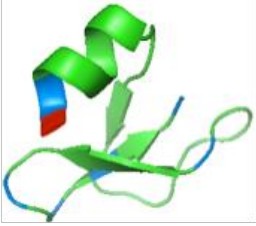
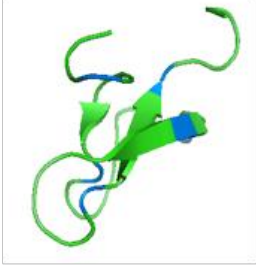
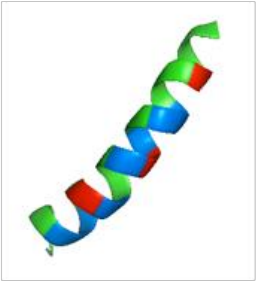
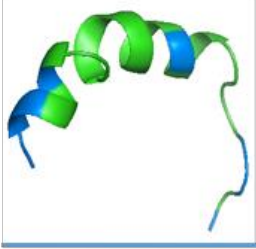
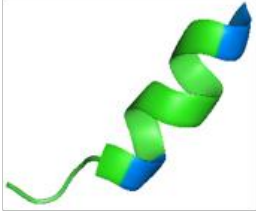
	Human β -Defensin-1	Folded β -sheet defensin peptides contain disulfide linked β -sheets and cationic residues.
A 	Avian β -Defensin-2	
B 	LL37, α -helical human peptide	Non-folded α -helical cathelicidins do not contain any disulfide linkages and have cationic residues.
	Fowlcidin-1, α -helical chicken peptide	
C 	Indolicidin, a tryptophan rich bovine peptide.	Non-folded linear CAMPs are similar to cathelicidins and often contain a strong bias toward certain amino acids.

Figure 4: The three main classes of ribosomally produced CAMPs. (A) the defensins, characterised by their folded structure and disulfide bonds. (B) the linear cathelicidins and (C) the shorter linear peptides. All three groups share a net positive charge and are ribosomally synthesised. Positive residues are shown in blue and negative residues are shown in red. All structure taken from the protein data bank (<http://www.rcsb.org/pdb/home/home.do>) and visualized with pymol.

1.9.1 The model CAMP polymyxin-B

CAMPs produced by higher eukaryotes typically fall into one of three classes, as discussed in the previous section. CAMPs may also be produced by bacteria and are typically produced using non ribosomal peptide synthesis. The CAMP polymyxin-B was originally found in the organism *Paenibacillus polymyxa* (originally known as *Bacillus polymyxa*), it is a cyclic peptide antimicrobial which contains a mixture of L-amino acids, D-amino acids and other non-proteinogenic amino acids (Paulus and Gray, 1964). There is some evidence to suggest that the non-ribosomal synthesis of polymyxin-B may be a defence mechanism against other bacteria that produce protein synthesis inhibiting antibiotics, as polymyxin-B production is roughly doubled in *P. polymyxa* when treated with chloramphenicol (Paulus and Gray, 1964). Polymyxin-B is produced by the *pmxABCDE* gene locus from *P. polymyxa*, and is more active against Gram-negative bacteria (Kim *et al.*, 2015). Polymyxin-B has been shown to bind to the lipid-A major outer membrane lipid from Gram-negative bacteria (Yin *et al.*, 2003). The binding appears to increase the surface charge of the outer membrane lipopolysaccharide (LPS) and induces LPS aggregation which can reduce the severity of infection (Domingues *et al.*, 2012). It is not known exactly how polymyxin-B causes cell death and there are competing models for the exact mechanism as the concentrations of polymyxin-B required to cause membrane permeabilisation are often higher than the reported inhibitory concentrations (Hancock, 1997). It is thought that at low concentrations polymyxin-B may induce exchange of lipids between the cytoplasmic and outer membranes, compromising the integrity of the outer membrane and causing cell death or inhibition of growth (Clausell *et al.*, 2003).

1.9.2 Cathelicidins and β -defensins

The cathelicidin classes of CAMPs are generally simple α -helical peptides with multiple positively charged residues. The class includes the human CAMP LL37, and the chicken CAMPs Folwlicidin-1 and Fowlicidin-2 (Mukhopadhyaya *et al.*, 2010). The human cathelicidin LL37 has been shown to not only lyse bacterial cells but also to act as a localised modulator of the immune response by potentially acting as a chemotaxin for mast cells (Niyonsaba *et al.*, 2002). LL37 has also been implicated in promoting epithelial repair at wound sites (Heilborn *et al.*, 2003).

The β -defensins are characterized by their folded structure often containing 6 or more cysteine residues forming up to 3 disulfide bridges (Pasupuleti *et al.*, 2012). There are 3 different classes of defensins (α , β and θ) where α and β are synthesised as a single pro-peptide chain and are stored in Paneth cells or as mature peptides in neutrophils. θ defensins are not found in humans and are formed by the end to end post translational ligation of two 9 residue

peptides into a cyclic peptide (Tang *et al.*, 1999). Artificial θ defensins have been shown to be effective *in-vitro* inhibitors of the herpes simplex virus adhesion and entry into host cells (Yasin *et al.*, 2004). Antimicrobial peptides can also act as stimulators of the immune system in response to infection (Arnett *et al.*, 2011). It has recently been shown that the human defensin (HD1) is significantly more potent against bacteria when the disulfide bonds are broken whereas another defensin (HD3) shows a slight reduction in potency when in its reduced form (Schroeder *et al.*, 2011), suggesting that the disulfide bonds are not required for activity in all defensins but may help to stabilize the peptide during storage or transport. A third human defensin (HD5) has been shown to bind around a single zinc ion when in its reduced form and is protected from proteolytic degradation in this state. Since HD5 is primarily localized to the intestines, this metal bound state may protect the defensin from accidental digestion in the gut (Zhang *et al.*, 2013).

1.10 Mechanisms of antimicrobial peptide activity

The primary target for antimicrobial peptides appears to be the membrane bilayer found in all bacteria. The outer leaflet of the eukaryotic cell membrane is composed of zwitterionic phospholipids and usually carries a net neutral charge, both leaflets of the gram negative external membrane show a net negative charge due to a larger proportion of acidic phospholipids (Matsuzaki, 1999). Thus cationic AMPs are preferentially attracted to the negatively charged bacterial membranes. Since many CAMPs are also amphipathic, the hydrophobic region is likely preferentially inserted into the cell membrane. This action is also thought to be a reason for the anti-tumor effect seen in some CAMPs as many types of tumor cells contain unusually high numbers of negatively charged gangliosides lowering the net charge of the cell membranes (Lee *et al.*, 2008). While there is no clear agreement on the exact mechanism of cell killing, there are 3 primary models of how CAMPs can interact with the membrane to cause cell leakage.

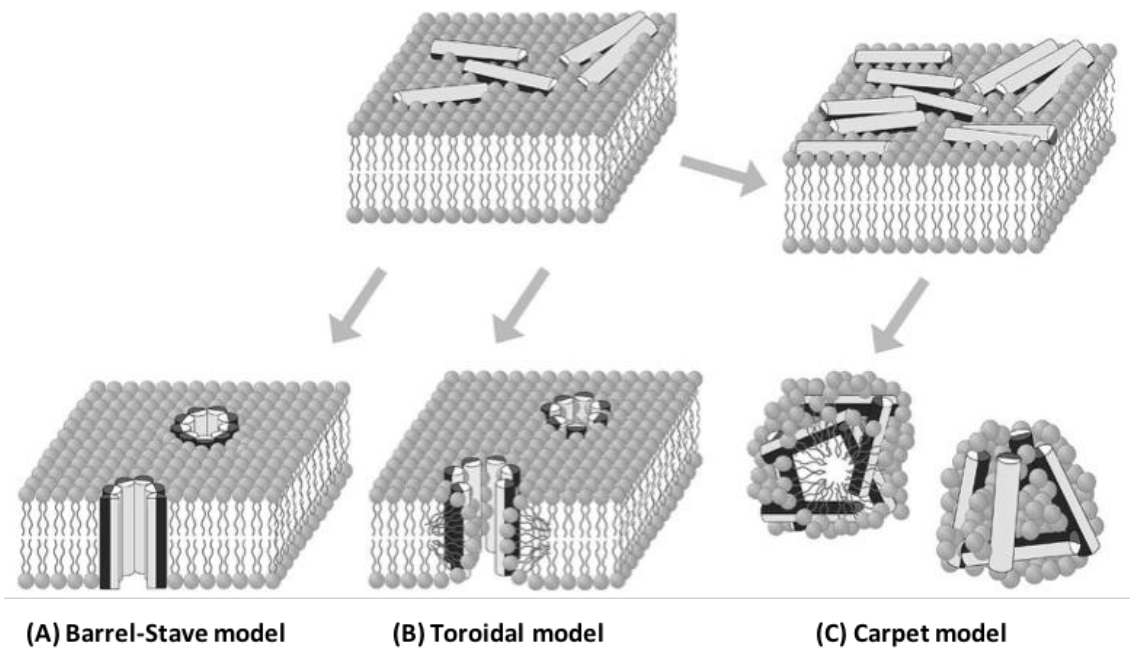


Figure 5: The three models for CAMP interactions with lipid membranes. Initially CAMPs are thought to attach to the lipid bilayer surface and cluster together to form pores. **(A)** the barrel-stave model hypothesizes that the hydrophobic residues of the CAMPs align with the hydrophobic acyl chains in the lipid bilayer forming a straight pore through the bilayer. **(B)** the toroidal model is similar to the barrel-stave model except that the hydrophilic heads of the bilayer associate along the edge of the pore bending the bilayer around the hole. **(C)** the carpet model is thought to require a threshold concentration of CAMPs on the membrane surface before small micelles or peptide-lipid aggregates are formed away from the cell. The CAMPs are represented as linear when bound to the surface, hydrophilic and lipophilic parts of the CAMPs are represented by grey and black respectively. Image adapted from (Wiesner and Vilcinskas, 2010).

1.10.1 *The barrel-stave model*

The barrel stave model was considered the archetypal model for peptide-induced pore formation (Wiesner and Vilcinskas, 2010). This model depicts spontaneous pore formation by insertion of the peptide through the entire lipid bilayer, which requires the peptide to be of equal or greater length to the bilayer. Since it would be energetically unfavorable for a single peptide to transverse the hydrophobic and hydrophilic regions of the lipid membrane, this model is hypothesized to be dependent on a local 'threshold' concentration of surface bound CAMPs before the pore is formed (Pasupuleti *et al.*, 2012). Only a few AMPs have been shown to act in this way, including the mammalian C9 protein from the complement pathway of the adaptive immune system (Rosado *et al.*, 2008).

1.10.2 *The toroidal model*

The toroidal (worm-hole) model is similar to the barrel-stave model and is the preferred model for the action of the majority of CAMPs including the cathelicidins and defensins (Wiesner and Vilcinskas, 2010, van Dijk *et al.*, 2008). The toroidal model is 'hypothetically' dependent on the hydrophilic head of the lipids aiding in pore formation by bending with the peptide which is likely preceded by localised membrane thinning due to the insertion of peptides into the outer leaflet of the lipid membrane (Chen *et al.*, 2003).

1.10.3 *The carpet model*

The carpet model is a more general model for the action of CAMPs exhibiting a detergent like effect, where localised surface aggregation of CAMPs leads to the removal of micelle like 'bundles' of phospholipids (Chang *et al.*, 2008). This method of pore formation has been shown to be more easily repairable than the other models as the peptides are removed from the cell surface along with the micelles (Chang *et al.*, 2008).

Much of the work characterising which model a particular CAMP exerts upon the lipid membrane has been carried out using artificial membranes as models and so what effect differences in membrane composition and trans-membrane proteins may have between species has not been well studied (van Dijk *et al.*, 2008). There also does not yet appear to be a strong consensus about whether different families of CAMPs preferentially form one of the three models of pore formation.

Some CAMPs are able to transverse the microbial membrane and affect intracellular components, for example Buforin-II and Magainin-II are both amphipathic α -helical CAMPs isolated from frogs. Magainin-II has been shown to form toroidal membrane pores causing cell

lysis (Ludtke *et al.*, 1996). Buforin-II however was shown to cause cell death without causing cell lysis but by strongly binding to DNA and RNA (Park *et al.*, 1998). Another example is the silk moth CAMP Attacin, which was shown to prevent outer membrane protein synthesis at the pre-translational level in *E. coli* (Carlsson *et al.*, 1991).

1.11 Sensing and defending against CAMPs

While the majority of CAMPs target a fundamental and not easily altered component of the microbial cell membrane, there are five main ways in which Gram-negative bacteria can defend against host CAMPs, (1) degradation of host CAMPs, both *Pseudomonas aeruginosa* and *Proteus mirabilis* have been shown to produce outer membrane proteins which can degrade the human α -helical cathelicidin LL37 (Schmidtchen *et al.*, 2002). (2) modification of the cell membrane, *Salmonella typhimurium* possess a lipid modification protein (*pagP*) which attaches acyl groups to lipid-A, this is hypothesised to alter the fluidity of the outer membrane making it harder for CAMPs to form pores (Guo *et al.*, 1998). *P. aeruginosa* possess a system for modifying components of the outer membrane prior to being flipped into the outer leaflet, by attaching aminoarabinose moieties to the negatively charged phosphate groups on lipid-A, the net membrane charge becomes more neutral which is thought to attract fewer CAMPs (Moskowitz *et al.*, 2004). (3) Shielding of the outer membrane, strains of *Klebsiella pneumoniae* with mutations in capsule polysaccharide synthesis pathways have been shown to be more sensitive to CAMPs (Campos *et al.*, 2004). Another study showed that secretion of only anionic capsular polysaccharide increased resistance to CAMPs (Llobet *et al.*, 2008), (4) Pumping CAMPs either into the cell for degradation or out of the cell. A well-studied example from *Salmonella typhimurium* is the sensitivity to antimicrobial peptide (*sapABCDF*) operon containing an ABC transporter, which was, required for CAMP resistance (Parra-Lopez *et al.*, 1993). Another example is the *N. gonorrhoeae* RND efflux transporter *mtrCDE* that was shown to be required for resistance to LL37 (Shafer *et al.*, 1998). (5) Down-regulation of host CAMP expression, this is a mechanism some Gram-negative pathogens use to resist killing by host derived peptides, *Salmonella typhimurium* has been shown to lower the expression of the mouse defensin Cryptdin in paneth cells, using a process involving a type III secretion system and the *phoP* regulon (Salzman *et al.*, 2003, Gruenheid and Le Moual, 2012).

One of the best-studied mechanisms of defence against CAMPs in Gram-negative bacteria is the PhoP/PhoQ two component sensor regulator system in *S. typhimurium*. This was first shown to provide resistance to CAMPs by up-regulating the *pagP* gene, which alters the structure of lipid A, reducing the ability of CAMPs to bind to the lipid bilayer (Guo *et al.*, 1998). This modification system was shown to be inducible by CAMPs by sensing membrane bound

CAMPs on the cell surface via displacement of divalent metal cations (Bader *et al.*, 2005). While CAMPs were able to induce this system it was also shown that a drop in pH and a decrease in divalent metal cation concentration could act as inducers. Further investigation showed that a large number of genes are under the control of the PhoP/Q system, including some for survival following internalization within a host cell, leading to speculation that this system is a global host survival regulator rather than a dedicated CAMP resistance system (Groisman and Mouslim, 2006). Homologues of parts of the PhoP/Q system have been found in several Gram-negative pathogens including *Yersinia pestis* and *Shigella flexneri* (Otto, 2009). More recently CAMP activation of the PhoP/Q system was shown to induce not only Lipid-A modification in *Klebsiella pneumoniae*, but also to induce virulence factors. The authors also showed that exposure to sub-inhibitory concentrations of the model CAMP polymyxin-B increased short-term resistance to higher concentrations of both polymyxin-B and other CAMPs (Llobet *et al.*, 2011).

1.12 CAMP resistance in *Campylobacter jejuni*

One of the early *Campylobacter* selective medias contained the CAMP polymyxin-B as a selective agent, showing that *Campylobacter* possesses an intrinsic resistance to this particular CAMP (Skirrow, 1977). Much of the work on the effect of CAMPs upon *Campylobacter* species has focused on the roles of the unique LOS (lipooligosaccharide) layer. Disruption of the lipooligosaccharide layer by deletion of the heptosyltransferase gene *waaF* in *C. jejuni* shows an increase in susceptibility to polymyxin-B, but interestingly disruption of the capsular polysaccharide (CPS) layer by deletion of a putative CPS transporter showed no increased sensitivity (Jeon *et al.*, 2009). Other studies on aspects of the *Campylobacter* LOS layer have shown similar increases in polymyxin-B sensitivity, such as modification of lipid-A (Van Mourik *et al.*, 2010) and truncation of the LOS core (Naito *et al.*, 2010). Mutagenesis of the phosphoethanolamine (pEtN) transferase (*cj0256*) causes a large increase in sensitivity to polymyxin-B, this deletion also causes a near complete loss of flagellar production (Cullen and Trent, 2010). Further work looking for specific resistance mechanisms in *C. jejuni* 81-176 using high throughput transposon mutagenesis and polymyxin-B sensitivity screening has highlighted genes involved in synthesis of cell surface carbohydrates, modulation of membrane potential, and further genes involved in membrane and LOS synthesis (Lin *et al.*, 2009). There does not appear to be any dedicated CAMP sensing / resistance system, such as PhoPQ, in *Campylobacter*.

1.13 The type VI secretion system

The type VI secretion system (T6SS) is a Gram-negative specific, secretory apparatus for the export of proteins through the membranes of neighboring cells. The T6SS was discovered in *Vibrio cholerae* as being required for virulence and further genetic analysis of the T6SS gene cluster revealed homologies between the T6SS export apparatus and bacteriophage tail spike apparatus (Pukatzki *et al.*, 2006, Pukatzki *et al.*, 2007). The T6SS was shown to export virulence factors in both *V. cholerae* and *P. aeruginosa* (Mougous *et al.*, 2006), yet non-pathogenic bacteria were also shown to possess homologues of the T6SS export apparatus (Ho *et al.*, 2014). It was also discovered that *P. aeruginosa* is able to export toxic effector proteins directly into the periplasm of other Gram-negative cells via the T6SS (Russell *et al.*, 2011). *P. aeruginosa* was shown to export two peptidoglycan amidase toxins into other bacteria, the toxins are exported directly from the attacking cell cytoplasm to the prey cell periplasm and so never interact with the cell's own peptidoglycan layer. To prevent attack from closely related species, *P. aeruginosa* produces and exports antitoxins into their own periplasms to quench attacks from close relatives. The crystal structure of the *P. aeruginosa* T6SS amidase toxin and antitoxin has been solved multiple times and has been shown to contain a cysteine-histidine catalytic site and a papain like fold (Chou *et al.*, 2012, Ding *et al.*, 2012). Some of the best studied antibacterial T6SS systems are in *V. cholerae*, *Pseudomonas*, *Burkholderia* and *S. marcescens* (Schell *et al.*, 2007, Murdoch *et al.*, 2011), it is estimated that 25% of all Gram-negative bacteria may possess related systems (Ho *et al.*, 2014).

Some strains of *C. jejuni* do possess a type VI secretion system but it is seemingly related to host cell invasion and pathogenesis rather than interbacterial competition. The *C. jejuni* strain ACCT 43431 was shown to be defective in chicken colonisation and shows reduced adhesion and invasion of host cells when the T6SS was inactivated by mutagenesis (Lertpiriyapong *et al.*, 2012).

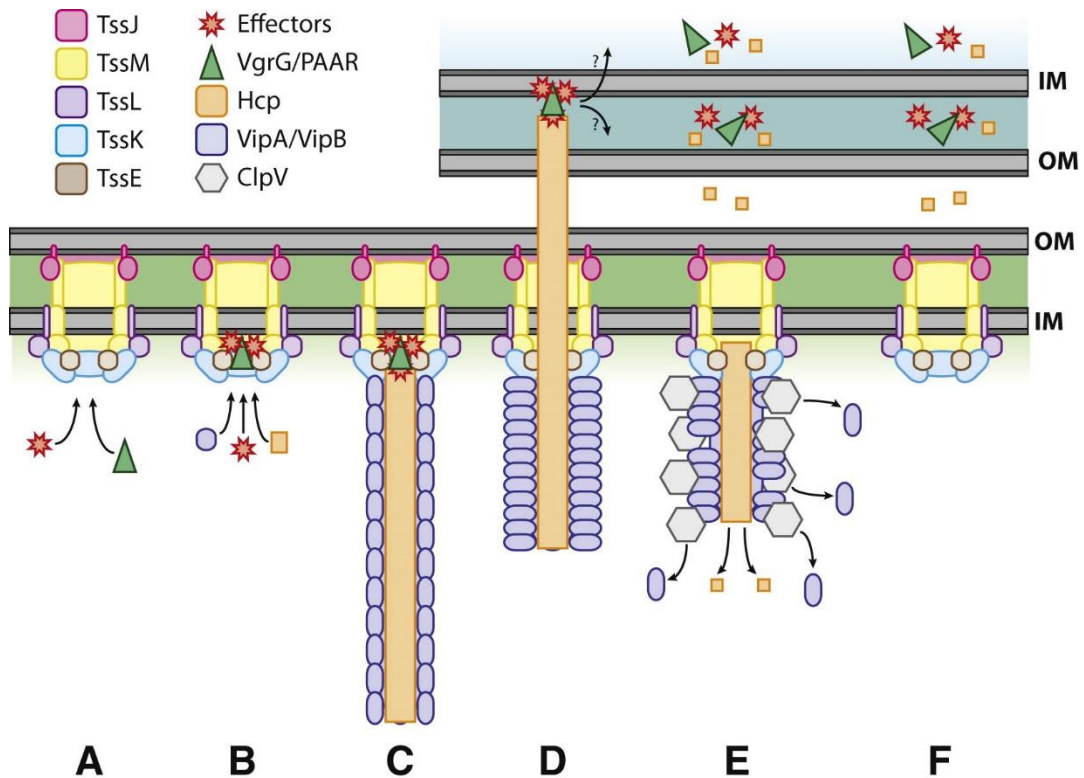


Figure 6: Model for the assembly and function of the antibacterial type VI secretion system (T6SS). (A) the formation of the baseplate complex consisting of TssEJKLM. (B) the recruitment and assembly of the effector proteins VgrG/PAAR to the baseplate complex, it is unknown if they are localised to the cytoplasm, periplasm or inner membrane at this point. (C) the Hcp effector delivery tube polymerises from the baseplate complex with the VipA/B contractile sheath polymerizing around the growing Hcp tube. (D) conformational changes in VipA/B propels the Hcp tube outside the cell and through the outer membrane of a neighbouring cell. The VgrG/PAAR proteins act as both ‘wahead’ proteins to pierce the membrane as well as toxic effector proteins. Other effector proteins are delivered from the Hcp tube. (E) ClpV remodels the contractile sheath using ATP and disassembles the tube components. The recycled components can be immediately re-used or degraded. (F) the baseplate complex can also be re-used or recycled depending on the activation state of the T6SS. Image adapted from (Ho et al., 2014).

1.13.1 The type VI secretion system toxin-antitoxin system

Since the discovery of the T6SS a wide range of toxin-antitoxin pairs have been characterised in Gram-negative bacteria. A recent study in *V. cholera* has shown that while the T6SS is widespread and exports both host-targeted and anti-bacterial effectors, there are often different types of anti-bacterial targeting effector toxins, usually found with an antitoxin gene immediately downstream (Unterweger et al., 2014). From *V. cholera* species alone there are 3 classes of toxin-antitoxin systems, multiple types of peptidoglycan amidase and muramidase enzymes, a class of membrane acting lipases (which presumably act from within the periplasm) and a class membrane-spanning pore forming toxins, each with their respective antitoxins. The antitoxins for the enzymatic effectors are typically active site blocking inhibitors. While the antitoxins for pore-forming toxins are smaller membrane spanning proteins, which

presumably act as inhibitors of pore formation (Russell *et al.*, 2014). The *S. marcescens* DB10 genome encodes 6 putative toxic effectors, all of which have been shown to be active against *E. coli* (Fritsch *et al.*, 2013). Two of these toxins (Ssp1 and Ssp2) have been characterised as peptidoglycan amidase toxins (English *et al.*, 2012) while the others remain unknown, though Ssp3, Ssp5 and Ssp6 have been shown to be active against unknown cytoplasmic targets (Fritsch *et al.*, 2013).

A study of a *P. aeruginosa* amidase toxin showed that the inhibiting antitoxin, which is expressed in the periplasm, does not share any structural homology to a more general class of cysteine containing protease inhibitors called cystatins. They hypothesize that having a non-specific peptidoglycan amidase inhibitor in the periplasm would hinder cell wall turnover, leading to the evolution of a highly specific inhibitor for the toxin (Key *et al.*, 2012). The T6SS is a diverse and under-characterised way for bacteria to interact with each other in both environmental and infection niches. The toxin-antitoxin system ensures that closely related species do not inhibit each other during times of stress. To the best of the authors knowledge no defense mechanisms has yet been discovered for bacteria to actively inhibit foreign T6SS effector proteins.

1.14 A cluster of genes in *Campylobacter jejuni* NCTC11168 which may protect against Cationic Antimicrobial Peptides (CAMPs)

1.14.1 Previous work on the gene cluster

The antimicrobial peptide polymyxin-B is a commonly used model peptide for studying CAMP resistance mechanisms in bacteria. While *Campylobacter* species are known to be more resistant to polymyxin-B than other Gram-negative bacteria (Skirrow, 1977), no specific or active defense mechanism has been found. Previous work in this lab has suggested that a 5 gene cluster in *C. jejuni* NCTC11168 (*cj0421c-cj0425*) may be involved in active resistance to CAMPs. These genes were provisionally named as the Rid system (Resistance to Innate Defenses).

One of the genes in this cluster is a DNA-binding protein (Cj0422c), which was initially discovered as part of another project looking at differences in gene regulation in response to lowering atmospheric oxygen in chemostat cultures. This work showed a small up-regulation (4.5 fold) of *cj0422c* by microarray at 1.88% oxygen compared to the standard 10% oxygen (E.J. Guccione, R.K. Poole and D.J. Kelly, unpublished data). Because it is still unknown how *C. jejuni* is able to 'sense' and respond to oxygen levels this putative DNA-binding protein was thought of as a candidate regulator for oxygen stress response genes. Due to the predicted DNA binding domain of Cj0422c a mutant was produced and RNA extracted for microarray analysis. The microarray transcriptome of this mutant showed multiple changes in gene expression compared to wild type *C. jejuni*, including both up and down regulation of genes, suggesting that Cj0422c is able to act as both a repressor and activator of transcription. The microarray results (performed and analysed by Dr Ed Guccione) are shown in (Figure 7). The genes showing the greatest change in expression do not appear to have any obvious role in oxygen stress response, instead the largest differences in expression are in the genes immediately upstream of Cj0422c itself.

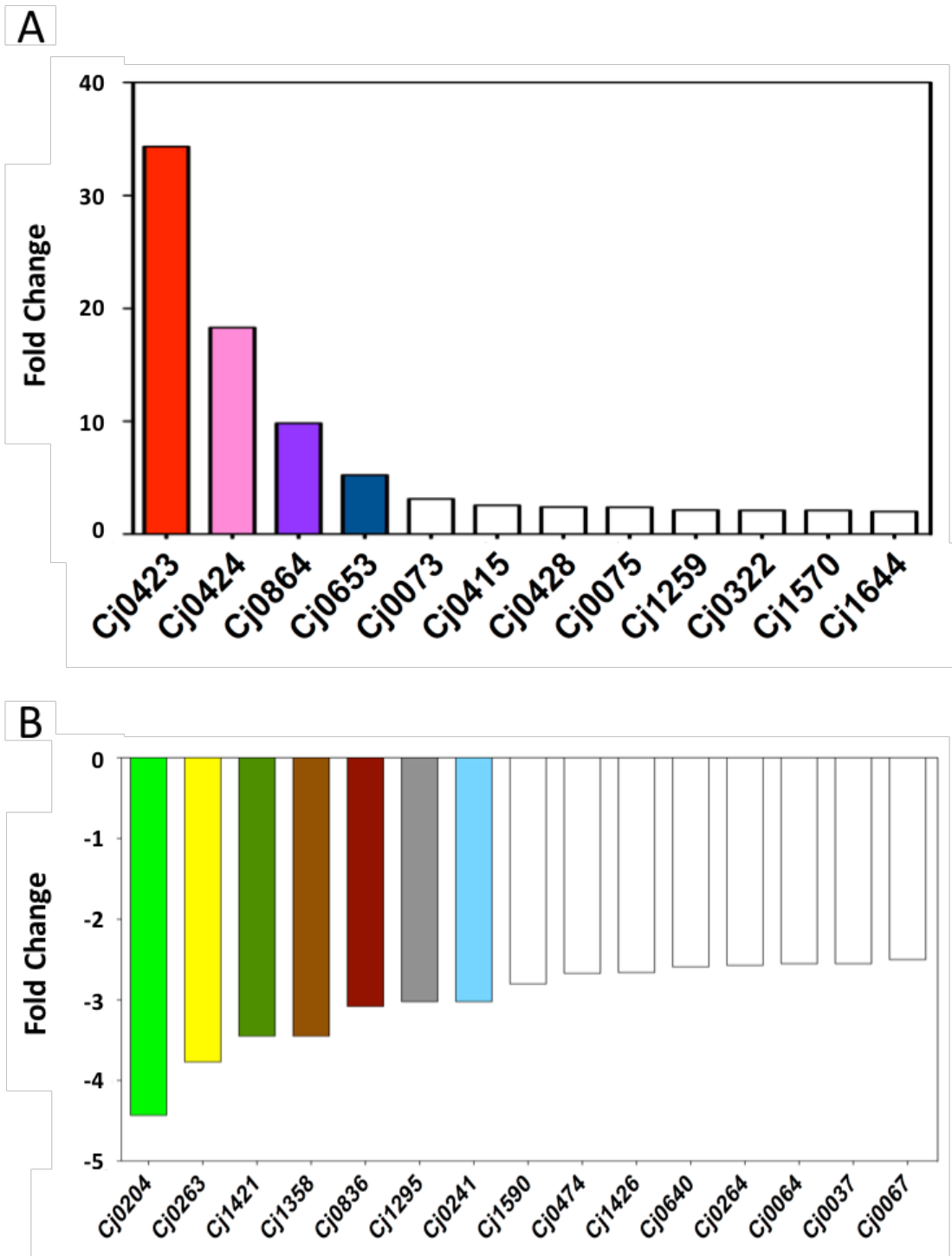


Figure 7: Microarray analysis of the *cj0422c* mutant compared to wild type. RNA was extracted from cultures grown in steady state chemostat culture. (A) shows genes which are up-regulated, (B) shows genes which are down-regulated.

This microarray analysis of the *cj0422c* mutant revealed that while it may not be involved in the oxygen stress response it does appear to regulate a number of genes throughout the *C. jejuni* NCTC11168 genome with no clear link between them. The largest changes in expression are in *cj0423* and *cj0424* (34 and 18-fold increases respectively), implying that the two are transcriptionally linked in an operon (a further gene *cj0425* is found immediately downstream in the same orientation but this does not appear on the microarray). The roles of these genes are unknown, analysis of the protein sequence has shown that Cj0423 contains 2 transmembrane domains and Cj0424 contains 7 MORN (Membrane Occupation and Recognition Nexus) motif repeats and an N-terminal membrane lipid anchor sequence. Cj0425 contains a periplasmic export sequence and two separate CXXT motifs, potentially implying a role in redox reactions in the periplasm. None of these 3 proteins show any strong homologies to proteins outside of *Campylobacter* species so their roles are unknown. Other genes which are significantly up-regulated in the *cj0422c* mutant are *cj0864* which encodes a DsbA like periplasmic protein (9.8 fold) and *cj0653c* which encodes as cytoplasmic aminopeptidase (5.2 fold). Several genes are also down-regulated including *cj0204c*, a predicted peptide transporter (-4.4 fold) and *cj0263* a ZupT like zinc transporter (-3.8 fold).

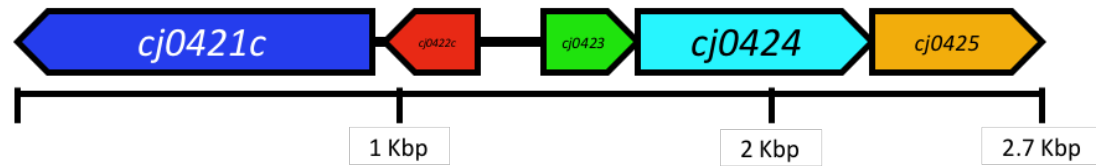
Cj0424 is the only protein from the *cj0423-cj0425* operon which contains a characterised motif, the membrane occupation and recognition nexus or MORN motif. MORN proteins are split into 2 families, MORN 1 and 2, with MORN 1 motifs being found mostly in eukaryotes and MORN 2 motifs in prokaryotes, though there are exceptions (PFAM database (<http://pfam.xfam.org>), MORN 1-PF02493, MORN 2-PF07661). MORN 2 proteins are characterised by a 22-residue variable amino acid motif that is typically repeated multiple times within a single protein (Takeshima *et al.*, 2000).

MORN motifs were originally found in junctophilin proteins which mediate the junctional complex between the cytoplasmic membrane and endoplasmic/sarcoplasmic reticulum in higher eukaryotes (Takeshima *et al.*, 2000). MORN motifs are often replicated within a single protein, sometimes up to 17 individual motifs per protein, that are often clustered at the C or N terminal ends of a protein (Habicht *et al.*, 2015). The exact role of MORN domains is not fully understood but they were initially hypothesised to bind to the phospholipid membrane as a way of localising other protein domains to the lipid membrane (Shimada *et al.*, 2004). It has since been shown that some MORN domains are required for cell division in *Toxoplasma gondii* (Gubbels *et al.*, 2006). Some genomes encode a surprisingly large number of MORN

domain proteins including *Helicobacter bilis* (>100 MORN domains), *Fusobacterium periodonticum* (234), *Tetrahymena thermophile* (129). The presence of large numbers of MORN domains appears to strongly correlate with organisms which actively invade host cells (McGuire *et al.*, 2014, Habicht *et al.*, 2015). A study on four MORN domain proteins from *Tetrahymena thermophile* has shown that all four proteins localise to distinctly different locations within the cell though the mechanism for this localisation is unknown (Habicht *et al.*, 2015). There are currently no reported studies on individual MORN proteins in bacteria and the structure-function relationships in MORN motifs are also not known.

The microbial MORN 2 motif is variable between species but will typically contain multiple tyrosine and glycine residues, with a central YYxNGKL motif. The *C. jejuni* genome encodes a single MORN 2 motif protein Cj0424, which contains 7 repeated (xeGxxkxYYeNGKLxxexxYkN) motifs, where uppercase letters represent heavily conserved amino acid residues and lowercase represents less conserved residues and x represents variable amino acid residues.

1.14.2 The *Rid* operon



Gene	Description	Domain Architecture
<i>cj0421c</i> <i>ridS</i>	37 kDa protein, contains 6 transmembrane helices with globular C-terminal cytoplasmic domain. Some weak homology to GGDEF domain proteins.	
<i>cj0422c</i> <i>ridR</i>	8.4 kDa protein containing a helix-turn-helix domain. It binds to an 18bp recognition sequence in the <i>cj0423</i> promoter region repressing expression.	
Promoter	168 bp region between <i>cj0422c</i> - <i>cj0423</i> . 18 bp palindromic repeat sequence found upstream of <i>cj0423</i> which <i>Cj0422c</i> has been shown to bind to.	
<i>cj0423</i> <i>ridM</i>	8.6 kDa inner membrane protein containing 2 transmembrane helices.	
<i>cj0424</i> <i>ridL</i>	24 kDa periplasmic protein. Contains 7 MORN motifs and forms an antiparallel β -sheet ladder structure.	
<i>cj0425</i> <i>ridP</i>	15.6 kDa periplasmic protein. Contains 2 CXXT motifs, potentially involved in redox reactions.	

Table 1: A brief description of the 5 genes within the primary *Rid* operon, the diagrams show the predicted domain architecture of the proteins using data obtained from (<http://blast.ncbi.nlm.nih.gov/Blast.cgi>) and (<http://smart.embl-heidelberg.de>).

1.14.3 Early characterisation of the *rid* system

Since there is no immediately obvious role that links all the genes that are regulated by Cj0422c, initial work focused on the roles of some of the individual proteins. It was shown that Cj0422c does bind to a very specific 18bp palindromic repeat sequence immediately upstream of *cj0423* and binding would likely block transcription. Purified recombinant Cj0422c was shown to tightly bind the 18 bp sequence ($K_d < 1 \mu\text{M}$) and less so to an 18 bp sequence altered by site directed mutagenesis ($K_d \sim 5 \mu\text{M}$), the protein was also shown to bind upstream of *cj0864*, *cj0204* and *cj0263* however the binding was notably weaker at these promoters, shown by electrophoretic mobility shift assays (Hitchcock, 2011).

The Cj0424 MORN domain protein was purified and crystallised by Dr Andrew Hitchcock in collaboration with Dr John Rafferty, the crystal structure was solved to 2.1 Å, which to our knowledge is the first reported structure of a MORN domain protein (unpublished data). The crystal structure showed that Cj0424 contains 15 folded antiparallel β -sheet strands arranged in a 'ladder like' formation, with the MORN domains located along one edge of the protein, (see Figure 8). The structure also shows a small protruding loop designated the ED loop composed of negatively charged residues (Glutamic acid and Aspartic acid).

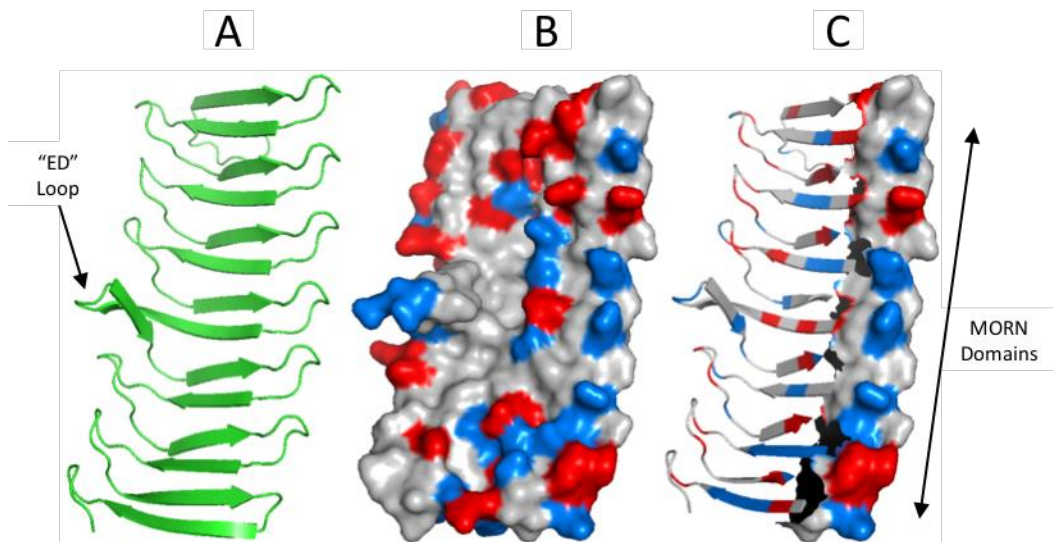


Figure 8: The crystal structure of Cj0424 (RidL). The 2.1 Å structure of Cj0424 (residues 21-205), (A) shows the protein structure represented by ribbons showing the 15 antiparallel β -sheet strands, the protruding 'ED' loop is highlighted. (B) shows the structure in the same orientation showing the surface electrostatic potential (blue shows negatively charged residues and red shows positively charged residues). (C) shows the structure in the same orientation with the MORN domains filled with the surface charge and the rest of the protein represented by the ribbon structure. The protein's structure was analysed in PyMOL (<https://www.pymol.org>).

The Cj0425 periplasmic protein contains 2 CXXT motifs which may be involved in redox reactions within the periplasm, however the protein has no close homologues outside the *Campylobacter* genus and previous studies have not revealed anything about the role of Cj0425 in *Campylobacter*. A *cj0425* mutant showed a small but statistically significant increase in biofilm formation when grown in high oxygen conditions compared to wild type *C. jejuni*, the *cj0425* mutant also showed a slight increase in sensitivity to peroxide and sulphide (Hitchcock, 2011).

1.14.4 How the Rid system may be involved in CAMP defence

The data obtained from the microarray on the *cj0422c* mutant showed large changes in gene expression in the *cj0423-cj0425* operon and smaller, yet significant changes elsewhere in the genome of *C. jejuni* NCTC11168, including both up and down-regulation of genes. This implies that the role of these genes collectively may be specific to a particular niche condition or stress and the data showing that Cj0422c acts as a strong repressor implies that some type of condition or stress may act as an inducer or 'on switch' for the Rid system, and that the *cj0422c* mutant in effect mimics this condition. Further data from previous students has shown that none of the mutant strains appear to show any growth defects when grown under normal conditions, implying that these genes are not essential for normal growth. While the roles of the genes in the primary operon *cj0423-cj0425* are not known, the microarray reveals that the cytoplasmic aminopeptidase *cj0653c* is up-regulated and the peptide transporter *cj0204* is down regulated. This lead to the hypothesis that the whole Rid system may be involved in resistance to Cationic Antimicrobial Peptides (CAMPs). This hypothesis was initially tested by assaying the sensitivity of the *rid* mutant strains to polymyxin-B a model CAMP. Wild type *C. jejuni* is able to effectively resist 200 $\mu\text{g ml}^{-1}$ polymyxin-B for 2 hours in microtiter assays whereas the *cj0422c* mutant showed a complete loss of viability at only 20 $\mu\text{g ml}^{-1}$ polymyxin-B over the same time period, the *cj0424* mutant also showed increased sensitivity to polymyxin-B. This hypersensitivity strongly suggested that the Rid system acts as a defence mechanism against polymyxin-B and probably other CAMPs since they share a similar mechanism of action. Further work in assaying the sensitivities of Rid mutants to polymyxin-B and other CAMPs as well as characterising how the primary Rid proteins (Cj0423-Cj0425) act to defend against CAMPs was undertaken by another PhD student Halah Al-Haideri. This work showed that the mutants in the other Rid genes showed large increases in sensitivity to polymyxin-B as well as other CAMPs from both humans and chickens. Further work in this area showed that heterologous expression of Cj0424 in the periplasm of *E. coli* afforded extra protection against CAMPs. NMR analysis of purified Cj0424 also showed weak binding to

polymyxin-B suggesting its role may be to bind and inhibit CAMPs in the periplasm. This data suggested that the whole Rid system is involved in defence against CAMPs and may be the reason why *Campylobacter* species are intrinsically so resistant to polymyxin-B. Further work on the roles of the individual proteins within the Rid operon was continued alongside work to examine more closely the roles of the primary regulator Cj0422c and the downstream gene Cj0421c.

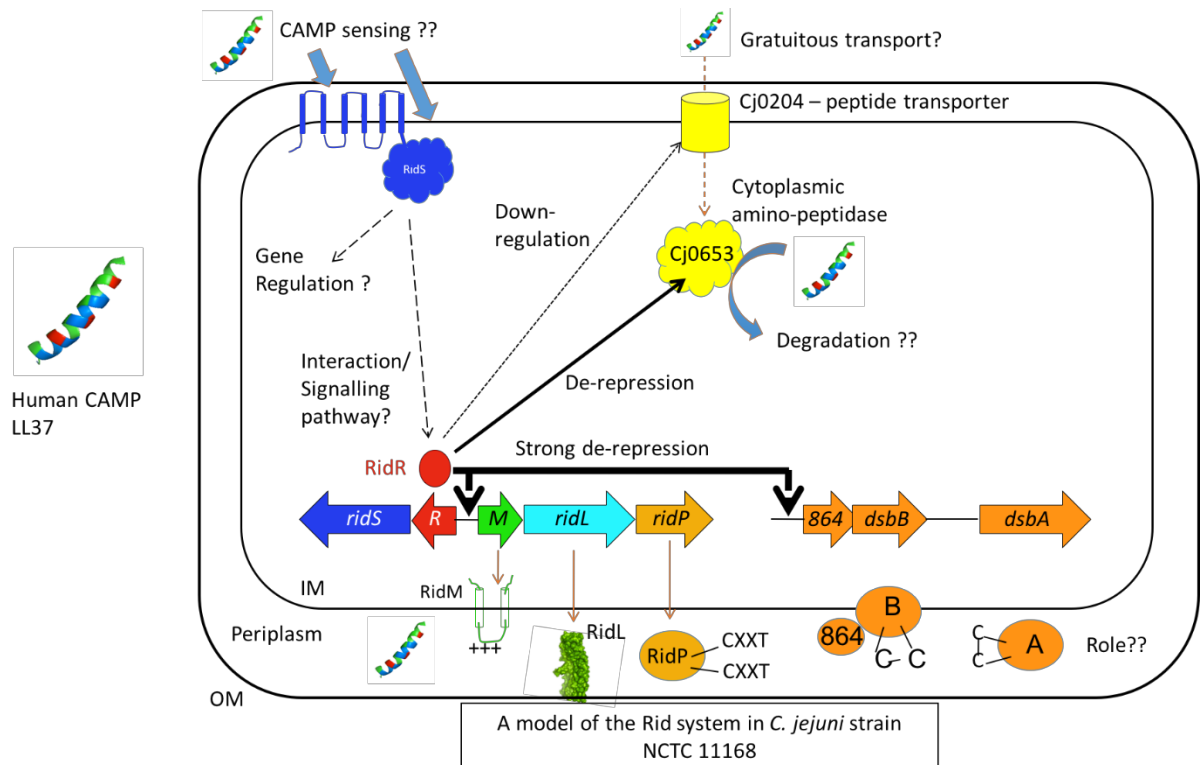


Figure 9: The hypothetical model of how the Rid system would work to defend against CAMPs. The model is based on the difference in gene expression observed in the *cj0422c* (*ridR*) mutant strain. This assumes that the 'on' state for the Rid system is mimicked by the *cj0422c* mutant. The model is based on most of the genes which show strong up or down-regulation being part of a system to defend against CAMPs. The individual roles for each of the genes is listed in (Table 2).

Protein	Microarray Fold Change	Gene Annotation	Predicted Role In CAMP Defence
Cj0421c	X	Hypothetical protein	Potentially acts as a 'sensor' for CAMPs or other stimuli
Cj0422c	X	DNA binding H-T-H	Master regulator, acts to repress whole system during normal conditions
Cj0423	34.33	Hypothetical membrane protein	Contains positively charged residues, possibly acting to repel positively charged CAMPs
Cj0424	18.31	Outer membrane lipid anchor MORN protein	Outer membrane bound protein, possibly acts to 'soak up' CAMPs by binding
Cj0425	X	Periplasmic protein	Contains 2 CXXT motifs so may be involved in redox reactions, role unknown
Cj0864	9.83	Putative periplasmic Dsb protein	Forms part of the Dsb operon so may act to re-fold some families of CAMPs which become more active when unfolded
Cj0653c	5.22	Putative M23 family cytoplasmic aminopeptidase	May act to degrade CAMPs that reach the cell cytoplasm
Cj0263	-3.77	Zinc transporter	Likely transports multiple 2+ metal cations, role unknown
Cj0204	-4.43	Putative oligopeptide transporter	May gratuitously transports CAMPs so is down-regulated to prevent accidental transport into the cell.

Table 2: A table detailing how the hypothetical CAMP resistance model would work using the genes altered from the *cj0422c* mutant microarray data. The genes listed show the largest difference in expression in the *cj0422c* mutant microarray data or are in an operon with those that are. The model is based on the genes being up or down-regulated by Cj0422c in response to some kind of external stimuli which is currently unknown but assumed to be CAMPs. Fold changes shown by X contained no data.

1.15 Project Aims:

- To determine the sensitivity phenotypes of the two regulator mutants *cj0421c* and *cj0422c* against a wide range of CAMPs and other antimicrobials.
- Bioinformatically analyse the *rid* genes to look for homologues in other *Campylobacter* strains and to produce knockout mutants of the *rid* homologues in *C. jejuni* 81116.
- To confirm the microarray data by qRT-PCR and to examine the role of Cj0421c as a potential regulator by qRT-PCR.
- To produce a *lacZ* reporter construct and to screen for potential inducers of the *rid* system by CAMPs or other conditions.
- To overexpress and purify Cj0421c and Cj0422c to look for binding to CAMPs or protein-protein interactions with each other.
- To attempt crystallisation of both Cj0421c and Cj0422c.
- To overexpress and purify Cj0425 to examine its role in the *C. jejuni* periplasm.

2 Chapter 2 Materials and Methods

2.1 *Materials used in this study*

All chemicals used were obtained from BDH, Bibco, Oxoid, Sigma-Aldrich, Acros, Duchefa, Melford, VWR, Apollo Scientific or Thermo-Fisher scientific. Antimicrobial peptides were synthesized by Peptide Synthetics. Gasses were supplied by BOC. Molecular biology reagents were supplied by New England Biolabs, Promega, Roche, Ambion, Bioline, Fermentas or Invitrogen.

2.2 *Organisms used in this study*

All strains used in this study are listed in Tables 3-5, *C. jejuni* was stored at -80°C in Brain Heart Infusion (BHI) broth containing 20% [v/v] glycerol as cryoprotectant. *E. coli*, *S. marcescens* and *P. aeruginosa* strains were preserved at -80°C in Luria-Bertani (LB) broth containing 25% [v/v] glycerol as cryoprotectant.

2.3 *Campylobacter growth Media*

C. jejuni was routinely grown on Columbia blood agar base containing 5% lysed horse blood with 10 µg ml⁻¹ amphotericin-B and vancomycin. *C. jejuni* was also grown on Mueller-Hinton (MH) agar and CCDA agar for colony counts. Liquid cultures of *C. jejuni* were grown in (BHI) or MH broth. Both were made as per manufacturer's instructions and autoclaved for 20 min at 121°C. Amphotericin B and vancomycin were added as standard to 10 µg ml⁻¹. Mueller-Hinton broth was supplemented with 20 mM L-serine prior to autoclaving and is referred to as MHS broth.

2.4 *E. coli, S. marcescens and P. aeruginosa growth Media*

Escherichia coli was grown routinely at 37 °C on LB Agar (Oxoid) which was made according to the manufacturer's instructions and sterilised by autoclaving. Liquid cultures of *E. coli* were grown in LB broth.

2.5 *Antibiotics*

Antibiotics were prepared in distilled water and filter sterilised through 0.2 µm filters except for chloramphenicol which was dissolved in ethanol. Amphotericin B was dissolved in water using a few drops of concentrated NaOH (10 M). Antibiotics were used at the following working concentrations: amphotericin-B 10 µg ml⁻¹, vancomycin 10 µg ml⁻¹,

kanamycin 50 $\mu\text{g ml}^{-1}$, chloramphenicol 20 $\mu\text{g ml}^{-1}$ (40 $\mu\text{g ml}^{-1}$ for *E. coli*), carbenicillin / ampicillin 50 $\mu\text{g ml}^{-1}$ and cefoperazone 32 $\mu\text{g ml}^{-1}$.

2.6 Growth of *C. jejuni*

C. jejuni strains were routinely grown at 37°C in microaerobic conditions (5% [v/v] O₂, 10% [v/v] CO₂ and 85% [v/v] N₂) in a MACS-VA500 Incubator (Don Whitley Scientific Ltd, UK). Typically, cells were plated on blood agar and grown for 1-2 days, cell material was then scraped off and used to inoculate 50-250 ml MH broth media. Cultures were routinely supplemented with 10 $\mu\text{g ml}^{-1}$ amphotericin-B and vancomycin, selective antibiotics such as kanamycin or chloramphenicol were not used for sensitive assays. Liquid cultures were typically incubated overnight and shaken at 200 rpm.

2.6.1 Growth of *C. jejuni* in MCLMAN minimal media

The MCLMAN minimal media was based on work by (Alazzam *et al.*, 2011), the media composition was modified for this study. The final concentration of the individual components is described here:

- CaCl₂.2H₂O 1.8 mM
- Fe(NO₃)₃.9H₂O 25 μM (dissolved in equimolar ascorbate solution)
- MgCl₂.6H₂O 1.75 mM
- KCl 5.4 mM
- NaCl 0.1 M
- NaHCO₃ 44 mM
- NaH₂PO₄ 0.9 mM
- Niacinamide 33 μM
- L-Serine 20 mM
- L-Cysteine 0.2 mM
- L-Methionine 0.2 mM
- L-Leucine 0.8 mM
- L-Aspartic acid 10 mM

The following changes in how the media was produced were also made:

- The Fe(NO₃)₃.9H₂O was dissolved to a 1000X stock solution in equimolar ascorbate to prevent oxidation.
- The salts (MgCl₂.6H₂O, KCl, NaCl, NaHCO₃, NaH₂PO₄) were mixed to at 3X stock solution and adjusted to pH 7.2 with concentrated HCl, the CaCl₂.2H₂O was added after adjustment to prevent precipitation.

All components were mixed together and made up to 75 ml with SDW, the compounds were filter sterilised and equilibrated for 30-60 minutes prior to inoculation.

2.6.2 Growth of *E. coli*, *S. marcescens* and *P. aeruginosa*

All strains were routinely cultured aerobically at 37°C on LB agar or broth. Liquid cultures were shaken at 250 rpm. *S. marcescens* was cultured in liquid MHs broth.

2.7 *Campylobacter* strains used in this study

Table 3

<i>Campylobacter jejuni</i>	Description	Source / Reference
Wild type NCTC11168 (DJK)	Laboratory wild type strain, original human clinical isolate	Parkhill <i>et al.</i> , 2000
Wild type NCTC11168-H	Hypermotile human clinical isolate	Karlyshev <i>et al.</i> , 2002
Wild type 81116	Genetically stable strain	Pearson <i>et al.</i> , 2007
Wild type 81-176	Highly virulent strain with pVir and pTet plasmids	Hofreuter <i>et al.</i> , 2006
$\Delta c8j_0398$	<i>C. jejuni</i> 81116 <i>c8j_0398</i> deletion :: Kan	This Study
$\Delta c8j_0399$	<i>C. jejuni</i> 81116 <i>c8j_0399</i> deletion :: Kan	This Study
$\Delta c8j_0400$	<i>C. jejuni</i> 81116 <i>c8j_0400</i> deletion :: Kan	This Study
$\Delta c8j_0398$-$c8j_0400$ (3X)	<i>C. jejuni</i> 81116 triple gene deletion :: Kan	This Study
$\Delta cj0421c$	<i>C. jejuni</i> 11168-DJK <i>cj0421c</i> deletion :: Kan	This Study
$\Delta cj0421c$ / <i>metK</i>+	<i>C. jejuni</i> 11168-DJK $\Delta cj0421c$ <i>metK</i> complementation :: Kan / Cat	This Study
$\Delta cj0421c$ / <i>metK</i> C+	<i>C. jejuni</i> 11168-DJK $\Delta cj0421c$ C-terminal <i>metK</i> complementation :: Kan / Cat	This Study
$\Delta cj0422c$	<i>C. jejuni</i> 11168-DJK <i>cj0422c</i> deletion :: Cat	This Study
$\Delta cj0422c$ / Nat +	<i>C. jejuni</i> 11168-DJK $\Delta cj0422c$ Natural promoter complementation :: Kan / Cat	This Study
$\Delta cj0421c$-$cj0422c$ (2X)	<i>C. jejuni</i> 11168-DJK double gene deletion :: Kan	This Study
$\Delta cj0423$	<i>C. jejuni</i> 11168-DJK <i>cj0423</i> deletion :: Kan	This Study
$\Delta cj0424$	<i>C. jejuni</i> 11168-DJK <i>cj0424</i> deletion :: Kan	This Study
$\Delta cj0425$	<i>C. jejuni</i> 11168-DJK <i>cj0425</i> deletion :: Kan	This Study
$\Delta cj0423$-$cj0425$ (3X)	<i>C. jejuni</i> 11168-DJK triple gene deletion :: Kan	This Study
$\Delta cj0421c$-$cj0425$ (5X)	<i>C. jejuni</i> 11168-DJK quintuple gene deletion :: Kan	This Study
<i>cj0423</i> <i>fdxA</i>+	<i>C. jejuni</i> 11168-DJK <i>cj0423</i> <i>fdxA</i> complementation :: Kan / Cat	This Study
<i>cj0425</i>-His <i>fdxA</i>+	<i>C. jejuni</i> 11168-DJK His-tagged <i>cj0425</i> <i>fdxA</i> complementation :: Kan / Cat	This Study
<i>lacZ</i>-F-pK46	<i>C. jejuni</i> 11168-DJK <i>cj0423</i> promoter <i>lacZ</i> reporter strain :: Kan	This Study
<i>lacZ</i>-F-pC46	<i>C. jejuni</i> 11168-DJK <i>cj0423</i> promoter <i>lacZ</i> reporter strain :: Cat	This Study
<i>lacZ</i>-R-pC46	<i>C. jejuni</i> 11168-DJK <i>cj0422</i> promoter <i>lacZ</i> reporter strain :: Kan	This Study
$\Delta cj0422c$ <i>lacZ</i>-F-pK46	<i>C. jejuni</i> 11168-DJK $\Delta cj0422c$ deletion containing the <i>lacZ</i> -F-pK46 reporter	This Study

2.8 *E. coli* strains used in this study

Table 4

<i>Escherichia coli</i>	Genotype	Source
DH5 α TM	F- Φ 80 <i>lacZ</i> Δ M15 Δ (<i>lacZ</i> YA- <i>argF</i>) U169 <i>recA1</i> <i>endA1</i> <i>hsdR17</i> (rK-, mK+) <i>phoA</i> <i>supE44</i> λ - <i>thi-1</i> <i>gyrA96</i> <i>relA1</i>	Invitrogen
BL21 (DE3)	F- <i>ompT</i> <i>hsdSB</i> (rB-, mB-) <i>gal dcm</i> (DE3)	Invitrogen

2.9 Other strains used in this study

Table 5

Strain	Genotype	Source
<i>Serratia marcescens</i> DB10	Wild type insect pathogen	Dr Sarah Coulthurst (University of Dundee)
<i>Serratia marcescens</i> Δ <i>tssE</i>	Silent deletion of the <i>tssE</i> gene	Dr Sarah Coulthurst (University of Dundee)
<i>Pseudomonas aeruginosa</i> PA01	Wild type wound isolate	Professor Colin Manoil transposon library (University of Washington)

2.10 DNA manipulation

2.10.1 Isolation and purification of DNA

Genomic DNA was isolated using the GenElute genomic extraction kit, plasmid DNA was extracted using the GenElute miniprep and midiprep kits. DNA was extracted from agarose gels using the GenElute gel extraction kit and purified using the GenElute PCR purification kit. All kits were purchased from Sigma and the manufacturers instruction were followed.

2.10.2 DNA manipulation techniques

Unless otherwise stated all standard DNA manipulation techniques used were based on those described in (Sambrook *et al.*, 1989).

2.10.3 Polymerase chain reaction

Standard PCR reactions were carried out in a final volume of 50 μ l, two types of polymerase were used, Phusion (Thermo) for high fidelity cloning and MyTaq (Bioline) for screening. Each reaction was made up with the following components.

2X Polymerase solution	25 μ l (Phusion)	10 μ l (MyTaq)
100 μ M Primer solutions	2 μ l	1 μ l
Template DNA	1 μ l	1 μ l
dH ₂ O	20 μ l	7 μ l

Conditions were occasionally modified according to requirements. The PCR reactions were performed in a 48 well (Techgene) thermal-cycler using the settings described in (Table 6). All primers were purchased from (Sigma).

Table 6

Stage	Temperature	Duration	Cycles	Description
1	98°C 95°C	5 mins (Phusion) 10 mins (Taq)	1	Initial Denaturation
2	98°C 95°C	10 seconds (Phusion) 10 seconds (Taq)	30-32	Denaturation
	45-55°C 50-60°C	20 seconds (Phusion) 20 seconds (Taq)		Annealing
	72°C 72°C	1 minute kb ⁻¹ (Phusion) 1 minute kb ⁻¹ (Taq)		Extension
3	72°C	5 minutes	1	Final Extension
4	4°C	Hold	1	Final Hold

2.10.4 PCR primers used in this study

Table 7

<i>C. jejuni</i> 81116 knockout primers (5' – 3')	
C8j_0397-KO-F1F	GAGCTCGGTACCCGGGATCCTCTAGAGTCTTAACAAGCCACAACAAACC
C8j_0397-KO-F1R	AAGCTGTCAAACATGAGAACCAAGGAGAATGCCATATCACGCTTGCTCTT
C8j_0397-KO-F2F	GAATTGTTTTAGTACCTAGCCAAGGTGTGCACTATACAAGATGAGATTGC
C8j_0397-KO-F2R	AGAATACTAAGCTTGCATGCCTGCAGGTCTAAAAATGAGTATTAAGCCG
C8j_0398-KO-F1F	GAGCTCGGTACCCGGGATCCTCTAGAGTCAAGGATAGCACAAGTGCTGA
C8j_0398-KO-F1R	AAGCTGTCAAACATGAGAACCAAGGAGAATCAATTTATCGCCAATGCTGA
C8j_0398-KO-F2F	GAATTGTTTTAGTACCTAGCCAAGGTGTGCGGGATAATATATGTTTTGTT
C8j_0398-KO-F2R	AGAATACTAAGCTTGCATGCCTGCAGGTCAAATCGCTCATAAAACCGCT
C8j_0399-KO-F1F	GAGCTCGGTACCCGGGATCCTCTAGAGTCTAGGGCTTATACGCTTGGGA
C8j_0399-KO-F1R	AAGCTGTCAAACATGAGAACCAAGGAGAATCTGCCAAAATTCCAACAAAC
C8j_0399-KO-F2F	GAATTGTTTTAGTACCTAGCCAAGGTGTGCATTCTCGCCCTTACAATGG
C8j_0399-KO-F2R	AGAATACTAAGCTTGCATGCCTGCAGGTCCCACCAAATAATGCCAAT
C8j_0400-KO-F1F	GAGCTCGGTACCCGGGATCCTCTAGAGTCTTTGTTTTGTGGCAAGTGA
C8j_0400-KO-F1R	AAGCTGTCAAACATGAGAACCAAGGAGAATCTATCGATTGCCAACCAACC
C8j_0400-KO-F2F	GAATTGTTTTAGTACCTAGCCAAGGTGTGCGGCATTATTTGGTGGGGAGT
C8j_0400-KO-F2R	AGAATACTAAGCTTGCATGCCTGCAGGTACACATCACCGCATCTTTGA
C8j_0398-400-KO-F1R	AAGCTGTCAAACATGAGAACCAAGGAGAATCAATTTATCGCCAATGCTGA
C8j_0398-400-KO-F2F	GAATTGTTTTAGTACCTAGCCAAGGTGTGCGGCATTATTTGGTGGGGAGT
<i>C. jejuni</i> 11168 knockout primers (5' – 3')	
Cj0421c-KO-F1F	GAGCTCGGTACCCGGGATCCTCTAGAGTCATACTATACTTAATTAATA
Cj0421c-KO-F1R	AAGCTGTCAAACATGAGAACCAAGGAGAATGGATAATACAAGTGCTGAAA
Cj0421c-KO-F2F	GAATTGTTTTAGTACCTAGCCAAGGTGTGCACAAAGTCTAAGAGCAAGAC
Cj0421c-KO-F2R	AGAATACTAAGCTTGCATGCCTGCAGGTCCCTGCGAGTGCTGAATTTAA
Cj0422c-KO-F1F	GAGCTCGGTACCCGGGATCCTCTAGAGTCACCACTTAACAACATCGCAA

Cj0421c-pET28-F (NdeI)	GGAATTCCATATGGACACCTTAACAAAGCTACCCAATG
Cj0421c-pET28-R (XhoI)	ATCCACTCGAGTTAGTCTAAGAGTCTTGCTCTTAGAC
Cj0422c-pET21-F (NheI)	AGGTAAGCGCTAGCATGACAAAAAAGAGCAAGC
Cj0422c-pET21-R (XhoI)	AGTGATTCTCGAGTTTAAATTTAGCAATTCATCT
Cj0422c-pET28-F (NheI)	AGGTAAGCGCTAGCACAAAAAAGAGCAAGCGTGATATGGC
Cj0422c-pET28-R (XhoI)	ATCCACTCGAGTTATTTAAATTTAGCAATTCATCTT
Cj0425-pET22-F (NcoI)	TTAATACCATGGATAACTCATTAGACAAATGT
Cj0425-pET22-R (XhoI)	AATATTCTCGAGTTGGAAATCTCCATTG
RT-PCR primers (5' – 3')	
GyrA-RT-F	ATGCTCTTTCAGTAACCAAAAA
GyrA-RT-R	GGCCGATTCACGCACTTTA
Cj0421c-RT-F	AAAATCAAGCTTTAAATCATCTTGC
Cj0421c-RT-R	TTATCCAATTTTCTTCACTTTCTTG
Cj0422c-RT-F	AGGCTAAATTTTTAAGGTAA
Cj0422c-RT-R	CCATATCACGCTTGCTCTTTT
Cj0423-RT-F	GCCCGCTATTATTGGTTTGA
Cj0423-RT-R	AAAACCTCCCGTAAAAGACCA
Cj0424-RT-F	CGCGGATATGGTGATTTTG
Cj0424-RT-R	TCTAAGGCGCCATTTTCATC
Cj0425-RT-F	TCTTAATGGGGTTTGCCTTG
Cj0425-RT-R	CATTCCATCATGCTTGGCTA
Cj0204-RT-F	TTATCATCAATTCAGCTGTG
Cj0204-RT-R	ATCACTCCAATACCCACACATAA
Cj0653-RT-F	GGGTAGATGGAAGATATTGGCT
Cj0653-RT-R	CAAGCTATATCATCAAGGCTGGAG
Cj0864-RT-F	GCTAGCGCATTAAAGTAAGGTTAAAG
Cj0864-RT-R	TCCATTAACAACAAAAGCAGGG
Isothermal assembly construct primers (5' – 3')	
KO Kanamycin cassette-F	ATTCTCCTTGGTTCTCATGTTTGACAGCTTAT
KO Kanamycin cassette-R	GCACACCTTGGCTAGTACTAAAACAATTC
KO Chloramphenicol cassette-F	ATTCTCCTTGGGAATTCCTCGAGCCC
KO Chloramphenicol cassette-R	GCACACCTTGGACTAGTGGATCCCGG
ISA p46 Kan internal-F	AAGACTCCATTTAAAGATCCGCGGAGC
ISA p46 Kan internal-R	GCTCGCGGGATCTTTAAATGGAGTGTCTT
ISA p46 Cat internal-F	AAAAGTTATACCAACTCTTTTATATGGAG
ISA p46 Cat internal-R	CTCCATATAAAAGAGTTGGGTATAACTTTT
ISA pK46-F	CATGTATTGACAATACTGATAAGATAATATATAATTAATACTGTAGAAA
ISA pK46-R	CATGTGAGACGTTTTAATTTATCTTTAGCAAAAGTAGAAGCATTAGGCGT
ISA pC46-F	CATGGATTGAAAAGTGGATAGATTTATGATATAGTGGATAGATTTATGAT
ISA pC46-R	CATGTGAGACGTTTTAATTTATCTTTAGCAAAAGTAGAAGCATTAGGCGT
ISA p46 MetK-F	TGAGACGTTTTAATTTATCTTTAGCAAAAG
ISA p46 MetK-R	CATGAAAAGTCCCTTCATTTAAAATGAAC
ISA p46 FdxA-F	GTTTTCTCTTTTAAATTAAGATTTAAA
ISA p46 FdxA-R	CATGTGAGACGTTTTAATTTATCTTTAGCAAAAGTAGAAGCATTAGGCGT

2.10.5 Agarose gel electrophoresis

0.8 – 2% agarose gels in TAE buffer (40 mM Tris-acetate pH 8.0, 1 mM EDTA) with added ethidium bromide ($0.1 \mu\text{g ml}^{-1}$) were used to separate and visualise DNA fragments using the 10 Kb hyperladder-1 (Bioline) as a size marker. 6X loading buffer (Bioline) was added to all DNA samples before loading and the samples were separated by electrophoresis using a constant voltage of 100V for varying lengths of time (typically 1 hour).

For extraction of DNA from agarose gels after electrophoresis, the desired bands of DNA were excised with a scalpel and the DNA extracted using the Sigma-Aldrich GenElute gel extraction kit according to the manufacturer's instructions.

2.10.6 Restriction enzyme digestion of DNA

Restriction digestions of PCR products and plasmids were carried out using NEB or Fermentas enzymes according to the manufacturer's instructions based on the concentration of DNA being digested, a typical reaction lasted for 3-4 hours at 37°C using 20-100 units of enzyme. The samples were then separated by agarose gel electrophoresis for analysis or purification using the (Sigma) gel extraction kit.

2.10.7 Ligation of DNA

The concentration of digested plasmid and PCR products was analysed on a Genova Nano Spectrophotometer (Jenway) and the volumes required for an approximate 3:1 ratio of insert : vector was calculated. Appropriate volumes were mixed with 1 μl of T4 DNA ligase (Thermo) and 2 μl of the associated 10X buffer and made up to 20 μl total reaction volume. Reactions were incubated at room temperature for 2-3 hours.

2.10.8 Short fragment sequencing of DNA

DNA samples were sequenced using a drop-off sequencing service (GATC-Biotech). Read lengths were typically 0.8-1.2 Kb in length.

2.11 Isothermal Assembly Cloning

Isothermal assembly (ISA) cloning was used to generate mutant and complementation plasmids for transformation into *C. jejuni*. The method is based on (Gibson *et al.*, 2009). This method allows for multiple overlapping DNA fragments to be incorporated into a vector in a single step without the need for multiple restriction digestion steps. An ISA mastermix was prepared by mixing 40 μl 5 x ISA buffer (25 % polyethylene glycol [PEG-8000], 500 mM Tris-HCl pH 7.5, 50 mM MgCl_2 , 50 mM dithiothreitol [DTT], 1 mM of each dNTP and 5 mM NAD), 0.125

µl T5 exonuclease (Cambio), 2.5 µl Phusion polymerase (NEB) and 20 µl Taq ligase (NEB) (made up to 150 µl with dH₂O). The mastermix was divided into 15 µl aliquots and stored at -20°C.

For *C. jejuni* knockout mutants the ISA reaction was performed using 4 fragments, HincII digested pGEM3Zf(-) vector, the resistance cassette and two flanking regions. The pGEM3Zf(-) vector was linearised with HincII, the kanamycin or chloramphenicol resistance marker was amplified from pJMK30 or pAV35 respectively. Approximately 400 bp of the flanking regions of the gene of interest were amplified (typically removing most of the ORF). The left flanking region for the gene of interest was amplified using primers named F1F and F1R, the right flanking region was amplified by F2F and F2R. All PCR amplifications were performed with Phusion. The F1F and F2R primers contain 30 bp adapters for the pGEM3Sf(-) vector cut with HincII and the F1R and F2F primers contain 30 bp adapters for either the kanamycin or chloramphenicol resistance markers.

For *C. jejuni* complementation and *lacZ* reporter construction the ISA reaction was performed using 3 fragments, the large fragment of a p46 vector, the small fragment of the same p46 vector and the gene of interest. The two vector fragments were amplified by Phusion PCR directly from the plasmid, the two fragments shared a 30 bp overlapping region within either the kanamycin or chloramphenicol resistance marker. The gene of interest for complementation or the *lacZ* gene for the reporter system were amplified by Phusion PCR.

All the PCR products and fragments were purified using the PCR purification kit (Sigma). The ISA mastermix was gently thawed on ice and the DNA fragments were added, typically a 3:1 ratio of each fragment to the vector was used for cloning. The reaction was made up to 20 µl total with SDW. ISA reactions were typically incubated at 50°C for 4 hours and chilled for storage prior to transformation.

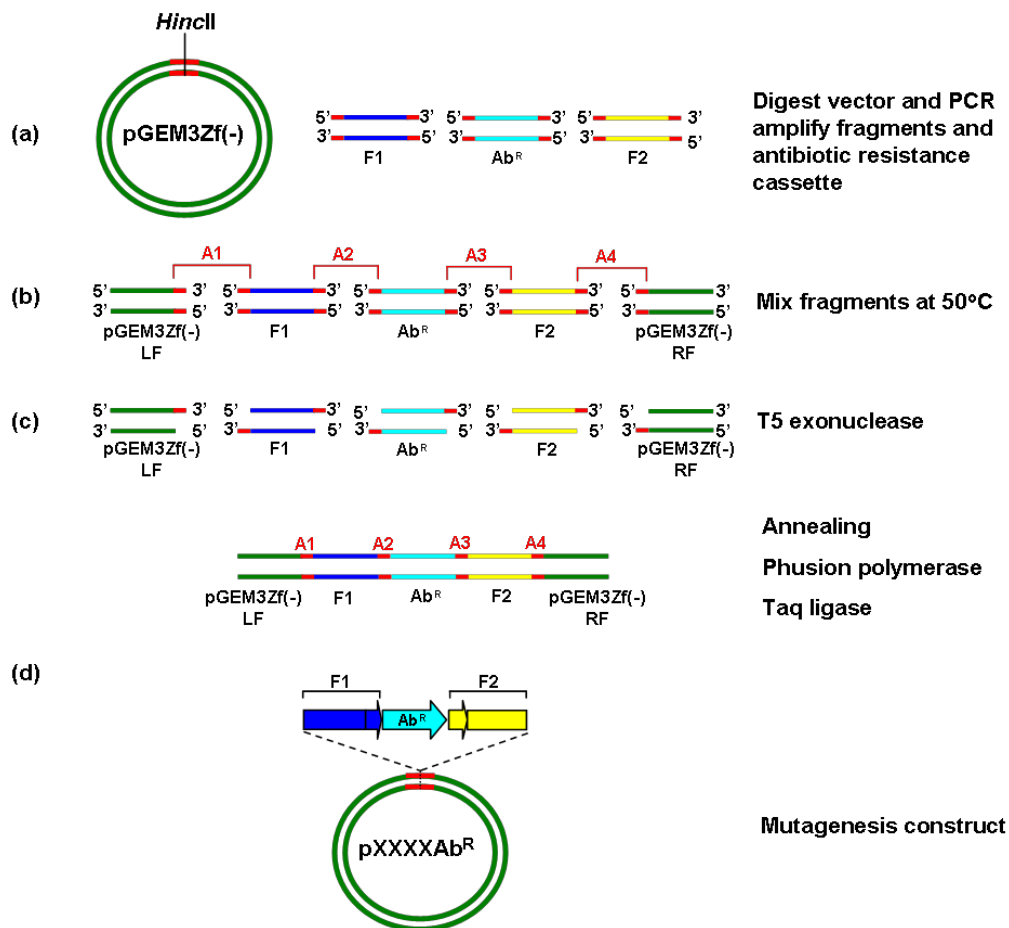


Figure 10: Isothermal assembly (ISA) cloning. (a) pGEM3Zf(-) was digested with *HincII*. The flanking regions F1 and F2 and the resistance marker (Ab^R) were amplified by Phusion PCR. The region highlighted in red are the overlapping adapter regions. (b) The vector and fragments were mixed with the ISA reaction buffer and incubated for 4 hours at 50 °C. (c) The T5 exonuclease removes nucleotides from the 5' end of each DNA fragment, the T5 enzyme is heat labile and will become inactive during the course of the reaction. (d). The homologous adapter regions anneal and the single strand nicks are filled in by Phusion polymerase. The final construct contains the flanking regions of the gene of interest with a resistance marker between them allowing for the gene of interest to be replaced with the resistance marker. Figure adapted from Gibson *et al.*, 2009.

2.12 Preparation of chemically competent *E. coli*

Competent *E. coli* cells for plasmid transformation were produced using methods described by (Hanahan, 1983). *E. coli* was grown in LB broth at 37°C until the OD_{600nm} reached 0.6. Cells were then incubated on ice for 15 min before centrifugation (6000 x g, 20 min, 4 °C). The supernatant was discarded and the cells re-suspended in 50 ml solution RF1 (100 mM KCl, 50mM MnCl₂·4H₂O, 30 mM CH₃COOK, 10 mM CaCl₂·2H₂O, 15% [w/v] glycerol), adjusted to pH 5.8 with 0.2 M acetic acid. Following incubation on ice for 15 min cells were harvested by centrifugation (as above) and re-suspended in 8 ml solution RF2 (10 mM MOPS, 10 mM KCl, 75 mM CaCl₂·2H₂O, 15% [w/v] glycerol) adjusted to pH 6.8 with NaOH. Cells were then incubated for a further 15 min at 4°C before being aliquoted and stored at -80°C.

2.12.1 Transformation of competent *E. coli*

200 µl of competent cells were thawed on ice and 10-20 ng plasmid DNA added. The cells were incubated for 2 minutes on ice then heat shocked at 42 °C for 1 min, then placed on ice for 5 minutes. 1 ml of SOC broth was added to the cells and placed in a 37°C water bath for 1 hr. Cells were then harvested by centrifugation (5,000 x g 5 min), resuspended in 200 µl plain LB broth and plated out onto selective LB agar and left at 37 °C overnight.

2.13 Plasmids used in this study

Table 8

Plasmid	Description	Resistance Marker	Source
pGEM[®] 3Zf(-)	Standard cloning vector used for making mutagenesis constructs. MCS in frame with <i>lac</i> operon to allow blue/white colour selection	Amp	Promega
pJMK30	Cloning vector containing the <i>aphAIII</i> gene encoding kanamycin resistance	Amp Kan	Van Vliet <i>et al.</i> , 1998
pAV35	Cloning vector containing the chloramphenicol acetyl transferase (<i>cat</i>) inserted at <i>Bam</i> HI site	Amp Cat	Van Vliet <i>et al.</i> , 1998
p(K/C)46 (Metk / FdxA)	Group of vectors for complementation of <i>C. jejuni</i> mutants by insertion at the <i>cj0046</i> pseudogene locus	Kan or Cat	Gaskin <i>et al.</i> , 2007
pET21a(+)	Used for over-expression of proteins with C-terminal His-tag under control of IPTG inducible T7 promoter	Amp	Novagen
pET22b(+)	Used for over-expression of proteins with N-terminal <i>peIB</i> signal sequence and C-terminal His-tag under control of IPTG inducible T7 promoter	Amp	Novagen
pET28a(+)	Used for over-expression of proteins with N-terminal His-tag and thrombin cut site under control of IPTG inducible T7 promoter	Kan	Novagen
pGEM-c8j_0397	pGEM3Zf(-) containing the flanking regions of <i>c8j_0397</i> around a Kan cassette	Amp Kan	This study
pGEM-c8j_0398	pGEM3Zf(-) containing the flanking regions of <i>c8j_0398</i> around a Kan cassette	Amp Kan	This study
pGEM-c8j_0399	pGEM3Zf(-) containing the flanking regions of <i>c8j_0399</i> around a Kan cassette	Amp Kan	This study

pGEM-c8j_0400	pGEM3Zf(-) containing the flanking regions of <i>c8j_0400</i> around a Kan cassette	Amp Kan	This study
pGEM-c8j_0398-400	pGEM3Zf(-) containing the flanking regions of <i>c8j_0398-400</i> around a Kan cassette	Amp Kan	This study
pGEM-cj0421c	pGEM3Zf(-) containing the flanking regions of <i>cj0421c</i> around a Kan cassette	Amp Kan	This study
pGEM-cj0422c	pGEM3Zf(-) containing the flanking regions of <i>cj0422c</i> around a Cat cassette	Amp Cat	This study
pGEM-cj0421c-422c	pGEM3Zf(-) containing the flanking regions of <i>cj0421c-422c</i> around a Kan cassette	Amp Kan	This study
pGEM-cj0423	pGEM3Zf(-) containing the flanking regions of <i>cj0423</i> around a Kan cassette	Amp Kan	Halal Al-Haideri
pGEM-cj0424	pGEM3Zf(-) containing the flanking regions of <i>cj0424</i> around a Kan cassette	Amp Kan	Halal Al-Haideri
pGEM-cj0425	pGEM3Zf(-) containing the flanking regions of <i>cj0425</i> around a Kan cassette	Amp Kan	Halal Al-Haideri
pGEM-cj0423-425	pGEM3Zf(-) containing the flanking regions of <i>cj0423-425</i> around a Kan cassette	Amp Kan	This study
pGEM-cj0421c-425	pGEM3Zf(-) containing the flanking regions of <i>cj0421c-425</i> around a Kan cassette	Amp Kan	This study
pCMetK46-Cj0421c	pCMetK46 with the <i>cj0421c</i> ORF under the <i>metK</i> promoter	Cat	This study
pCMetK46-Cj0421c-C	pCMetK46 with the cytoplasmic domain of <i>cj0421c</i> under the <i>metK</i> promoter	Cat	This study
pK46-Cj0422c	pK46 with the <i>cj0422c</i> ORF under the natural promoter	Kan	This study
pCFdxA46-Cj0423	pCFdxA46 with the <i>cj0423</i> ORF under the <i>fdxA</i> promoter	Cat	This study
pCFdxA46-Cj0425His	pCFdxA46 with the <i>cj0425</i> ORF under the <i>fdxA</i> promoter with a C-terminal 6His tag	Cat	This study
pK46-LacZ-F	pK46 with the <i>lacZ</i> gene under the <i>cj0423</i> promoter	Kan	This study
pC46-LacZ-F	pC46 with the <i>lacZ</i> gene under the <i>cj0423</i> promoter	Cat	This study
pC46-LacZ-R	pC46 with the <i>lacZ</i> gene under the <i>cj0422c</i> promoter	Cat	This study
pET28-Cj0421c	pET28a(+) with the cytoplasmic domain of <i>cj0421c</i> , with a N-terminal His tag	Kan	This study
pET21-Cj0422c	pET21a(+) with the cytoplasmic domain of	Amp	Dr Ed Guccione

	<i>cj0421c</i> , with a C-terminal His tag		
pET28-Cj0422c	pET28a(+) with the <i>cj0422c</i> ORF, with a N-terminal His tag	Kan	This study
pET22-Cj0425	pET22b(+) with the <i>cj0425</i> ORF, with the native signal sequence replaced with the <i>peIB</i> signal sequence and with a C-terminal His tag	Amp	Halal Al-Haideri

2.14 Preparation of chemically competent *C. jejuni*

C. jejuni was grown on blood agar overnight, scrapped off and re-suspended in 1 ml BHI broth. The cells were centrifuged (15,000 x g, 5 minutes, 4°C) and re-suspended in 1ml chilled wash buffer (9% sucrose w/v, 15% glycerol v/v in SDW). This was repeated two more times and the cells re-suspended in 300 µl chilled wash buffer. The cells were then separated into 150 µl aliquots and stored at -80°C.

2.14.1 Transformation of competent *C. jejuni*

150 µl of competent *C. jejuni* was thawed on ice and mixed with 200-500 ng plasmid DNA, the mixture was incubated on ice for 15 minutes and transferred to a pre-chilled electroporation cuvette (VWR). The cells were electroporated with a pulse of 25 F, 2.5 kV and 200 Ω, giving time constants for 4 – 5 ms in a Gene pulsar chamber (Biorad). 150 µl of BHI broth was added and the cells were plated onto 2 non selective blood agar plates and grown for 24 hours. The cell material was harvested and plated onto 4 selective blood agar plates and grown for 2-5 days until individual colonies formed. The colonies were re-plated onto selective blood agar and screened by PCR. The procedure was scaled up as necessary.

2.15 Whole cell RNA extraction and purification

Typically, *C. jejuni* was grown in triplicate in MHS broth culture to a mid-log phase OD_{600nm} (0.5-0.6) under standard conditions unless otherwise stated. RNA was extracted directly from the cultures using the 'SV total RNA isolation system' (Promega) as recommended by the supplier. The only modification was the use of a 1 mg ml⁻¹ lysozyme solution instead of the recommended 0.3 mg ml⁻¹. Purified RNA samples were DNase treated using the 'Turbo-DNA Free' kit (Ambion) to remove any contaminating DNA according to the manufacturer's instructions. The RNA concentration and purity were determined by using a 'Genova nano micro-volume spectrophotometer' (Jenway). The treated RNA samples were matched to 10 ng µl⁻¹ in nuclease-free water and stored at -80°C. The RNA samples were checked for

contaminating DNA by performing a PCR reaction without any reverse transcriptase. All water used for RT-PCR is DEPC treated nuclease free water (Thermo).

2.15.1 Real time quantitative reverse transcriptase PCR

qRT-PCR gene specific primers (Table 7), were designed to amplify a 100-300 bp fragment within the gene of interest, with the *C. jejuni gyrA* gene being used as a reference. RT-PCR primers were checked for specificity prior to use by performing a standard PCR reaction. The primers were diluted to 25 μ M in nuclease free water prior to use. Each qRT-PCR reaction was carried out in a 20 μ l volume in a MicroAmp[®] 96-well optical reaction plate (ABI prism). Reactions were performed using the Sensifast SYBR Lo-ROX one step kit (Bioline, UK). Each reaction contained 10 μ l Sensifast SYBR 2x buffer, 0.2 μ l of each primer, 0.2 μ l reverse transcriptase, 0.4 μ l RNase inhibitor, 2 μ l of matched RNA or DNA template and 7 μ l nuclease free water. Each reaction using RNA was repeated in triplicate; reactions using genomic DNA for the standard curve were replicated in duplicate. Some reactions were performed using the Sensifast SYBR Hi-ROX one step kit. All other components remained the same. PCR amplification was carried out in a Stratagene MX3005p thermal cycler (Agilent) at 45°C for 10 min; 95°C for 2 min followed by 40 cycles of 95°C for 20 s; 55°C for 30s and 72°C for 20s. Data was collected with the associated MxPRO QPCR software (Agilent). A standard curve for each gene was generated using a series of *C. jejuni* genomic DNA dilutions. The relative expression levels of the target genes were calculated following the standard curve protocol described in the *User Bulletin #2 (ABI Prism 7700 Sequence Detection System, Subject: Relative Quantification of Gene Expression)* provided by Applied Biosystems. Gene expression was calculated as relative to *gyrA* expression. No-template controls were included for each primer set being used.

2.16 Preparation of *C. jejuni* cell free extracts

1 litre of *C. jejuni* was grown overnight in 4X 250 ml MHS broth cultures under standard conditions. Cells were harvested by centrifugation (8,000 x g, 5 minutes) and re-suspended in 100 ml 10 mM Tris-HCl pH 7.4, 500 mM NaCl. The cells were lysed using a French press (SIM Aminco). The resulting cell free extract was stored at 4°C prior to use or at -20°C for long term storage.

2.17 *C. jejuni* growth curves

C. jejuni strains were grown overnight on blood agar plates with selective antibiotics. Cell material was harvested by centrifugation (10,000 x g, 5 minutes) and re-suspended in sterile

saline water. Pre-equilibrated MHS broth (without selective antibiotics) was distributed into 6-well plates (Greiner) and the media inoculated to a starting OD_{600nm} of 0.05. OD_{600nm} readings were taken at 0, 2, 4, 6, 8 and 24 hours to generate a growth curve.

2.18 Antimicrobial disc diffusion assay

100 ml cultures of *C. jejuni* were grown to an OD_{600nm} of 1.0. Individual 50 ml aliquots of MH agar were cooled to 40°C in a water bath and 10 ml of the cell culture was added to each. The agar-cell culture mixture was poured into individual petri dishes and allowed to set. Using sterilized forceps, the antibiotic discs (Mast Diagnostics, disc number M14) were placed onto the agar and gently pressed down to ensure complete contact. The plates were incubated under standard conditions for 24 hours and the zones of inhibition measured in millimeters.

2.19 Antimicrobial sensitivity microtiter assay

C. jejuni starter cultures were cultured overnight in standard conditions. The cells were diluted to an OD_{600nm} of 0.6 in fresh MHS broth (without selective antibiotics) and briefly incubated. Sterile 200 µl, 96 well microtitre plates (Greiner) were prepared for the assays by adding 100 µl of MHS broth into the wells in row A and mixing 160 µl of MHS broth with 20 µl of the appropriate antimicrobial dilution into the wells in row B. 180 µl of MHS broth was added to all remaining wells in rows C-H and the plates equilibrated for 30 minutes under standard conditions. Typically, the plates contain 12 wells per row and these are divided into 4 sets of 3 replicates. The 4 sets were used for the different antimicrobial concentrations with the first set being used as the negative control which contained only SDW. To start the assay 100 µl of the diluted *C. jejuni* culture was added to the 100 µl MHS broth in the wells in row A. 20 µl of these cultures were diluted 1:10 into the wells in row B containing the antimicrobial compound. The dilutions were performed using a 12-channel pipette. The plates were incubated for typically 2 or 4 hours, depending on the antimicrobial, under standard conditions. Following the incubation the cultures were serially diluted down the 96 well plate using a multichannel pipette at 1:10 dilutions (20 µl : 200 µl). 10 µl was transferred from each well to CCDA agar plates, using an 8-channel pipette, to perform colony counts. The plates were incubated for 2 days and the colonies counted. The CFU ml⁻¹ was calculated in Microsoft excel and the data expressed in Graphpad prism.

2.20 LacZ expression (Miller) assays

To measure the expression of the lacZ protein from broth cultures of *C. jejuni* reporter strains the OD_{600nm} was measured for each reading and 100 µl of culture was added to a 1 ml

Eppendorf tube containing 780 μl of Z-buffer (60 mM Na_2HPO_4 , 40 mM NaH_2PO_4 , 10 mM KCl, 1 mM MgSO_4 , pH7), 2.7 μl β -mercaptoethanol, 20 μl chloroform and 10 μl 0.1% [w/v] SDS. The mixture was briefly shaken and incubated at room temperature for 5 minutes. The reaction was started by adding 200 μl ONPG solution (ortho-Nitrophenyl- β -galactoside, 4 mg ml^{-1}) and the tubes incubated at 30°C for 1 hour (this was altered depending on the speed of the reaction). The reaction was stopped by adding 500 μl of 1 M Na_2CO_3 solution. The tubes were centrifuged (10,000 x g for 10 minutes) to pellet cell debris and 1 ml of the mixture was transferred to a cuvette for the OD420_{nm} reading. The relative expression of the LacZ protein is expressed in Miller units (Simons *et al.*, 1983) where the expression is calculated as relative to the cell density. The equation used is as follows:

$$M = 1000 \times \text{Abs}_{420\text{nm}} / (T \times V \times \text{Abs}_{600\text{nm}})$$

M – Relative expression (Miller units)

T – Time (minutes)

V – Volume (milliliters)

Abs420_{nm} – Absorption at 420_{nm}

Abs600_{nm} – Absorption at 600_{nm}

2.20.1 96 well Biolog phenotype microarray Miller assay

For high throughput screening of the LacZ reporter construct using the phenotype microarray system, the Miller assay was adapted for use in a 96 well plate format. Broth cultures of *C. jejuni* were grown under standard conditions to an OD600_{nm} of 0.6. 75 ml of the MCLMAN minimal media (Section 2.6.1) was prepared and equilibrated under standard conditions. Cells from the MHS broth culture were harvested by centrifugation (5,000 x g, 5 minutes, 37°C) and used to inoculate the MCLMAN culture to a starting OD600_{nm} of 0.5. The cultures were incubated for 1 hour and the OD600_{nm} measured to ensure the culture was growing. 100 μl of the culture was transferred to the 96 well phenotype microarray plates and the plates were incubated for 4 hours under standard conditions with gentle shaking.

During the incubation the 96 well Miller assay was prepared, the volumes and concentrations used for the Miller assay in a 96 well format are exactly half those described in (Section 2.20). The final step involving Na_2CO_3 uses 200 μl of 1.25 M instead of 250 μl of 1 M. The Z-buffer, β -mercaptoethanol, chloroform and SDS solutions were mixed together in 1 ml volume 96 well plates (Greiner) with each well corresponding to the same well from the Biolog phenotype microarray plates. The OD600_{nm} of the wells from the biolog phenotype microarray plates

were measured and 50 μ l of the culture from each of the 96 wells was added to the corresponding wells in the 1 ml 96 well plates. The reaction was started by adding 100 μ l ONPG solution and the plates incubated for 2 hours at 30°C. 200 μ l of 1.25 M Na₂CO₃ was added to each well to stop the reaction and the plates were centrifuged at 3,000 x g for 10 minutes to pellet the cell debris. 200 μ l of the solution from each well was transferred to a fresh 200 μ l flat bottomed 96 well plate and the OD_{420nm} measured. The absorptions at 600 and 420_{nm} were measured on a FLOUstar omega 96-well plate reader (BMG Labtech). The relative expression in Miller units for each well was calculated as described in (Section 2.20).

2.21 Type VI secretion competition assays with *S. marcescens*

C. jejuni strains were grown on blood agar plates overnight and *S. marcescens* strains were grown on LB agar plates overnight under standard conditions. 6 ml cultures of MHS broth were prepared in 6-well plates (Greiner) and equilibrated. Both the *C. jejuni* and *S. marcescens* strains were harvested from the agar plates and used to inoculate the 6 ml cultures to a starting OD_{600nm} of 0.5, the cultures were briefly incubated with gentle shaking. The *C. jejuni* and *S. marcescens* cultures were mixed together in duplicate in 1 ml Eppendorf tubes at a 50:1 ratio respectively (20 μ l added to 980 μ l). 25 μ l of these mixtures were spotted onto MH agar plates in duplicate and allowed to dry, the plates were inverted and incubated under standard *C. jejuni* growth conditions for exactly 24 hours. For each individual spot a single Eppendorf tube was prepared with pre-equilibrated PBS buffer (Sigma). The spot was scraped off the MH plates and transferred to the PBS using a sterile plastic loop. The cell suspensions were serially diluted down a 200 μ l 96 well plate using 1:10 dilutions in 180 μ l volumes of pre warmed PBS and 10 μ l samples were transferred to mCCDA agar plates (containing Amphotericin-B and Cefoperazone at 10 and 32 μ g ml⁻¹ respectively final concentration). The plates were incubated under standard *C. jejuni* conditions (except at 42°C) for 2 days and the colonies counted. The procedure was repeated using LB agar plates under aerobic conditions at 37°C for counting *S. marcescens* colonies. The CFU ml⁻¹ for both *C. jejuni* and *S. marcescens* was calculated from the serially diluted colonies using Microsoft excel and the data presented in Graphpad prism.

2.22 *C. jejuni* membrane rigidity assays

The method for measuring the rigidity of the *C. jejuni* membrane is adapted from work by (Wu *et al.*, 2015). The method uses a hydrophobic fluorescent dye 1, 6-diphenyl-1, 3, 5-hexatriene (DPH) that inserts into the membrane. *C. jejuni* strains were cultured in MHS broth under standard conditions and the assay was performed on both mid log phase cells and overnight cultures. 50 ml of *C. jejuni* cells were harvested by centrifugation (8,000 x g, 5 minutes, 37°C),

the cells were washed twice with pre-warmed PBS (Sigma) and diluted in PBS to an OD_{600nm} of 0.2 in 40 ml. DPH (7.5 mM stock solution in DMF) was added to the cells to a final concentration of 7.5 μM. The cells were incubated with gentle shaking for 30 minutes at 37°C. The cells were re-harvested by centrifugation and washed twice with PBS to wash away any non-incorporated DPH. The cells were re-suspended in PBS to an OD_{600nm} of 0.2.

The fluorescence readings were measured using a Cary Eclipse fluorimeter (Varian Ltd, UK) using a 3 ml quartz cuvette and a manual accessory polarizer (Varian). The excitation wavelength was 358 nm with a 10 nm slit, the emission wavelength was 428 nm with a 10 nm slit. The machine voltage was set to high. The fluorescence values were measured at V-V, V-H, H-H and H-V, where V is vertical and H is horizontal polarization of the excitation and emission respectively. The cuvette was maintained at 37°C at all times during the assay. Measurements were taken for 30 seconds for each polarization set and the average of the middle 20 seconds was used as the fluorescence value. The polarization value for the membrane-bound DPH was calculated using the following equation:

$$P = (I_{vv} - GI_{vh}) / (I_{vv} + GI_{vh})$$

Where

P – Polarization value (must be <0.5)

G – Correction factor (I_{hv}/I_{hh})

I – Fluorescence intensity

h – Horizontal polarization

v – Vertical polarization

2.23 Outer membrane permeability nitrocefin assay

Nitrocefin is a chromogenic cephalosporin that can be hydrolysed by periplasmic beta-lactamase. The rate of hydrolysis can be used as an indicator of membrane permeability after osmotic shock treatment. 20 ml *C. jejuni* cultures were grown overnight and matched to an OD_{600nm} of 0.5 under standard conditions and harvested by centrifugation (10,000 x g, 5 minutes). The cell pellets were re-suspended in osmotic shock buffer (10 mM Tris-HCl, pH 8, 8% [w/v] sucrose and 0.4% [w/v] EDTA) and incubated with gentle shaking for 5 minutes at room temperature. The pellets were re-harvested by centrifugation and re-suspended in 800 μl chilled 20 mM sodium phosphate buffer pH 7.5. The cells were incubated at 4°C with gentle shaking for 5 minutes and the soluble periplasmic extracts separated by centrifugation (15,000 x g, 10 minutes, 4°C). The supernatant was removed and kept on ice. For the assay a 1 ml

quartz cuvette containing 5 µg of nitrocefin (Sigma) in 900 µl 20 mM sodium phosphate pH 7.5, was checked for to ensure there was no background rate and 100 µl of the periplasmic extract added to start the reaction. The change in Abs_{495nm} was measured over 2 minutes using a Shimadzu UV-2401PC recording spectrophotometer, the rate of reaction calculated in Microsoft excel.

2.24 Outer membrane permeability lysozyme assay

Lysozyme is a glycoside hydrolase which degrades microbial peptidoglycan, Gram-negative bacteria are typically resistant to lysozyme due to the outer membrane. If the outer membrane is compromised Gram-negative bacteria become more sensitive to lysozyme. The rate of cell lysis due to lysozyme can be measured by the decrease in the Abs OD_{600nm} of a cell suspension. Overnight cultures of *C. jejuni* grown under standard conditions were matched to an OD_{600nm} of 0.5 in 20 mM sodium phosphate buffer pH 7.5 with 5 mM sodium azide. Lysozyme (Sigma) was prepared in fresh aliquots of 1 mg ml⁻¹ in 20 mM sodium phosphate buffer. Lysozyme was added to a final concentration of 50 µg ml⁻¹ in a 1 ml cuvette in with 870 µl of cell suspension. The background rate of OD_{600nm} was measured for 20 seconds and a stressor compound such as sodium deoxyholate or buffer as a negative control was added and the decrease in OD_{600nm} measured over 2 minutes using a Shimadzu UV-2401PC recording spectrophotometer, the rate of reaction calculated in Microsoft excel.

2.25 Protein manipulations

2.25.1 Protein concentration determination

Soluble (cell-free) protein concentration was determined using a Bio-Rad Protein Assay Kit according to the manufacturer's instructions. For approximate determination of soluble protein concentration, the method was adapted as follows: 1-5 µl of protein solution was added to a 1 ml cuvette containing 0.8 ml of SDW and 0.2 ml Bio-Rad Dye Reagent Concentrate. The cuvette was mixed by inversion and absorbance measured at 595 nm. The approximate protein concentration (mg ml⁻¹) was calculated using the following formula: (OD₅₉₅ x 15)/volume of protein (µl). For more accurate determination of soluble protein from whole cell free extracts, the Bio-Rad reagent was used in a 96-well plate format and compared to a standard BSA curve.

For accurate determination of pure protein concentration by spectroscopy, the protein was diluted into 1 ml of buffer and the absorption at 280 and 320_{nm} measured using a Shimadzu

UV-2401PC recording spectrophotometer. The concentration of pure protein was calculated using the following equation:

$$M = \text{Abs}_{280\text{nm}} - \text{Abs}_{320\text{nm}} / \epsilon$$

Where:

M – Molar concentration

E – Extinction coefficient

The extinction coefficient for each protein was calculated from the complete amino acid sequence using the ExPasy ProtParam service (<http://web.expasy.org/protparam/>).

2.25.2 SDS poly acrylamide gel electrophoresis

SDS-PAGE was performed using the Mini-Protean Tetra system (Bio-Rad), 12% resolving gels were prepared (30% [w/v] acrylamide with 0.8% [w/v] bis-acrylamide was diluted in 1 M Tris-HCl pH 8.8, 10% [w/v] SDS and dH₂O to create a 375 mM Tris-HCl pH 8.8, 0.1 % [w/v] SDS, 12.5% acrylamide mixture). Addition of 0.1% [w/v] ammonium persulphate (APS) and 0.01% N,N,N',N'-Tetramethylethylenediamine (TEMED) initiated polymerisation. The components were mixed by gentle swirling and pipetted into assembled gel casts. 100% Ethanol was added to the top of the mixture to ensure an even spread, this was removed by filter paper and gentle rinsing prior to the addition of the stacking gel. 5% stacking gels were prepared (30% [w/v] acrylamide with 0.8% [w/v] bis-acrylamide was diluted in 1 M Tris-HCl pH 6.8, 10% [w/v] SDS and dH₂O to create a 125 mM Tris-HCl pH 6.8, 0.1% [w/v] SDS. 6% acrylamide mixture). Polymerisation was initiated as described above and the mixture poured on top of the resolving gel with a loading comb which was removed upon polymerization. Protein samples were boiled for 5 minutes in equal volumes of sample buffer (60 mM Tris-HCl pH 6.8, 2% [w/v] SDS, 0.05% [w/v] bromophenol blue, 5% [v/v] β-mercaptoethanol, 10 % [w/v] glycerol. Samples were loaded into the gel with the prestained EZ-Run protein ladder (Fisher). The gel was loaded into a gel tank containing 1X running buffer (25 mM Tris, 250 mM glycine, 0.1% [w/v] SDS). The samples were separated by electrophoresis at 180V until the tracking dye had reached the bottom of the gel. Gels were stained with coomassie brilliant blue (50 % [(v) methanol, 10 % [v/v] glacial acetic acid, 0.1 % [w/v] coomassie brilliant blue (Sigma-Aldrich)) and de-stained (50 % [v/v] methanol, 10 % [v/v] glacial acetic acid) until individual bands were visible.

2.25.2.1 Silver staining

SDS-PAGE gels were silver stained for increased sensitivity, silver staining was performed using the PlusOne™ Silver Stainink Kit (GE Healthcare) according to the manufacturer's instructions.

2.25.2.2 SDS-PAGE tricine gels

SDS-PAGE Tricine gels were prepared in the same way as described in (Section 2.25.2) with the following exceptions. The acrylamide concentration was made up to 16% for the resolving gel and 6% for the stacking gel using the same gel buffer at pH 8.45. For the electrophoresis separate anode (0.1 M Tris-HCl pH 8.9) and cathode (0.1 M Tris-HCl, 0.1 M Tricine, 0.1 % [w/v] SDS, pH 8.25) buffers were used. All other steps were the same as for standard SDS-PAGE gels.

2.25.3 Preparation of C. jejuni cell free extracts for western blotting

Overnight cultures of *C. jejuni* cells were harvested by centrifugation at 8,000 x g for 10 minutes at 4°C and re-suspended in 10 mM Tris-HCl pH 8. The cells were sonicated for 4 x 15 second pulses at a frequency of 16 amplitude microns using a Soniprep 150 ultrasonic disintegrator (SANYO). The cell debris was removed by centrifugation at 15,000 x g for 30 minutes at 4°C. The remaining supernatant was stored at -20°C.

2.25.4 Western blotting for detection of Cj0424 from C. jejuni cell free extracts

Cell free extracts were separated by SDS-PAGE, the transfer of proteins was carried out using a Mini Trans-Blot Electrophoretic Cell (Bio-Rad) according to manufacturer's instructions. The protein samples were transferred to a nitrocellulose membrane (Hybond-C Extra, Amersham Biosciences) at a constant voltage of 100 V for 90 min at 4 °C in ice cold transfer buffer (25 mM Tris, 190 mM glycine, 20 % [v/v] methanol). All immuno-detection steps were carried out at room temperature with constant agitation. TBS-T20 buffer (25 mM Tris-HCl pH 7.4, 137 mM NaCl, 2.7 mM KCl, 0.1 % Tween 20) was used as both a base for blocking agent (5 % dried skimmed-milk powder, incubated overnight) and for washing (15 minutes and 2 x 5 minutes). Polyclonal antibodies for the Cj0424 protein was raised from rats and provided by Halah Al-Haideri. This was diluted 1:20,000 and applied to the membrane for 1 hour. The membrane was then washed 3 times with TBS-T20. The secondary antibody (peroxidase linked goat anti-rat IgG (Sigma) was diluted (1:2000) in TBS-T and applied to the membrane for 1 hr. After washing in TBS-T 4 times, antibody binding was visualised by means of enhanced chemiluminescence (ECL Kit, GE Healthcare), according to manufacturer's instructions.

2.26 Protein purification procedures

Three individual proteins were purified during the course of this work, the exact concentrations of the buffers used for each purification step are detailed in the results chapters.

2.26.1 Overexpression of recombinant protein in *E. coli* BL21 (DE3)

All protein overexpressions were performed using the T7 promoter in the pET vector system in *E. coli* BL21 (DE3) as the expression strain. Cultures were grown in LB broth with selective antibiotics to an OD_{600nm} of 0.6 and induced with isopropyl-β-D-thiogalactopyranoside (IPTG). The concentration of IPTG used and the incubation times and temperatures are detailed in the results chapters for each individual protein. Cells were harvested by centrifugation (8,000 x g, 5 minutes, 4°C) and stored at -80°C before use.

2.26.2 Overexpression of selenomethionine incorporated protein

For production of selenomethionine incorporated protein the *E. coli* BL21 (DE3) overexpression strain was grown in 1 L volumes of M9 minimal media containing 6.78 g Na₂HPO₄, 3 g KH₂PO₄, 0.5 g NaCl, 1 g NH₄Cl and 5 ml glycerol, the total volume was made up to 950 ml with SDW. The media was autoclaved and allowed to cool prior to the addition of the following components from 0.2 μm filter sterilised stock solutions to final concentrations of: 50 mg l⁻¹ carbenicillin, 0.1 mM CaCl₂, 2 mM MgSO₄, 2 mg l⁻¹ thiamine hydrochloride, 40 mg/l L-selenomethionine and 100 mg l⁻¹ of each of L-lysine, L-threonine, L-phenylalanine, L-isoleucine, L-valine and L-leucine. The culture was grown under standard conditions till the cells reached an OD_{600nm} of 0.6 and IPTG was added. As with standard protein overexpression the exact IPTG concentrations, length and temperature of the induction is explained in the results chapters. The cells were harvested in the same way for standard protein expression.

2.26.3 Preparation of *E. coli* cell free extracts

The cell pellets from protein overexpression samples were thawed gently on ice and re-suspended in buffer solution, typically 20 mM sodium phosphate buffer with 500 mM NaCl was used (the individual buffers used are described for each protein in the results chapters). 5 mg DNase I (Sigma) was added to the cell suspension to remove DNA and the soluble protein extracted using a French press (SIM Aminco) according to the manufacturer's instructions. The extracts were centrifuged (40,000 x g, 30 minutes, 4°C) and the soluble fraction was filtered through a 0.45 μm filter prior to protein purification.

2.26.4 Nickel affinity chromatography

The cell extracts were fractionated on a HisTrapTM HP 5 ml column (GE Healthcare) connected to an Akta Prime purification system (GE healthcare) by affinity chromatography. The proteins were bound to the column in individual buffers containing 0.5M NaCl and 20mM imidazole and

eluted from the resin by a linear gradient from 20-500mM imidazole in the same buffer. Fractions containing eluted protein were pooled and kept on ice.

2.26.5 Ion exchange chromatography

Pooled elutions from His trap purification containing the protein of interest were de-salted using PD10 de-salting columns (GE healthcare) according to the manufacturers instructions. The fractions containing protein were pooled and loaded onto a HiTrap™ Phenyl HP column (GE healthcare) and eluted with a gradient of 0-1 M NaCl in the same buffer over 10 column volumes.

2.26.6 Hydrophobic interaction chromatography

Pooled elutions from His trap purification containing the protein of interest were mixed with $(\text{NH}_4)_2\text{SO}_4$ to a final concentration of 1.5 M. The protein solution was loaded onto a HiTrap™ HIC column (GE healthcare) and eluted with a gradient of 1-0 M $(\text{NH}_4)_2\text{SO}_4$ in the same buffer over 10 column volumes.

2.26.7 Gel filtration chromatography

The pooled protein was concentrated to less than 5 ml using vivaspin concentration columns (GE healthcare) with a molecular weight cutoff (MWCO) of less than half the protein of interest. The protein was loaded onto a HiLoad Superdex 200 gel filtration column (GE healthcare) according to the manufacturer's instructions. The protein was eluted into whichever buffer was desired for final purification.

All elutions were checked for purity by SDS-PAGE analysis and the final protein concentration determined by spectroscopic analysis.

2.26.8 Protein dialysis

Pooled protein fractions were dialysed to remove imidazole and other contaminants using benzoylated dialysis tubing with a MWCO less than half the protein of interest (Sigma). Typically, dialysis was performed for 1 hour, the buffer was replaced and the sample was dialysed overnight, the buffer replaced again with sterilised buffer and the protein dialysed for 2 hours. All dialysis steps were performed at 4°C unless otherwise stated.

2.27 Recombinant Cj0425 pull down assays

2.5 L of *C. jejuni* cells were cultured under standard conditions overnight. The cells were harvested by centrifugation (8,000 x g, 5 minutes, 4°C) and the soluble protein extracted as described in (2.26.3). The proteins were extracted into loading buffer (20 mM sodium phosphate buffer at pH 7.4 with 100 mM NaCl). *C. jejuni* soluble cell free extracts were loaded onto a HisTrap column and the column was washed with 5 column volumes (CVs) loading buffer and the pooled fractions collected. The column was then washed with 5 CVs of binding buffer (loading buffer with 20 mM Imidazole) and the fractions collected. The column was then washed with 5 CVs of elution buffer (loading buffer with 300 mM imidazole) and the fractions collected. The column was re-equilibrated with loading buffer and purified Cj0425 was loaded onto the column. The column was then washed with 5 CVs of loading, binding and elution buffer and the fractions pooled together. Samples from all the wash steps were analysed by SDS-PAGE.

2.28 Thermal shift analysis of Cj0421c

All thermal shift (thermofluor) screens were performed using an Mx3005P qRT-PCR machine (Stratagene) and the data collected with the associated mxpro software (Stratagene). Each 50 µl well contained 50 µM purified Cj0421c in 20 mM sodium phosphate buffer with 500 mM NaCl pH7.4 and 5 µl of the 10X SYPRO orange dye (Invitrogen), the potential ligand of interest was added to whichever concentration was required and the difference made up with buffer. The SYPRO dye was stored in darkness and was added last. The assays were performed in a MicroAmp® 96-well optical reaction plate (ABI prism) over a temperature gradient of 25-95°C, with the fluorescence measured at each degree increase. The fluorescence was measured using the same settings for the measurement of SYBR green for qRT-PCR reactions. The thermofluor reaction is described in (Niesen *et al.*, 2007). The data was analysed in Microsoft excel using publicly available analysis packages available at (<ftp://ftp.sgc.ox.ac.uk/pub/biophysics>). The graphs were generated in Graphpad prism.

2.29 DTNB thiol assay

To measure the concentration of free thiol groups the compound 5,5'-Dithiobis(2-nitrobenzoic acid (DTNB) also known as Ellman's reagent was used to determine the number of free thiol groups in a protein solution, thereby acting as an indicator of disulfide bond formation in purified proteins. A 10 mM stock solution of DTNB (dissolved in DMSO) was diluted to 100 µM in whichever buffer the protein of interest is stored in. 50 µl of the sample was added to 950 µl of the DTNB solution and the absorption at 412_{nm} measured after a brief incubation at room

temperature. A standard curve was generated using acetyl-cysteine (Sigma) to calculate the exact thiol molar concentration lysozyme was used as a control protein.

2.30 Papain assay

Papain activity was assayed by measuring the rate of liberation of methylcoumarin from *N*_α-Benzoyl-L-arginine-7-amido-4-methylcoumarin (BAEE-Coumarin) (Sigma). Purified papain (Sigma) was dissolved in activation buffer (20 mM sodium phosphate, 5 mM EDTA, 100 mM NaCl, pH 6.2) containing 5 mM L-cysteine and 67 μM β-mercaptoethanol. The reaction was performed in a 3 ml quartz cuvette and the final concentration of papain was calculated to be 1 unit per 3 ml, where 1 unit should hydrolyse 1 μmol BAEE per minute at 25°C pH 6.2. The reaction was performed at 37°C due to the higher temperature requirement of *C. jejuni*. The papain solution was pre-warmed to 37°C and transferred to the reaction cuvette and a final concentration of 50 μM BAEE-Coumarin (dissolved in 1:1 methanol:DMSO) was added to start the reaction. Once a repeatable reaction could be achieved inhibitor compounds were added to the reaction to assay for papain inhibition.

The fluorescence data was collected on a Cary Eclipse fluorimeter (Varian Ltd, UK) with a λ_{ex} of 345 nm with a 5 nm slit width and a λ_{em} of 442 nm with a 10 nm slit width, the machine voltage was set to low. A standard curve of 7-amido-4-methylcoumarin (Sigma) fluorescence was generated to calculate the rate of hydrolysis. Data was collected over a 2 minutes and the rate of reaction calculated using Microsoft excel.

2.31 Cathepsin-B assay

Human cathepsin-B activity was assayed by measuring the rate of liberation of methylcoumarin from Z-Arg-Arg-7-amido-4-methyl-coumarin (ZAA-Coumarin) (Sigma). Cathepsin-B (Sigma) was dissolved in a 0.1% [w/v] chilled Brij35 solution in SDW. Assay buffer (100 mM sodium potassium phosphate, 2 mM EDTA, pH 6) was prepared containing 5 mM L-cysteine and 67 μM β-mercaptoethanol. The reaction was performed in a 3 ml quartz cuvette and the final concentration of cathepsin-B was calculated to be 0.2 units per 3 ml, where 1 unit should hydrolyse 1 nmol BAEE per minute at 25°C pH 6. The reaction was performed at 37°C due to the higher temperature requirement of *C. jejuni*. The cathepsin-B solution was added to the pre-warmed reaction buffer and transferred to the reaction cuvette and a final concentration of 50 μM ZAA-Coumarin (dissolved in DMSO) was added to start the reaction. Once a repeatable reaction could be achieved inhibitor compounds were added to the reaction to assay for papain inhibition.

The fluorescence data was collected on a Cary Eclipse fluorimeter (Varian Ltd, UK) with a λ_{ex} of 348 nm with a 5 nm slit width and a λ_{em} of 440 nm with a 10 nm slit width, the machine voltage was set to low. A standard curve of 7-amido-4-methylcoumarin (Sigma) fluorescence was generated to calculate the rate of hydrolysis. Data was collected over 30 minutes and the data presented in Graphpad prism.

2.32 Protein crosslinking

Purified protein-protein crosslinking was performed using dithiobis(succinimidyl propionate (DSP) (Thermo-Fisher). The proteins of interest were mixed at different ratios in their respective buffers, to a 50 μl final volume (no Tris buffer was used for the reaction as Tris reacts with DSP) and DSP added to a final concentration of 0.5 or 2 mM and incubated for 30 minutes at 25°C. The reaction was stopped by adding 5 μl of 1M Tris-HCl, pH 7.4 to each reaction. The samples were analysed on SDS-PAGE gels without boiling or reducing with β -mercaptoethanol to keep the crosslinked proteins intact.

2.33 Crystallisation screening

Purified protein was screened for crystallisation using 5-10 mg ml^{-1} of pure protein solution in individual buffer solutions. Microdrops of 200 nl protein and 200 nl precipitant were set up in sitting drop vapour diffusion trials using a Matrix Hydra II Plus One crystallisation robot in collaboration with Dr John Rafferty. Proteins were screened using the PACT, JCSG+, Ammonium Sulphate, Proplex, MPD and classic crystal screens (Qiagen).

2.33.1 Crystallisation optimisation

Once individual crystallisation conditions were determined hanging drop trials were performed where 3 μl of purified protein (5-10 mg ml^{-1}) and 3 μl of crystallisation buffer were suspended from siliconized cover slips in sealed wells and allowed to vapor diffuse until crystals formed. Typically, during a crystallisation optimization trial the concentration of the precipitant and the pH values of the buffer were slightly altered in each individual well to allow for a greater range of conditions to be screened.

2.33.2 Crystal cryoprotectant and X-ray diffraction

Crystals were looped from the hanging drop trials and stored in cryoprotectant (typically the same buffer that the crystal formed in with 10 % ethylene glycol). Cryoprotected crystals were

stored in liquid nitrogen. X-ray diffraction analysis was performed by Dr John Rafferty at the Diamond Light Source (Oxfordshire, UK).

3 [Chapter 3 – The role of the rid system in Campylobacter sub strains and the role of Cj0422c in CAMP defence.](#)

3.1 Introduction

Previous work had identified a novel gene cluster in *Campylobacter jejuni* 11168 which was thought to provide resistance to Cationic Antimicrobial Peptides (CAMPs). This 5 gene cluster spans the *cj0421c-cj0425* region within the *C. jejuni* 11168 genome and is organised into two operons separated by a divergent promoter region. One operon contains the hypothetical regulator genes (*cj0421c* and *cj0422c*) and the other contains the structural genes (*cj0423*, *cj0424* and *cj0425*). Data from a previous PhD student had shown that when these genes are deleted the strains show large increases in sensitivity to CAMPs compared to wild type. For this reason, the genes have been renamed as the **R**esistance to **I**nnate **D**efences or *rid* operon for this study; a table of the genes and their names is shown in (Table 1). This table and the model depicted in (Figure 9) shows what was known about the *rid* system at the start of this project.

So far all of the work on this project had been completed using our laboratory standard variant of *Campylobacter jejuni* NCTC11168-GS (Parkhill *et al.*, 2000). Some previous work has established that the *rid* genes found in this strain (which we are using as our archetypal *rid* system) are also found in other *Campylobacter* strains. Using the NCBI BLAST tool (<http://blast.ncbi.nlm.nih.gov/Blast.cgi>) to search for *rid* genes in other bacteria showed that most *C. jejuni* strains contain the *rid* regulator genes (*cj0421c* and *cj0422c*) but only about half contain the structural genes (*cj0423*, *cj0424* and *cj0425*). It was decided to utilise the recent advances in whole genome sequencing (WGS) to examine a large number of sequenced *Campylobacter* genomes for the presence of *rid* genes, this was done in collaboration with Dr Sam Sheppard who provided summary data on a sample of 182 *C. jejuni* and *C. coli* genomes isolated from multiple animal and human sources. The data revealed that the *rid* regulator genes (*cj0421c* and *cj0422c*) are found in around 90% of *C. jejuni* strains whereas the 3 structural genes (*cj0423*, *cj0424* and *cj0425*) are found in about 40%. Following this it was decided to produce mutant strains in the *rid* genes of a different laboratory strain, *C. jejuni* 81116. This strain is known to possess the *rid* regulator genes *cj0421c* and *cj0422c* but does not possess the 3 structural genes *cj0423-cj0425*. Instead the strain appears to have 3 different genes located in an operon immediately upstream of the regulatory genes. Since the regulatory genes from *C. jejuni* NCTC11168, *cj0421c-cj0422c* share near perfect homology at the protein level with their counterparts in *C. jejuni* 81116 (96% and 99% amino-acid sequence

respectively) it seems that the regulation of the operon is conserved between the species yet strangely the genes being regulated are not.

The aim of this chapter was first to bioinformatically analyse how conserved the *rid* genes are between different *Campylobacter* sub strains. I also produced knockout mutations for the 3 *rid* genes in *C. jejuni* 81116 to determine how sensitive the mutants are to CAMPs. A further aim was to complete some previous work on the *cj0422c* mutant by using a genetic complementation strain (produced by a previous PhD student) in CAMP sensitivity assays to check that the wild type phenotype is restored. I used a variety of different CAMPs to check for sensitivity including the human cathelicidin LL37, the chicken cathelicidin Fowlicidin-2 and the model CAMP polymyxin-B.

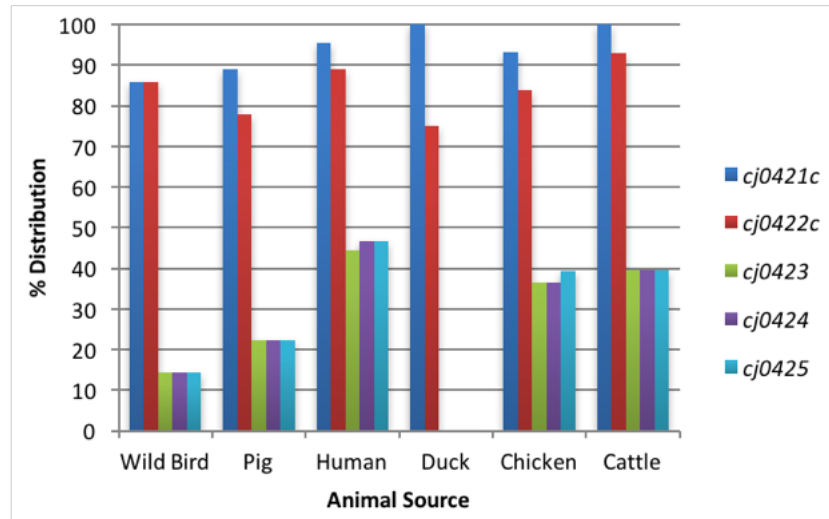
3.2 Chapter 3 Results

3.2.1 Bioinformatic analysis of the *rid* operon in *Campylobacter jejuni* sub strains

3.2.2 Prevalence of the *rid* operon in *Campylobacter* strains isolated from animal sources

The lab of Dr Sam Sheppard utilises large scale whole genome sequencing to analyse the genomes of hundreds of *Campylobacter* strains, conveniently one of the project areas involves using multiple genomes isolated from different animal sources to look for gene prevalence in *Campylobacter* strains from these sources, with an aim to determine which genes may be specially adapted to that particular animal niche (Sheppard *et al.*, 2010). Data from 182 *Campylobacter* genomes was analysed for the presence of the 5 *rid* genes, the genomes were taken from 6 animal sources (human, chicken, duck, wild bird, pig and cattle). The data was expressed for each gene shows the number isolates containing the gene of interest as a percentage of the total (Figure 11). The data shows that the 5 genes within the operon are split into two groups, the regulators (*cj0421c-cj0422c*) and the structural genes (*cj0423-cj0425*).

A



B

Source	Sample Size
Chicken	74
Human	45
Cattle	43
Pig	9
Wild Bird	7
Duck	4
Total	182

C

Gene	Distribution (%)
<i>cj0421c</i>	95
<i>cj0422c</i>	87
<i>cj0423</i>	37
<i>cj0424</i>	37
<i>cj0425</i>	38

Figure 11: Whole genome analysis of multiple *Campylobacter* strains for the prevalence of the *rid* operon. (A) The distribution of the 5 *Rid* genes (arranged by colour) expressed as a percentage of the total number of isolates from a particular animal source. This graph highlights that the regulator genes (red and blue) are found together in the majority of strains analysed, whereas the other genes (green, purple, light blue) are also found grouped together but in less than half of all strains analysed. **(B)** A table showing the total genome sample size from each animal source. **(C)** The total percentage distribution of each of the 5 *Rid* genes throughout the 182 *Campylobacter* genomes analysed. This data indicates that though around 90% of *Campylobacter* strains possess the regulator genes *cj0421c* and *cj0422c*, only around 40% of strains contain the structural genes. Data was obtained from Dr Sam Sheppard and analysed with MS Excel.

3.2.3 Bioinformatic analysis reveals different sub types of *rid* system

The majority of *Campylobacter* species analysed in (Figure 11) (around 90%) appear to contain the two regulator genes *cj0421c* and *cj0422c*, yet only around 40% contain the 3 structural genes *cj0423-cj0425*. This implies that while the *rid* system as a whole is widespread in *Campylobacter*, the structural genes within the operon may be variable. Following on from this it was decided to align the *rid* regions from a group of fully annotated *Campylobacter*



Figure 12: Multi alignment of the *rid* gene cluster from *Campylobacter* sub strains. The 10 annotated genomes of *Campylobacter* from the XBase database were aligned using the region alignment tool (<http://rid.xbase.ac.uk/> accessed on July 2013). The order of the genomes are as follows (all are *C. jejuni* unless otherwise stated) (1) NCTC11168, (2) IA3902, (3) ICDCJ07001, (4) *C. jejuni* subsp *doylei* 269.97, (5) RM1221, (6) S3, (7) 81117, (8) M1, (9) *C. coli* RM2228, (10) 81-176. The blue lines separate the different regions of the gene cluster, highlighting that while all strains have *cj0421c* (some are probably pseudogenes), not all strains have *cj0422c* and the structural genes are highly variable.

genomes to determine how variable the *rid* system is.

From the 10 genomes analysed by regional alignments of the *rid* gene cluster in (Figure 12) it appears that the *rid* system can be sub-categorised into 3 distinct groups A, B and C. A is strains 1-3, B is strains 4-6, C is strains 7-9 and X is *C. jejuni* 81-176 which does not appear to possess a *rid* system. Since the majority of work in this study is being done on *Campylobacter jejuni* NCTC11168, this strain is considered the archetypal *rid* system.

3.2.4 Representation and transcription of the different rid sub-groups

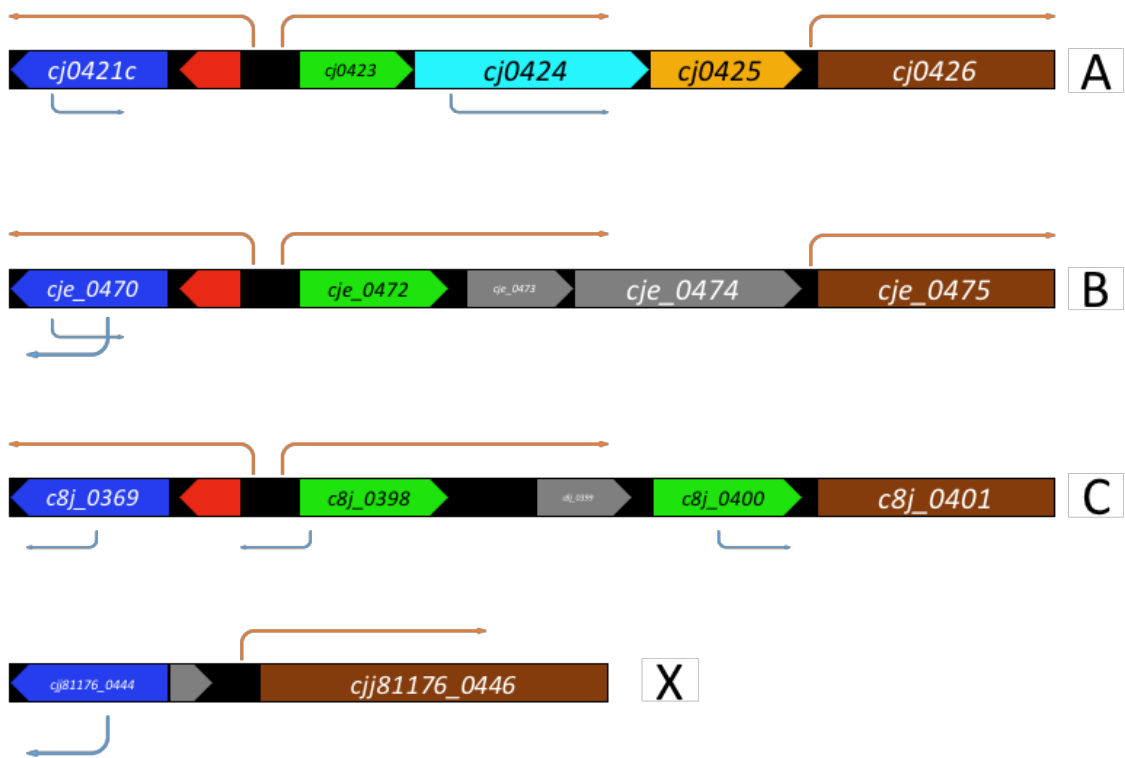


Figure 13: A representative diagram of the 4 primary varieties of Rid system. The figure highlights the high variability between the Rid structural genes of (A) NCTC11168 and those found in other *Campylobacter* isolates, including (B) *C. jejuni* RM1221, (C) *C. jejuni* 81116 and (X) *C. jejuni* 81-176. None of the genes from any of these groups show any close similarity to any other genes of known function in the NCBI database (<http://blast.ncbi.nlm.nih.gov/Blast.cgi>) and are all designated genes with unknown function. The arrows represent transcriptional start sites (TSS) for the operons, these are based on data from a whole cell RNA sequencing study on *Campylobacter* species which happened to include these 4 strains (Dugar et al., 2013). The orange arrows show primary TSS, which are conserved between strains, the blue arrows show internal TSS. The genes highlighted in green, while not similar at the nucleotide level are structurally similar and likely share a common function; this is discussed further in the next section.

3.2.5 Sequence alignments of the *rid* transmembrane proteins

The genes highlighted in green from (Figure 13) are structurally similar small membrane proteins which appear to be the only family of proteins conserved between the different sub-groups of the *rid* system. The alignment shown in (Figure 14) suggests that the membrane proteins from *C. jejuni* 81116 and RM1221 share a common evolutionary origin. While Cj0423 from *C. jejuni* 11168 appears to have originated separately yet likely shares a common function due to the similar domain architecture.

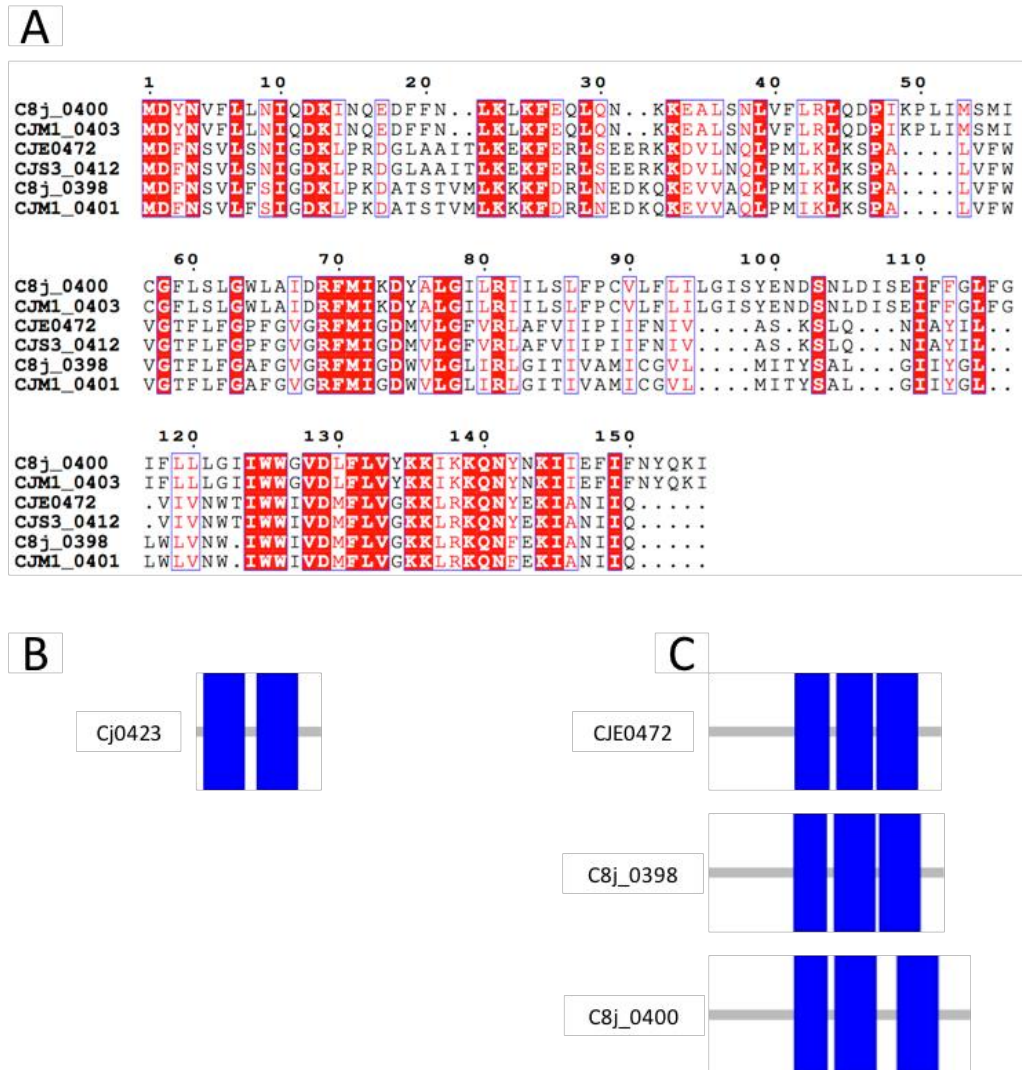


Figure 14: Protein sequence alignment of a conserved family of proteins from the *rid* system. The regional alignment shown in (Figure 12) reveals that while the *Rid* structural genes vary between different *Campylobacter* sub strains some share a degree of structural similarity. (A) Protein sequence alignment of the triple transmembrane proteins which are conserved between different *Rid* systems. Cj0423 was excluded from this alignment as it does not show strong homology at the sequence level to any of the other proteins, possibly implying a different ancestral origin. (B) Domain architecture of Cj0423, with the transmembrane regions represented in blue. (C) Domain architecture of CJE0472, C8j_0398 and C8j_0400. The protein sequence alignment was generated from (<http://rid.ebi.ac.uk/Tools/msa/clustalo/>) and represented in (<http://esprict.ibcp.fr/ESPrict/ESPrict/>), the protein domain architecture images were generated by (<http://smart.embl-heidelberg.de>).

The conservation of the small transmembrane proteins between *rid* systems implies that this family of proteins is essential for the role of the *rid* system between strains. BLAST analysis of the Cj0423 protein sequence shows some homology to the T4 immunity protein from T4 bacteriophage. T4 immunity proteins exclude foreign DNA from entering the cytoplasmic membrane thereby preventing superinfection by multiple phage (Lu and Henning, 1989). However, this homology is not found in the membrane proteins from *C. jejuni* 81116 or RM1221. Since the *rid* membrane proteins are so small and most of the proteins length is occupied with transmembrane domains, searching for proteins with similar domain architecture rather than sequence homology may give a better indication of the proteins role. Searches revealed that a family of proteins known as holins (also derived from bacteriophage) share similar domain architecture to the transmembrane *rid* proteins. Holins are small ‘hole-forming’ transmembrane proteins which are used by phage to lyse the cytoplasmic membrane to allow phage endolysins to escape the cell and degrade peptidoglycan. Holins may also be used to mediate pre-programmed cell death (Reddy and Saier, 2013). Structurally holins are small membrane proteins which vary in the number of transmembrane domains they possess (see Figure 15).

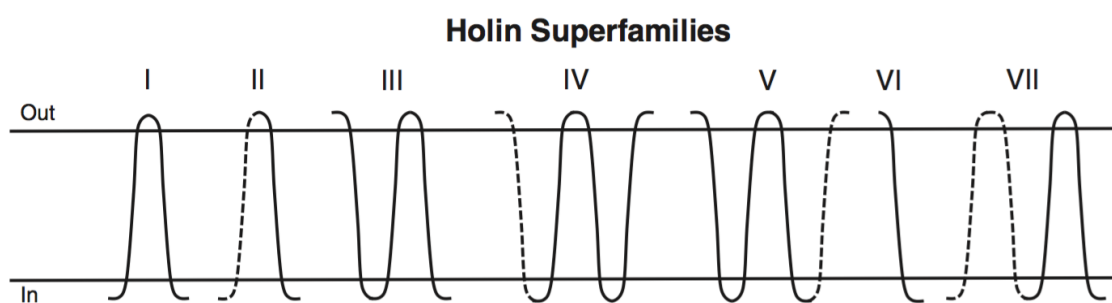


Figure 15: Bacterial holin superfamilies. Transmembrane topologies of members of holin superfamilies, dashed lines show transmembrane regions present in some but not all holin families. Figure adapted from (Reddy and Saier, 2013).

The similarities between the domain architecture of holins and the transmembrane *rid* proteins Cj0423, C8j_0398, C8j_0400 and CJE0472 imply a similar function. The possible role of the transmembrane domain proteins and holins is discussed in (Section 3.3.2).

The variability of the *rid* structural genes between *Campylobacter* strains indicates that individual *rid* systems may have evolved to defend against different niche stresses. Since data from a previous student had shown that *rid* mutant strains show sensitivity to CAMPs, it may be that the variable *rid* systems have evolved to counter specific sub types of CAMP. The varieties of CAMP families are discussed in the introduction (Section 1.9).

3.2.6 Generation of knockout mutants in *C. jejuni* 81116 by Isothermal Assembly Cloning (ISA)

The *rid* system of *C. jejuni* NCTC11168 has been shown to be involved in resistance to Cationic Antimicrobial Peptides (CAMPs); this phenotype is based on previous work showing knockout mutations of the *rid* genes being more sensitive to CAMPs than wild type NCTC11168. Since it has been shown that the *rid* system is highly variable between *Campylobacter* strains it was decided to knockout some of the *rid* genes from another *Campylobacter* strain, *C. jejuni* 81116. The *rid* operon for this strain is showed as (C) in (Figure 13). Since the *cj0422c* mutant from NCTC11168 shows the greatest sensitivity to CAMPs it was decided to mutate the homologue of this as well as the 3 *rid* structural genes in 81116. These mutants would then be tested for sensitivity to CAMPs.

Knockout constructs were produced using pGEM-3Zf(-) plasmids which were assembled using Isothermal Assembly (ISA) cloning (Section 2.11). These were then transformed into *C. jejuni* 81116 to remove most of the genes of interest while not disrupting flanking genes. The mutations in the structural genes were produced relatively easily, however despite multiple attempts, using both chloramphenicol and kanamycin resistance cassettes a mutant in *c8j_0397* (the *cj0422c* homologue) was unable to be produced. Since this was attempted numerous times it may be that this gene is unable to be deleted or is potentially an essential gene. The following section details how the mutant strains were produced in *C. jejuni* 81116.

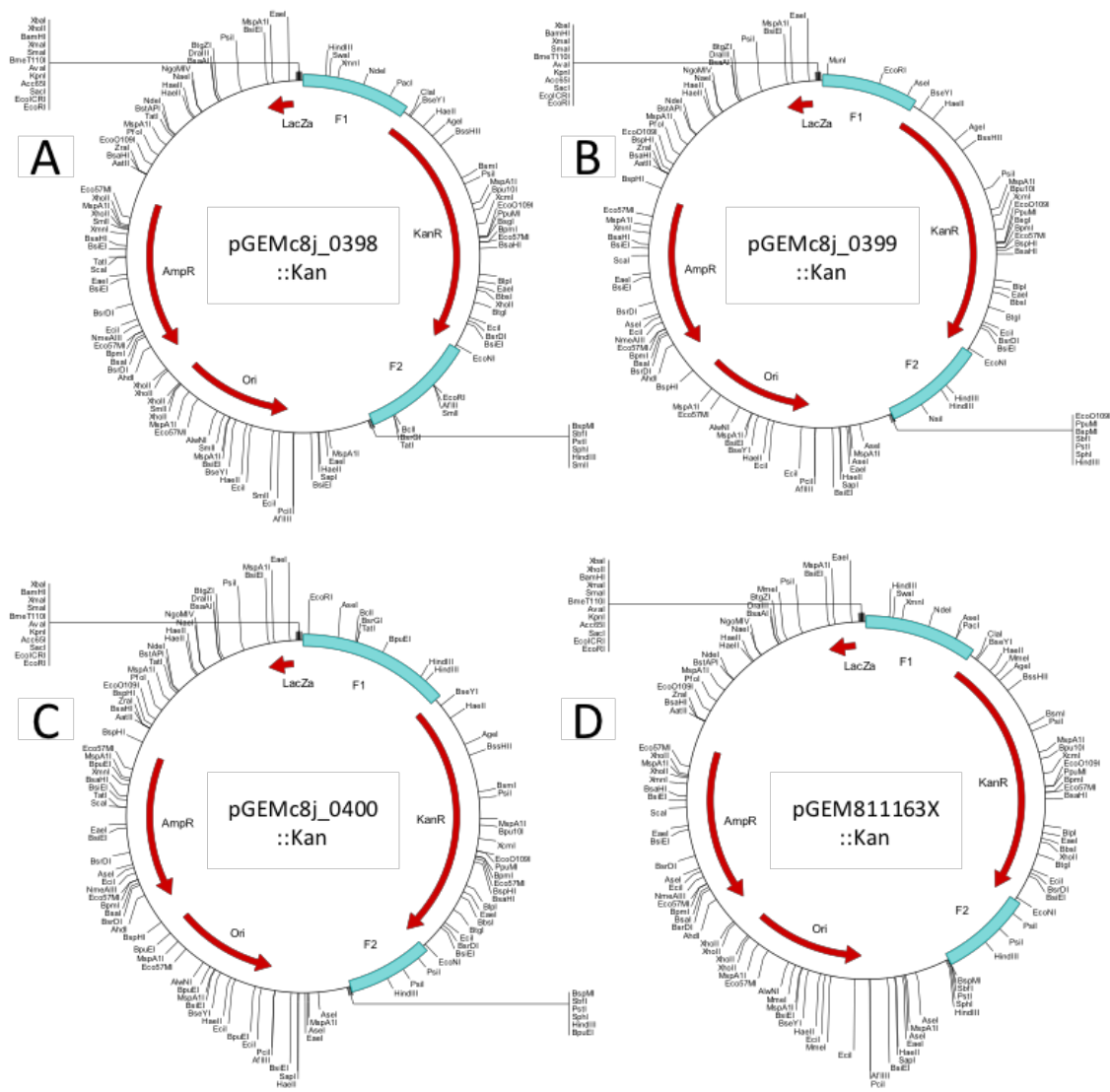


Figure 17: Plasmid maps of the *C. jejuni* 81116 knockout vectors. All plasmids shown were produced by ISA cloning in the same way as (Figure 16), all constructs shown used the kanamycin resistance cassette (*kanR*). The maps show the knockout constructs for *c8j_0398* (A), *c8j_0399* (B), *c8j_0400* (C) and a 3 gene deletion *c8j_0398-c8j_0400* (D). The 3 gene deletion utilised the flanking regions F1 from (A) and F2 from (C). All plasmids were confirmed by DNA sequencing of the inserted fragments (Data not shown).

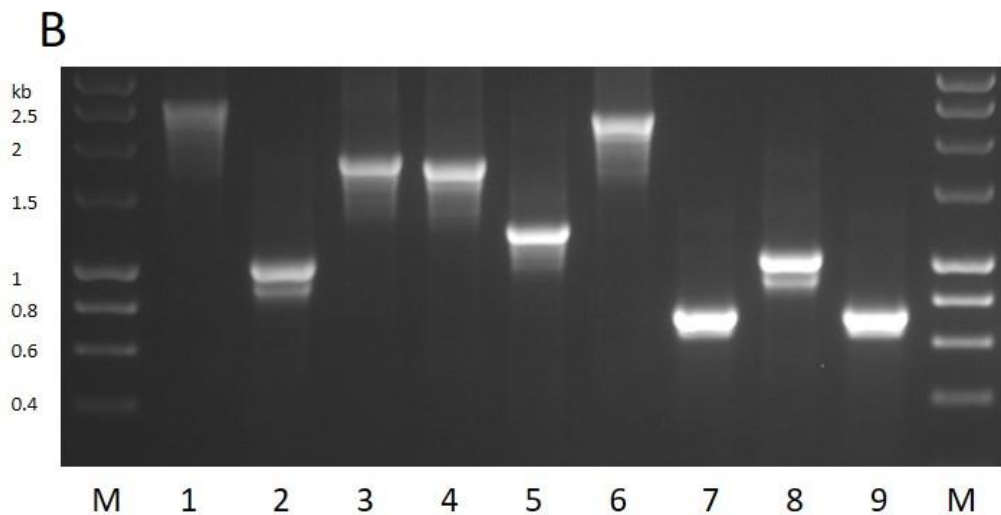
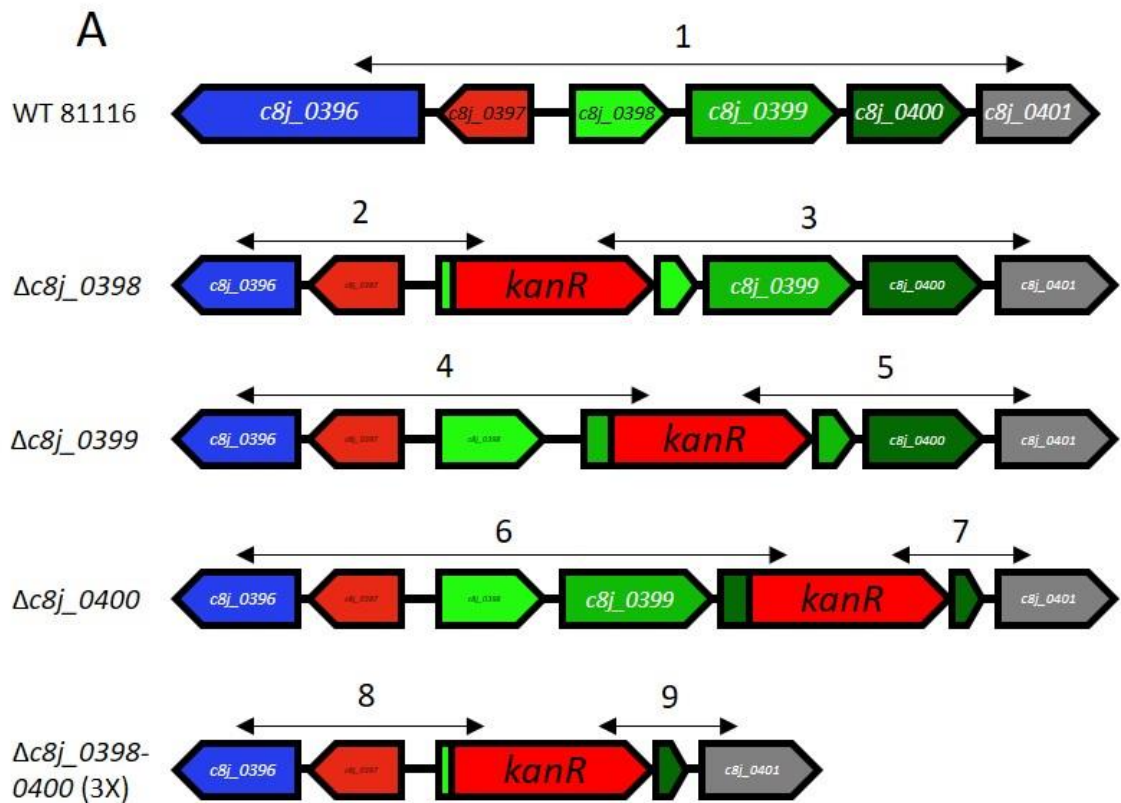


Figure 18: Mutagenesis of Rid genes in *C. jejuni* 81116. The ISA vectors shown in (Figure 17) were transformed into *C. jejuni* 81116 to remove the genes of interest. (A) shows the gene arrangements of WT 81116 and the 4 mutant strains following removal of the gene and insertions of the kanamycin resistance cassette. The mutants were confirmed by PCR analysis. The numbers correspond to the PCR products expected using the knockout screening primers. The PCR confirmation bands are shown in (B). The lane numbers correspond to the numbers shown above the arrows, the band sizes also correspond to the arrow lengths. The expected PCR product sizes in bp are 1-2616, 2-1046, 3-1879, 4-1815, 5-1243, 6-2378, 7-742, 8-1046, 9-742. The PCR primers were designed to be outside the flanking primers used to produce the construct, this was to show that the construct was correctly inserted in the correct orientation and that the double recombination had removed the remaining vector DNA.

3.2.7 Sensitivity of wild type *C. jejuni* strains and 81116 mutants to the CAMP polymyxin-B

The new mutations in *C. jejuni* 81116 were tested for sensitivity to CAMPs using methods described in (Section 2.19). Briefly, overnight broth cultures of cells were checked to ensure they had all grown to a similar OD_{600nm} (typically around 1.1-1.3) and were diluted to a starting OD of 0.6. These cells were transferred to a 96-well plate and were mixed with appropriate volumes of CAMPs (or SDW as a negative control) to a final volume of 200 µl. The cells were then incubated for 2 hours under normal growth conditions. Typically, there were 3 concentrations of CAMPs used and a negative control per assay, each individual concentration was repeated in triplicate. The cells were then serially diluted down the 96-well plate (1:10) and 10 µl from each dilution was spotted onto Mueller-Hinton agar. The plates were incubated for 2 days and the colonies counted.

In this experiment 3 wild type strains of *C. jejuni* were also tested for sensitivity to the model CAMP polymyxin-B. The 3 strains (NCTC11168, 81116 and 81-176) are useful as both NCTC11168 and 81116 contain *rid* systems yet they contain different sets of structural genes. *C. jejuni* 81-176 however does not contain a *rid* system, it does contain a pseudogene which shows strong homology to *cj0421c* but no other genes (Figure 12-13). The data shown in (Figure 19) suggests that the wild type *C. jejuni* 81-176 strain appears slightly more resistant to polymyxin-B compared to 11168 and 81116. And that none of the mutant strains produced in *C. jejuni* 81116 show the same level of sensitivity as the Rid mutants from 11168 (comparing this data to data from Halah Al-Haideri on the NCTC 11168 mutant strains) one of the strains ($\Delta c8j_0400$) does appear to be slightly more sensitive to polymyxin-B.

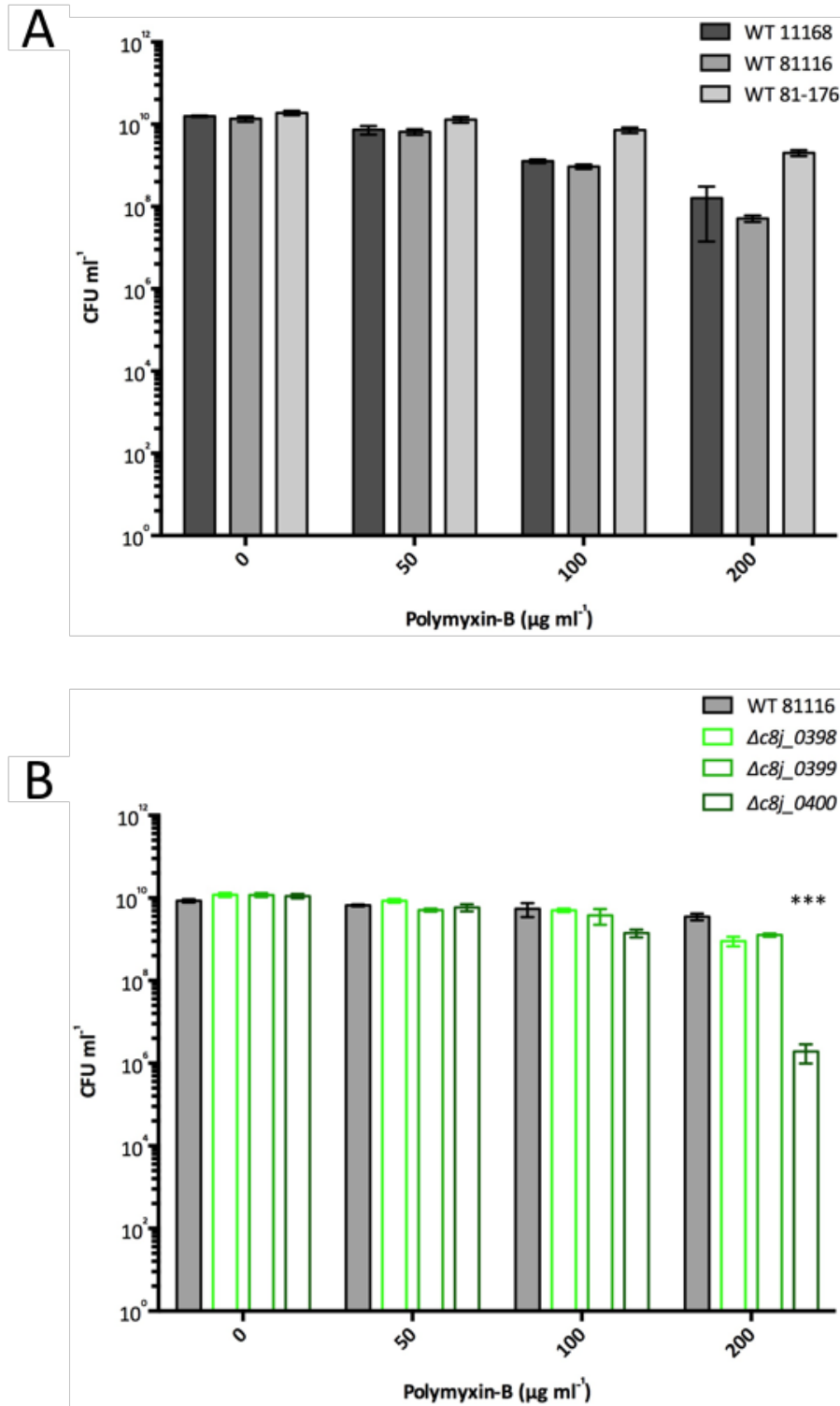


Figure 19: Sensitivity of 3 wild type *C. jejuni* strains and the *C. jejuni* 81116 mutants to polymyxin-B. Microtitre sensitivity assays were performed using methods described in (Section 2.19) with the strains incubated for 2 hours. **(A)** 3 wild type strains of *C. jejuni* were tested for innate polymyxin-B sensitivity. **(B)** The 3 mutant strains produced in *C. jejuni* 81116 were also tested for polymyxin-B sensitivity. The asterisks represent a P-value < 0.05 comparing the wild type and *c8j_0400* mutant strain. All error bars show the standard deviations from at least 3 biological replicates.

3.2.8 Sensitivity of the *cj0422c* mutant to a range of CAMPs

Since the *rid* mutants in *C. jejuni* 81116 did not show much sensitivity to the model CAMP polymyxin-B it was decided to suspend this line of enquiry and to focus on the archetypal *rid* system in *C. jejuni* NCTC11168. Since polymyxin-B is a model CAMP and is produced by *Bacillus polymyxa* using non-ribosomal peptide synthesis (Paulus and Gray, 1964) it is not necessarily an accurate model for short chain CAMPs produced by higher organisms. To study whether the *rid* system is involved in resistance to human and chicken CAMPs a selection of synthetic CAMPs was acquired including the human cathelicidin LL37, and the chicken cathelicidins Fowlicidin-1 and Fowlicidin-2. The *cj0422c* mutant and a newly produced complementation strain (both provided by Halah Al-Haideri) were used to test for sensitivity to these CAMPs. As a control the strains were also tested for sensitivity to the anionic detergent sodium dodecyl sulphate (SDS). SDS was used as it is active against the cell membrane in a non-specific manner, so if the *rid* system is protecting against pore forming CAMPs, then there should be no difference in sensitivity to SDS. The data shown in (Figures 20-21) revealed that the *cj0422c* mutant does show increased sensitivity to polymyxin-B, LL37 and Fowlicidin-2 as expected, while no increase in sensitivity was observed against the SDS control, however the complementation strain of *cj0422c* did not show any restoration of wild type resistance.

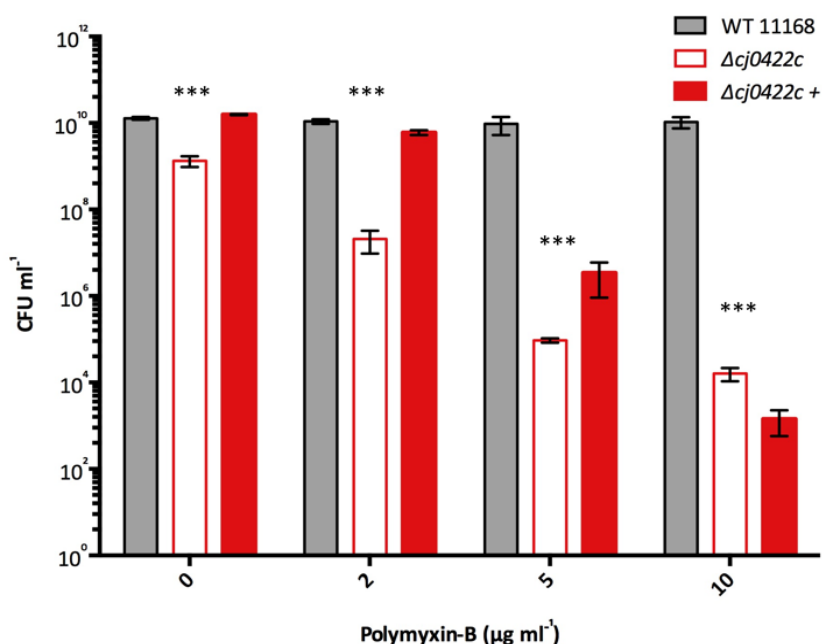


Figure 20: Sensitivity of the *cj0422c* mutant and complementation strains to the model CAMP polymyxin-B. Microtitre sensitivity assays were performed using methods described in (Section 2.19) with the strains incubated for 2 hours. The error bars show the standard deviation from at least 3 biological replicates for each data point. The asterisks represent a T-test P value <0.05 comparing the wild type and mutant strains.

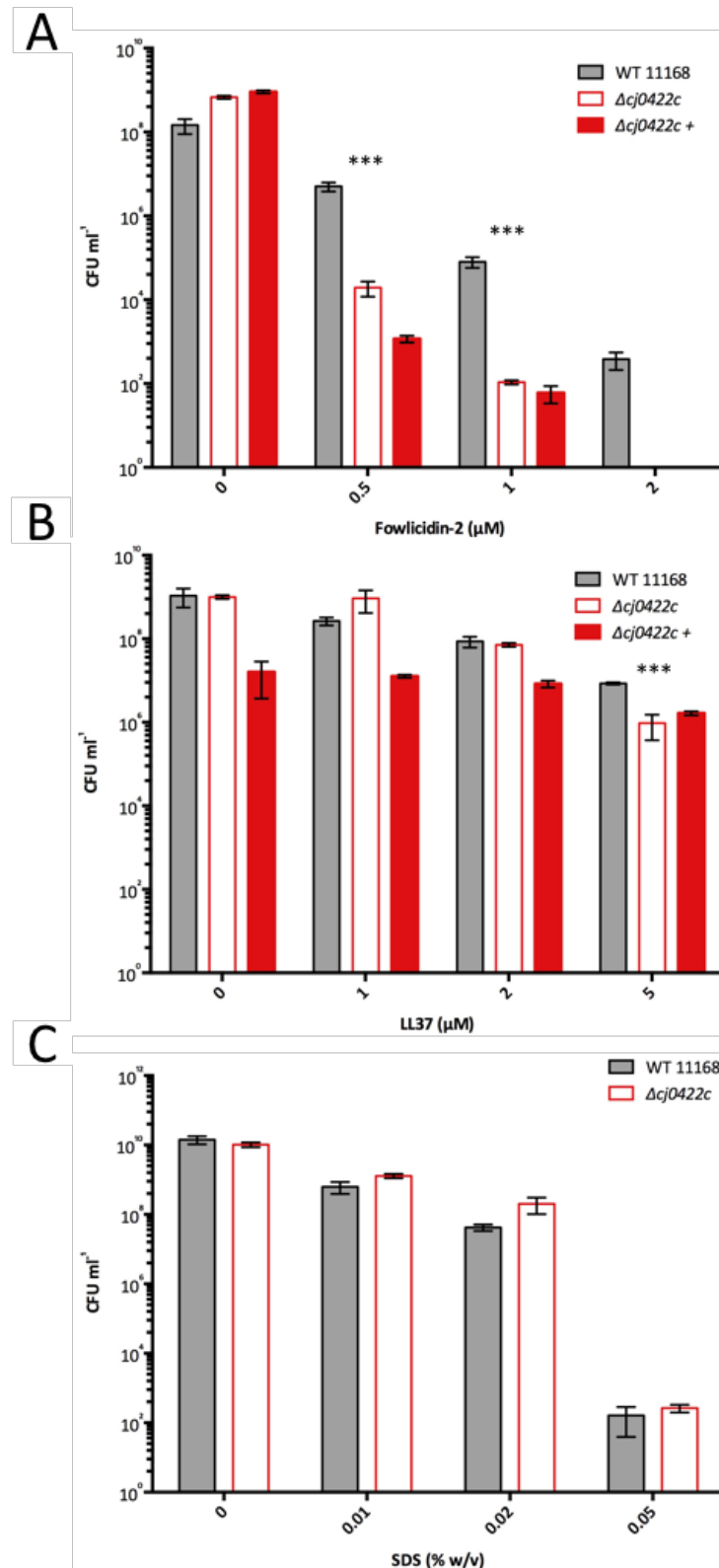


Figure 21: Sensitivity of the *cj0422c* mutant and complementation strains to LL37, Fowlicidin-2 and SDS. Microtitre sensitivity assays were performed using methods described in (Section 2.19) with the strains incubated for 4 hours (2 hours for SDS). (A) shows that like polymyxin-B (Figure 20) the *cj0422c* mutant is much more sensitive to fowlicidin-2, and slightly more sensitive to LL37 as shown in (B). (C) shows that the *cj0422c* mutant is no more sensitive to SDS compared to wild type. Asterisks represent a T-test P value <0.05 between the wild type and mutant strains.

The data presented shows that while the *cj0422c* mutant is highly sensitive to CAMPs (particularly polymyxin-B and fowlicidin-2) this phenotype is not reversed, when the *cj0422c* complementation strain is tested. The complementation strain used was produced using the *C. jejuni metK* promoter which is constitutively expressed at a moderate level in *C. jejuni* (Van Vliet *et al.*, 2001). It may be that this promoter is unable to completely mimic the wild type promoter. It was decided to re-produce the complementation strain using the natural promoter. The construction of this complementation strain is discussed further in the next chapter.

3.2.9 *The rid operon is not up-regulated by polymyxin-B*

Since transcriptomic microarray data from the *cj0422c* mutant shows that the *rid* structural genes are highly up-regulated in the mutant strain, (Figure 7), it seems peculiar that this strain should be highly sensitive to polymyxin-B since the model for CAMP resistance assumes that the up-regulation of the *rid* genes is what promotes resistance. To test that it is up-regulation of the *rid* structural genes that promotes resistance, both western blot analysis and qRT-PCR were used to look for up-regulation of the *rid* structural proteins and genes respectively in response to polymyxin-B. As part of the previous work on this project a polyclonal rat antibody for Cj0424 was produced. Cultures of wild type *C. jejuni* 11168 were grown for 24 hours in the presence of 200 ng ml⁻¹ and 2 µg ml⁻¹ polymyxin-B with samples taken at 8 and 24 hours. These concentrations were chosen as they are the approximate minimum inhibitory concentrations of the *cj0422c* mutant and wild type *C. jejuni* respectively, over 24-hour growth curve (data not shown). The samples were matched by whole cell protein concentration using the Bio-Rad assay (Section 2.25.1) and separated on a 12% SDS-PAGE gel. A western blot was performed using the anti-Cj0424 antibody in conjunction with a goat anti-rat HRP conjugated antibody (Section 2.25.4). To test for induction of the *rid* operon over a short time period, qRT-PCR was used to determine expression of *cj0423* in response to a higher concentration of polymyxin-B (25 µg ml⁻¹) over a 15-minute time period. The expression of *cj0423* was measured at both T=0 and T=15 minutes. The data shown in (Figure 22) shows no observable increase in the expression of Cj0424 in response to polymyxin-B.

3.2.10 Western blot analysis suggests Cj0424 is not up-regulated in response to polymyxin-B

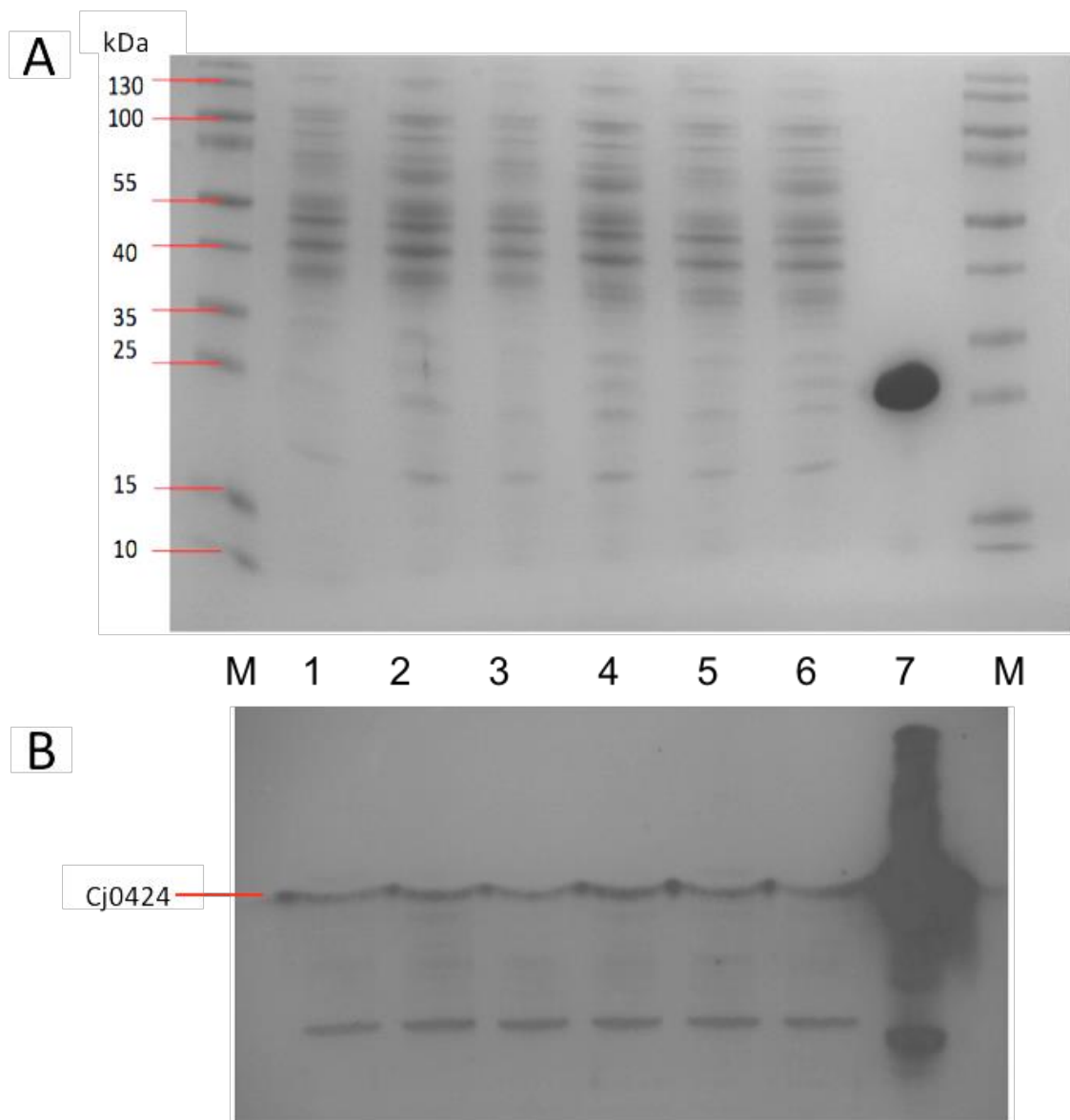


Figure 22: Western blot analysis of the expression of Cj0424 in wild type *C. jejuni* NCTC11168 in the presence of polymyxin-B. (A) shows whole cell protein extracts from wild type cells after matching by BioRad assay (Section 2.25.1) and separated by 12% SDS-PAGE (Section 2.25.2). Lanes 1 and 2 show WT *C. jejuni* grown under normal conditions with no polymyxin-B and samples taken at 8 and 24 hours respectively. Lanes 3 and 4 show WT *C. jejuni* grown in the presence of $2 \mu\text{g ml}^{-1}$ polymyxin-B with samples taken at 8 and 24 hours respectively. Lanes 5 and 6 show WT *C. jejuni* grown in the presence of 200 ng ml^{-1} polymyxin-B with samples taken at 8 and 24 hours respectively. Lane 7 shows purified recombinant Cj0424 used as a control (provided by Halah Al-Haideri). Figure (B) shows the same SDS-PAGE gel following western blotting with anti-Cj0424 rat antibody and anti-rat HRP conjugated goat antibody (Section 2.25.4).

3.2.11 Quantitative reverse transcriptase PCR (qRT-PCR) analysis suggests *cj0423* is not up-regulated in response to polymyxin-B.

The expression of *cj0423* was assayed at the transcriptional level by qRT-PCR in response to polymyxin-B shock over a 15-minute time period. The data presented in (Figure 23) shows only a slight increase in *cj0423* expression (2.5-fold) in response to polymyxin-B, which is less than the increase in expression seen in the negative control (4-fold).

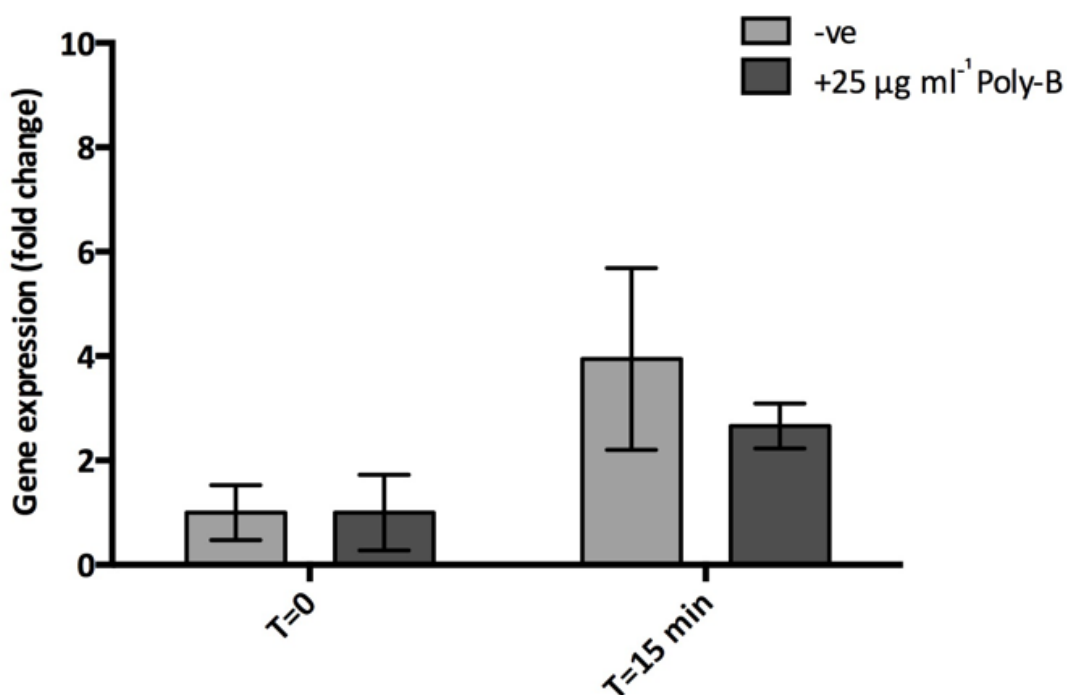


Figure 23: qRT-PCR analysis of *cj0423* gene expression in response to polymyxin-B. 6 biological replicates of wild type *C. jejuni* were grown to an OD_{600nm} of 0.5 and polymyxin-B was added to 3 of them at a final concentration of 25 µg ml⁻¹, SDW was added to the control group. The cells were incubated under normal conditions for 15 minutes and whole cell RNA was extracted and matched to 10 ng µl⁻¹ in nuclease free water (RNA was also extracted prior to adding polymyxin-B) (Section 2.15). qRT-PCR reactions were performed according to the methods described in (Section 2.15.1), the *gyrA* gene was used as an internal control. The data is expressed as a fold change in *cj0423* gene expression at 15 minutes compared to expression at 0 minutes immediately prior to adding polymyxin-B. The error bars represent the standard deviations from 9 replicates.

3.2.12 Checking the *cj0422c* mutant strain for changes in gene expression.

The data shown so far in this chapter has confirmed that while the *cj0422c* mutant strain is more sensitive to CAMPs than wild type *C. jejuni*, resistance to CAMPs is not restored in the complementation strain. There appears to be no significant up-regulation of the *rid* operon in response to the model CAMP polymyxin-B and mutations in the *rid* genes of *C. jejuni* 81116 do not show much change in CAMP sensitivity. Since so far all the data on the role of Cj0422c regarding gene regulation has come from the original microarray data (Figure 7), it was decided to analyse the expression of *rid* genes in the *cj0422c* mutant and complementation strains by qRT-PCR to determine whether the complementation strain is successfully repressing the *rid* genes as it should. The data shown in (Figure 24) shows that the expression of *cj0423* and *cj0424* in the *cj0422c* are not strongly up-regulated, and are actually down-regulated by around 0.5-fold for *cj0423* and 0.3-fold for *cj0424*.

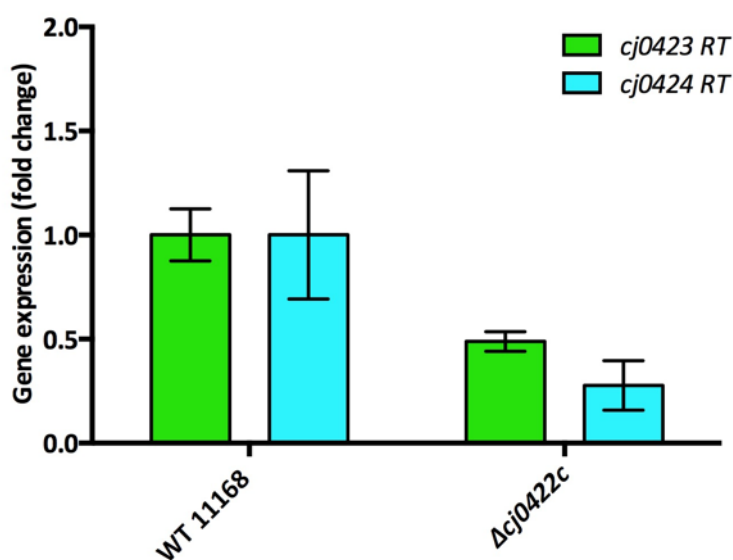


Figure 24: qRT-PCR analysis of the *cj0422c* mutant strain compared to wild type *C. jejuni* 11168. The expression of the *Rid* structural genes *cj0423* and *cj0424* was measured by qRT-PCR analysis of the *cj0422c* mutant. Wild type *C. jejuni* 11168 and the *cj0422c* mutant were grown to an OD_{600nm} of 0.5 and whole cell RNA was extracted and matched to $10 \text{ ng } \mu\text{l}^{-1}$ in nuclease free water (Section 2.15). qRT-PCR reactions were performed according to the methods described in (Section 2.15.1), the *gyrA* gene was used as an internal control. The data is expressed as a fold change in *cj0423* and *cj0424* expression in the *cj0422c* mutant compared to wild type, with wild type expression for each gene being matched to 1.

3.2.13 Checking the promoter of the *cj0422c* mutant strain for sequence changes

The qRT-PCR data shown in (Figure 24) shows that *cj0423* and *cj0424* are not strongly up-regulate in the *cj0422c* mutant, in contradiction to the microarray data. This is the same mutant strain that was used to produce the microarray data shown in (Figure 7), it is also the same mutant that shows high sensitivity to CAMPs. It was decided to sequence the promoter region of the *cj0422c* mutant strain to determine whether any secondary mutations may have affected gene expression. The sequencing data, represented by (Figure 25), reveals that the *cj0422c* mutant is missing a 160bp fragment from the *cj0423* promoter which would likely prevent gene expression. Since the role of the Cj0422c protein is to bind at this promoter and repress expression, removal of *cj0422c* leads to a large increase in gene expression as shown in the original microarray (Figure 7). This overexpression may be detrimental to the cell when grown under normal conditions, or it may simply be wasteful of resources. It appears the *cj0422c* mutant strain has at some point acquired this secondary mutation, though it is not known when.

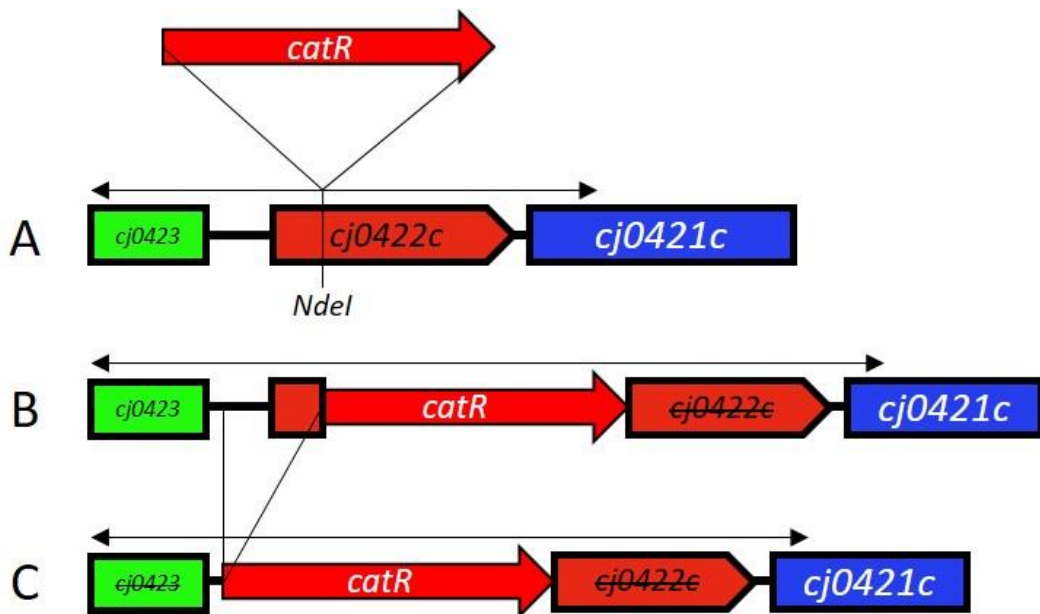


Figure 25: Sequencing the *Rid* promoter region of the *cj0422c* mutant. The original *cj0422c* mutant was generated by insertional activation of the gene by insertion of a chloramphenicol cassette (*catR*). The cloning strategy is shown in (A) whereby the *catR* cassette was cloned into a unique *NdeI* site within the *cj0422c* gene. (B) represents what the mutant should look like when sequenced with the *catR* cassette inserted into the *cj0422c* gene and promoter region for *cj0423* unaffected. However, sequencing the region revealed that a 160bp fragment is missing from the genome. This is shown in (C) where most of the promoter region between *cj0423* and *cj0422c* has been removed. The arrows show the region covered by the DNA sequencing reaction.

3.2.14 Re-isolation of the *cj0422c* mutant strain

Since the *cj0422c* mutant strain which has so far been used in this project appears to have acquired a secondary mutation it calls into question the CAMP sensitivity data so far presented in this chapter. However, it is worth noting that the high sensitivity to CAMPs seen in the *cj0422c* mutant strain shown in (Figure 20) may now be explained by the secondary mutation as the *rid* structural genes are no longer up-regulated as shown in (Figure 24), it may also explain why the complementation construct was unable to restore the wild type phenotype. It was decided to re-isolate the *cj0422c* mutant from the original stock produced by Dr Ed Guccione in 2010. Cell material from the original mutant sample was streaked on blood agar plates with 20 $\mu\text{g ml}^{-1}$ chloramphenicol and 5 colonies were picked and grown for re-stocking and screening. These 5 single isolates were first checked by DNA sequencing of the promoter region between *cj0423* and *cj0422c*, all 5 contained the expected gene arrangement with no evidence of any secondary mutations (data not shown). As a further check all 5 isolates were assayed for polymyxin-B sensitivity. The data is shown in (Figure 26) and shows that a single variant within the original mutant strain appears considerably more sensitive to polymyxin-B.

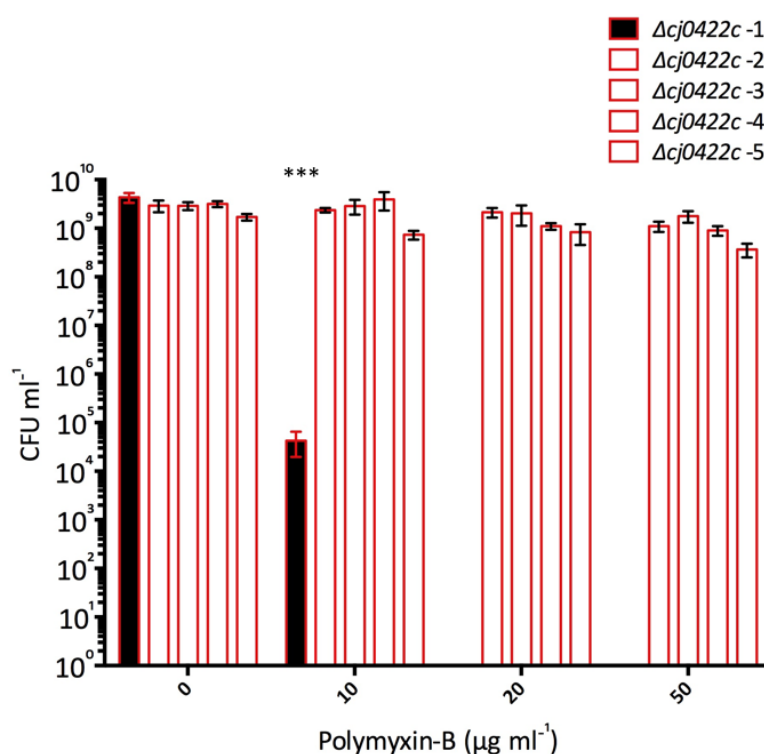


Figure 26: Polymyxin-B sensitivity of the 5 re-isolated *cj0422c* mutants. Microtitre sensitivity assays were performed using methods described in (Section 2.19) with the strains incubated for 2 hours. The error bars show the standard deviation from at least 3 biological replicates for each data point. The data shows that while 4 out of the 5 strains showed no increase in sensitivity to polymyxin-B, a single isolate ($\Delta cj0422c$ -1) shows high sensitivity to polymyxin-B. Asterisks represent a T-test P value <0.05 comparing the $\Delta cj0422c$ -1 and $\Delta cj0422c$ -2 strains.

The data shown in (Figure 26) shows that a single seemingly random variant of the $\Delta cj0422$ strain from the original mutant stock is hyper-sensitive to polymyxin-B and presumably to other CAMPs (this was not tested). This suggests that the earlier hypothesis about the polymyxin-B sensitivity seen in the $cj0422c$ mutant being the result of the secondary mutation within the *rid* system (as shown in Figure 25), is in fact not true. DNA sequencing of the *rid* regions from all 5 $\Delta cj0422$ mutant strains from (Figure 26) shows that the regions are genetically identical within sequenced promoter region (data not shown). This data leads to two conclusions; the high level of CAMP sensitivity seen earlier (Figures 20-21) is likely the result of a mutation or single nucleotide polymorphisms (SNPs) elsewhere in the genome, and also that the $cj0422c$ mutant (with no secondary mutations or SNPs) is no more sensitive to polymyxin-B than wild type. These data would still fit with the CAMP resistance model we have built as it solves a logic flaw in the original hypothesis that the $cj0422c$ mutant overproduces other *rid* proteins and therefore should in theory be just as resistant if not more so than wild type.

The whole *rid* system hypothesis rests primarily on the mutant strains $\Delta cj0423$ and $\Delta cj0424$ being more sensitive to polymyxin-B and other CAMPs than wild type, this work was done by a previous student Halah Al-Haideri. Following the data showing that the high CAMP sensitivity seen in the $cj0422c$ mutant was not related to the *rid* system it was decided to repeat some of the polymyxin-B sensitivity assays in the other mutant strains. Some of the data is shown in the next chapter. In essence it was shown that the high sensitivity to polymyxin-B and other CAMPs observed in the $cj0423$ and $cj0424$ mutants was false, the reasons for this are still unclear.

Strains of *Campylobacter* are known to be genetically variable (Gaynor *et al.*, 2004), (SNPs) and phase variable genes mean that random phenotypes can be acquired or lost quickly, such as cell shape, growth rate or ability to colonise chickens. This high rate of variation between strains of *Campylobacter* can in theory lead to mutant strains acquiring phenotypes which are not directly due to the mutation, this is likely due to producing mutants by selecting single colonies which may contain random variations when compared to the host wild type. For many types of experiments this may not be a problem, however when assaying for survival under a stress condition, such as exposure to CAMPs, random variations between strains can lead to an apparent difference in sensitivity between mutants whereas this is actually due to other factors such as growth rate, motility or variations in membrane composition, all of which

may affect viability. This is still a poorly understood area of microbiology yet it does have real consequences, DNA sequencing has proved that the polymyxin-B sensitivity seen in the *cj0422c* mutant is not related to the mutation or variations in another part of the *rid* system and is likely due to another genetic variation elsewhere in the genome.

Due to these problems it was decided to re-isolate a fresh wild type *C. jejuni* NCTC11168 strain from an older laboratory -80°C frozen stock and to sequence the entire genome as a fresh starting point. All the *rid* mutants would then be re-produced in this background strain which was renamed as *C. jejuni* NCTC11168 DJK. Two of the *cj0422c* knockout strains shown in (Figure 26) would also be genome sequenced, the strain which is sensitive to polymyxin-B ($\Delta cj0422c-1$) and a strain which is resistant to polymyxin-B ($\Delta cj0422c-2$). These were genome sequenced to try and determine how the extreme sensitivity seen in $\Delta cj0422c-1$ originated. These strains would be genome sequenced alongside another wild type variant of *C. jejuni*, 11168-H, which is known for being hypermotile (Karlyshev *et al.*, 2002). This strain is commonly used in chicken models as motility greatly increases the chance of colonisation (Wassenaar *et al.*, 1993). The strain was donated from the laboratory of Dr Dennis Linton.

3.2.15 Whole genome sequencing (WGS) of *C. jejuni*

Whole genome sequencing (WGS) of the 4 strains of *Campylobacter* was performed by MicrobesNG using the Illumina sequencing platform, the raw data was collected and assembled into a whole genome using the original NCTC11168 as a reference by Dr Roy Chaudhuri. The data was visualised in a standard web browser using Biodalliance.



Figure 27: Biodalliance web server showing the WGS data. A screenshot example of the WGS data, the entire genome sequence extends across the width of the figure. The figure shows Illumina sequencing read coverage (shown as graphs across the sequence) and variations within the genome (shown as blue and red markers for substitutions and deletions respectively). Red arrows with short sequences show single insertions. This figure shows summary data for 4 genomes JB1 (NCTC11168-RID wild type), JB3 (NCTC11168 DJK lab wild type), JB3 ($\Delta cj0422c-1$ polymyxin sensitive), JB4 ($\Delta cj0422c-2$ polymyxin resistant).

What is immediately obvious from the WGS data shown in (Figure 27) is that the newly named WT DJK strain contains many SNPs and small difference compared to the reference sequence. Compared to the reference NCTC11168 sequence the WT-DJK strain contains 49 differences, the WT 11168-H strains contains 6 differences, the $\Delta cj0422c-1$ strain contains 21 unique differences and the $\Delta cj0422c-2$ strain contains 19. Most of these differences are SNPs while some are slightly longer variations in sequence. No large changes in the genome such as large fragment insertions or deletions could be detected. The analysis of these genomes is shown below.

Genome Sequencing Table-9: WT DJK strain, variations in intergenic regions									
Position	Genes	Strand	Gene Names	Description (<i>C. jejuni</i> NCTC11168 Annotation)	Reference Poly Tract	Reference	Variant	Variant Type	Illumina Read Coverage
199139	<i>cj0203 - cj0204</i>	++	_ _	Citrate Transporter, Oligopeptide Transporter	GTTTTTTTG	-	T	Insertion	12
514227	<i>cj0551 - cj0552</i>	++	<i>efp</i> , _	Elongation Factor P, Hypothetical Protein	ATTTTTTTA	-	T	Insertion	20
1338384	<i>cj1403c - cj1404</i>	- +	<i>gapA</i> , <i>NadD</i>	Glyceraldehyde 3-phosphate dehydrogenase, Nicotinate-nucleotide adenyltransferase	CAAAAAAAG	-	A	Insertion	60
1470420	<i>cj1537c - cj1538c</i>	--	<i>acs</i> , _	Acetyl-CoA synthetase, Anion-uptake ABC transporter		G	T	Substitution	3
1473189	<i>cj1540 - cj1541</i>	++	_ _	Tungstate transport system substrate binding protein, LamB / YcsF family protein		T	-	Deletion	20
1546467	<i>cj1618c - cj1619</i>	- +	_ <i>kgtP</i>	Radical SAM domain-containing protein, apha-ketoglutarate permease		A	T	Substitution	29
1603971	<i>cj1681c - cj1682c</i>	--	<i>cysQ</i> , <i>gltA</i>	3' (2'),5'-bisphosphate nucleotidase, Citrate synthase		C	T	Substitution	31

Table 9: Wild Type 11168 DJK strain intergenic region variations. The table lists the variations found within intergenic regions of the new lab wild type strain. Because these variations are found between gene ORFs it is unknown whether they have a meaningful effect on gene expression.

Genome Sequencing Table-10: WT DJK strain, in-frame amino acid changes								
Position	Genes	Strand	Gene Names	Description (<i>C. jejuni</i> NCTC11168 Annotation)	Reference	Variant	Amino Acid Change	Illumina Read Coverage
108021	<i>cj0099</i>	+	<i>birA</i>	Biotin-protein ligase transcriptional regulator	G	A	Ala 120 - Thr	62
136901	<i>cj0136</i>	+	<i>infB</i>	Translation initiation factor IF-2	G	A	Asp 16 - Asn	75
168234	<i>cj0172c</i>	-		Saccharopine dehydrogenase	A	G	His 260 - Arg	374
199708	<i>cj0204</i>	+		Oligopeptide Transporter	G	A	Gly 158 - Asp	439
224012	<i>cj0240c</i>	-	<i>iscS</i>	Cysteine desulfurase	C	T	Pro 23 - Ser	198
253191	<i>cj0276</i>	+	<i>mreB</i>	Rod shape-determining protein	A	G	Asp 48 - Gly	448

262345	<i>cj0284c</i>	-	<i>cheA</i>	Chemotaxis histidine kinase	T	C	Ile 290 - Thr	983
554938	<i>cj0597</i>	+	<i>fba</i>	Fructose-biphosphate adolase	C	T	Arg 296 - Cys	523
643379	<i>cj0688</i>	+	<i>pta</i>	Phosphate acetyltransferase	C	T	Ala 497 - Val	95
753450	<i>cj0802</i>	+	<i>cysS</i>	CysteinyI-tRNA synthetase	A	G	Asp 69 - Gly	89
759961	<i>cj0807</i>	+		7-alpha-hydroxysteroid dehydrogenase	C	T	Ala 122 - Val	88
760188	<i>cj0807</i>	+		7-alpha-hydroxysteroid dehydrogenase	A	G	Lys 198 - Glu	126
843351	<i>cj0903c</i>	-		Amino acid transport protein	C	T	Thr 124 - Ile	178
861381	<i>cj0927</i>	+	<i>apt</i>	Adenine phosphoribosyltransferase	T	C	Val 110 - Ala	148
880877	<i>cj0942c</i>	-	<i>secA</i>	Preprotein translocase subunit	C	T	-	71
1159310	<i>cj1231</i>	+	<i>kefB</i>	Glutathione-regulated potassium-efflux system protein	G	A	Gly 48 - Asp	248
1189659	<i>cj1259</i>	+	<i>porA</i>	Major outer membrane protein	A	G	Glu 180 - Gly	950
1190075	<i>cj1259</i>	+	<i>porA</i>	Major outer membrane protein	G	A	Glu 319 - Lys	1868
1434480	<i>cj1502c</i>	-	<i>putP</i>	Sodium/Proline symporter	G	A	Thr 357 - Ile	220
1526322	<i>cj1597</i>	+	<i>hisG</i>	ATP phosphoribosyltransferase	G	A	Glu 295 - Lys	114
1546746	<i>cj1619</i>	+	<i>kgtP</i>	Alpha-ketoglutarate permease	C	A	Ser 84 - Tyr	404

Table 10: Wild Type 11168 DJK strain in frame amino acid substitutions. The table lists the SNPs which results in amino acid substitutions within the ORFs of the new lab wild type strain. It is difficult to predict what, if any, changes these substitutions may have on protein function so no hypothetical changes are listed. It is likely that most of them do not result in any significant change in function.

Genome Sequencing Table-11: WT DJK strain, gene deletions												
Position	Gene	Strand	Gene Name	Description (<i>C. jejuni</i> NCTC11168 Annotation)	Reference Poly Tract	Reference	Variant	Variant Type	Predicted Effect (Translation)	Percentage Lost / Altered	Predicted Effect (Phenotype)	Illumina Read Coverage
87327	<i>cj0076c</i>	-	<i>lctP</i>	L-lactate permease		-	T	Insertion	Thr 465 - Tyr / Asn 468 - STOP	17%	Probable loss of function	539
97789	<i>cj0088</i>	+	<i>dcuA</i>	Anaerobic C4-dicarboxylate transporter		G	-	Deletion	Trp 100 - Gly / Leu 105 - STOP	77%	Complete loss of function	341
291007	<i>cj0319</i>	+	<i>fliG</i>	Flagellar motor switch protein		C	-	Deletion	Ser 290 - Leu / Frame Shift	15%	Probable loss of function	627
305103	<i>cj0337c</i>	-	<i>motA</i>	Flagellar motor protein	TGGGGGA	G	-	Deletion	Lys 206 - Asn / Leu 107 - STOP	21%	Complete loss of function	391
818022	<i>cj0882c</i>	-	<i>fliH</i>	Flagellar biosynthesis protein		G	-	Deletion	Asp 577 - Ile / Leu 582 - STOP	20%	Complete loss of function	205
859539	<i>cj0923c</i>	-	<i>cheR</i>	Chemotaxis protein methyltransferase	GAAAAAAAT	A	-	Deletion	Ile 5 - STOP	98%	Complete loss of function	24
933483	<i>cj1002c</i>	-		Phosphoglycerate/bisphosphoglycerate mutase	TAAAAAAC	-	A	Insertion	Leu 36 - Thr / Lys 38 - STOP	78%	Complete loss of function	50
1074329	<i>cj1139c</i>	-	<i>wlaN</i>	Beta-1,3 galactosyltransferase	TGGGGGGGGT	G	-	Deletion	Gly 113 - Val / Ile 131 - STOP	63%	Complete loss of function	49
1106849	<i>cj1179c</i>	-	<i>fliR</i>	Flagellar biosynthesis protein		-	A	Insertion	Met 80 - Asn / Gln 98 - STOP	68%	Complete loss of function	140
1219393	<i>cj1287c</i>	-		Malate oxidoreductase		T	-	Deletion	Tyr 200 - STOP	52%	Complete loss of function	78
1278680	<i>cj1345c</i>	-		M99 family peptidase		A	-	Deletion	Leu 57 - STOP	88%	Probable loss of function	238
1425977	<i>cj1491c</i>	-		Two component regulator	GAAAAAT	A	-	Deletion	Asn 184 - Met / Ile 187 - STOP	19%	Probable loss of function	67
1492035	<i>cj1564</i>	+		Methyl-accepting chemotaxis signal protein		AA	-	2X Deletion	Met 12 - Glu / Asn 13 - STOP	98%	Complete loss of function	23

Table 11: Wild Type 11168 DJK strain gene deletions. The table lists the variations which will likely result in gene deletions in the new lab wild type strain. The majority of these changes originate as SNPs which result in a frame shift and a subsequent change to an early stop codon. The percentage lost/alterd column details how much of the amino acid sequence is lost or severely altered as a result of the change. Interestingly 4 of the genes shown here encode for crucial components of the motility complex and 2 genes encode for chemotaxis components. This is discussed later.

Genome Sequencing Table-12: WT DJK strain, pseudogene re-activations											
Position	Gene	Strand	Gene Name	Description (<i>C. jejuni</i> NCTC11168 Annotation)	Reference Poly Tract	Reference	Variant	Variant Type	Predicted Effect (Translation)	Predicted Effect (Phenotype)	Illumina Read Coverage
420550	<i>cj0455c</i>	-		Hypothetical Protein (Pseudogene)		T	C	Substitution	TAA (STOP) - CAA (Gln)	Pseudogene active	243
1001550	<i>cj1064</i>	+	<i>nfsB</i>	Oxygen-insensitive nitroreductase (Pseudogene)		-	A	Insertion	Phe 112 - Ile / STOP 120 - Met	Pseudogene active	106
1404343	<i>cj1470c</i>	-	<i>gspF</i>	General secretion pathway protein (T2 Secretion) (Pseudogene)	TAAAAAT	-	A	Insertion	Met 270 - Asn / STOP 280 - Leu	Pseudogene active	12

Table 12: Wild Type 11168 DJK strain pseudogene re-activations. The table lists the variations found within pseudogene loci which result in restoration of a complete open reading frame. This occurs seemingly by SNPs causing a frame shift to remove a stop codon. It is unknown whether these restorations of complete ORFs actually lead to a functioning protein as gene expression is not known.

Genome Sequencing Table-13: WT DJK strain, other variations											
Position	Gene	Strand	Gene Name	Description (<i>C. jejuni</i> NCTC11168 Annotation)	Reference Poly Tract	Reference	Variant	Variant Type	Predicted Effect (Translation)	Predicted Effect (Phenotype)	Illumina Read Coverage
180707	<i>cj0184c</i>	-		Serine/threonine protein phosphatase		GT	-	2X Deletion	Frame shift, 12 additional AAs added onto C-terminal	Minor or no effect on function	172
221822	<i>cj0238</i>	+		Mechanosensitive ion channel family protein		-	G	Insertion	Frame shift, 23 additional AAs added onto C-terminal	Minor or no effect on function	108
393542	<i>cj0431</i>	+		ATP/GTP-binding protein	CATAAAAG	T	A	Substitution	Substitution alters stop codon, 41 additional AAs added onto C-terminal	Both short and long versions of Cj0431 exist in NCBI database	272
1078651	<i>cj1143</i>	+	<i>neuA1</i>	Bifunctional beta-1,4-N-acetylgalactosaminyltransferase / CMP-Neu5Ac synthase	CAAAAAAT	T	-	Deletion	Frame shift leads to stop codon 66% through the ORF	Protein loses C-terminal CMP-Neu5Ac synthase domain, N-terminal domain remains intact.	78

1121265	<i>cj1192</i>	+	<i>dctA</i>	C4 dicarboxylate transport protein		G	-	Deletion	Frame shift alters AA sequence for final 5% of sequence, protein shorter by 2 AA	Minor or no effect on function	574
---------	---------------	---	-------------	------------------------------------	--	---	---	----------	--	--------------------------------	-----

Table 13: Wild Type 11168 DJK strain other strain variations. The table lists variations found within the DJK strain genome which do not fall into any of the previous categories. Those listed here show variations which may influence or modify protein function without a complete loss of function.

Genome Sequencing Table-14: WT 11168-Hypermotile												
Position	Gene	Strand	Gene Name	Unique to 11168-H	Description (<i>C. jejuni</i> NCTC11168 Annotation)	Reference Poly Tract	Reference	Variant	Variant Type	Predicted Effect (Translation)	Predicted Effect (Phenotype)	Illumina Read Coverage
180707	<i>cj0184c</i>	-		No	Serine/threonine protein phosphatase		GT	-	2X Deletion	Frame shift, 12 additional AAs added onto C-terminal	Minor or no effect on function	172
393542	<i>cj0431</i>	+		No	ATP/GTP-binding protein	CATAAAAG	T	A	Substitution	Substitution alters stop codon, 41 additional AAs added onto C-terminal	Both short and long versions of Cj0431 exist in databases	272
420550	<i>cj0455c</i>	-		No	Hypothetical Protein (Pseudogene)		T	C	Substitution	TAA (STOP) - CAA (Gln)	Internal stop codon altered to allow for complete ORF, gene function unknown.	243
760188	<i>cj0807</i>	+		No	7-alpha-hydroxysteroid dehydrogenase		A	G	Substitution	Lys 198 - Glu	Minor or no effect on function	126
1336117	<i>cj1401c</i>	-	<i>tpiA</i>	Yes	Triosephosphate isomerase		A	G	Substitution	Asn 10 - Ser	Minor or no effect on function	65
1604692	<i>cj1682c</i>	-	<i>gltA</i>	Yes	Citrate synthase		C	G	Substitution	Ala 187 - Tyr	Minor or no effect on function	141

Table 14: Wild Type 11168-H strain variations. The table lists all 6 variations seen between the NCTC11168-RID strain and the reference 11168 genome. Only two of the changes are unique to 11168-H (*cj1401c* and *cj1682c*) and both of these are amino acid substitutions which are unlikely to have much change on gene function.

Genome Sequencing Table-15: *Δcj0422c* strains

Position	Gene	Strand	Gene Name	<i>Δcj0422c</i> strain	Description (<i>C. jejuni</i> NCTC11168 Annotation)	Reference Poly Tract	Reference	Variant	Variant Type	Predicted Effect (Translation)	Percentage Lost / Altered	Predicted Effect (Phenotype)	Illumina Read Coverage
199139	<i>cj0203 - cj0204</i>			2	Citrate Transporter, Oligopeptide Transporter	GTTTTTTTG	-	T	Insertion	Intergenic region	-	Minor or no effect on function	12
199853	<i>cj0204</i>	+		1, 2	Oligopeptide transporter		-	A	Insertion	Leu 207 - Thr, Glu 241 - STOP	64%	Likely complete loss of function	424
221827	<i>cj0238</i>	+		1, 2	Mechanosensitive ion channel		-	T	Insertion	Ser 608 - Lys, Ser 610 - STOP	3%	Minor or no effect on function	98
234820	<i>cj0256</i>	+		1	Lipid A ethanolaminephosphotransferase	CTTTTTTA	-	T	Insertion	Leu 76 - Phe, Ser 82 - STOP	84%	Likely complete loss of function	21
613964	<i>cj0653c</i>	-		1, 2	Aminopeptidase		T	C	Substitution	Tyr 351 - His	-	Minor or no effect on function	438
613974	<i>cj0653c</i>	-		1, 2	Aminopeptidase		G	A	Substitution	-	-	Minor or no effect on function	406
613996	<i>cj0653c</i>	-		1, 2	Aminopeptidase		T	C	Substitution	Val 340 - Ala	-	Minor or no effect on function	388
614021	<i>cj0653c</i>	-		1, 2	Aminopeptidase		C	T	Substitution	-	-	Minor or no effect on function	337
614033	<i>cj0653c</i>	-		1, 2	Aminopeptidase		A	G	Substitution	Lys 328 - Glu	-	Minor or no effect on function	315
614052	<i>cj0653c</i>	-		1, 2	Aminopeptidase		C	A	Substitution	-	-	Minor or no effect on function	312
614128	<i>cj0653c</i>	-		1, 2	Aminopeptidase		C	T	Substitution	Ala 296 - Val	-	Minor or no effect on function	185
614181	<i>cj0653c</i>	-		1, 2	Aminopeptidase		T	C	Substitution	-	-	Minor or no effect on function	138
614249	<i>cj0653c</i>	-		1, 2	Aminopeptidase		G	A	Substitution	Glu 256 - lys	-	Minor or no effect on function	90
614355	<i>cj0653c</i>	-		1, 2	Aminopeptidase		C	T	Substitution	-	-	Minor or no effect on function	38
614473	<i>cj0653c</i>	-		1, 2	Aminopeptidase		C	T	Substitution	Ala 181 - Val	-	Minor or no effect on function	103
615242	<i>cj0654c</i>	-		1, 2	Transmembrane transport protein (pseudogene)		C	T	Substitution	-	-	Pseudogene remains inactive	133
615250	<i>cj0654c</i>	-		1, 2	Transmembrane transport protein (pseudogene)		A	G	Substitution	-	-	Pseudogene remains inactive	142

615268	<i>cj0654c</i>	-		1, 2	Transmembrane transport protein (pseudogene)		A	G	Substitution	-	-	Pseudogene remains inactive	122
615283	<i>cj0654c</i>	-		1, 2	Transmembrane transport protein (pseudogene)		C	T	Substitution	-	-	Pseudogene remains inactive	116
615621	<i>cj0654c</i>	-		1	Transmembrane transport protein (pseudogene)	CTTTTTTTG	-	T	Insertion	-	-	Pseudogene remains inactive	32
615635	<i>cj0654c</i>	-		1, 2	Transmembrane transport protein (pseudogene)		C	T	Substitution	-	-	Pseudogene remains inactive	30
639006	<i>cj0685c</i>	-	<i>cipA</i>	1	Invasion protein	ACCCCCCCA	C	-	Deletion	His 296 - Ile, Leu 300 - STOP	33%	Likely complete loss of function	50
1545190	<i>cj1617</i>	+	<i>chuD</i>	1	Hemin uptake system substrate-binding protein		TATTTAAGACTT	-	12X Deletion	Leu 176 - Ile 179 Lost	1%	Minor or no effect on function	53

Table 15: $\Delta cj0422c-1$ and $\Delta cj0422c-2$ strain variations. The table lists the variations which are unique to either one or both of the $\Delta cj0422c$ strains. Other variations are found but they are also found in the 11168-DJK strain and are not listed here. Both the strains shown contain a chloramphenicol resistance cassette inserted within the *cj0422c* gene, which is also not shown here. The table shows that the gene *cj0653c* and the upstream pseudogene *cj0654c* contain many SNPs with seemingly not change in function, the reason for so many SNPs within a single gene is unknown. The genome sequences shown here are discussed further in section (Section 3.3.3). As shown in (Figure 26) the $\Delta cj0422c-1$ strain is polymyxin-B sensitive and the $\Delta cj0422c-2$ strain is not.

3.2.16 Genomic analysis of the *cj0422c* mutant strains

As shown by the data in (Figure 20) the original *cj0422c* mutant strain was highly sensitive to the CAMP polymyxin-B, however this was un-related to the intended mutation and in fact appears to have been acquired at some point as an unknown secondary mutation. The whole genome analysis shown in (Table 15) reveals that the strain ($\Delta cj0422c-1$) contains a single SNP variation within the *cj0256* ORF. The insertion of an additional thymine nucleotide leads to a frame shift resulting in an early stop codon 16% through the open reading frame. This almost certainly leads to a complete loss of function as the full gene is no longer translated. The Cj0256 protein is annotated as a LipidA modification enzyme (Lipid A ethanolaminephosphotransferase) which has been studied in a previous publication (Cullen and Trent, 2010). This work showed that Cj0256 is responsible for attaching pEtN (phosphoethanolamine) to not only Lipid A, but also to the flagellar rod protein (FlgG). The study also showed that deletion of *cj0256* resulted in a 20-fold increase in sensitivity to polymyxin-B. This strongly suggests that the high sensitivity seen in the *cj0422c* mutant strain was the result of this randomly acquired mutation, the other genome sequenced *cj0422c* strain ($\Delta cj0422c-2$) does not contain this SNP and is polymyxin-B resistant. Other members of the lab re-produced the *cj0423* and *cj0424* mutant strains in the new wild type DJK background strain and these showed no notable difference in sensitivity to polymyxin-B. This leads to the conclusion that the *cj0421c-cj0425* gene cluster is not involved in CAMP resistance and from this point onwards the project is primarily about finding a role for the genes.

3.3 Chapter 3 Discussion

The initial aim of this chapter was to bioinformatically analyse the *cj0421c-cj0425* gene cluster (previously known as the *rid* genes) to determine how widespread these genes are between *Campylobacter* strains. Following this a series of mutant strains were created in *C. jejuni* 81116 which are located within the same locus but are structurally different to the archetypal genes from *C. jejuni* 11168. It was thought that the project would then focus on the roles of Cj0421c and Cj0422c and how they are able to respond to and defend against cationic antimicrobial peptides, however as the project proceeded the original data showing the gene cluster was involved in resisting CAMPs did not stand up to further scrutiny and much of the hypothesis broke down. As such most of the data presented in this chapter was collected while assuming that the genes being studied were involved in CAMP resistance. For this discussion I will re-assess the data shown in this chapter without assuming a role in CAMP resistance.

3.3.1 Bioinformatic analysis of the *rid* operon

Members of the *Campylobacter* genus are known for their high levels of genetic diversity (Meinersmann *et al.*, 2002). Much of the current research on the epidemiology of *Campylobacter* uses whole genome sequencing to assess which genes are required for transit through the food processing industry, the so called 'farm to fork' transit (Wassenaar, 2011). As part of this work many complete *Campylobacter* genome sequences are available for analysis with data on when and where they originated (Sheppard *et al.*, 2010). The bioinformatic analysis shown in (Figure 11) used data kindly provided from the lab of Dr Sam Sheppard to assess how prevalent the *cj0421c-cj0425* genes are in other *Campylobacter* strains. It was initially thought that there may be some correlation between the presence of the genes and the animal source the strain was isolated from. This turned out not to be the case, however it should be noted that the number of genomes analysed is comparatively small and that with ever larger numbers of *Campylobacter* genomes being sequenced a correlation with a certain source may emerge in the future. The data did however show that the genes are (a) not found in all *Campylobacter* strains and (b) the structural genes *cj0423-cj0425* are only found in around 40% of the strains analysed. This led on to the analysis in (Figures 12-13) showing that there are 3 sub types of these gene clusters distributed between different *Campylobacter* strains, there may also be other groups that have not been found yet. This adds complexity to the system as whatever the roles of these genes are, different *Campylobacter* species appear to need different groups of genes to respond to the same stimuli.

3.3.2 *Cj0423 and holin like proteins*

The analysis of the protein sequences shown in (Figure 14) shows that between the gene clusters from different *C. jejuni* sub strains, a single family of small inner membrane proteins is conserved between them, making this the only protein type which is found in all 3 sub types. These proteins are all quite small and most of the length is composed of transmembrane domains (either 2 or 3) leaving little room for any other functional domains. It was initially thought that these proteins may act as a way of stabilising the inner membrane in response to CAMP attack or possibly acting to repel positively charged CAMPs by the presence of some positively charged residues facing the periplasm. Protein BLAST analysis of Cj0423 shows some similarity with T4 bacteriophage immunity proteins which exclude phage DNA to prevent superinfection from competing phage (Lu and Henning, 1989). The T4 immunity protein is a similar length to Cj0423 and also contains 2 transmembrane domains so it may be that the BLAST similarity is due to the shared domain architecture rather than a shared role. However, the other small transmembrane proteins from *C. jejuni* 81116 and RM1221 within the same operon do not show any homology to predicted phage immunity proteins. The other family of proteins with a similar domain architecture to Cj0423 are holins.

Holins are small membrane spanning-proteins, generally produced by some bacteriophages that spontaneously form large flexible pores in the cytoplasmic membrane of both Gram-positive and Gram-negative bacteria, sometimes up to the micron scale in diameter (Savva *et al.*, 2014). The term holin was first used to describe the 'λS' protein from λ phage which forms part of the λS-R lysis cassette (Young, 2014). Deletion of the λs gene resulted in phage particles being unable to escape the host cell cytoplasm and the λR protein was shown to degrade peptidoglycan but could not be exported outside the cytoplasmic membrane without λS. Further work showed holin proteins are associated with the timing of bacteriophage lysis, the holin protein is rapidly produced and permeabilises the cytoplasmic membrane allowing various peptidoglycan amidases to reach the cell wall and lyse the cell (Wang *et al.*, 2000). Holins are often found with antiholin proteins which inhibit the formation of the pores, the antiholins are sometimes found within the same ORF as the holin where the two are co-expressed from alternate start codons (Neely and Friedman, 1998, Tran *et al.*, 2005). This co-expression of holins with antiholins causes the phage to enter a 'lysis inhibition' (Lin) state where the two proteins are in a state of equilibrium. Through an as yet unknown mechanism the equilibrium suddenly shifts to favour the holins and spontaneous pores form in the membrane (Young *et al.*, 2000). The Lin equilibrium state can also be broken by the addition of energy inhibitors such as cyanide or dinitrophenol (Žiedaite *et al.*, 2005), the authors

hypothesize that the loss ATP may act as a signal for the phage to lyse the host cells as the host is most likely near complete exhaustion at this point. How cellular energy levels maintain this equilibrium is unknown. The chaperone GroEL complex has been shown to bind to the λ phage antiholin at a 6:1 ration whereas the holin is bound at up to 350:1, both of which require ATP, this may be related to the timing of induced lysis (Deaton *et al.*, 2004). Holins typically contain one or more transmembrane domains and polymerize within the cytoplasmic membrane, there are thought to be up to 7 families of holins distributed throughout various phage genomes, all are characterized by containing one or more transmembrane domains (Reddy and Saier, 2013).

As shown in (Figure 15) holins can contain a number of transmembrane domains and form pores by polymerising within the membrane. The exact role of Cj0423 itself is not a part of this study so the data presented is only based on sequence analysis. Several hypotheses about what the gene cluster may do are tested in later chapters, Cj0423 and the similar inner membrane proteins from other *C. jejuni* strains are assumed to be holing-like genes.

3.3.3 Secondary mutations in the *cj0422c* mutant and whole genome sequencing

The CAMP sensitivity data presented in this chapter aimed to show that deletion of the *cj0422c* mutant resulted in increased sensitivity to CAMPs and that complementation would restore the wild type resistant phenotype. As shown in (Figures 20-21) the mutant strain does show increased sensitivity to CAMPs but could not be effectively complemented, this was shown to be due to a single SNP found within the *cj0256* ORF as discussed in (Section 3.2.16). This data from the genome sequences of the two *cj0422c* mutant strains effectively dispels the entire CAMP resistance mechanism and explains why the western blot and qRT-PCR data shown in (Figures 22-23) show no up-regulation of the *cj0423-cj0425* operon in response to polymyxin-B.

Another interesting result from the *cj0422c* mutant genome sequences is that some of the genes which are differentially expressed in the microarray data (Figure 7) also contain SNPs from the sequencing data. Expression of both *cj0204* and *cj0653c* is altered in the microarray study (with *cj0204* being down-regulated -4.4 fold and *cj0653c* being up-regulated +5.2 fold). In both the genome sequenced *cj0422c* mutant strains *cj0204* contains an insertion that most likely leads to a loss of gene function (Table 15). The *cj0422c* mutant strains also show 11 SNPs within the *cj0653c* ORF (making up almost half of all the unique SNPs within the *cj0422c*

mutant strains), this is a strangely large number of SNPs for a single gene and all of them are nucleotide substitutions. Out of these 11 substitutions 6 of them result in amino acid changes and 5 result in no changes. None of these amino acid changes are within the active site of the Cj0653c peptidase domain so it is unknown what if any changes in protein function these substitutions lead to. It was first thought that these alterations in the *cj0204* and *cj0653c* ORFs may be due to the *cj0422c* mutant altering their expression to such an extent that the genes are altered or removed to compensate (this theory is along the same lines as the data shown in (Figure 25) whereby the *cj0423* promoter was naturally removed in response to being continuously overexpressed). However, an alternative theory is that the changes in gene expression observed in the original microarray data are in fact because of the SNPs rather than causing them. The microarray data relies on a fluorescent oligonucleotide probe, specific for individual genes, hybridizing to cDNA or RNA samples. The relative difference between the fluorescence of each gene is calculated to produce a fold change in gene expression. This assumes that the nucleotide sequence between each strain is identical as the probes are usually designed from an annotated genome sequence. It also assumes that even if the probe sequence is slightly different then the differences will cancel out as the two strain will share the same differences. However, should the two strains have a different sequence for the same gene, this could lead to an artificial difference in recorded gene expression, where in fact it is due to variations in the genome sequence rather than a difference in cDNA or RNA levels of that particular gene. This theory is tested in the next chapter where a new *cj0422c* mutant strain is produced in the new WT-DJK background strain and qRT-PCR is performed to validate the microarray data.

3.3.4 Genomic analysis of the wild type DJK strain

Whole genome sequencing of the 2010 laboratory wild type strain has revealed many interesting differences between the lab strain and the original *C. jejuni* wild type NCTC11168-GS which was first sequenced in 2001 (Parkhill *et al.*, 2000). The data shown in (Tables 9-13) show the 49 changes between the two strains. These are split up into SNPs in intergenic regions, in frame amino acid changes, gene deletion, potential pseudogene re-activations and other changes. Many of these changes are likely the result of randomly acquired variations and SNPs in the genome sequence.

3.3.5 Wild type DJK strain intergenic regions and in frame substitutions

The WT DJK lab strain contains 7 SNPs within intergenic regions, since these changes are not within any ORFs it is difficult to predict what if any effects these changes may have. Some may affect gene expression by altering the promoter regions. The data is shown in (Tables 9-10). The lab strain also contains 21 nucleotide substitutions within ORFs, the majority of which result in a single amino acid change. It is possible that some of these amino acid changes may affect protein function.

3.3.6 Wild type DJK strain gene deletions

The WT DJK strain contains 13 nucleotide changes within ORFs that lead to frame shift changes which likely lead to a loss of gene function. The list of these changes is shown in (table 11). From these 13 genes 4 are involved in flagellar production and 2 are involved in chemotaxis which explains why the lab strain is non motile, a feature which is common amongst heavily passaged *Campylobacter* lab strains (Gaynor *et al.*, 2004). The loss of motility and chemotaxis is likely due to the lack of any need for motility in laboratory environments and the large amount of resources expended on assembling and maintaining a functional flagellar. This may also explain why non motile laboratory strains of *Campylobacter* are able to grow at a faster rate than wild type strains under the same conditions as all the resources saved from the motility apparatus can be used elsewhere. Another common feature of laboratory adapted *Campylobacter* strains is the loss of the spiral shape (Gaynor *et al.*, 2004). Formation of the spiral shape in *Campylobacter* has been shown to involve specific modifications of peptidoglycan chains (Firdich *et al.*, 2014). The Cj1345c protein shows some homology to an M99 family peptidase which has been shown to be responsible for modifying peptidoglycan in *Helicobacter pylori* (Kim *et al.*, 2014). Since this is the only known peptidoglycan modification enzyme which is altered in this new genome sequence, its removal may be responsible for the lack of a spiral shape. The DJK strain also shows further adaptations to the lab environment as 2 genes involved in nutrient transport have been lost, both the *lctP* and *dcuA* genes (L-lactate permease and C4-dicarboxylate transporter respectively) contain frame shift mutations. This is likely because the strain is routinely cultured on rich growth media and so does not require all available carbon sources when easier to use alternatives (such as serine) are present. The lack of the L-lactate permease is relevant to another part of the project and is discussed later on (Section 7.1).

3.3.7 *Wild type DJK strain pseudogene re-activations*

The WT DJK strain contains 3 SNPs within pseudogene loci which when analysed show a restoration of the full ORF, the 3 genes are shown in (Table 12). This is not a well-studied area of microbiology and the reasons for these genes becoming re-activated is unknown.

Pseudogene formation in bacteria is thought to be the result of generally random SNPs forming within coding regions causing a frame shifts or early stop codon formation (Lerat and Ochman, 2005). While it was generally thought that a pseudogene would typically be lost from the normally efficient bacterial genome reasonably quickly, due to the wastefulness of producing fragmented gene products and replicating unused DNA (Goodhead and Darby, 2015), there is some evidence suggesting that pseudogenes may be longer lasting in some microbial populations than previously thought (Goodhead and Darby, 2015). However, the authors note that this may be because the pseudogenes are under some (if small) form of selection pressure due to either a fragmented gene product or possibly even RNA interference affecting gene expression elsewhere. The concept of a pseudogene re-activating by a single SNP within the ORF is by its very nature highly unlikely. Single random SNPs almost anywhere within an open reading frame could render a gene non-functional (as seen in Table 12), while the 3 genes are shown here as 're-activating' because of a single incredibly specific nucleotide changes (1 has a substitution and 2 have insertions) to become functional again. DNA sequence BLAST analysis shows that the SNPs within these ORFs causing them to be annotated as pseudogenes are only found in the original annotated NCTC11168-GS sequence. It seems much more likely that the original genome sequence contains errors which led to these 3 genes being mis-annotated as pseudogenes.

3.3.8 *Wild type DJK strain other variations*

The remaining 5 SNPs within the new DJK strain (Table 13) occur inside ORFs and their effects are harder to categorise. Four of these SNPs cause the gene to become slightly longer or shorter which may not have much of an effect on gene function (this also may be due to the original NCTC11168 sequence containing sequence errors as discussed previously). One of the changes however might have interesting effects. A nucleotide deletion in *cj1143c* encoding a bifunctional beta-1,4 N-acetylgalactosiminyltransferase / CMP-Neu5Ac synthase (at the N and C-terminal ends respectively) may cause the final product to lose the C-terminal domain of the protein but retain an active C-terminal CMP-Neu5Ac synthase.

3.3.9 Genomic analysis of the NCTC 11168-Hypermotile strain

The hypermotile variant of *C. jejuni* NCTC11168 was originally isolated in a study looking at phase variable motility genes, cultured isolates of *C. jejuni* NCTC11168 were assayed for spontaneous changes in motility (Karlyshev *et al.*, 2002). This led to the culture of the NCTC11168-Hypermotile strain which is presented here. This strain is used as a good model organism for studying *Campylobacter* in chicken colonisation studies as motility is required for effective colonisation. This strain is used by other lab members to study the roles of Cj0423 and Cj0424 in chicken colonisation experiments. The data is shown in chapter 4.

At this point in the project it was decided to use the newly sequenced wild type NCTC11168-DJK strain as a fresh starting point in order to determine what the roles of Cj0421c and Cj0422c are in regulating the *cj0423-cj0425* operon. The roles of the Cj0423, Cj0424 and Cj0425 proteins were being studied by other members of the lab in tandem within with this study.

4 [Chapter 4 – Testing the potential roles of the cj0421c-cj0425 cluster by mutagenesis.](#)

4.1 [Chapter 4 Introduction](#)

Data presented in the previous chapter showed that the 5 gene cluster spanning the *cj0421c-cj0425* region of the *C. jejuni* NCTC1168 genome is not involved in resistance to cationic antimicrobial peptides as was previously hypothesised. Following on from this it was decided to re-sequence the genome of the laboratory strain used in this study, now named *Campylobacter jejuni* NCTC 11168-DJK, which is now the default wild type for the rest of the study unless otherwise stated. The primary aim of this chapter is to determine the roles of Cj0421c and Cj0422c in regulating the rest of the operon. Other lab members working on the same project area will focus on the roles of the individual structural proteins Cj0423, Cj0424 and Cj0425.

Cj0422c is a DNA-binding Helix-Turn-Helix domain protein which has been shown to bind to a specific 18bp palindromic repeat sequence found slightly upstream of *cj0423* thereby blocking transcription (Hitchcock, 2011). Microarray data from the *cj0422c* mutant (Figure 7) shows that a broad range of genes are differentially expressed throughout the genome in the mutant strain. However, the recent analysis of the *cj0422c* mutant genome sequence suggests this may be an artifact caused by seemingly random SNPs, this is discussed in (Section 3.3.3). This chapter aims to more accurately dissect the role of Cj0422c as a master regulator by producing a new mutant construct and assaying any changes in gene expression by qRT-PCR. The other main focus of this project is the role of Cj0421c, a protein that contains 6 transmembrane regions within the N-terminal domain and a cytoplasmic facing globular domain at the C-terminal end. BLAST searches of the C-terminal domain have shown no strong hits though there is some weak homology to a class of proteins containing GGDEF motifs. This class of proteins are diguanylate cyclases which produce the second messenger cyclic-di-GMP which typically controls the switch from motile to sessile states in bacteria (Romling *et al.*, 2013). Two conserved motifs within this family of proteins (the GGDEF active site and the RXXD inhibition site) are essential for the enzymatic activity of these proteins. The Cj0421c protein does not possess either the conserved GGDEF or RXXD motifs associated with this family of proteins. Further still there are other families of proteins that are associated with c-di-GMP signaling in bacteria, such as the c-di-GMP degrading HD-GYP and EAL domains and the c-di-GMP sensing PilZ domain. The genome of *Campylobacter jejuni* NCTC11168 shows no close homologies with any of these families of c-di-GMP related proteins, indicating that even if Cj0421c was a degenerate GGDEF binding protein, *C. jejuni* could not have a working c-di-GMP

signaling pathway. The roles of the Cj0421c and Cj0422c proteins are examined in detail in Chapter 6, this chapter will focus primarily on mutagenesis and complementation of the two genes. Since the new genome sequenced lab strain is now being used as the primary wild type for studying these genes, this chapter will also focus on producing mutant strains in *cj0423*, *cj0424* and *cj0425*. A series of further mutant strains will also be produced to delete multiples of these genes, a double mutant will delete both the regulatory genes *cj0421c* and *cj0422c*. A triple mutant will delete all 3 structural genes *cj0423*, *cj0424* and *cj0425*. And a quintuple mutant will delete the entire gene cluster *cj0421c-cj0425*.

The first aim of this chapter is to confirm the role of Cj0422c as a master regulator by qRT-PCR analysis of the mutant strain. The chapter then moves onto determining the roles of the individual genes by mutagenesis, and to assay for differences between the strains. The biggest challenge is that there is currently no evidence to even suggest or imply a role for most of these genes. Over the course of the work described in this chapter a variety of experiments were performed to test for phenotype difference under a variety of conditions and stresses. Since there is no overall theory being tested here the hypothesis behind each experiment is explained throughout the chapter.

During the course of the work described in this chapter the crystal structure of Cj0425 was solved to a 2 Å resolution by Halah Al-Haideri and Dr John Rafferty (Unpublished data). The protein shows strong similarity to a class of cysteine protease inhibitor proteins known as cystatins. The structure revealed that protein possesses a disulfide bond and is composed of 4 antiparallel β -sheet strands wrapped around a central α -helix. Cystatin proteins are a class of cysteine protease inhibitors, cysteine proteases such as papain hydrolyse peptide bonds using a reactive thiol group from a cysteine residue. In papain a reactive ion pair is formed by the interaction between a Cys free thiol group and a protonated His residue. The imidazole group on the His residue is protonated by the action of a nearby Trp residue (Polgár, 1973), other cysteine proteases function in a similar way using Cysteine and Histidine residues. The cystatin family act to inhibit cysteine proteases by competitively blocking the cysteine containing active site; since there are many types of cysteine proteases the K_d binding constant between cystatins and proteases can vary between different proteins (Turk and Bode, 1991). Cystatins are well studied in eukaryotes as they can often play a crucial role in disease progression, the role of cystatins in higher eukaryotes appears to be as a way to post translationally regulate the action of cysteine proteases (Turk *et al.*, 2008). Eukaryotic cystatins appear to be reasonably non-specific inhibitors and do not differentiate between different cysteine

protease enzymes (though they can differentiate between endo and exo-peptidase enzymes), typically cystatins inhibit cysteine proteases in a 1:1 ratio (Jenko *et al.*, 2003).

Cystatins are not well studied in bacteria, probably due to the lack of annotated cystatins in microbial genomes (Kordiš *et al.*, 2009), it may be that many bacteria contain cystatins but they cannot be identified bioinformatically. Many bacteria also encode other families of cysteine protease inhibitors such as chagasins (Rigden *et al.*, 2002), which are structurally different from cystatins. One of the better studied examples of a microbial cystatin is the *E. coli* protein YebF, which is secreted outside the cell and acts to protect against the secreted toxin colicin-M (Gérard *et al.*, 2011). This toxin is also secreted by *E. coli* strains so YebF acts as an immunity protein as part of a secreted toxin-antitoxin system. The YebF cystatin has been shown to be folded by the DsbA oxidase in the periplasm and then exported by outer membrane porins into the extracellular environment (Prehna *et al.*, 2012).

The protein sequence for Cj0425 encodes a periplasmic signal sequence and 2 cysteine residues which are likely oxidized to form a disulfide bond by the DsbA system in the *C. jejuni* periplasm. There is no evidence to suggest that Cj0425 is exported outside the periplasm since western blot analysis of culture media could not find any evidence of Cj0425 export. This work was performed by Halah Al-Haideri (data not shown). The potential role of this protein as part of the whole *cj0421c-cj0425* operon is examined in this chapter and in chapter 6.

4.2 Chapter 4 Results

4.2.1 Generation of mutant and complementation strains in *C. jejuni* 11168-DJK

4.2.2 Construction of *cj0421c* and *cj0422c* mutants in *C. jejuni* 11168-DJK

The mutant constructs were generated by isothermal assembly cloning using methods previously described in (Section 2.11) and previously used in chapter 3 (Section 3.2.6).

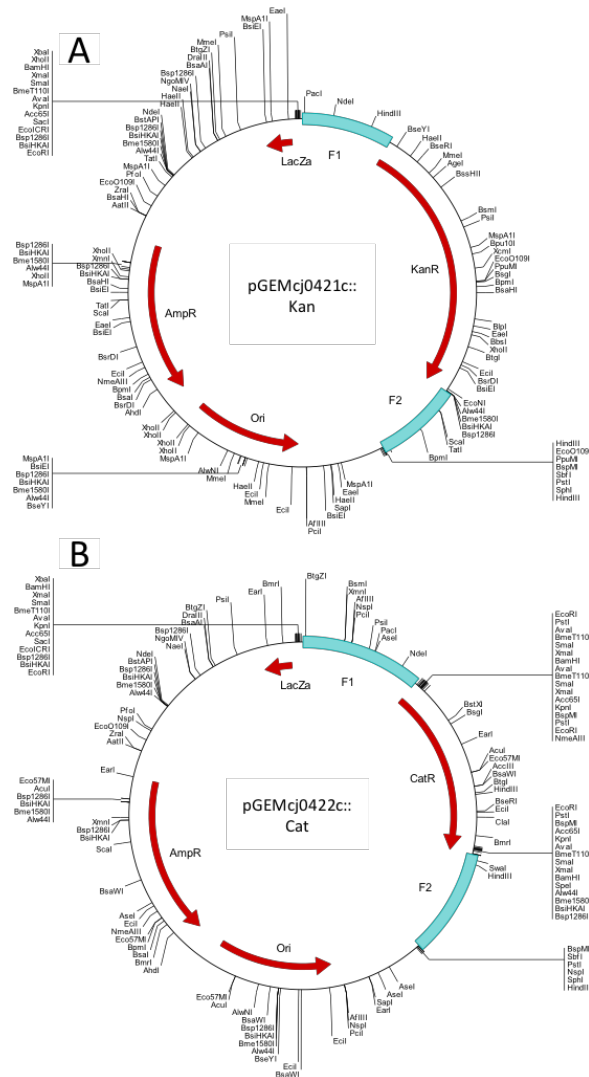


Figure 28: Plasmid maps of the *cj0421c* and *cj0422c* knockout vectors. All plasmids shown were produced by ISA cloning in the same way as (Figure 16). The *cj0421c* mutant (A) used the kanamycin resistance cassette (*kanR*) and the *cj0422c* mutant (B) used the chloramphenicol resistance cassette (*catR*). Both plasmids were confirmed by DNA sequencing of the inserted fragments (Data not shown).

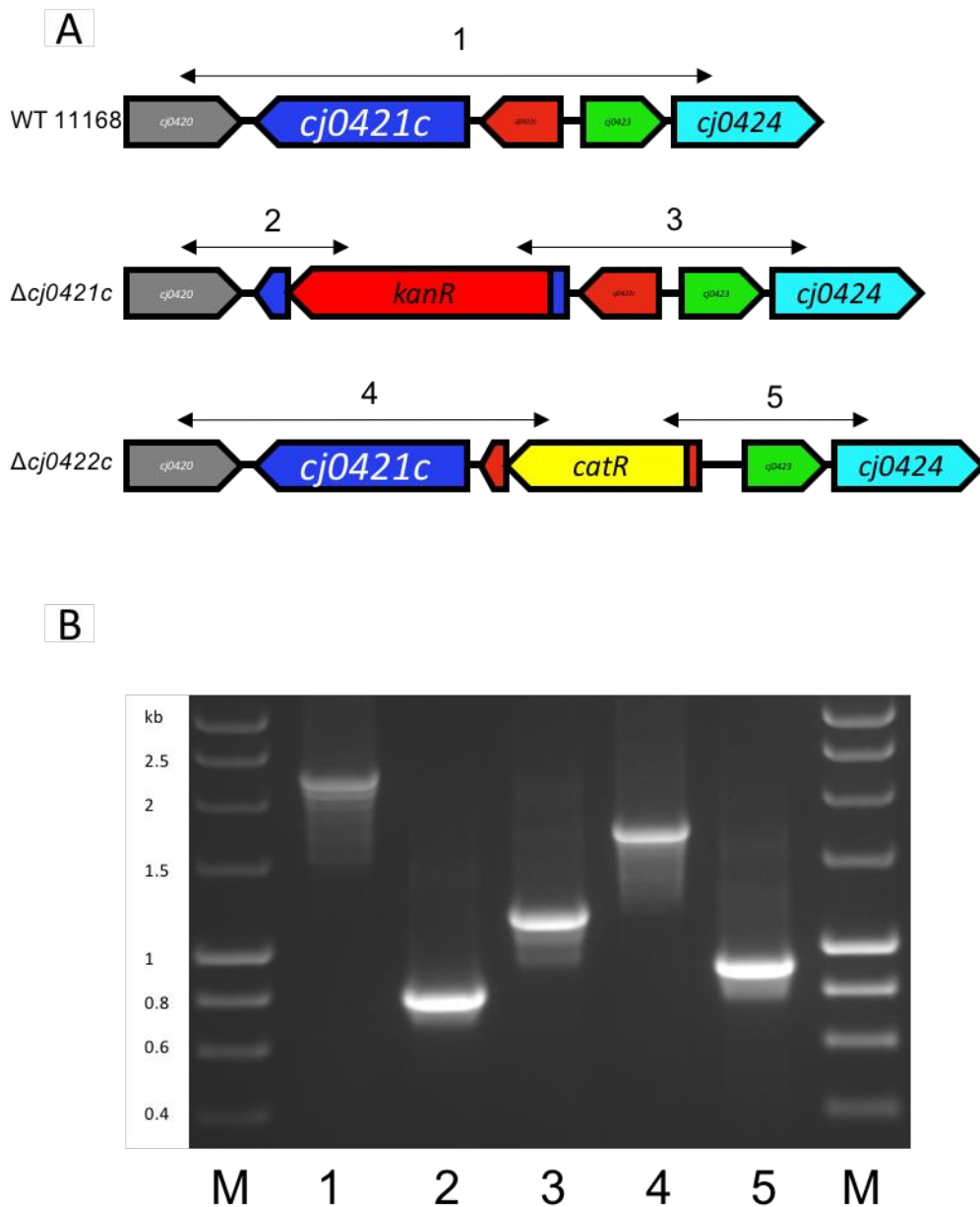


Figure 29: Mutagenesis of *cj0421c* and *cj0422c* in *C. jejuni* 11168-DJK. The ISA vectors shown in (Figure 28) were transformed into *C. jejuni* 11168 to remove most of the genes of interest. (A) shows the gene arrangements of WT 11168 and the 2 mutant strains following removal of the gene and insertions of the kanamycin resistance cassette for *cj0421c* and the chloramphenicol resistance cassette for *cj0422c*. The mutants were confirmed by PCR analysis. The numbers correspond to the PCR products expected using the knockout screening primers. The PCR confirmation bands are shown in (B). The lane numbers correspond to the numbers shown above the arrows, the band sizes also correspond to the arrow lengths. The expected PCR product sizes in bp are 1-2306, 2-822, 3-1285, 4-1769, 5-911. The PCR primers were designed to be outside the flanking primers used to produce the constructs; this was to show that the construct was correctly inserted in the correct orientation and that the double recombination had removed the remaining vector DNA.

4.2.3 Construction of *cj0423*, *cj0424* and *cj0425* mutants in *C. jejuni* 11168-DJK

The mutant constructs were generated by isothermal assembly cloning using methods described in (Section 2.11).

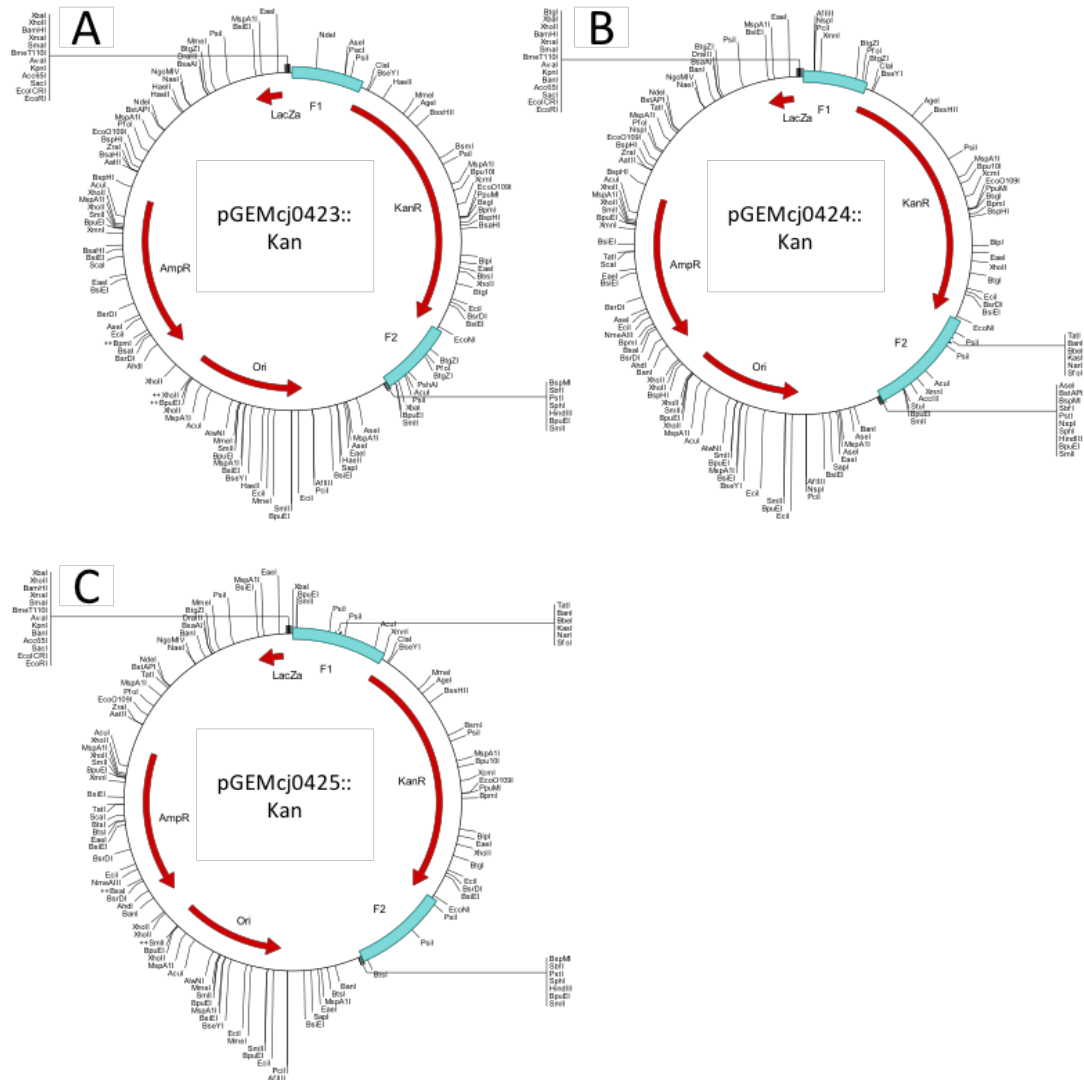


Figure 30: Plasmid maps of the *cj0423*, *cj0424* and *cj0425* knockout vectors. All plasmids shown were produced by ISA cloning in the same way as (Section 3.2.6) by Dr Andrew Hitchcock and Halah Al-Haideri, all constructs shown used the kanamycin resistance cassette (*kanR*). The maps show the knockout constructs for *cj0423* (A), *cj0424* (B) and *cj0425* (C). All plasmids were confirmed by DNA sequencing of the inserted fragments (Data not shown).

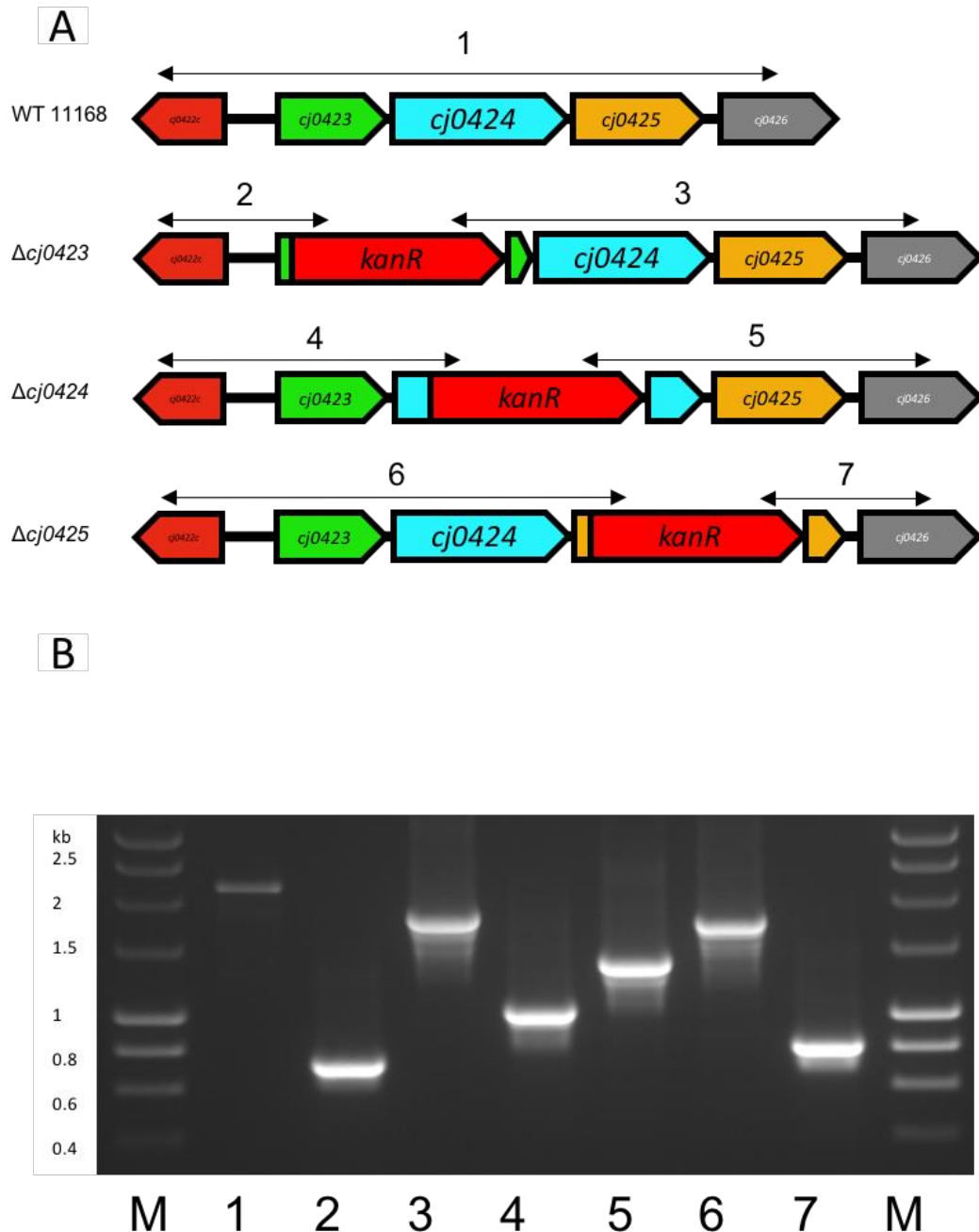


Figure 31: Mutagenesis of *cj0423*, *cj0424* and *cj0425* in *C. jejuni* 11168-DJK. The ISA vectors shown in (Figure 30) were transformed into *C. jejuni* 11168 to remove the genes of interest. (A) shows the gene arrangements of WT 11168 and the 3 mutant strains following removal of most of the gene and insertions of the kanamycin resistance cassettes. The mutants were confirmed by PCR analysis. The numbers correspond to the PCR products expected using the knockout screening primers. The PCR confirmation bands are shown in (B). The lane numbers correspond to the numbers shown above the arrows, the band sizes also correspond to the arrow lengths. The expected PCR product sizes in bp are 1-2170, 2-747, 3-1863, 4-1041, 5-1413, 6-1698, 7-826. The PCR primers were designed to be outside the flanking primers used to produce the construct, this was to show that the construct was correctly inserted in the correct orientation and that the double recombination had removed the remaining vector DNA.

4.2.4 Construction of double, triple and quintuple mutants in *C. jejuni* 11168-DJK

The mutant constructs were generated by isothermal assembly cloning using methods described in (Section 2.11).

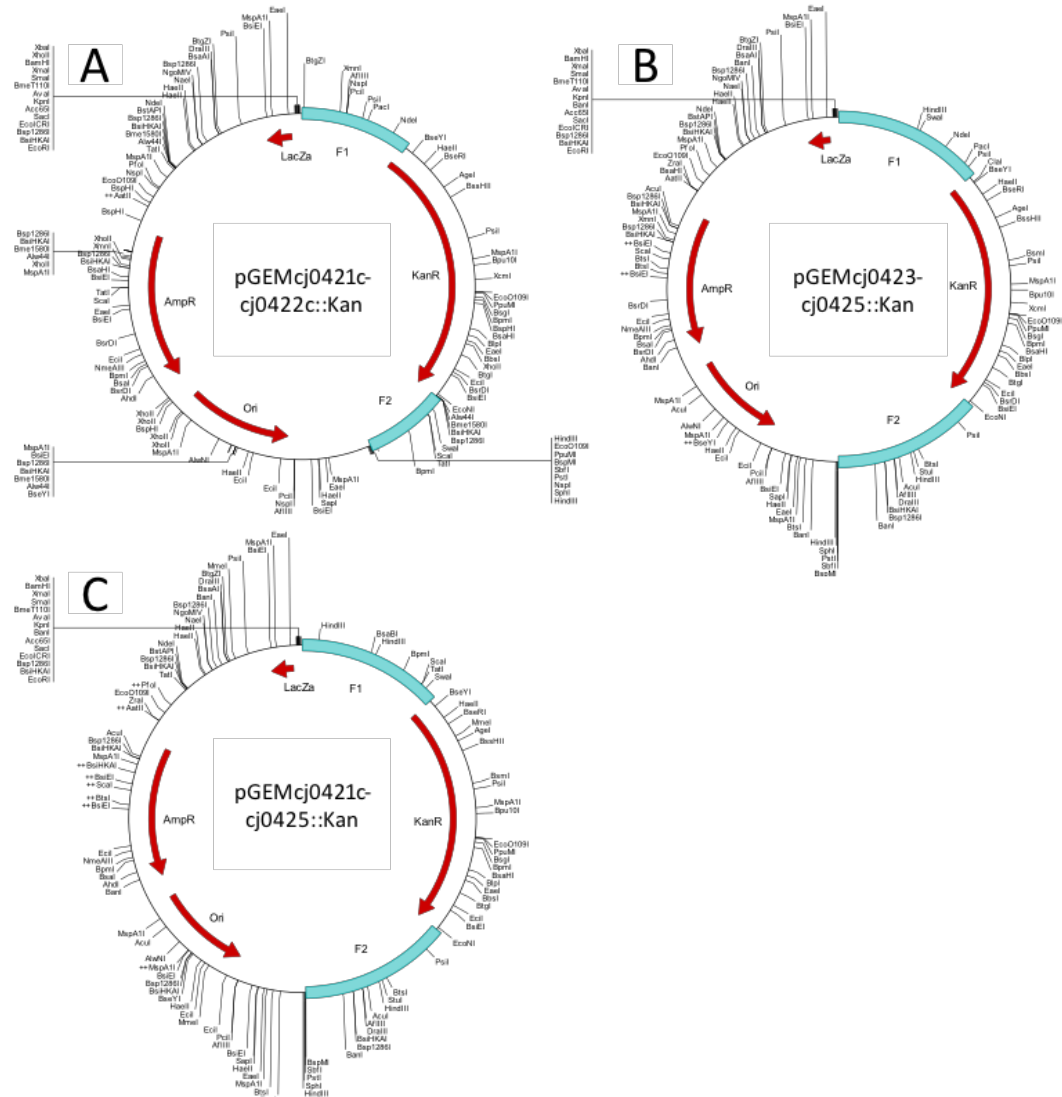


Figure 32: Plasmid maps of the double, triple and quintuple knockout vectors. All plasmids shown were produced by ISA cloning in the same way as (Figure 16), plasmids (B and C were produced by Dr Jonathan Butler. All constructs shown used the kanamycin resistance cassette (*kanR*). The maps show the knockout constructs for the double mutant (*cj0421c-cj0422c*) (A), the triple mutant (*cj0423-cj0424-cj0425*) (B) and the quintuple mutant (*cj0421c-cj0422c-cj0423-cj0424-cj0425*) (C). All plasmids were confirmed by DNA sequencing of the inserted fragments (Data not shown).

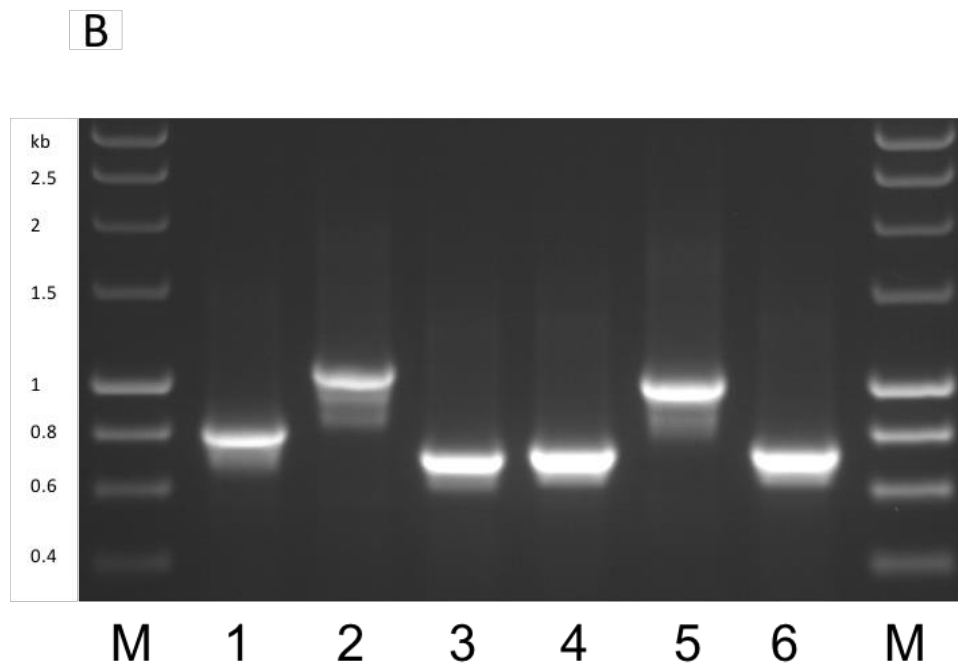
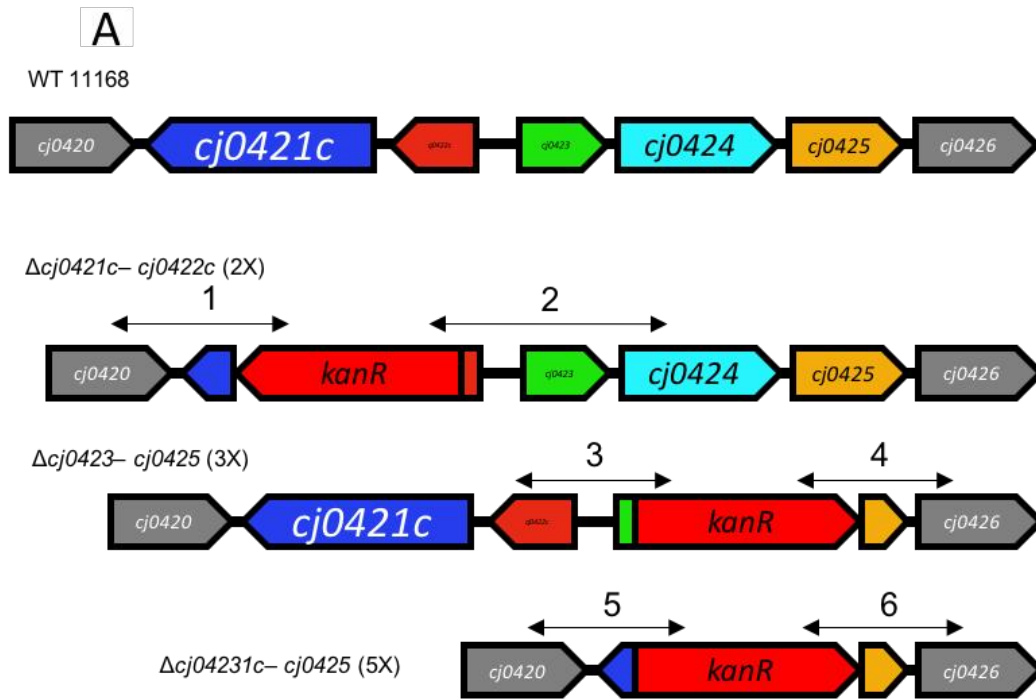


Figure 33: Production of the double, triple and quintuple mutants in *C. jejuni* 11168-DJK. The ISA vectors shown in (Figure 32) were transformed into *C. jejuni* 11168 to remove the genes of interest. (A) shows the gene arrangements of WT 11168 and the 3 mutant strains following removal of most of the gene and insertions of the kanamycin resistance cassettes. The mutants were confirmed by PCR analysis. The numbers correspond to the PCR products expected using the knockout screening primers. The PCR confirmation bands are shown in (B). The lane numbers correspond to the numbers shown above the arrows, the band sizes also correspond to the arrow lengths. The expected PCR product sizes in bp are 1-822, 2-1072, 3-732, 4-752, 5-1030, 6-752. The PCR primers were designed to be outside the flanking primers used to produce the construct, this was to show that the construct was correctly inserted in the correct orientation and that the double recombination had removed the remaining vector DNA.

4.2.5 qRT-PCR analysis of the *cj0421c* and *cj0422c* mutants

Much of the previous work on the *cj0422c* mutant is based on the microarray results shown in (Figure 7). This shows that the Cj0422c protein acts to repress the *cj0423-cj0425* operon under normal growth conditions. The new mutant strains produced in the NCTC11168-DJK background strain were tested for changes in gene expression by qRT-PCR analysis. As mentioned in the previous chapter the *cj0422c* mutant contained a variety of secondary mutations, including a complete loss of the *cj0423* promoter region (Figure 25). To try and prevent this happening again frozen stocks of the mutant strains were produced quickly from individual colonies from the transformation plates. Four of these individual colonies were analysed by qRT-PCR for changes in *cj0423* gene expression. There was some evidence from previous work that Cj0421c may have a role in affecting gene expression, this hypothesis was also tested by qRT-PCR analysis. The data in (Figure 34) shows a strong up-regulation of *cj0423* in the *cj0422c* mutant strain (around 50-fold) and a similar up-regulation in the double mutant (around 30-fold). There is a slight drop in expression in the *cj0421c* mutant (around 0.5-fold).

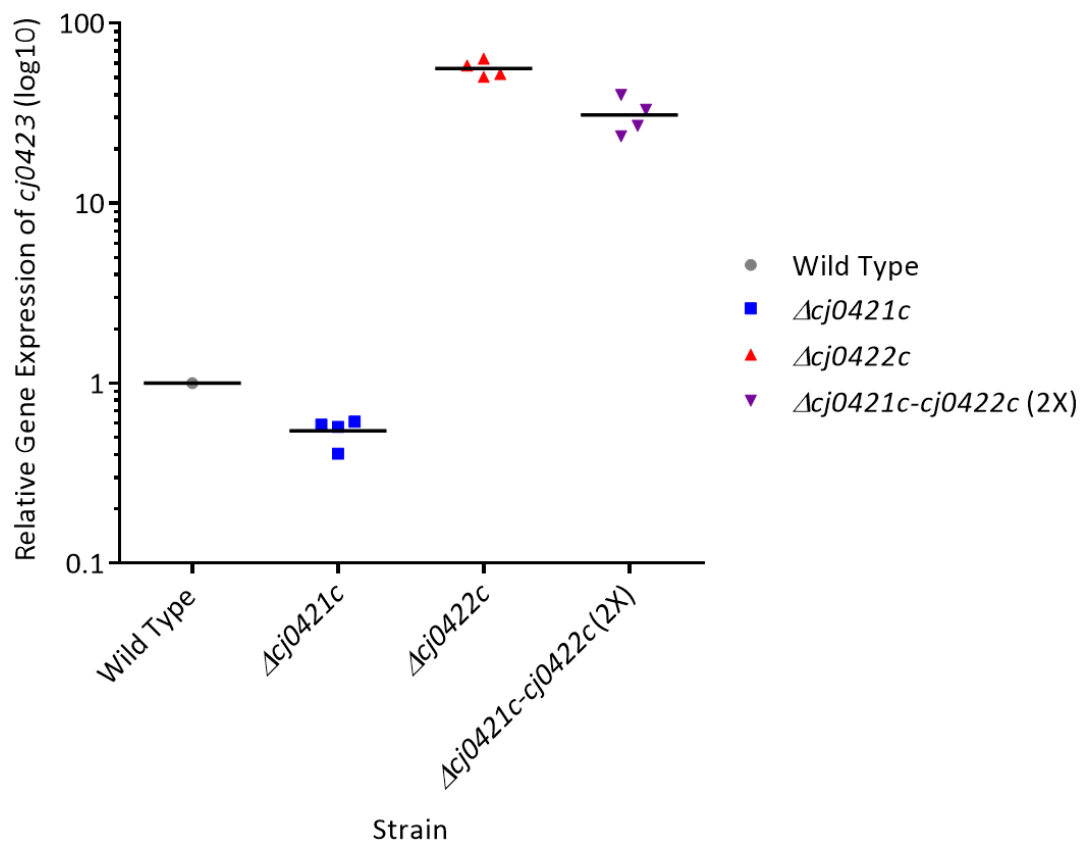


Figure 34: Quantitative Reverse Transcriptase PCR analysis of *cj0423* in the *cj0421c* and *cj0422c* mutants. Whole cell RNA was extracted and analysed using methods described previously (Section 2.15). 4 separate biological replicates of the *cj0421c*, *cj0422c* and the double mutants were analysed by assaying the expression of *cj0423*, the data was matched to the wild type expression which is given a value of 1. The error bars show standard deviations from the 4 biological replicates shown as each data point.

4.2.6 Construction of complementation constructs by Isothermal Assembly Cloning (ISA)

Following construction and screening of the mutant strains, complementation constructs were produced for *cj0421c* and *cj0422c*. The complementation system used in *C. jejuni* involves inserting the gene of interest into the pseudogene locus *cj0046*. This is achieved by using a family of plasmids known as the pK/C46 plasmids (Thomas *et al.*, 2011). These plasmids contain either a kanamycin or chloramphenicol resistance cassette located between two fragments of the *cj0046* pseudogene locus. The gene of interest is usually amplified by PCR with a *BsmBI* restriction site at either end, this is then ligated into the *BsmBI* site located between the *cj0046* fragments within the plasmid. The genes of interest can either be cloned into the plasmid downstream of the *metK* Promoter (medium level constitutive expression), the *fdxA* promoter (Iron inducible promoter) or they can be cloned with the native promoter (Van Vliet *et al.*, 2001). The native promoter is always used for complementation if possible or unless there is a particular reason not to. Typically, *C. jejuni* complementation requires cloning into the *BsmBI* restriction site of one of the p46 plasmids; however the *BsmBI* (or *Esp3I*) restriction enzyme is not very efficient at digesting DNA. Since no additional antibiotic selection markers are being inserted into the vector, the plasmid will often re-ligate with no insertion since the *BsmBI* sticky ends are compatible. Since ISA cloning has proved so efficient at producing knockout constructs for *Campylobacter*, as part of this project I attempted to improve the complementation system employed in the lab by modifying the complementation protocol to use ISA cloning.

The ISA system is efficient at incorporating multiple linear DNA fragments into a single vector, thereby eliminating the need for multiple restriction enzyme cloning steps. For this to work the DNA products need to be amplified by high fidelity PCR with overlapping 'adapter' fragments attached to each end of the sequence. These complementary adapters act like longer sticky ends and allow the fragments to attach during the ISA reaction. This technique was employed to insert a single fragment into the p46 family of vectors. Since the p46 families of vectors contain a single antibiotic resistance marker (kanamycin or chloramphenicol) the transformants cannot be selected for using a newly inserted marker. To overcome this, the resistance marker already in the plasmid was amplified as two separate fragments by high fidelity PCR, the fragments contained a 20bp overlapping adapter region which allowed for the ISA reaction to re-incorporate the two fragments into a complete resistance marker. This allowed the resistance cassette to act as a selective marker whereas before it could not. This is explained in further detail below.

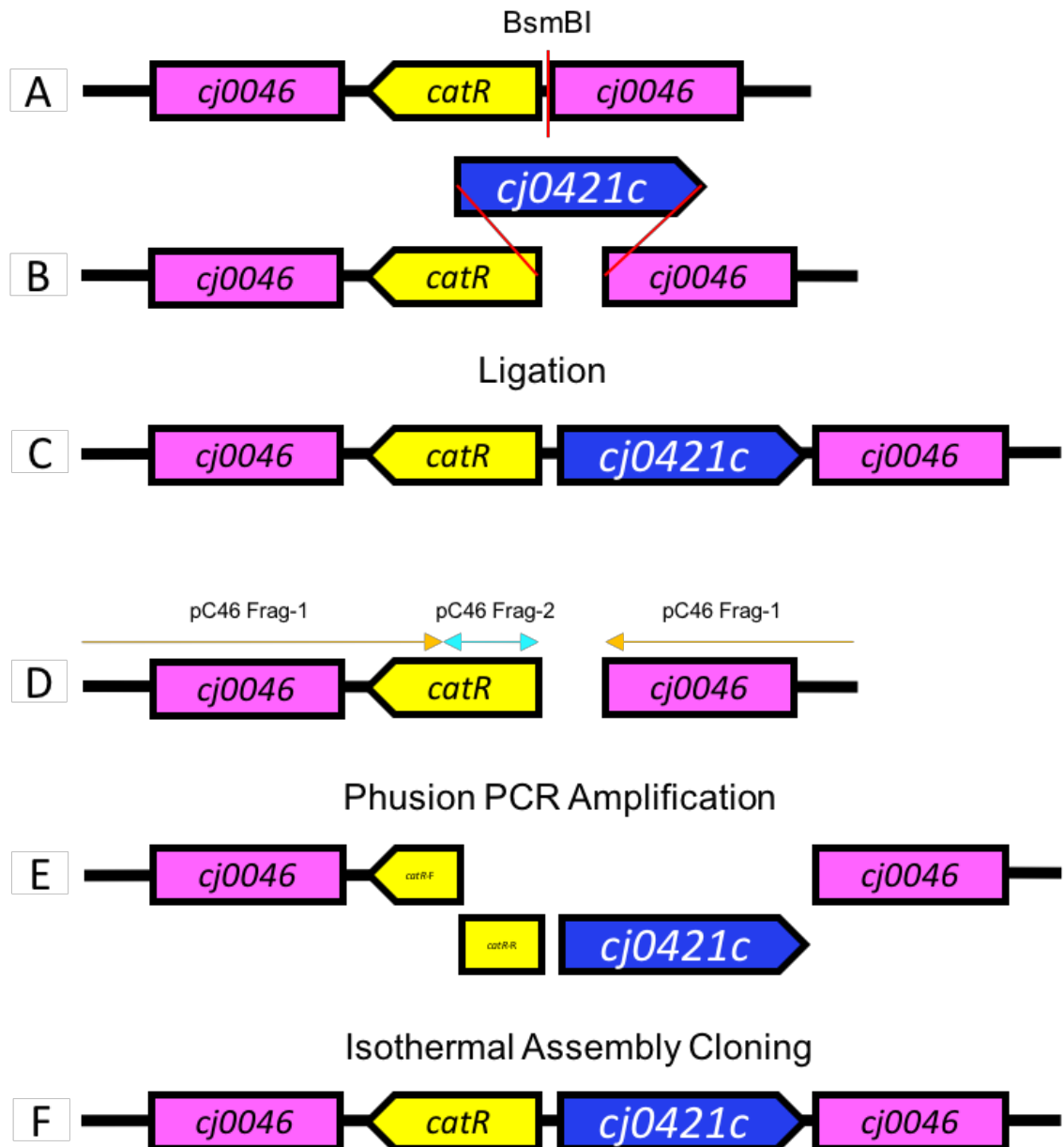


Figure 35: Generation of a complementation construct by Isothermal Assembly (ISA) cloning. (A-B-C) all show the normal restriction site cloning method for producing complementation plasmids in pC46. (A) shows the location of the BsmBI restriction site within the pC46 plasmid. (B) shows the plasmid after digestion with BsmBI and (C) shows the ligation step to insert *cj0421c* into the vector. This method is slow and often results in very low product yield as the BsmBI enzyme is inefficient at digesting DNA. (D-E-F) all show the new method for producing complementation vectors used in this study. (D) shows the linearised pC46 plasmid, high fidelity PCR reactions amplify the two fragments shown by the orange and blue arrows (the orange arrow continues around the rest of the pC46 plasmid). These two fragments can then be used in an ISA reaction. (E) shows the ISA fragments used in a typical reaction. The *cj0421c* fragment is amplified from genomic DNA with adapter fragments on either end to allows for ligation into the plasmid. (F) shows the completed plasmid following the ISA reaction.

Using this new cloning method means that a fully formed plasmid can only be made if the ISA reaction has successfully incorporated the gene of interest and it becomes much less likely to form an empty vector. It also allows for the gene of interest to be attached to the small

fragment (pC46 Frag-2) by overlap extension PCR which makes it practically impossible for the plasmid to re-form without the gene of interest. This technique is used in the next chapter. This method also allows for the large and small fragments to be re-used in later cloning procedures and since the small fragments contain the different promoter regions used in the *cj0046* complementation system these can be interchanged at will. This cloning system was used for each of the complementation vectors produced in this study and it did not once result in a reformed empty vector.

Since this study is primarily focused on the roles of Cj0421c and Cj0422c only these genes have been complemented. *cj0422c* contains its own promoter immediately upstream of the gene, so the complementation construct will include the native promoter and will be produced in the pK46 plasmid with a kanamycin resistance marker as the mutant was produced using the chloramphenicol marker. The *cj0421c* gene is located in an operon downstream of *cj0422c* so it cannot be complemented under its own promoter, instead it will be complemented using the *metK* promoter in the pC46-*metK* plasmid. The Cj0421c protein is predicted to contain 6 transmembrane domains and a cytoplasmic C-terminal domain. For this reason, I decided to produce 2 complementation strains for *cj0421c* with one using the complete gene under the *metK* promoter and a second construct only producing the C-terminal cytoplasmic domain, also under the *metK* promoter. The sequence used is shown below.

>Cj0421c

```
MFLLDFLISLSFIFEISALVLSFYFKNSKIFFLTLVLLGAKLPYFYTSFFQANLFVALFLPMIF
TLFCVGGKHHVLIILNKKNIASITTLIFIGILSIILPRNTTFNSAGLEFHFIALDFFKPVSELGFL
FFLVGLILIFIKTFKTKKEYYLLIAFFTAYFQFLFQEGAGIRYFEFASLVFCFYLLNHAYRLAFF
DTLTKLPNEKSLTRFTKGKNNYIIALLHFNELKDTKESYTKLILKQIAKILKRFRAKIFIVEND
FILIFNDKNQALNHLAFLESTLKNTEFNLENENFKPDFKLIWQESEENLDKNLQSLRARLLD
```

The transmembrane regions are highlighted in blue and the cytoplasmic domain is highlighted in yellow, for the C-terminal only complementation an extra methionine was added at the start of the domain as shown below. This is the same domain sequence used for the heterologous protein overexpression of Cj0421c used in a later chapter.

>Cj0421c-C-terminal

```
MDTLTKLPNEKSLTRFTKGKNNYIIALLHFNELKDTKESYTKLILKQIAKILKRFRAKIFIVEN
DFILIFNDKNQALNHLAFLESTLKNTEFNLENENFKPDFKLIWQESEENLDKNLQSLRARLLD
```

4.2.7 Construction of *cj0421c* and *cj0422c* complementation vectors

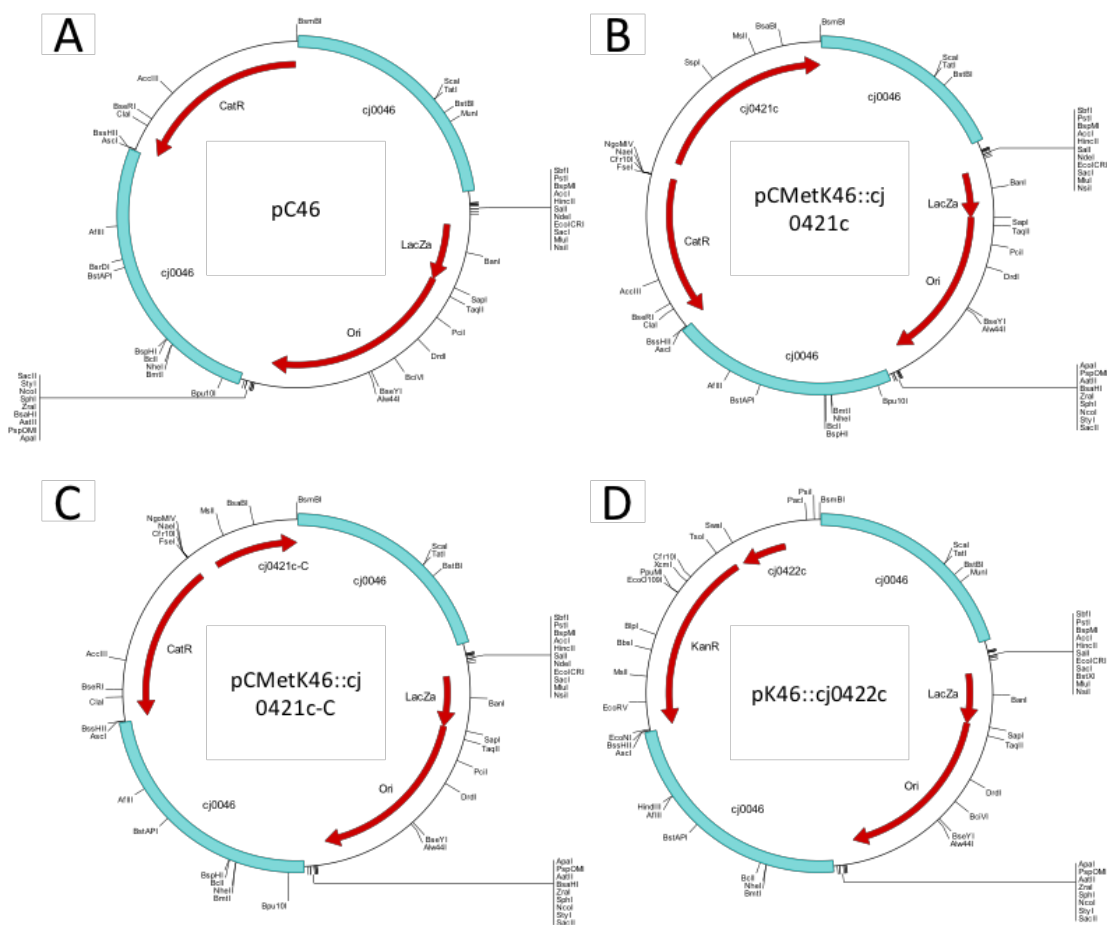


Figure 36: Plasmid maps of the *cj0421c* and *cj0422c* complementation plasmids. (A) shows the empty pC46 plasmid, (B) shows the full length *cj0421c* complementation plasmid *cj0421c* located downstream of the MetK promoter. (C) shows the truncated *cj0421c* gene as described in the previous section. (D) shows the *cj0422c* complementation plasmid in pK46 with its native promoter. The BsmBI cloning sites are all located at the top of the plasmid maps. All plasmids shown were produced by ISA cloning in the same way as described in (Figure 35). All plasmids were confirmed by DNA sequencing of the inserted fragments (Data not shown).

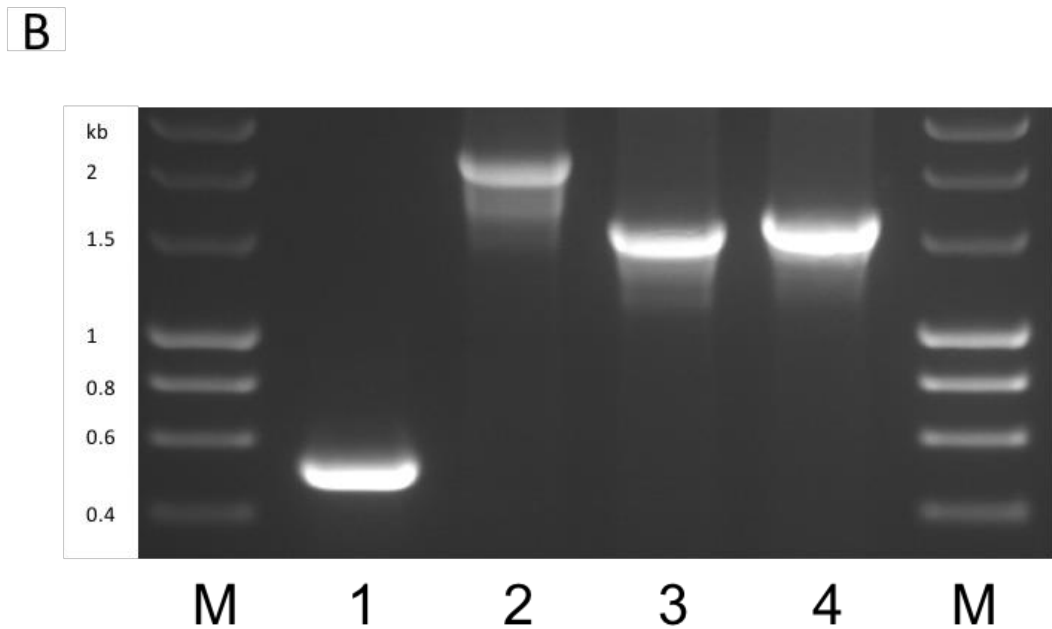
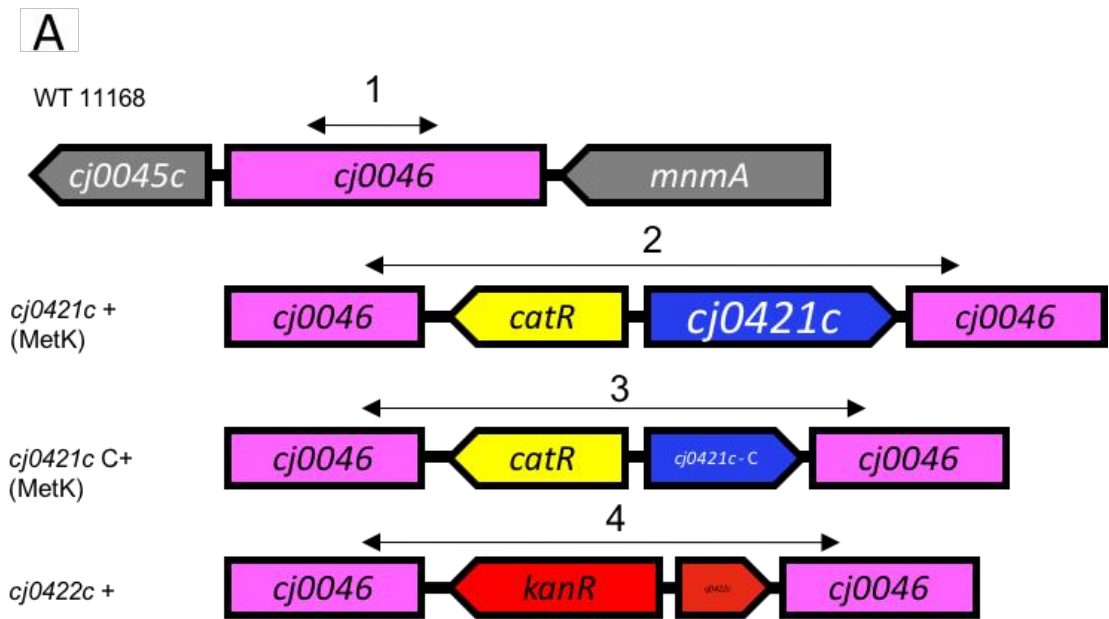


Figure 37: Production of *cj0421c* and *cj0422c* complementation strains in *C. jejuni* 11168-DJK. The ISA vectors shown in (Figure 36) were transformed into the *cj0046* pseudogene locus of respective *C. jejuni* 11168 mutant strains. (A) shows the gene arrangements of WT 11168 and the 3 complementation strains following insertion of the genes and the resistance cassettes. The strains were confirmed by PCR analysis. The numbers correspond to the PCR products expected using the p46 screening primers, the PCR confirmation bands are shown in (B). The lane numbers correspond to the numbers shown above the arrows, the band sizes also correspond to the arrow lengths. The expected PCR product sizes in bp are 1-544, 2-2195, 3-1622, 4-1676.

4.2.8 qRT-PCR analysis of the *cj0421c* and *cj0422c* complementation strains

The complementation plasmids were transformed into their respective mutant strains using methods described in (Section 2.14). To further analyse the role of Cj0421c in controlling gene expression the two *cj0421c* complementation strains were analysed by qRT-PCR analysis. It was hypothesised that Cj0421c may act as a 'sensor' domain for whichever signal activates the operon. While the *cj0421c* mutant shows no large change in *cj0423* gene expression, it may be that the C-terminal domain is able to influence gene expression either by interactions with the Cj0422c master regulator or by affecting gene expression directly. The data shown in (Figure 38) shows no significant changes in the expression of *cj0422c* or *cj0423* in the *cj0421c* mutant and complementation strains compared to wild type. The data shown in (Figure 39) shows that the expression of the *cj0423-5* operon is up-regulated in the *cj0422c* mutant while the expressions of *cj0204*, *cj0653c* and *cj0864* are not significantly altered.

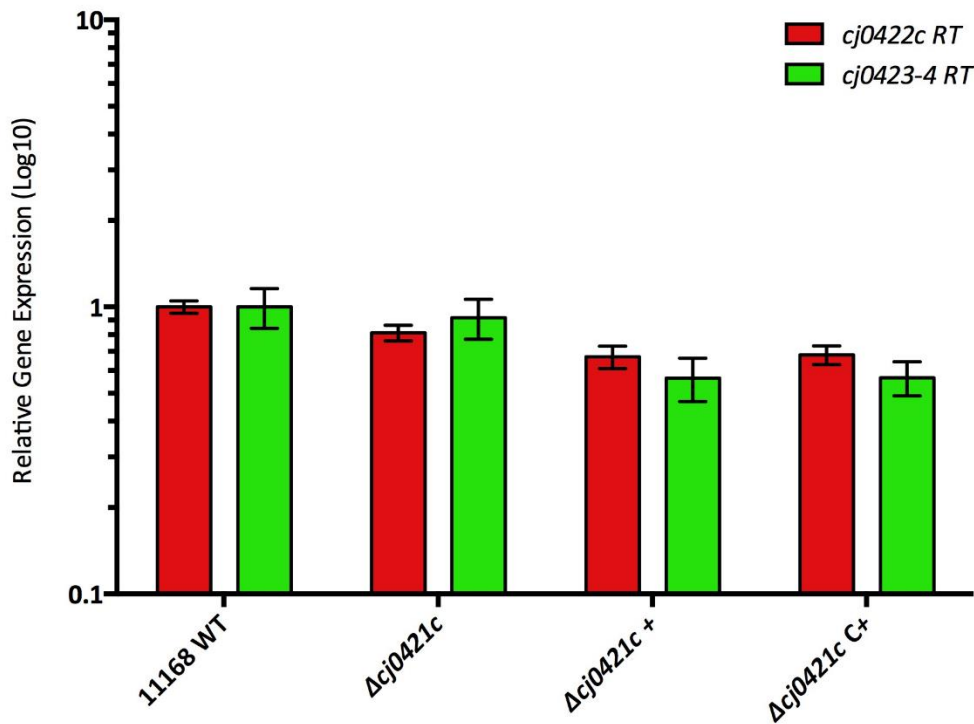


Figure 38: Quantitative Reverse Transcriptase PCR analysis of the *cj0421c* mutant and complementation strains. Whole cell RNA was extracted and analysed using methods described previously (Section 2.15). The red bars show the expression of *cj0422c* and the green bars show the expression of the *cj0423-cj0424* operon by using primers within each gene, the primers are listed in (Table 7). The error bars show the standard deviations from 3 technical repeats of 3 separately cultured biological repeats. The results for the mutant and complementation strains are shown as relative to the wild type expression.

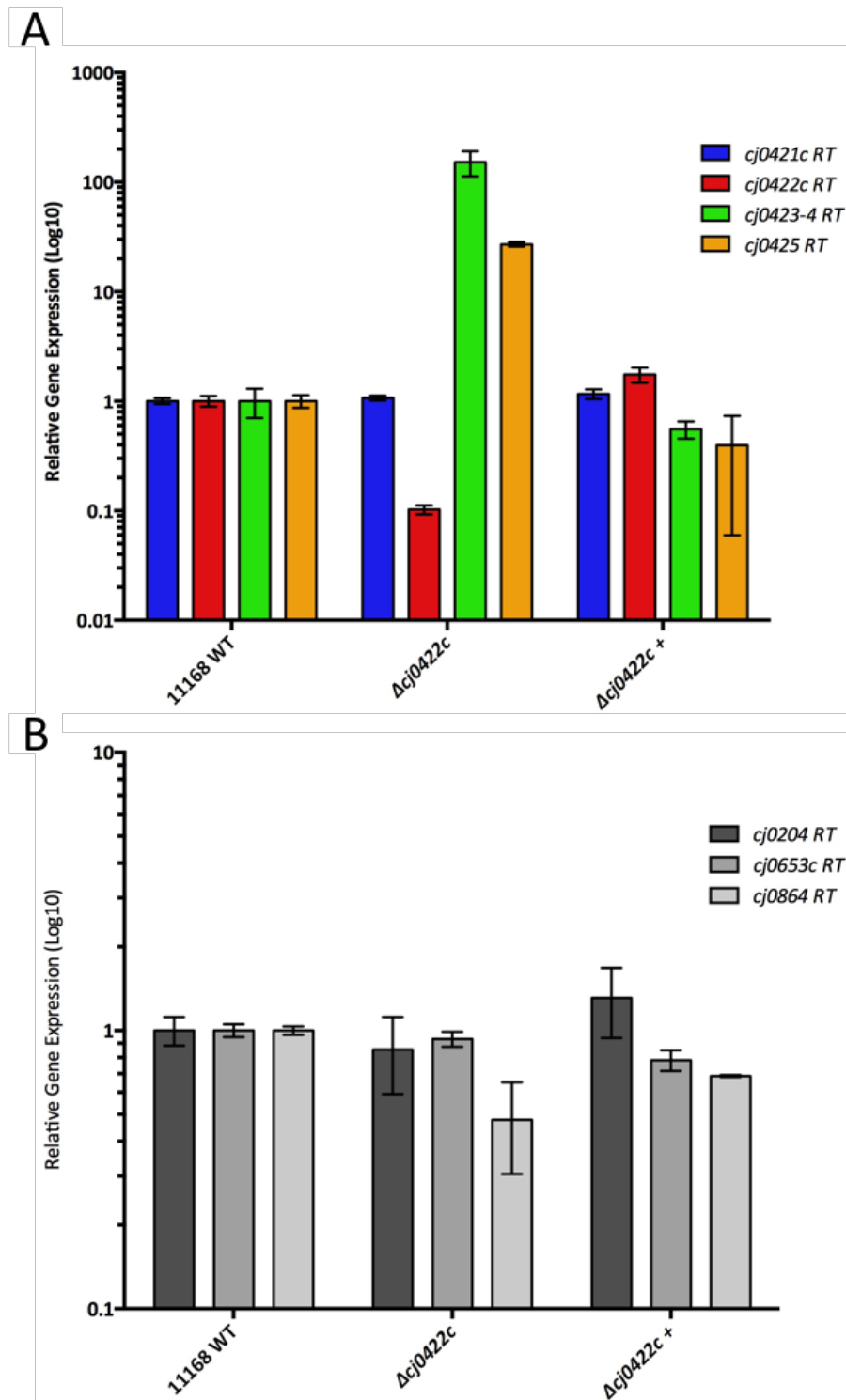


Figure 39: Quantitative Reverse Transcriptase PCR analysis of the *cj0422c* mutant and complementation strains. Whole cell RNA was extracted and analysed using methods described previously (Section 2.15). (A) shows that in the *cj0422c* mutant the expression of *cj0421c* is unchanged (blue bars) and the expression of the *cj0423-cj0425* operon is strongly up-regulated (green and orange bars). The red bar shows the expression of *cj0422c* itself in its own mutant strain. This was achieved by designing primers which bind upstream of the chloramphenicol insertion in the mutant thereby allowing transcription to be measured. (B) shows the expression of *cj0204*, *cj0653c* and *cj0864* in the *cj0422c* mutant and complementation strains, showing no real difference in gene expression in any of the genes. All primers are listed in (Table 7). The error bars show the standard deviations from 3 technical repeats of 3 separately cultured biological repeats. The results for the mutant and complementation strains are shown as relative to the wild type expression.

The data shown in (Figure 38) reveals that Cj0421c does not appear to have any direct effect on gene expression. While Cj0421c is still hypothesised to act as a 'sensor' protein for the gene cluster, it may need to be 'activated' in order to affect expression. The data shown in (Figure 39) shows that while Cj0422c does act as a repressor of the *cj0423-5* operon it does not seem to have any effect on the expression of *Cj0204*, *cj0653c* or *cj0684*. These 3 genes appeared to be differentially expressed in the microarray data shown in (Figure 7), which formed part of the hypothesis shown in (Figure 9) about CAMP resistance. The lack of any changes in gene expression shown here implies that the microarray data was inaccurate since qRT-PCR is a more sensitive and accurate way to determine gene expression. The reason for this inaccuracy is explained in the previous chapter (Section 3.3.3) whereby SNPs occurring within these genes may have altered the sensitivity of the microarray probes.

Following this confirmation of the *cj0422c* mutant phenotype I decided to continue looking for any changes in phenotype these mutants may possess. Initially this work focused on examining the mutant strains for any growth defects or any changes in antimicrobial sensitivity. It was decided that the *cj0422c* mutant is the best strain to use for detecting any changes in phenotype as the *cj0423-cj0425* operon is strongly repressed by Cj0422c under standard conditions, so in practical terms there is little difference in the expression of the structural genes between their respective mutant strains and wild type cells. Whereas in the *cj0422c* mutant strain the structural genes are strongly up-regulated making it useful as a way to study the structural genes.

4.2.9 The *cj0421c* and *cj0422c* mutant strains do not show any growth defects

To determine if the genes within the *cj0421c-cj0425* cluster have any effect on growth rate the *cj0421c* and *cj0422c* mutant strains were grown under normal conditions in broth cultures to measure growth rate. The 2X, 3X, and 5X mutant strains were also tested for any changes in growth rate. The data in (Figure 40) shows no appreciable difference in growth rate between the wild type DJK strain and the mutant strains.

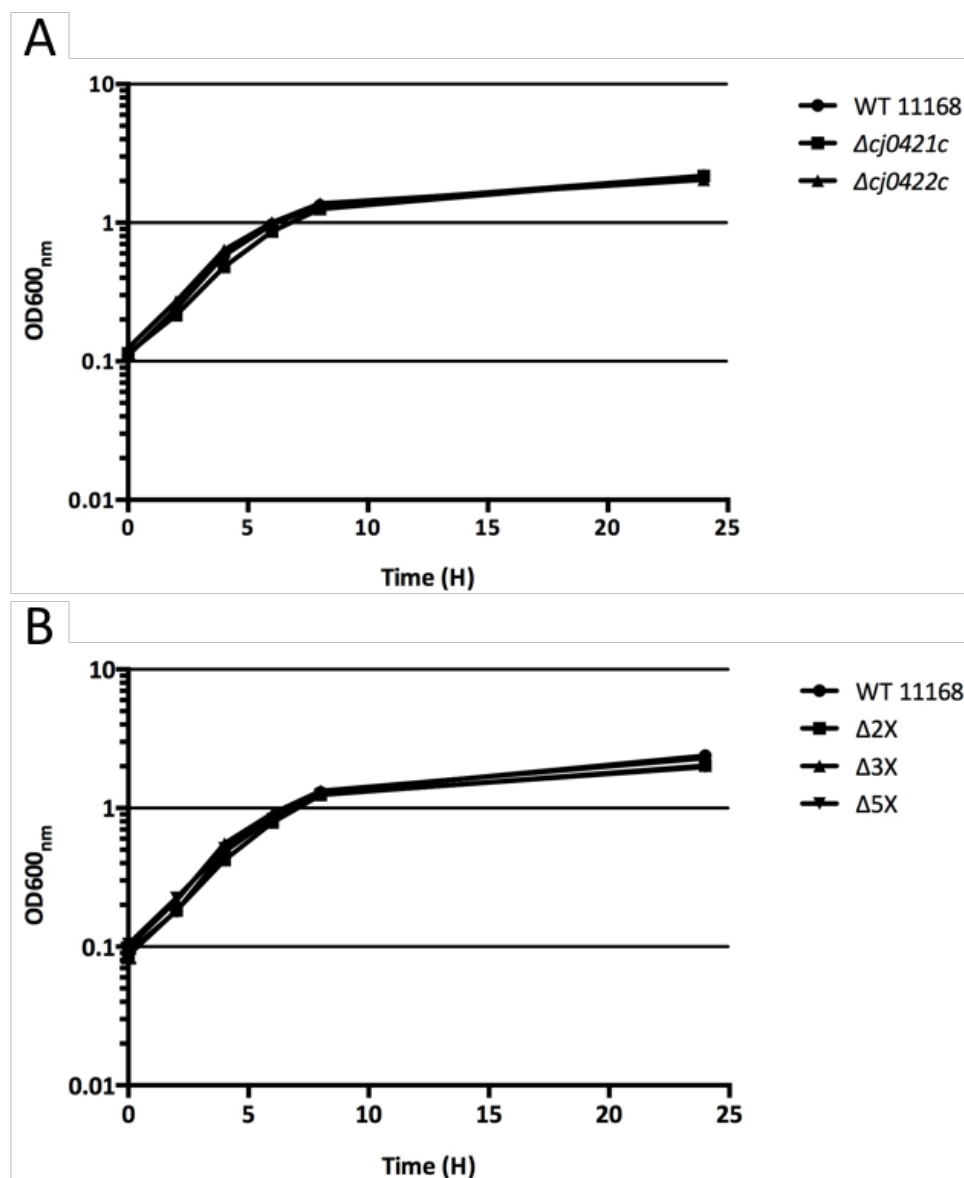


Figure 40: Growth curves of the *cj0421c-cj0425* mutant strains. Cells grown on blood agar plates were re-suspended in MHS broth to a starting OD600_{nm} of 0.1 and cultured over 24 hours with OD600_{nm} measurements taken at 0, 2, 4, 6, 8 and 24 hours (Section 2.17). (A) shows the individual *cj0421c* and *cj0422c* mutants. (B) shows the (*cj0421c-cj0422c*) 2X, (*cj0423-cj0425*) 3X and (*cj0421c-cj0425*) 5X mutant strains being tested. The data are the result of 3 separately grown replicates.

4.2.10 The *cj0421c*, *cj0422c* and *cj0424* mutant strains do not show any change in sensitivity to some antibiotics or CAMPs

The mutant strains were tested for sensitivity to the cell wall acting ampicillin and the membrane acting colistin sulphate (also known as polymyxin-E). All the mutant and complementation strains were tested against these antibiotics using disc diffusion assays where sensitivity is determined by the size of the zone of inhibition (Section 2.18). The *cj0422c* mutant and complementation strains were also tested by growth curve analysis for sensitivity to a range of ampicillin concentrations. The data shown in (Figure 41) shows no biologically significant difference in sensitivity between the wild type and mutant strains.

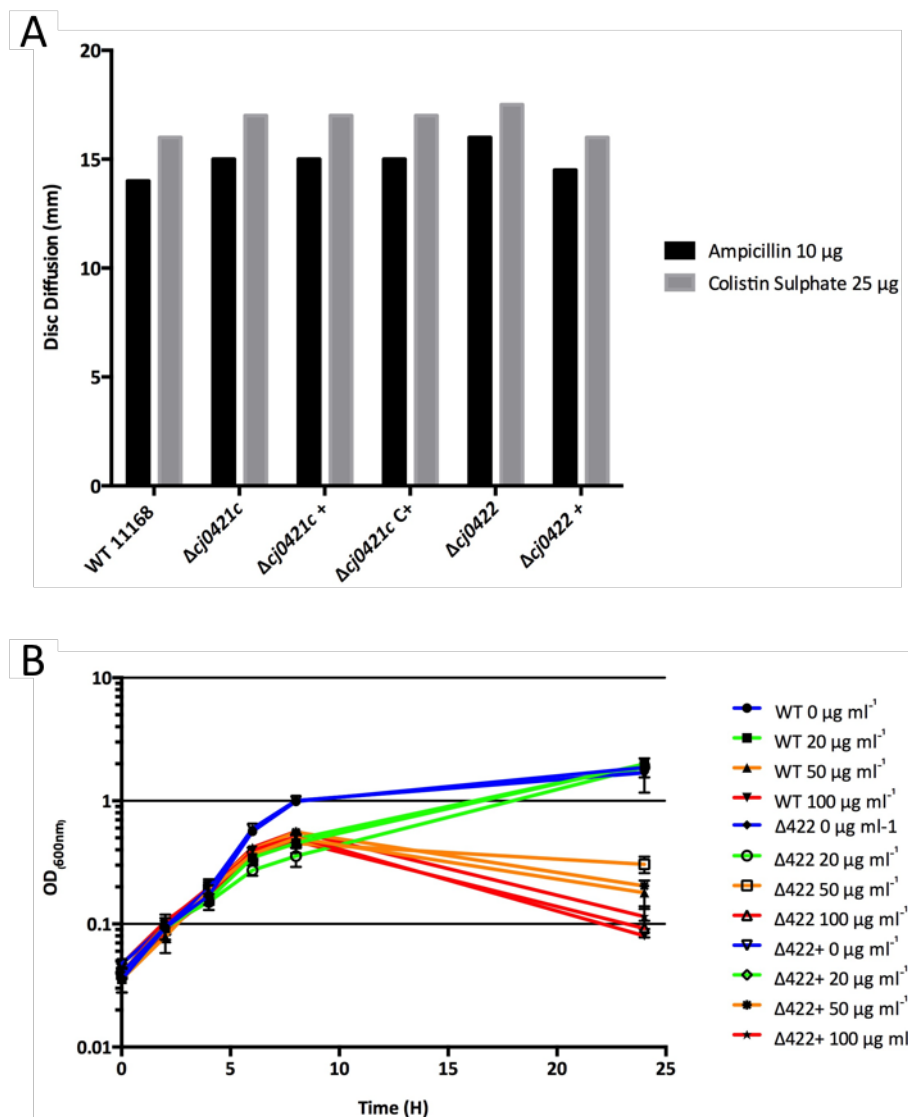


Figure 41: Antibiotic sensitivity of the *cj0421c* and *cj0422c* mutant strains. (A) shows the sensitivity profiles of the *cj0421c* and *cj0422c* mutant and complementation strains against ampicillin and polymyxin-E. (B) shows a more thorough test of the *cj0422c* mutant and complementation strains sensitivity to a range of ampicillin concentrations. The error bars represent the standard deviations of 2 independently grown biological replicates.

The *cj0422c* and *cj0424* mutant strains were also assayed by microtiter sensitivity to the model CAMP polymyxin-B, the human cathelicidin LL37, the chicken cathelicidin fowlicidin-2 and SDS as a control. The data shown in (Figures 42 and 43) shows some variations between the strains sensitivity however these are not considered biologically significant.

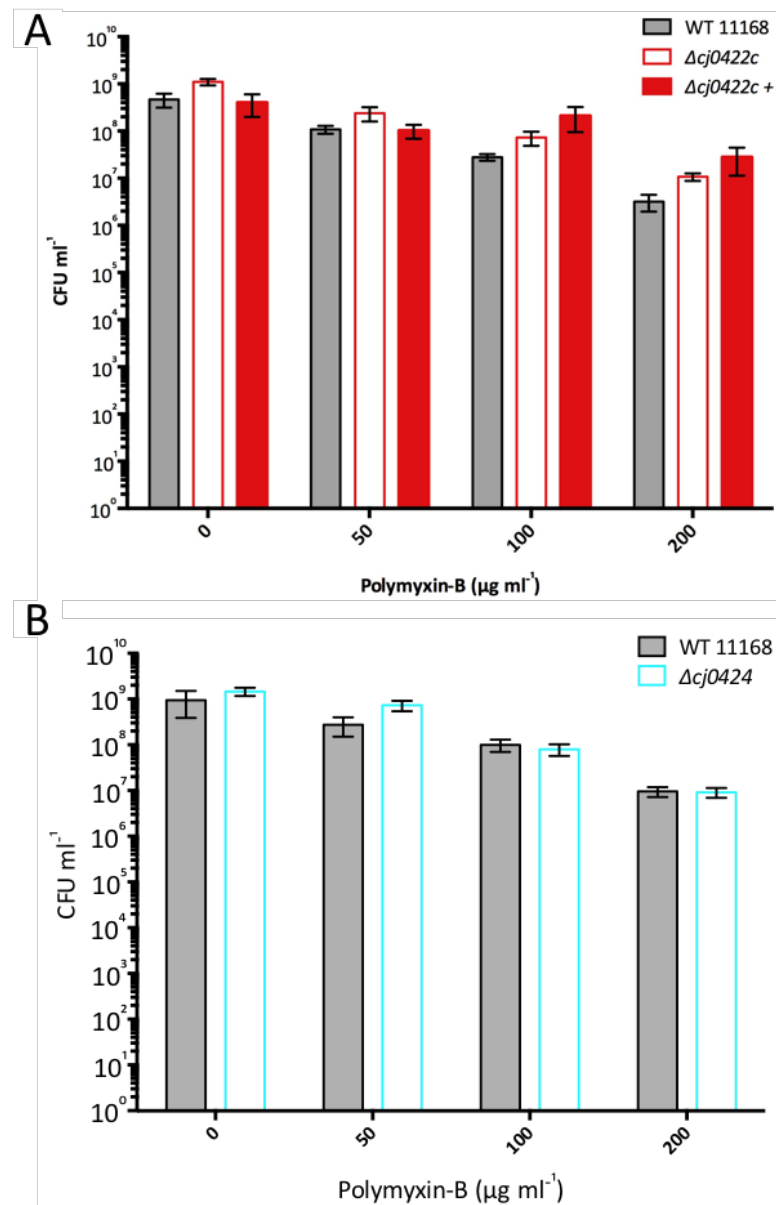


Figure 42: Polymyxin-B sensitivity of the *cj0422c* and *cj0424* mutant strains. Microtitre sensitivity assays were performed using methods described in (Section 2.19), with the strains incubated for 2 hours. The error bars show the standard deviation from at least 3 biological replicates for each data point. (A) shows the *cj0422c* mutant and complementation strains sensitivity to polymyxin-B and (B) shows the *cj0424* mutant sensitivity to polymyxin-B.

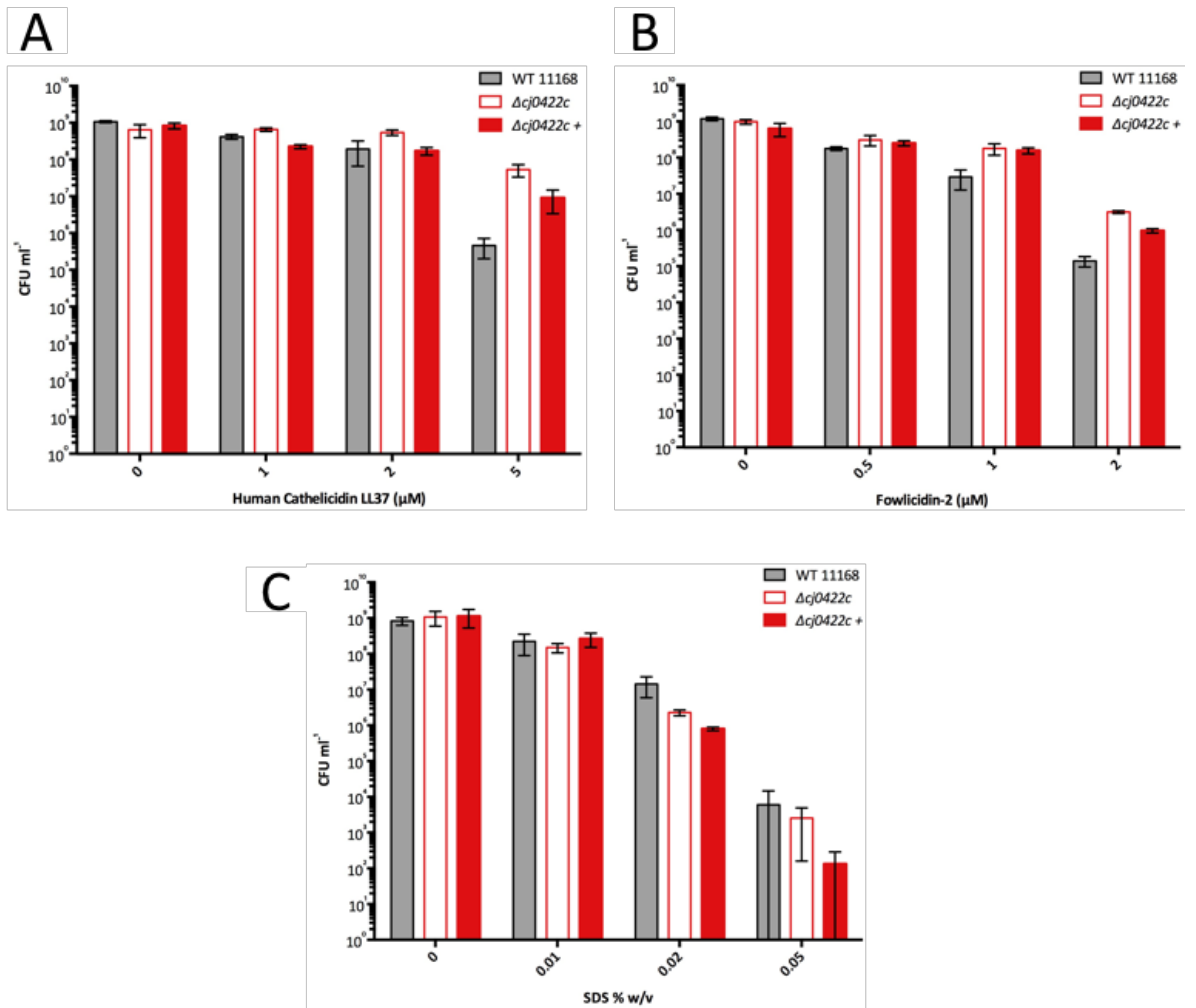


Figure 43: LL37, Fowlicidin-2 and SDS sensitivity of the *cj0422c* mutant and complementation strains. Microtitre sensitivity assays were performed using methods described in (Section 2.19), with the strains incubated for 4 hours (2 hours for SDS). The error bars show the standard deviation from at least 3 biological replicates for each data point. **(A)** shows the *cj0422c* mutant and complementation strains sensitivity to the human cathelicidin LL-37, **(B)** the *cj0422c* mutant and complementation strains sensitivity to the chicken cathelicidin Fowlicidin-2. **(C)** shows the *cj0422c* mutant and complementation strains sensitivity to SDS.

4.2.11 Investigating the rigidity of the cell membrane in the *cj0422c* mutant

The data presented in the previous section (Figures 42-43) shows that while there are some minor variations in sensitivity to antimicrobial compounds between wild type NCTC11168-DJK and the new mutant strains these are relatively minor and inconsistent. While this work was being done other work on the Cj0424 MORN domain protein showed that it is able to bind to lipid membranes and that when mixed with liposomes it is able to provide some degree of protection against leakage of a fluorescent dye marker inside the liposomes. This work is still ongoing but since the *cj0422c* mutant shows a strong up-regulation of the Cj0424 protein (as well as Cj0423 and Cj0425), it was decided to use this strain to analyse any effect these proteins may have on the *C. jejuni* membrane. Since the Cj0424 protein is able to protect against liposomal membrane leakage it was thought that it may help to order the outer membrane lipids (other work has shown Cj0424 is anchored to the inner leaflet of the outer membrane). To test this the strains were tested for membrane rigidity using methods described in (Section 2.22). Membrane rigidity is a method of determining the relative order of the membrane by examining the relative polarization of the hydrophobic dye DPH (1,6-diphenyl-1,3,5-hexatriene) when bound to the membrane. How polarized the DPH molecule is depends on how freely it is able to move when located in the hydrophobic part of the lipid membrane. The more freely the molecule is able to move the lower the polarization value will be as the DPH molecules spend less time in any one particular orientation. Other studies have shown that increased temperature or changes in membrane lipid composition can make a membrane less rigid which leads to a drop in the relative polarization. The data shown in (Figure 44) shows no statically significant difference in the membrane polarization of the *cj0422c* and *cj0424* mutant strains compared to wild type *C. jejuni*.

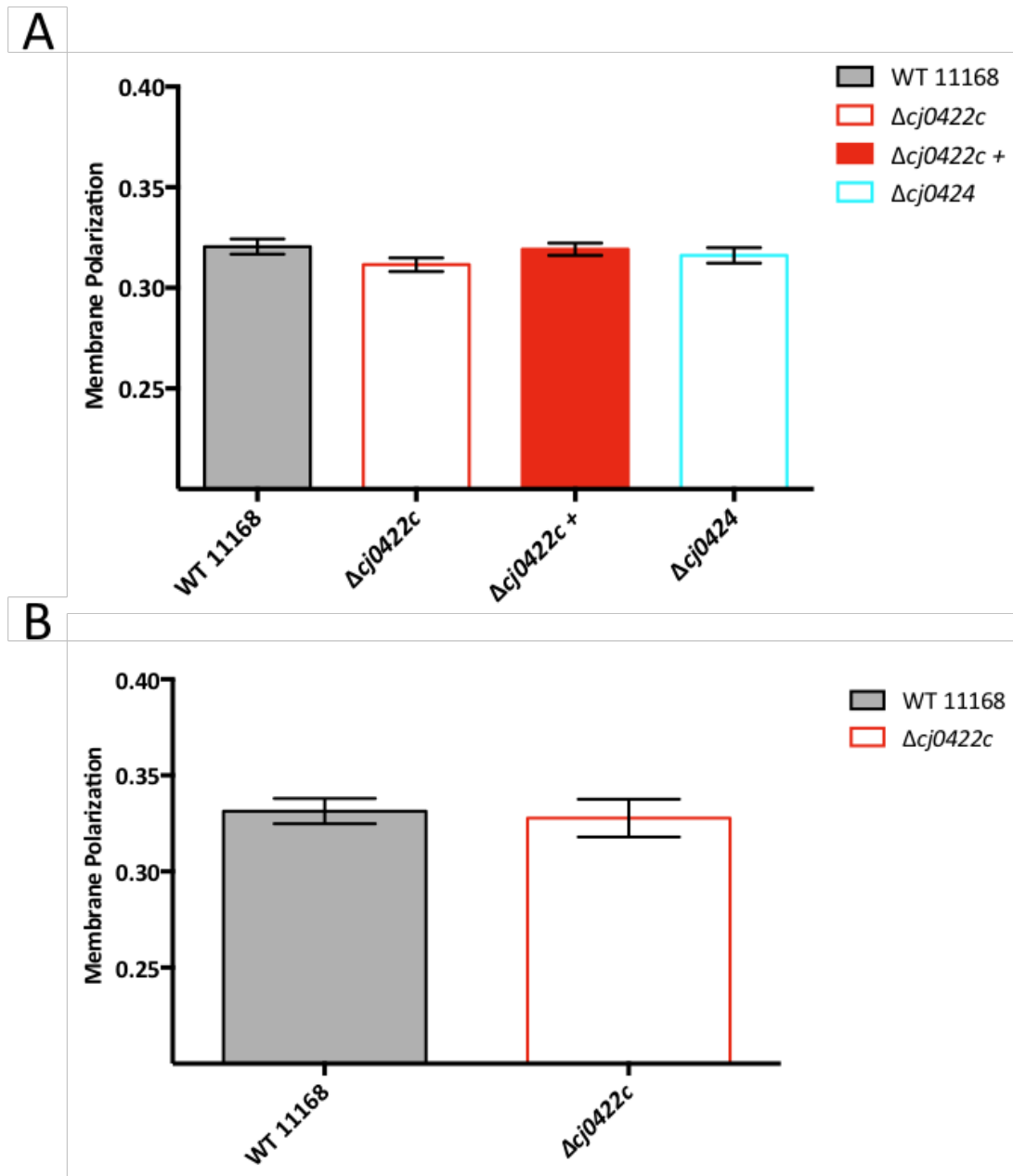


Figure 44: Membrane rigidity of the *cj0422c* mutant and complementation strains and the *cj0424* mutant strain. The assay was performed using methods described in (Section 2.22). **(A)** shows data for the strains cultured overnight under standard conditions before being assayed. **(B)** shows data for the strains grown to mid-log phase (OD_{600nm} 0.5-0.6) and then assayed. The error bars show the standard deviations from 3 technical repeats, each from 2 biological repeats.

4.2.12 Investigating the integrity of the cell membrane in the *cj0422c* mutant

The data shown in the previous section shows that the rigidity of the membrane structure is not altered by the presence of Cj0424. However, the lipid binding Cj0424 protein may still act to stabilize the outer membrane in other ways. This hypothesis was tested using two assays designed to test how 'leaky' the outer membrane is. These assays were performed by Dr Jonathan Smart using the *cj0422c* mutant strain I produced shown earlier in this chapter. The nitrocefin assay can be used as an indicator of outer membrane integrity by measuring the amount of 'leaked' periplasmic proteins following quick osmotic shock treatment, the protocol is explained in (Section 2.23). Briefly, overnight cultures of *C. jejuni* were matched to an OD_{600nm} of 0.5 and the periplasmic fraction collected by a short osmotic shock. Variations in membrane integrity are assayed by measuring the activity of periplasmic β -lactamase enzymes using nitrocefin as the substrate. The data is expressed as the rate of change in absorbance at 495 nm. The data (Figure 45) shows a slight but biologically insignificant difference between the wild type and *cj0422c* mutant strains.

Another method for testing the integrity of the outer membrane is by measuring cell sensitivity to lysozyme. This peptidoglycan hydrolase is unable to effectively cross the outer membrane of Gram-negative bacteria and so increased sensitivity to lysozyme indicates a defective outer membrane. The methods are described in (Section 2.24), briefly, overnight cultures of *C. jejuni* were matched to an OD_{600nm} of 0.5 and lysozyme added to the cells to a final concentration of 0.5 mg ml⁻¹. The OD_{600nm} was then measured over 3 minutes. The bile acid sodium deoxycholate was added to a final concentration of 10 mM to increase the rate of cell lysis. The experiment was performed by Dr Jonathan Smart using both wild type 11168 and the *cj0422c* mutant strains. The data shown in (Figure 46) shows some variations between the strains however the difference is not considered biologically relevant.

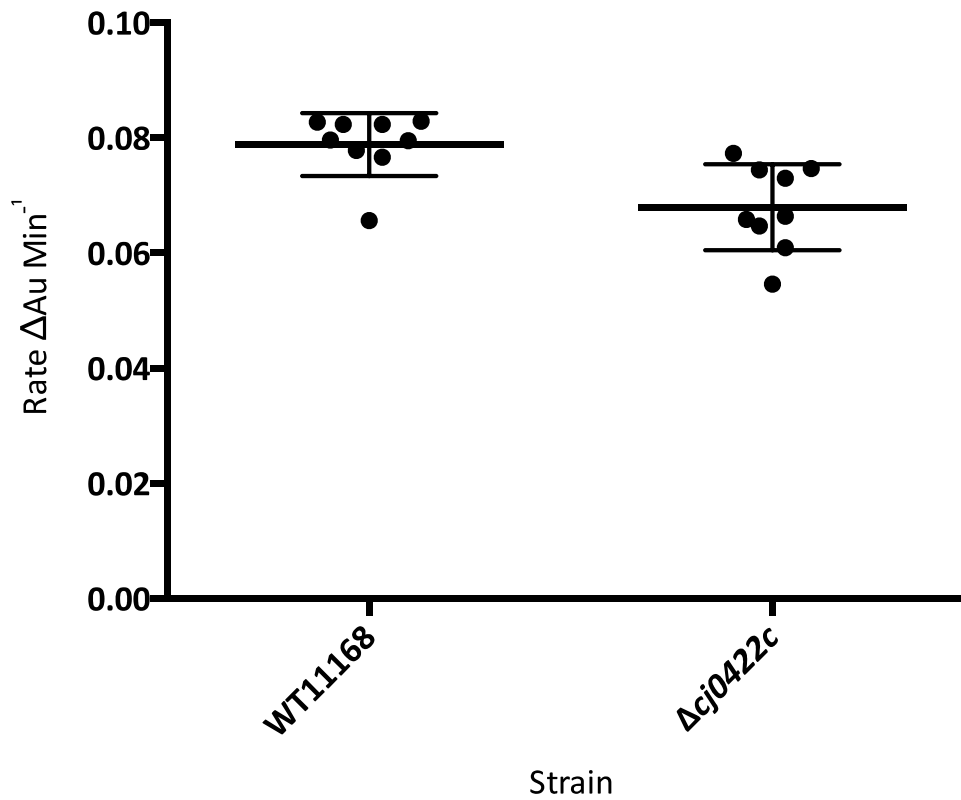


Figure 45: Determination of the activity of periplasmic β -lactamase in the wild type and *cj0422c* mutant strains. 3 independently grown replicates of the wild type and *cj0422c* mutant strains were grown overnight under standard conditions, the cultures were matched to an OD of 0.5 and the periplasmic fractions were extracted. The integrity of the outer membrane was measured by assaying the activity of the periplasmically located β -lactamase from 3 technical replicates of the 3 biological replicates. The activity of this enzyme was measured using methods described in (Section 2.23). The error bars represent the standard deviations from the mean of 9 replicates. The experiment was performed by Dr Jonathan Smart. Statistical analysis does show a significant difference between the data sets; however the difference is so small it is not considered biologically relevant.

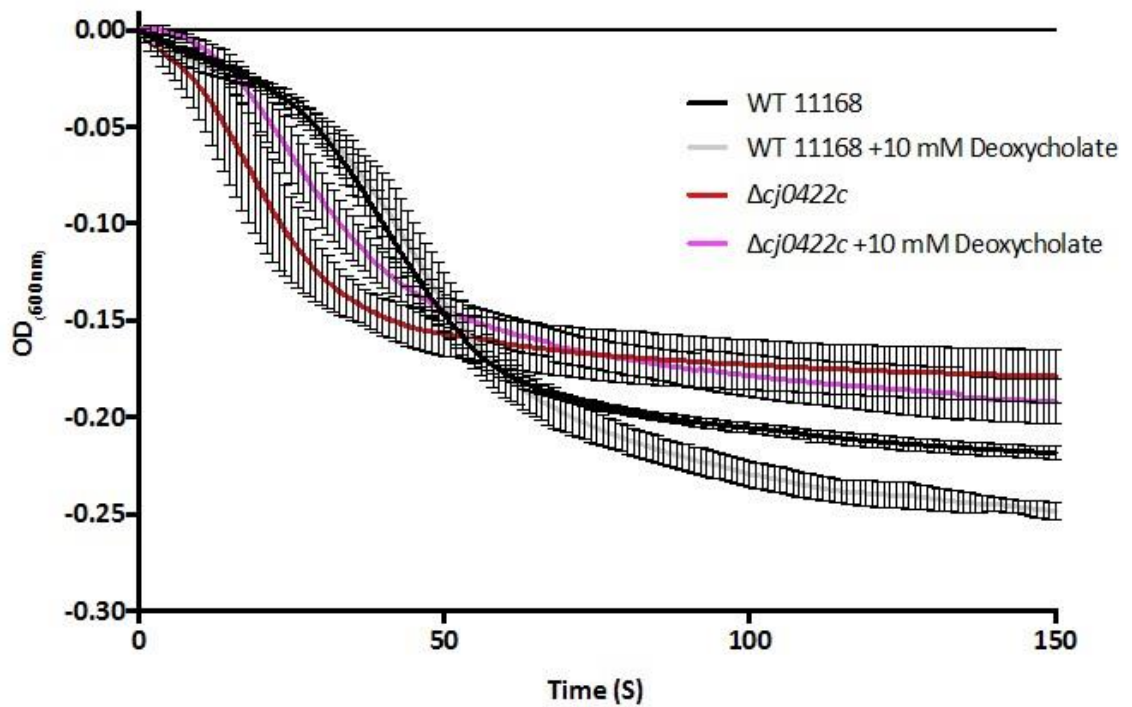


Figure 46: Lysozyme sensitivities of wild type and the *cj0422c* mutant strains. Strains were grown overnight under standard conditions and back diluted to an OD_{600nm} of 0.5. Lysozyme was added to a final concentration of 0.05 mg ml⁻¹ and the decrease in OD_{600nm} measured over 3 minutes. Sodium deoxycholate was added to increase the rate of uptake of the lysozyme. The data shown is matched to the starting OD_{600nm} after adding the lysozyme. The points show the average from 3 independently grown cultures with the error bars showing the standard deviations from the mean. The experiment was performed by Dr Jonathan Smart.

The data shown in (Figures 45-46) do not show biologically significant differences in outer membrane integrity between the wild type and *cj0422c* mutant strains. It is worth noting that when assaying for membrane integrity or stability the wild type is usually the more stable control and a mutant strain would normally show a decrease in stability. In this case however the hypothesis being tested is that the mutant strain makes the membrane more stable by up-regulating Cj0424. Since there is no obvious increase in membrane stability between the strains it was decided to discontinue this line of enquiry and to focus on what role the *cj0423-cj0425* operon as a whole is performing in *C. jejuni*.

4.2.13 Chicken colonisation studies using the *cj0423-4* mutant strain in the *C. jejuni* 11168-Hypermotile wild type.

As discussed in the previous chapter the laboratory wild type strain of *Campylobacter* (*C. jejuni* 11168-DJK) is non motile due to multiple SNPs within the structural components of the motility apparatus. Since motility is required for successful colonisation of chickens, some of the mutant strains produced earlier in the chapter were re-produced in the hypermotile variant of *Campylobacter* (Table 14). The strains tested were the *cj0424* mutant strain and a newly produced *cj0423-4* double mutant strain, both produced by Dr Jonathan Butler. These strains were tested for chicken colonisation in collaboration with Professor Mark Stevens and Cosmin Chintoan-Uta at the Roslin Institute. Briefly, 1 day old White Ledgehorn chicks were orally challenged with 50 μ l *C. jejuni* culture which had been diluted in PBS to 10^4 and 10^6 CFU ml⁻¹. Caecae were collected from 4-6 birds at weekly intervals for 3 weeks post challenge and 1 gram samples were re-suspended in Bolton Broth (Oxoid) and serially diluted to determine the CFU / gram caecal contents by plating on mCCDA selective agar. All chicken colonisation experiments were performed by Cosmin Chintoan-Uta according to home office guidelines and using all standard controls and procedures.

The chicken colonisation data shown below and other data not shown here, shows no difference in the ability of the mutant strains to colonise chickens compared to the wild type hypermotile strain. In order to successfully colonise chickens *C. jejuni* needs to be able to successfully resist a large number of potential stresses including acid shock, osmotic shock, bile salts, CAMPs and other components of the immune system. While this experiment does not provide any answers about the roles of the *cj0423-cj0425* operon, the lack of any colonisation defect in the mutant strain does imply that the genes are not involved directly in the process of chicken colonisation and therefore are not involved in resisting or responding to any of the associated stresses.

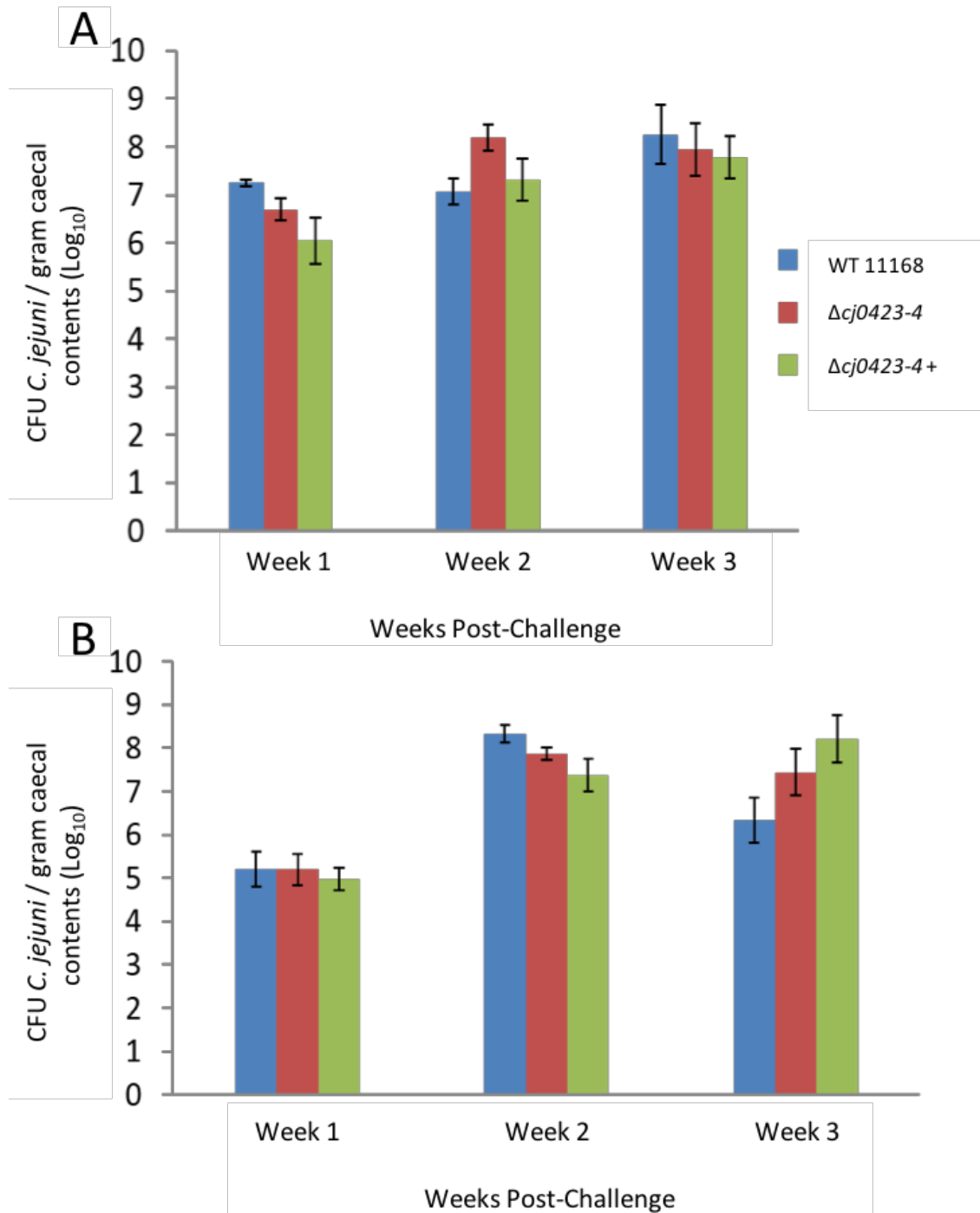


Figure 47: Chicken colonisation profile of wild type 11168-H and the *cj0423-4* double mutant and complementation strains. The 3 strains were tested against 1 day old chicks with (A) 10^4 CFU ml⁻¹ and (B) 10^6 CFU ml⁻¹ starting dose. 6 birds were sampled per strain at each of the weekly time points and the error bars represent the standard error of the means. The experiment was performed by Cosmin Chintoan-Uta in the laboratory of Professor Mark Stevens.

4.2.14 Examining the peptidoglycan structure of the *cj0422c* mutant strain

The other primary structural component of the Gram-negative cell envelope, apart from the membrane layers, is the peptidoglycan cell wall. The structure of the *C. jejuni* peptidoglycan layer is discussed in the introduction. Part of the reason for studying the peptidoglycan layer is that the crystal structure of Cj0425 revealed that it contains a cystatin like fold, this class of proteins act as cysteine protease inhibitors which directly bind to the active site regions of cysteine proteases such as papain. The protein structure and active site regions of some peptidoglycan modification enzymes is similar to that of cysteine proteases (Sanz-Gaitero *et al.*, 2014) so it was decided to look for any changes in the peptidoglycan structure of the *cj0422c* mutant to determine if an up-regulated Cj0425 might affect peptidoglycan turnover. To examine this hypothesis, the peptidoglycan structure of both wild type and the *cj0422* mutant strains was examined by HPLC analysis. This work was performed by Dr Jonathan Butler in collaboration with Dr Stéphane Mesnage.

The *C. jejuni* peptidoglycan was purified using standard extraction techniques based on (Glauner, 1988). The extraction was performed by Dr Jonathan Butler. The peptidoglycan was then digested with the N-acetylmuramidase enzyme mutanolysin (Sigma) which breaks apart the β -N-acetylmuramyl-(1 \rightarrow 4)-N-acetylglucosamine linkage of the bacterial cell wall peptidoglycan-polysaccharide. The soluble peptidoglycan fragments were separated on a Thermo Scientific Hypersil GOLD aQ column (250 x 4.6 mm, 3 μ m particle size), using a Waters HPLC system. The HPLC analysis was performed by Dr Stéphane Mesnage. The HPLC traces for wild type 11168 and the *cj0422c* mutant strain are shown in (Figure 48), the traces show no significant difference between the size or concentration of the peptidoglycan fragments between wild type *C. jejuni* or the *cj0422c* mutant (Dr Stéphane Mesnage personal communication). The size of the peaks in (Figure 48) does vary as does the elution time for the peaks, however the size is relative to the volume loaded onto the column and the 'drift' seen in the peak elution profile is typical for some HPLC separations.

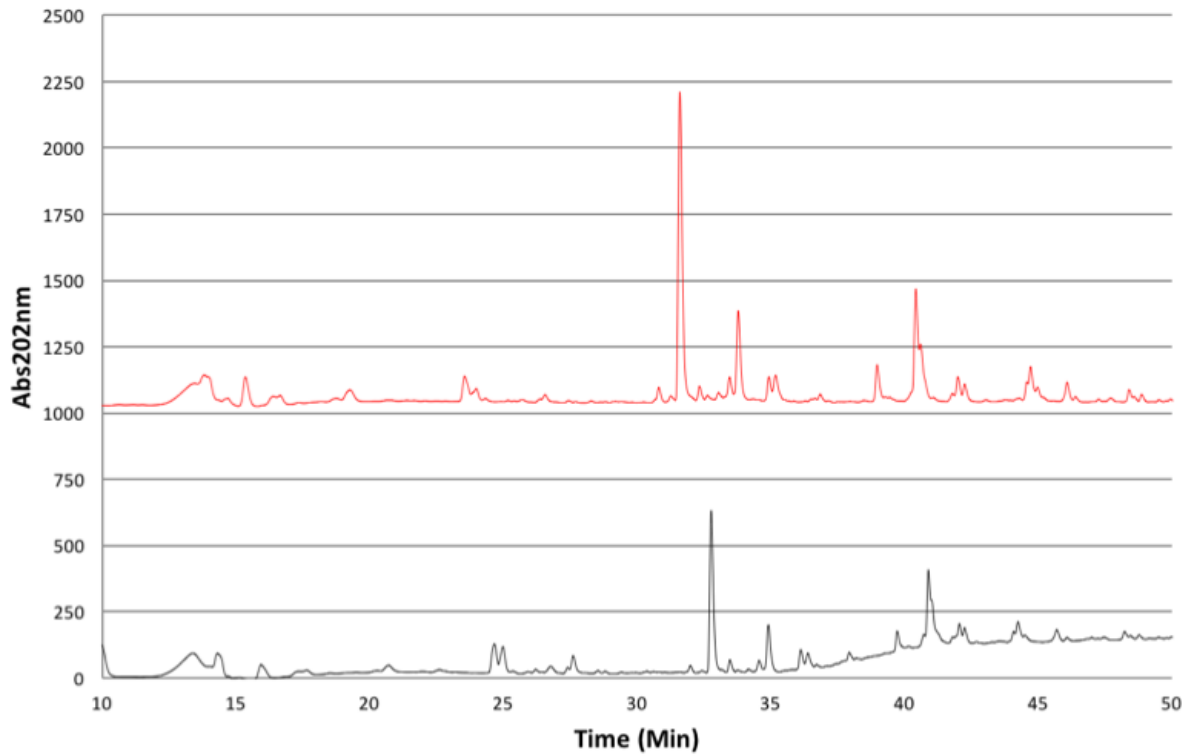


Figure 48: HPLC trace of the peptidoglycan fragments from wild type 11168 and the *cj0422c* mutant strain. The mutanolysin digested peptidoglycan fragments from a single wild type 11168 (black) and the *cj0422c* mutant (red) were separated by HPLC and the Abs202_{nm} measured over time to produce a trace of the *C. jejuni* peptidoglycan fragments. The peaks correspond to different peptidoglycan fragments though which fragments are unknown. While the traces show different peak heights this is likely due to differences in the column loading volumes.

4.2.15 Examining the potential role of the *cj0423-cj0425* operon as a defense against the antibacterial type VI secretion system

Because the *C. jejuni* peptidoglycan structure is apparently not altered in the *cj0422c* mutant strain and because pull down assays do not show any probable binding partners or targets for Cj0425 from *C. jejuni* cell free extracts (data shown in Chapter 6), it may be that Cj0425 does not inhibit or interact with any of the cysteine protease enzymes native to *Campylobacter*. Because of this I decided to look for potential ways in which foreign cysteine protease enzymes may enter the periplasm of *C. jejuni*. One potential source is via the antibacterial type VI secretion system (T6SS), this system is used by some Gram-negative bacteria to compete against other un-related Gram-negative bacteria. The T6SS is able to inject toxic effector proteins directly into the periplasm of neighboring cells whilst expressing immunity proteins to prevent self-damage (Ho *et al.*, 2014). The type VI secretion system of Gram-negative bacteria is reviewed in the introduction.

As discussed earlier the periplasmic protein Cj0425 possesses a similar structure to cystatin like proteins which inhibit cysteine protease enzymes. These enzymes are similar in structure to some peptidoglycan degrading enzymes exported by the T6SS of some bacteria (Srikannathasan *et al.*, 2013). Because of this similarity I decided to examine the possibility that Cj0425 may act to inhibit foreign peptidase enzymes. While preparing to test this hypothesis, I developed a model showing how the other genes in the operon (*cj0423* and *cj0424*) may also be involved in defence against the T6SS. This model is based on Cj0423 acting to inhibit the formation of pores by pore forming toxins and Cj0424 acting to inhibit the activity of secreted phospholipase enzymes potentially by blocking access to the membrane. This model is shown below.

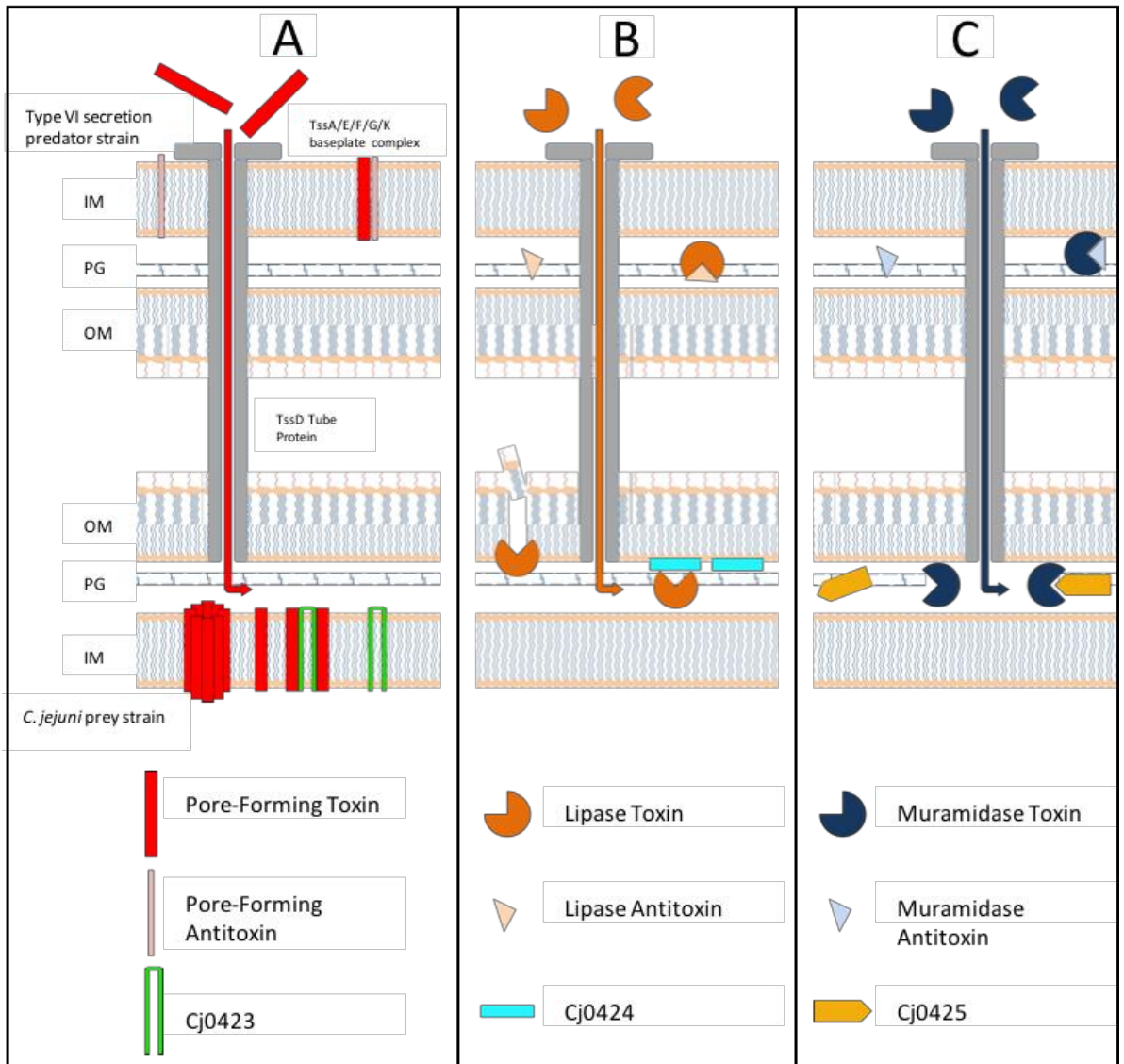


Figure 49: Proposed model for Cj0423-4-5 acting to defend against the type VI secretion system. The figure shows the proposed model for how the three proteins may individually help defend against different types of toxic effectors secreted by the type VI secretion system. The T6SS apparatus is represented by the grey tube connecting the cytoplasm of the 'predator' cell with the periplasm of the 'prey cell'. (A) Cj0423 is localised to the inner membrane and may act to inhibit or prevent the formation of pores from the T6SS secreted pore forming toxins. (B) Cj0424 which binds to the inner leaflet of the outer membrane may inhibit the action of phospholipase enzymes secreted by the T6SS. (C) Cj0425 which possesses a cystatin like structure may inhibit peptidoglycan degrading enzymes with similar mechanisms of action to cysteine proteases.

4.2.16 *Campylobacter jejuni* is sensitive to the *Serratia marcescens* type VI secretion system

In order to test the effectiveness of the T6SS toxins on *C. jejuni* I was kindly given a wild type and T6SS mutant strain of *S. marcescens* from Dr Sarah Coulthurst (University of Dundee). *S. marcescens* is a useful model for the T6SS as the system is continuously expressed (in other strains such as *Pseudomonas aeruginosa* it needs to be induced) and it exports a peptidoglycan degrading endopeptidase enzyme which contains a catalytic cysteine residue in the active site (Murdoch *et al.*, 2011, Srikannathan *et al.*, 2013). The T6SS mutant strain contains a silent deletion of the *tssE* gene which forms part of the baseplate complex, removal of this completely abolishes the activity of the type VI secretion system (English *et al.*, 2012).

Assays have previously been developed in a number of labs to study how effective at killing foreign cells T6SS possessing strains are, these typically involve simply spotting mixtures of 2 strains (predator and prey cells) onto solid agar plates and after a short incubation serially diluting the cells and plating onto selective media. Often using this method, the 'prey' strain contains a resistance marker allowing it to be cultured on selective agar while the 'predator' strain cannot (Dr Sarah Coulthurst personal communication). Since *Campylobacter* is relatively slow growing (compared to *Serratia*) and can only be cultured in a microaerobic environments, several trial and error experiments were performed to determine the best way to assay cell killing by the T6SS. The final assays protocol is described in (Section 2.21). Briefly, *Campylobacter* and *Serratia* strains were cultured on blood agar and MH agar respectively and then scrapped off and diluted in MHS broth to an OD_{600nm} of 0.5 and incubated microaerobically for 1 hour. Aliquots of the cultures were mixed together at a 50:1 ratio (*Campylobacter* : *Serratia*) and 25 µl spotted onto pre-warmed MH agar (with no selective antibiotics). These plates were incubated microaerobically at 37°C for 24 hours. The spots were then scrapped off the plates into phosphate buffered saline, serially diluted in a 96 well plate and spotted onto mCCDA agar plates (containing 10 µg ml⁻¹ Amphotericin-B and 32 µg ml⁻¹ Cefoperazone). These were incubated at 42°C for 2 days and the colonies counted. The procedure for counting the number of *Serratia* cells was identical apart from using standard Mueller-Hinton agar plates instead of mCCDA and incubating aerobically. The data is expressed as CFU ml⁻¹ for the final cell count or as a percentage survival of the *C. jejuni* strain against wild type *Serratia* compared to the *tssE* mutant strain. The data shown in (Figure 50) shows that wild type *C. jejuni* 11168 is killed by *S. marcescens* which is dependent on an active type VI secretion system.

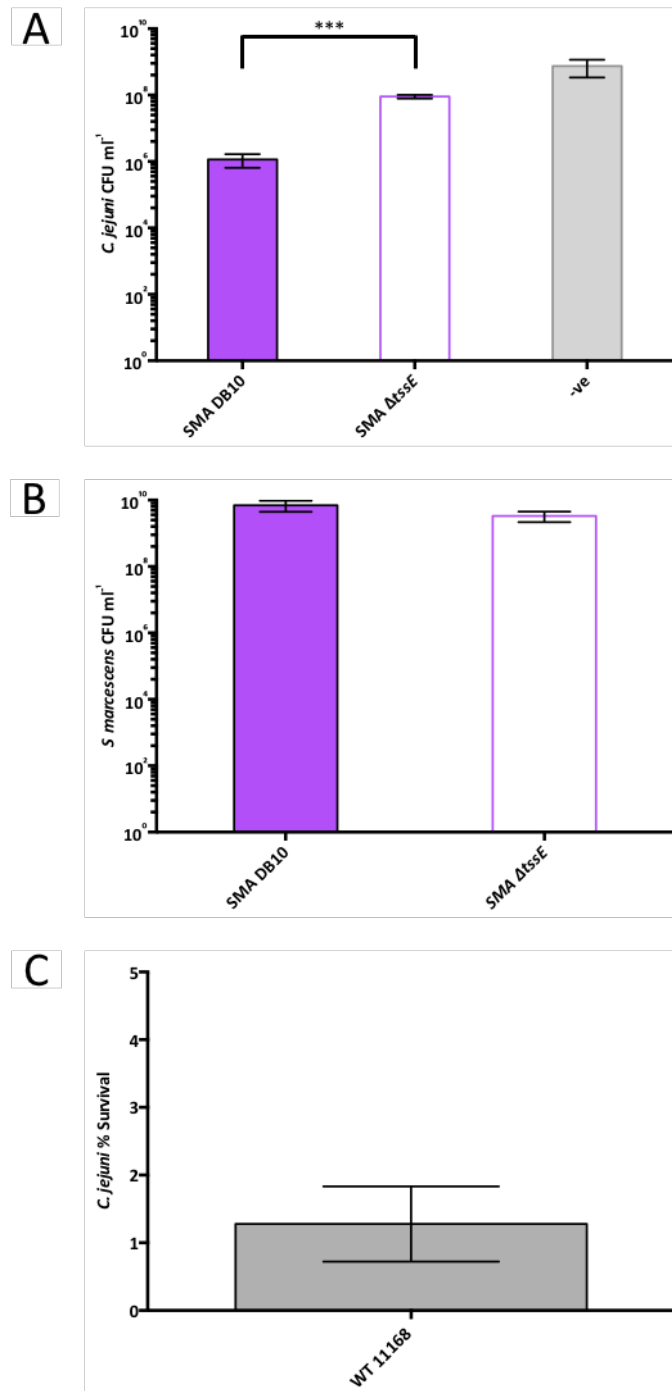


Figure 50: The *S. marcescens* type VI secretion system is active against *C. jejuni*. Interbacterial competition assays were performed using methods described in (Section 2.21). **(A)** shows the CFU ml⁻¹ of recovered *C. jejuni* WT11168 after incubation with wild type *Serratia marcescens* (SMA DB10), the *tssE* mutant ($\Delta tssE$) and a *C. jejuni* only control. The asterisks show a P value <0.01. **(B)** shows the average CFU ml⁻¹ of the recovered *S. marcescens* strains, this shows no large difference between the strains implying that the decrease seen in figure **(A)** is the result of the T6SS rather than other factors. **(C)** shows the percentage survival of wild type 11168 from the SMA DB10 strain compared to the *tssE* mutant strain as a control. All data points are the means of 2 technical replicates from 2 biological replicates with the error bars showing standard deviations. Statistical analysis was performed using Students T-test.

4.2.17 Different *C. jejuni* wild type strains vary in sensitivity to the *Serratia marcescens* type VI secretion system.

3 different laboratory strains of *C. jejuni* were assayed for sensitivity to the *S. marcescens* type VI secretion system. The new laboratory 11168-DJK strain, the highly virulent 81-176 strain and the 81116 strain. The 3X deletion strain in *C. jejuni* 81116 (produced in for the previous chapter (Section 3.2.6) was also used. The data shown in (Figure 51) shows statistically significant type VI dependent killing of all *C. jejuni* strains testes. The data also shows that the degree of killing between 11168 and 81116 is significantly different but the degree of killing between the 81116 wild type and the 81116 3X deletion strain is not.

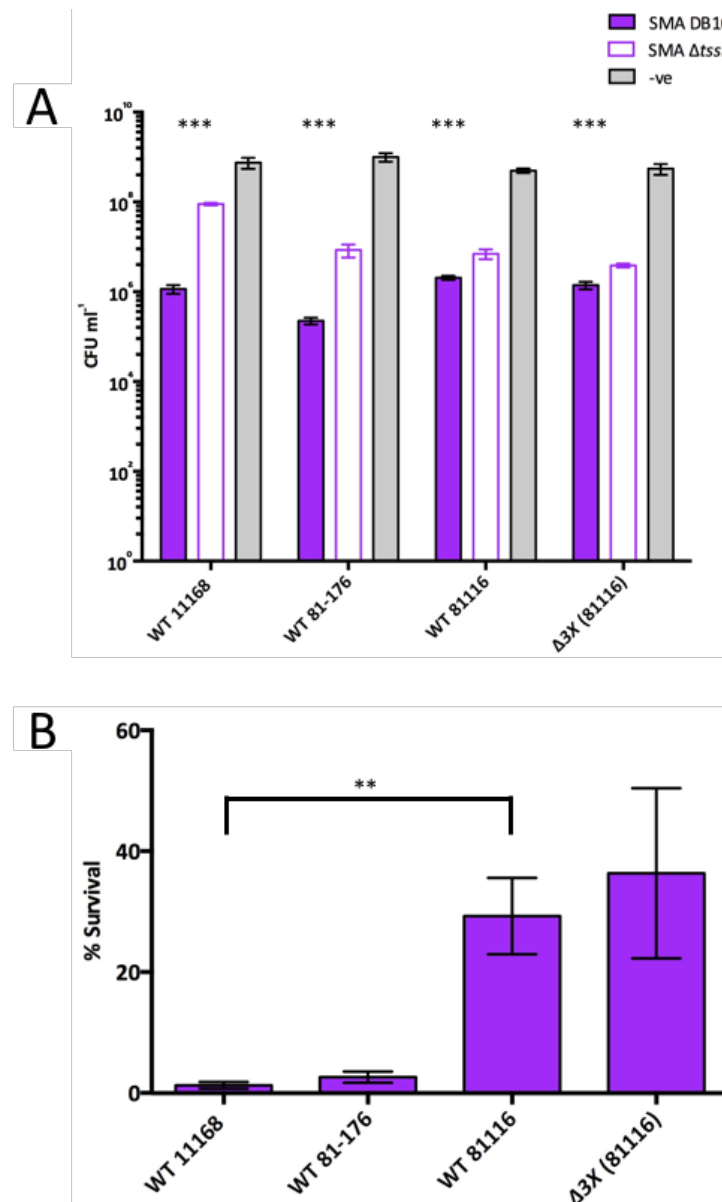


Figure 51: *C. jejuni* wild type strains vary in sensitivity to the T6SS. (A) Final CFU ml⁻¹ counts of wild type 11168, 81-176, 81116 and the 3X deletion of 81116 after assaying for sensitivity to the SMA T6SS. 3 sterisks represent a P value <0.01. **(B)** The percentage survival of each strain (comparing the CFU ml⁻¹ of recovered *C. jejuni* cells from the wild type SMA DB10 to the CFU ml⁻¹ of recovered *C. jejuni* cells from the $\Delta tssE$ strain. 2 Asterisks represent a P value <0.05. All data points are the means of 4 replicates (2 technical of 2 biological) and the error bars show standard deviations. Statistical analysis was performed using Students T-test.

The colony counts of *S. marcescens* strains were also counted to ensure that the difference in the degree of T6SS dependent killing was not the results of differences in the numbers of *S. marcescens* present in the assay. The data shown in (Figure 52) shows no significant difference in the numbers of *S. marcescens* present after performing the assay.

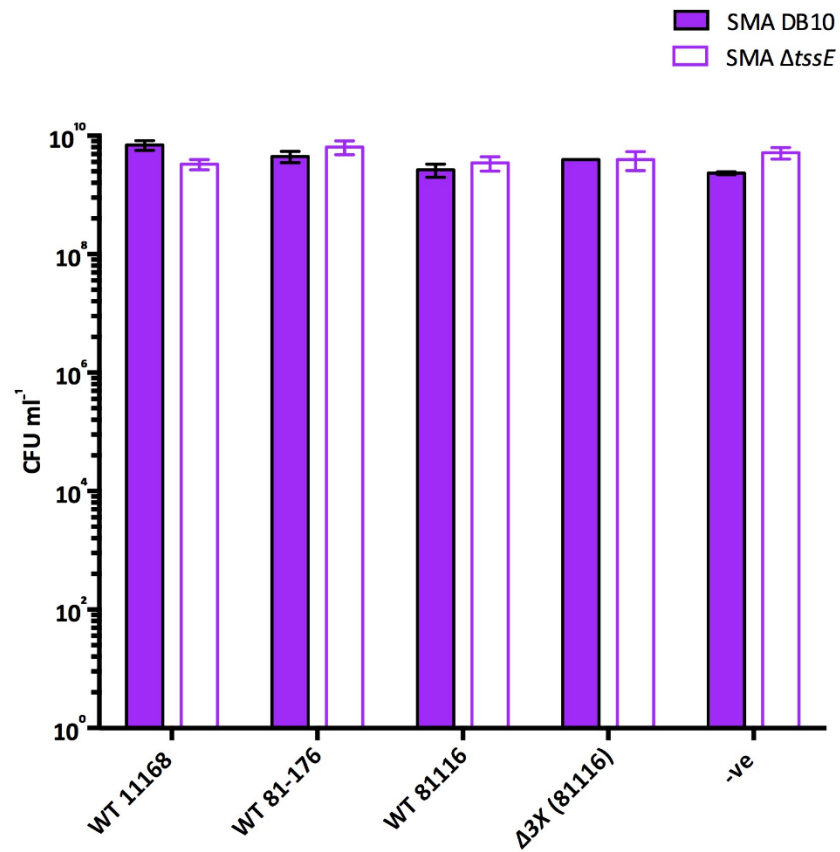


Figure 52: The competition assays do not affect the final viable counts of *S. marcescens*: The bars show the final CFU ml⁻¹ counts of *Serratia marcescens* after assaying with *Campylobacter*. The data shows that there is no change in viability between assays or with the negative control. This acts as a control for the standard competition assay showing that the numbers of *Serratia* predator cells remains constant. All data points are the means of 4 replicates (2 technical of 2 biological) and the error bars show standard deviations.

4.2.18 *The cj0423-4-5 genes do not appear to provide resistance to the S. marcescens type VI secretion system*

The T6SS competition assay was used to determine how sensitive the *cj0422c*, *cj0423*, *cj0424*, *cj0425* and 3X deletion strains are to the *S. marcescens* type VI secretion system. The data shown in (Figure 53) shows that there is a degree of variation between the wild type and mutant strains however these variations are not consistent with the hypothesis that the *cj0423-5* operon is able to defend against the *S. marcescens* T6SS. The data shows that only the 3X deletion strain shows a statistically significant change in sensitivity to the *S. marcescens* T6SS compared to wild type 11168. The 3X deletion strain shows a slight increase in resistance to wild type *S. marcescens* when the data is expressed as a percentage killing.

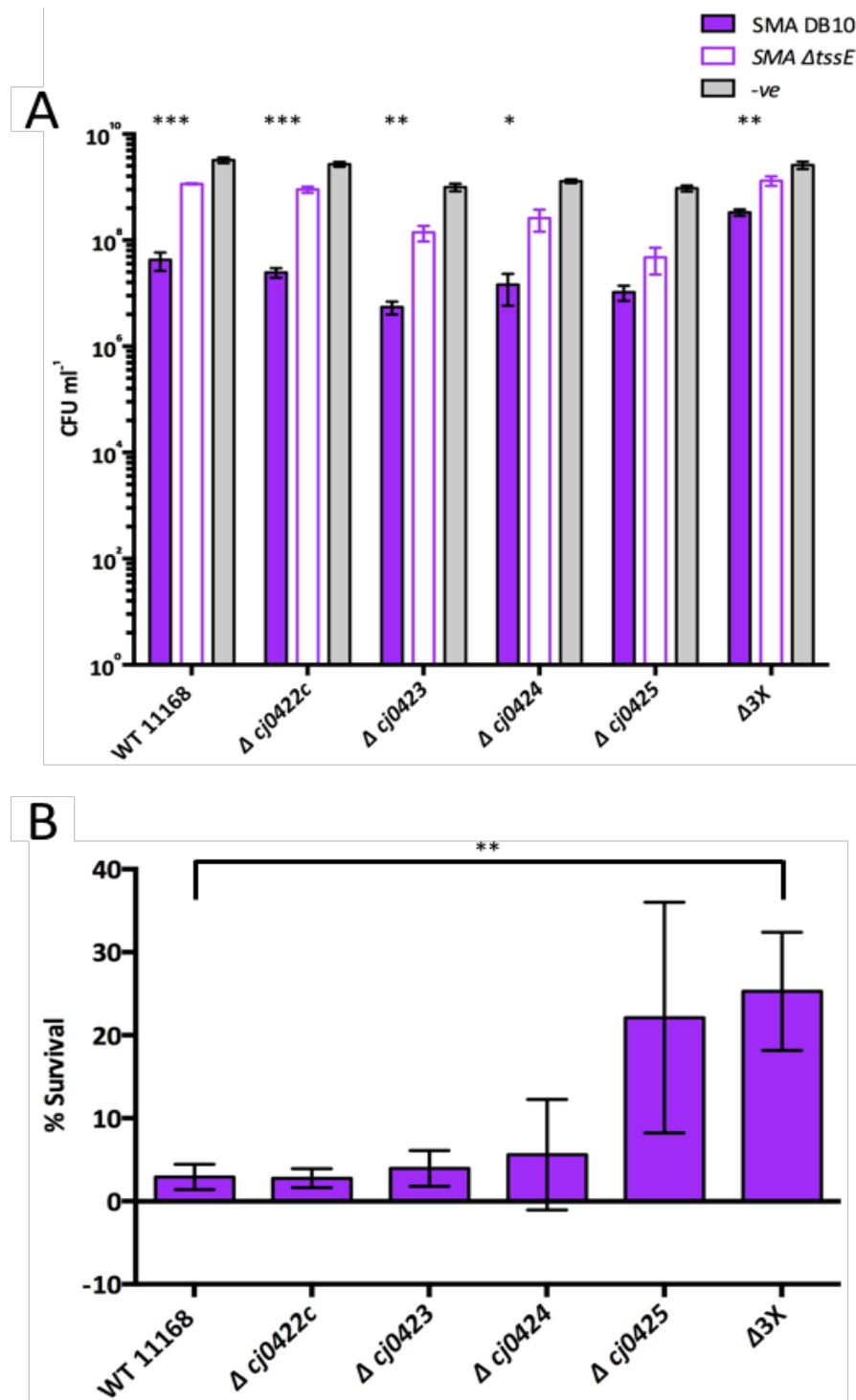


Figure 53: Susceptibility of the *cj0422c-cj0423-cj0424-cj0425* and 3X mutant strains to the *S. marcescens* type VI secretion system. (A) The bars show the final CFU ml⁻¹ counts for the *C. jejuni* mutant strains after assaying for sensitivity to the *S. marcescens* T6SS. (B) The percentage survival of each strain (comparing the CFU ml⁻¹ of recovered *C. jejuni* cells from the wild type SMA DB10 to the CFU ml⁻¹ of recovered *C. jejuni* cells from the $\Delta tssE$ strain. All data points are the means of 4 replicates (2 technical of 2 biological) and the error bars show standard deviations. Statistical analysis was performed using Students T-test.

4.3 Chapter 4 Discussion

The aim of this chapter was to produce all necessary mutant strains in the newly sequenced 11168-DJK lab strain of *C. jejuni* and to either confirm or disprove any phenotypes associated with these mutant strains. At the end of the previous chapter it was established that the increased sensitivity to cationic antimicrobial peptides was likely the result of a single SNP variant within the *cj0256* ORF and that the transcriptome microarray data on the *Cj0422c* mutant strain may have been affected by a large number of SNPs elsewhere in the genome. After re-producing the new *cj0421c* and *cj0422c* mutant strains and assaying by qRT-PCR it was shown that while the *Cj0422c* protein is responsible for repression of the *cj0423-5* operon, it does not appear to affect the expression of *cj0653c*, *cj0864* or *cj0204* as the microarray initially suggested. It appears then that the *cj0421c-cj0425* gene cluster is not part of a master regulatory network and it likely has a self-contained role.

4.3.1 Antimicrobial sensitivity of the mutant strains

Without any further information on the possible roles of the *cj0421c-cj0425* gene cluster I decided to initially assess whether the knockout mutations showed any growth defect or increased sensitivity to some antimicrobial compounds. The data shown in (Figures 40-41) shows that the mutant strains do not show any growth defect when cultured under normal conditions nor do they show any increased sensitivity to some basic antimicrobial compounds. I also tested the *cj0422c* and *cj0424* mutant strains against the cationic antimicrobial peptides polymyxin-B, human cathelicidin LL37 and fowlicidin-2 in order to finally confirm that the genes are not involved in CAMP resistance. The data shown in (Figures 42-43) shows no biologically relevant change in sensitivity to these CAMPs or to the SDS control. This data implies that the gene cluster is not involved in the normal growth of *C. jejuni* nor are they involved in resistance to antimicrobial compounds. Following this it was decided to examine the roles of the individual genes more closely to try and find clues about their function.

4.3.2 Membrane integrity of the mutant strains

Without any clear hypothesis about the role of the gene cluster as a whole I decided to examine the possible roles of the individual genes. Since the expression of the primary operon (*cj0423-cj0424-cj0425*) is strongly up-regulated in the *cj0422c* mutant strain (around 100-fold) it was decided that this strain is likely to show the largest change in phenotype compared to wild type *C. jejuni* as the operon is strongly repressed under normal conditions. The *Cj0424* protein contains 7 MORN repeat domains and the crystal structure showed the protein is arranged into a 'ladder like' structure with 15 antiparallel β -sheets. A paper published in 2015 showed that MORN domain proteins bind to lipid membranes (Habicht *et al.*, 2015) and data

from other members of the lab has shown that Cj0424 does indeed bind to a range of lipid membranes. The authors also explained that MORN domain proteins are often attached to other domains, some with known functions and others without, therefore it is assumed that the MORN domains may act to localize these domains to the membrane without the need for transmembrane regions or lipid anchors. The mature Cj0424 protein however does not contain any other domains and appears to be localised to the inner leaflet of the outer membrane in *C. jejuni*. Protein-protein interaction analysis by pull-down assays have not revealed any native binding partners for Cj0424 (though that does not rule out a potential foreign binding partner). Since all the evidence suggest that Cj0424 alone binds to the outer membrane it was decided to examine the integrity of the outer membrane by membrane polarization and cell leakage assays to determine if Cj0424 binding causes changes in the membrane structure. The membrane rigidity assays shown in (Figure 44) showed no change in light polarization between the wild type and *cj0422c* or *cj0424* mutant strains which implies that the presence of the Cj0424 protein does not significantly alter the stability of the outer membrane. The nitrocefin cell leakage assay shown in (Figure 45) showed no significant difference between the wild type and *cj0422c* mutant strain. The lysozyme assay shown in (Figure 46) showed slight variations between the strains but the changes are not large enough to be considered significant.

4.3.3 *Chicken colonisation of the mutant strains*

In order to successfully colonise chickens *Campylobacter* strains possess multiple colonisation factors including efflux pumps, motility and chemotaxis, protein glycosylation, bile resistance mechanisms, heat shock response, invasion proteins, iron regulation, oxidative and nitrosative stress, and various metabolic pathways. All of which appear essential for successful colonisation (Hermans *et al.*, 2011). To assess whether the *cj0421c-cj0425* gene cluster is involved in chicken colonisation a *cj0423-4* double mutant and complement strain were produced in the NCTC11168-Hypermotile background. These strains were produced by Dr Jonathan Butler and Halah Al-Haideri and the chicken colonisation experiments were performed by Cosmin Chintoan-Uta in the laboratory of Professor Mark Stevens. The data shows no apparent change in the colonising ability of the mutant strain compared to wild type. While this does not suggest a role for these genes it does imply that these genes are not chicken colonisation factors nor are they involved with other colonisation factor.

4.3.4 *Peptidoglycan structure of the cj0422c mutant*

Since the Cj0425 cystatin is exported into the *C. jejuni* periplasm and there is no evidence to suggest it is secreted, it is expected that the hypothetical 'target' protein for Cj0425 is also

localised in the periplasm. Because not all strains of *C. jejuni* possess a copy of *cj0425* (though there may well be other cystatins that are un-annotated elsewhere in the genome) and because there appears to be no obvious growth defect in the mutant strains, it seems Cj0425 is not essential for growth in standard conditions. The biochemical role of the Cj0425 protein is examined in greater detail in chapter 6.

The Gram-negative peptidoglycan layer forms a crucial component of the cell envelope and allows the cell to maintain a rigid structure which aids in virulence and motility (Firdich *et al.*, 2014). Controlling peptidoglycan synthesis and maintenance is a complex process requiring multiple enzymes and regulatory stages. The Gram-negative peptidoglycan structure is discussed in the introduction (Section 1.7). The peptidoglycan structure is primarily composed of an amino-sugar based backbone and short peptide side chains (which contain both L and D amino acids). These peptide side chains are often targets for degradation as part of normal peptidoglycan turnover or as targets for antibacterial proteins (Park and Uehara, 2008). The CHAP domain is a family of peptidoglycan degrading enzymes which contains a cysteine residue in the active site region, similar to other cysteine proteases (Bateman and Rawlings, 2003). The crystal structure of the CHAP domain protein LysK from a *Staphylococcal* bacteriophage showed it contains a papain like topology and the mechanism of action is likely very similar to that of papain (papain is the archetypal cysteine protease) (Sanz-Gaitero *et al.*, 2014).

While this project is not primarily about the peptidoglycan structure of *Campylobacter jejuni* the peptidoglycan targeting cysteine peptidase enzymes in the periplasm of Gram-negative bacteria may act as a suitable binding target for Cj0425 and many of these are likely involved in peptidoglycan modification or turnover (Park and Uehara, 2008). In order to assess whether Cj0425 acts to inhibit a cysteine protease like peptidoglycan modification enzyme the peptidoglycan structure of wild type 11168 and the *cj0422c* mutant strain was analysed by HPLC. The analysis showed no observable change in the peptidoglycan structure of the *cj0422c* mutant. From this it is possible to conclude that Cj0425 does not act upon any of the native *C. jejuni* peptidoglycan enzymes in the periplasm, therefore, it may be that the 'target' protein for Cj0425 is in fact a non-native cysteine protease like enzyme.

4.3.5 *The potential role of the cj0421c-cj0425 gene cluster in defence against the type VI secretion system*

The Gram-negative type VI secretion system (T6SS) is a recently discovered mechanism for directing effector toxins into the periplasm of a neighboring competitor cell (Ho *et al.*, 2014). The topic is reviewed in greater detail in the introduction (Section 1.13). The T6SS acts as an

export system for antibacterial toxins which are often active in the periplasm of other Gram-negative bacteria. These toxins can attack the prey cell in multiple ways, by degrading the cell membrane by lipase action or by pore forming toxins, degrading the cell peptidoglycan layer by amidase or muramidase action, or entering the cytoplasm and degrading prey DNA (Russell *et al.*, 2014). The bacteria which produce these T6SS toxins often produce antitoxins to defend against toxins from closely related species, one example is the VgrG3 protein from *Vibrio cholerae* which acts as both a structural component of the T6SS and as a peptidoglycan degrading muramidase. Immediately downstream of the *vgrG3* gene is the gene *tsaB* which encodes an antitoxin that binds to and inhibits VgrG3 (Brooks *et al.*, 2013). The presence of these toxin-antitoxin systems allows bacteria to not only prevent accidental self-killing from their own toxins but also to defend against toxins from closely related strains. After several trial and error experiments I managed to develop an assay to measure how sensitive different strains of *C. jejuni* are to the *S. marcescens* type VI secretion system. The data presented in (Figure 50) shows that wild type *C. jejuni* is indeed killed by *S. marcescens* wild type DB10 and that this is dependent on a functional T6SS. The data shown in (Figure 51-53) shows that different sub strains of *C. jejuni* differ in sensitivity to the *S. marcescens* T6SS. The reason for this difference is unknown, it is known that different strains of *Campylobacter* possess different lipooligosaccharide structures and these can also be varied by phase variation or by external factors such as temperature shock (Semchenko *et al.*, 2010, Gilbert *et al.*, 2002). The variation in the LOS structure between strains may contribute to the variation in sensitivity to the T6SS seen between *C. jejuni* strains. It may also be due to differences in the composition of the periplasm or more simply due to differences in growth rate between the strains.

The *cj0422c*, *cj0423*, *cj0424*, *cj0425* and 3X gene deletion strains were also assayed for sensitivity to the *S. marcescens* type VI secretion system. The hypothesis was that the Cj0425 cystatin like protein may inhibit the action of one or more cysteine protease like endopeptidase enzymes exported into the *C. jejuni* periplasm by the T6SS. The other proteins Cj0423 and Cj0424 may also inhibit or interact with other toxic effector proteins secreted by *S. marcescens*. The hypothesis would predict that deletions in *cj0425* would make the strain more sensitivity to the T6SS and that the *cj0422c* deletion (where Cj0425 is up-regulated) may lead to increased resistance to the T6SS. However, the data shown in (Figure 50-53) does not agree with this. The data appears to show no change in sensitivity between the wild type strains and the *cj0422c*, *cj0423* or *cj0424* mutant strains. There does appear to be a slight increase in resistance observed in both the *cj0425* and 3X deletion strains, however this is the opposite to what would be expected and is likely the result of random variation. Since the type VI secretion system is widespread throughout Gram-negative bacteria (Russell *et al.*,

2014), the data presented here does not disprove the potential role of Cj0425 acting as a peptidoglycan cysteine protease inhibitor. This would need to be tested *in-vitro* before any conclusion about the possible role of Cj0425 is to be uncovered.

This chapter sought to assign a role to the *cj0421c-cj0425* gene cluster by analysis of mutant phenotypes, unfortunately no observable phenotype could be found. The qRT-PCR data presented in this chapter implies that this 5 gene cluster is best thought of as an isolated cluster with little to no impact on genes elsewhere in the *C. jejuni* genome. The lack of any observable effect on growth rate, antimicrobial sensitivity or chicken colonising ability does suggest that whatever role these genes play it is likely highly specific, possibly to a very particular environmental niche. The fact that the *cj0423-5* operon is repressed during normal growth implies that there should be some kind of activating signal. In order to screen for potential 'activation' signals a *lacZ* reporter construct was generated to look for gene induction of the operon.

5.1 Introduction

The data presented in the previous chapter has so far failed to assign any role to the *cj0421c-cj0425* operon. qRT-PCR data from the *cj0422c* mutant strain has shown that the expression of the *cj0423-5* operon is strongly repressed during growth under normal conditions (Figure 39), and that the expression of *cj0423* is increase around by around 100-fold at the transcriptional level in the *cj0422c* mutant. Data from previous work in the Kelly lab has shown that the Cj0422c protein binds to an 18bp palindromic repeat sequence located upstream of *cj0423* (Hitchcock, 2011) unpublished data. This binding site is located slightly behind the -10 box within the promoter and so likely prevents RNA-polymerase from effectively transcribing the operon. This implies that the role of Cj0422c is to repress the transcription of the *cj0423-5* operon and that some kind of stimulus leads to the operon being expressed, presumably by the release of Cj0422c from the promoter region. Since there is currently no obvious role for the genes within the operon there is no obvious condition or chemical stimuli to test for gene induction. I decided to begin screening a large range of physical and chemical conditions to see if any up-regulation of the operon could be observed.

As a tool to screen multiple conditions I produced a series of plasmids using the *E. coli lacZ* gene as a reporter construct. The expression of the *lacZ* gene can be quickly assayed using methods described in (Section 2.20) which are based on (Zhang and Bremer, 1995). The *lacZ* gene was cloned downstream of the *cj0422c* and *cj0423* promoter regions and inserted into the wild-type genome as a single copy at the *cj0046* pseudogene locus used for complementation in *C. jejuni*. The *cj0423::lacZ* construct also was tested by transforming the plasmid into the *cj0422c* mutant from the previous chapter, where a strong up-regulation should be observed.

The aim of this chapter was to screen potential conditions for induction of the *cj0423-5* operon. Initially, the *lacZ* reporter constructs were produced and tested to ensure that they functioned as expected. Following successful construction of the reporter strains a series of antimicrobial compounds and various other membrane stressing compounds were tested for induction. As a way of testing multiple compounds simultaneously a novel assay method was developed using the Biolog© Phenotype Microarray system. These 96 well plates contain a range of compounds and are typically used to look for changes in cell growth rate when incubated with various different nutrient sources. For this study the plates were used to look for potential inducers of the *cj0423* operon.

5.2 Chapter 5 Results

5.2.1 Construction of the *lacZ* reporter strains in *C. jejuni*

The *lacZ* reporter constructs were generated using isothermal assembly cloning using methods described previously (Section 2.11). The constructs were generated in the p46 complementation plasmids using the same cloning system described in (Section 4.2.6).

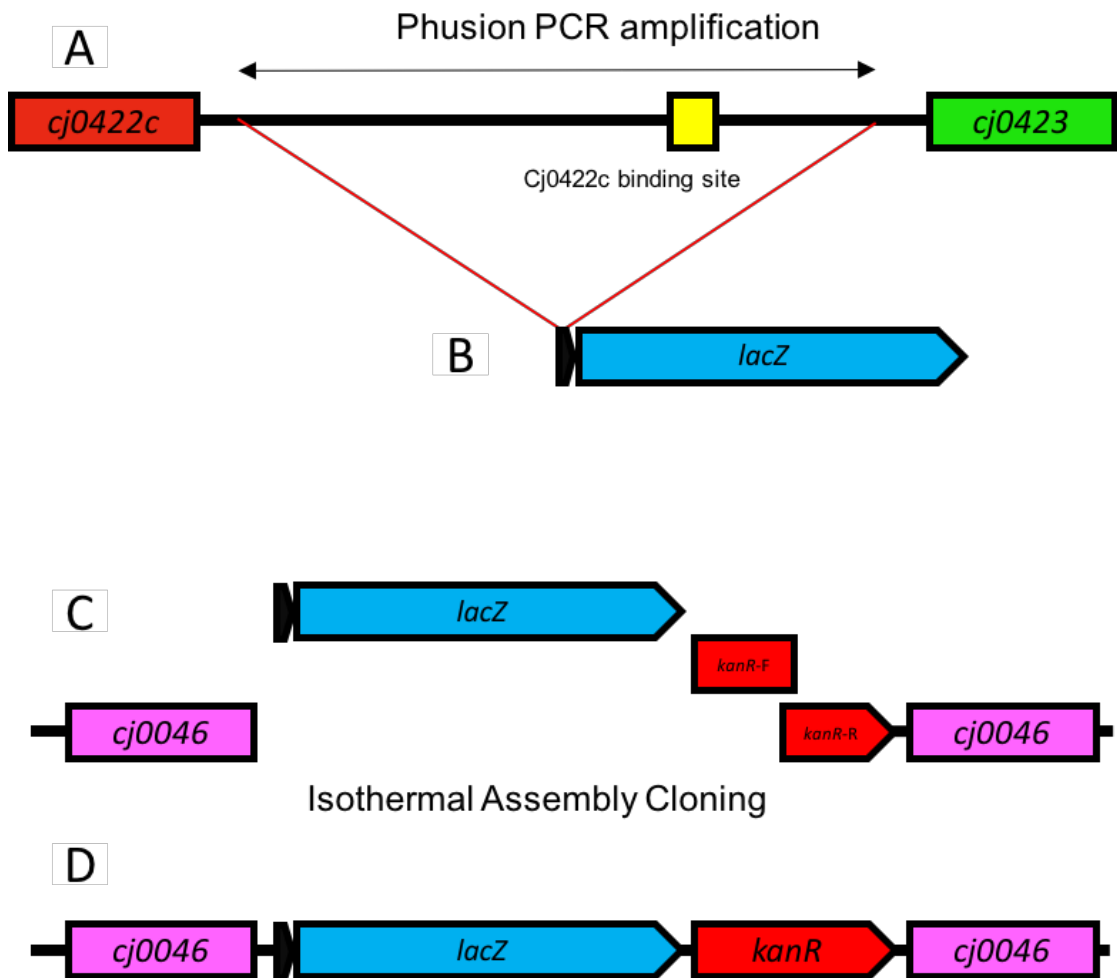


Figure 54: Generation of a *lacZ* reporter construct by Isothermal Assembly (ISA) cloning. (A) the intergenic region between *cj0422c* and *cj0423* was amplified using high fidelity Phusion polymerase. The primers were designed to amplify up the promoter region just before the predicted RBS and contained 30bp adapter regions to allow for ISA cloning (Table 7). (B) The promoter region was attached upstream of the *lacZ* gene (amplified from the pRS415 plasmid) by overlap extension PCR. (C) the ISA reaction was performed using the same technique described in the ISA complementation protocol (Section 4.2.6). (D) shows the fragments after insertion into the pK46 plasmid.

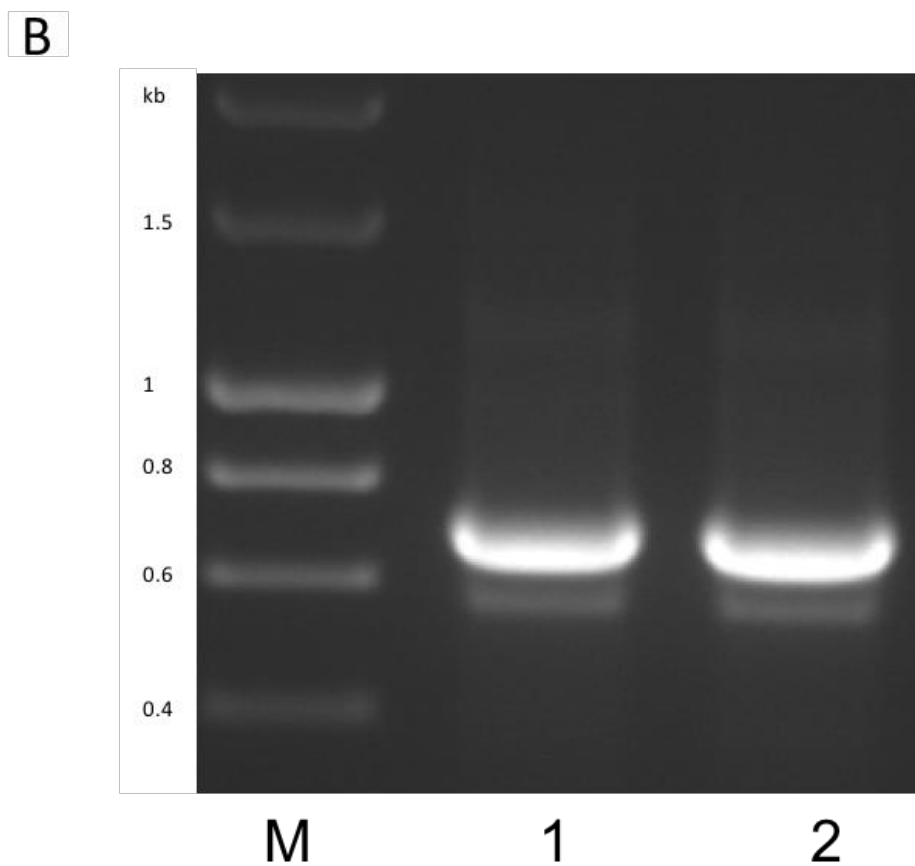
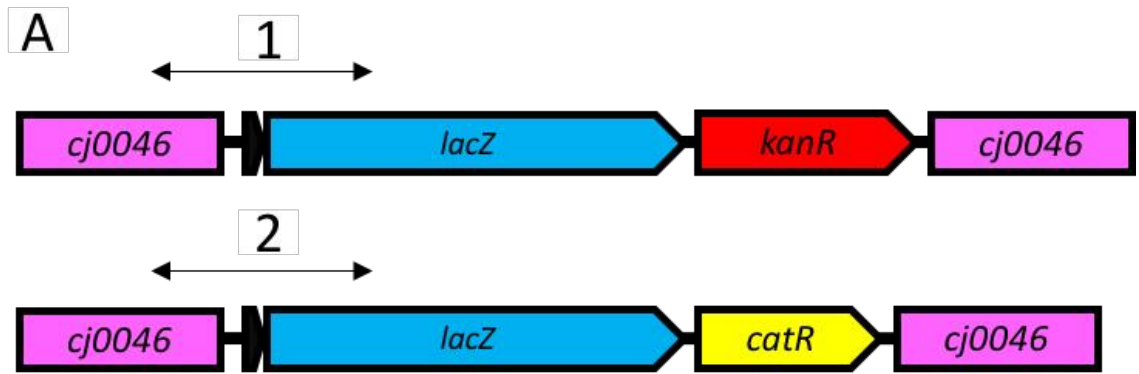


Figure 56: Production of the *lacZ* reporter constructs in *C. jejuni* 11168-DJK. The ISA vectors shown in (Figure 55) were transformed into the *cj0046* pseudogene locus of *C. jejuni* 11168. (A) shows the gene arrangement of the *lacZ* pF pK46 strain containing the forward facing promoter region with a kanamycin resistance marker and the *lacZ* pR pC46 strain containing the reverse facing promoter region with a chloramphenicol resistance marker. Successful transformation of the constructs was confirmed by the agarose gel shown in (B). The lane number correspond with the arrows shown in (A). Both bands are expected to be 725 bp in length.

5.2.2 Confirmation of the *lacZ* reporter strains

Unless otherwise stated all the data presented for the *lacZ* reporter constructs is expressed in Miller units. These are arbitrary units of β -galactosidase expression which measures the amount of o-nitrophenol liberated from the lactose analog ortho-nitrophenyl- β -galactoside by LacZ. The o-nitrophenol strongly absorbs light at 420_{nm} giving it a bright yellow colour. The full assay is described in (Section 2.20) which is based on (Zhang and Bremer, 1995). The absorbance at 420_{nm} is calculated as relative to the absorbance at 600_{nm} to give an estimation of *lacZ* expression per cell density. The assay was altered slightly between testing different compounds and conditions; these variations are explained for each individual assay.

As a start to the investigation three *lacZ* strains were tested for gene expression during a normal growth curve. The *cj0423::lacZ* strain contains the *lacZ* gene under the *cj0423* promoter with a kanamycin resistance marker. The *cj0422::lacZ* strain contains the *lacZ* gene under the control of the *cj0422c* promoter with a chloramphenicol resistance marker. The Δ *cj0422c cj0423::lacZ* strain contains the same construct as the *cj0423::lacZ* strain but was transformed into the *cj0422c* mutant strain. This strain acted as a positive control strain where in theory the expression of *lacZ* under the *cj0423* promoter should be strongly up-regulated when transformed into the *cj0422c* mutant strain. The strains were grown overnight on blood agar plates under normal conditions and the cell material scraped off and diluted to a starting OD_{600nm} of 0.05 in MHS broth with no selective antibiotics. The cultures were incubated under standard conditions for 24 hours with measurements being taken at 0, 2, 4, 6, 8 and 24 hours. The expression of *lacZ* was calculated at each time point and the data is shown in (Figure 57). As a negative control a sample of wild type *C. jejuni* 11168-DJK was also tested for *lacZ* expression. The 11168 genome does not contain a homologue of *lacZ* and there was no detectable change in the absorbance at 420_{nm} (data not shown).

The data presented in (Figure 57) shows that the expression from the *cj0423* promoter is tightly repressed under normal conditions and can fluctuate between around 50-150 Miller units. It also shows that the expression is at its lowest point during log phase growth. The expression from the *cj0422c* promoter is comparatively quite high and fluctuates between 200-300 Miller units. This is consistent with the role of Cj0422c as a repressor protein as high expression will lead to stronger repression of the *cj0423* promoter. The expression of *lacZ* under the control of the *cj0423* promoter when expressed in the *cj0422c* mutant is much higher and fluctuates between 2000 and up to 4000 Miller units. Unless otherwise stated only the *cj0423::lacZ* strain in the wild type background is used from this point onwards and all assays are performed using standard MHS media at 37°C unless otherwise stated.

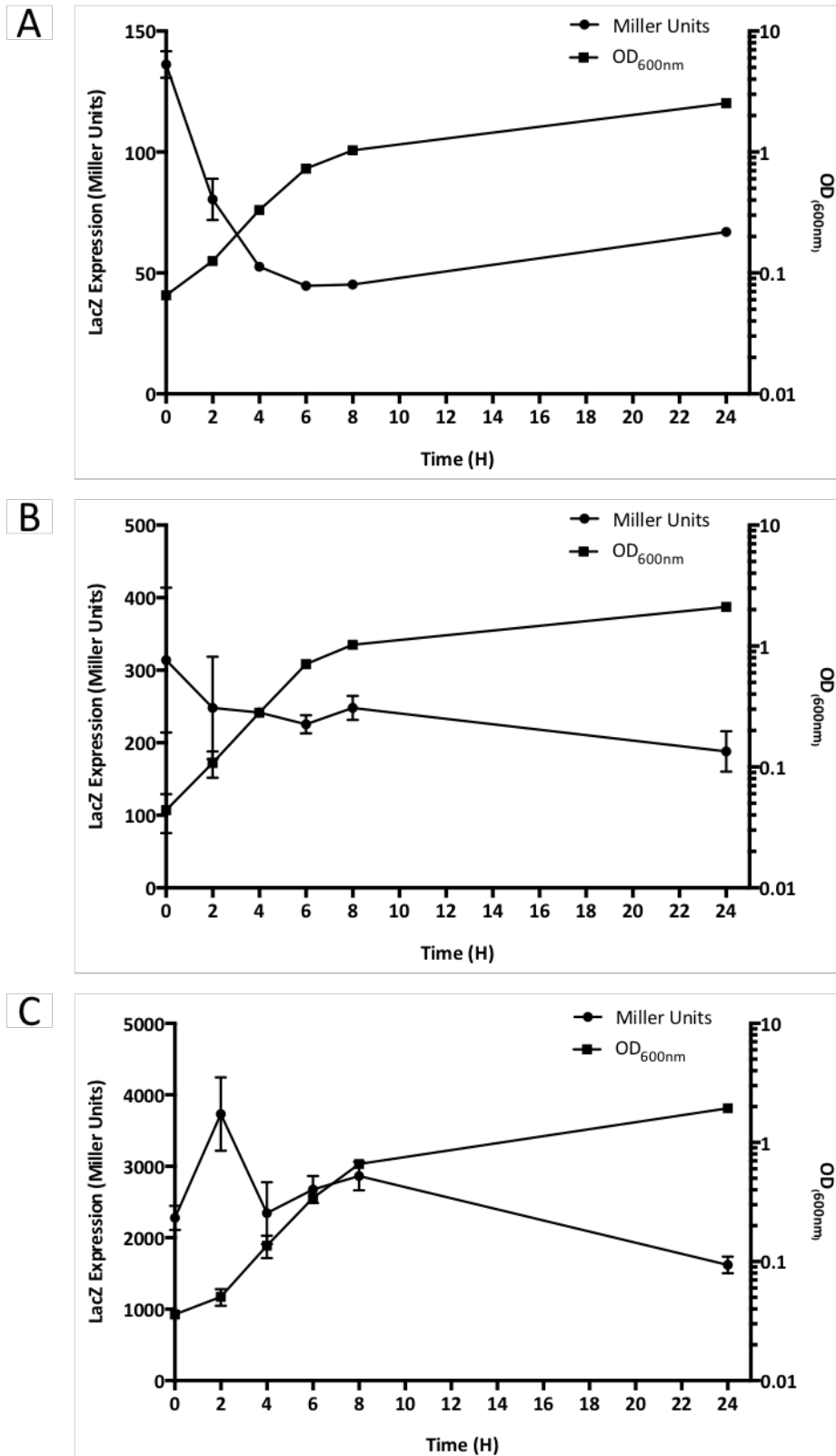


Figure 57: Expression of the *lacZ* reporter during normal growth. The expression of the *lacZ* gene was measured at time points 0, 2, 4, 6, 8 and 24 over a 24-hour growth curve. (A) shows the expression of the *lacZ* gene (expressed in Miller units) while under the control of the *cj0423* promoter. (B) shows the expression of the *lacZ* gene under the control of the *cj0422c* promoter. (C) shows the expression of the *lacZ* gene under the control of the *cj0423* promoter but expressed in the *cj0422c* mutant strain. The error bars show the standard deviations from 3 separately grown replicates.

5.2.3 Assaying antimicrobial compounds for induction of the *cj0423-5* operon

Having confirmed that the *lacZ* reporter strains are functional and that the expression was up-regulated as expected in the *cj0422c* mutant strain I began to test a series of antimicrobial compounds for possible up-regulation of the *cj0423-5* operon in wild type cells. These were chosen specifically to target different parts of the cell, including the cell wall, the cell membrane and protein synthesis. The data shown in (Figure 58) shows the expression of *lacZ* when cells were challenged with Ampicillin, Gentamycin, Erythromycin and the model CAMP Polymyxin-B; none of these antimicrobials produced an up-regulation of the *lacZ* strain. The strain was also challenged with non-therapeutic antimicrobials including SDS, Taurocholic acid (a bile acid), 1,2-Benzisothiazole-3(2H)-one (BIT) and ethanol (Figure 60), again none of these produced any significant up-regulation in gene expression. The expression of LacZ is apparently reduced in some of the data presented however since the operon is tightly repressed during normal growth this is likely due to the inhibitory effect of the antimicrobials being tested. The LacZ expression (in Miller units) appears to increase with increasing SDS concentrations (Figure 59) however this is due to the cells being lysed rather than because of increased expression as shown by the decreasing OD_{600nm}.

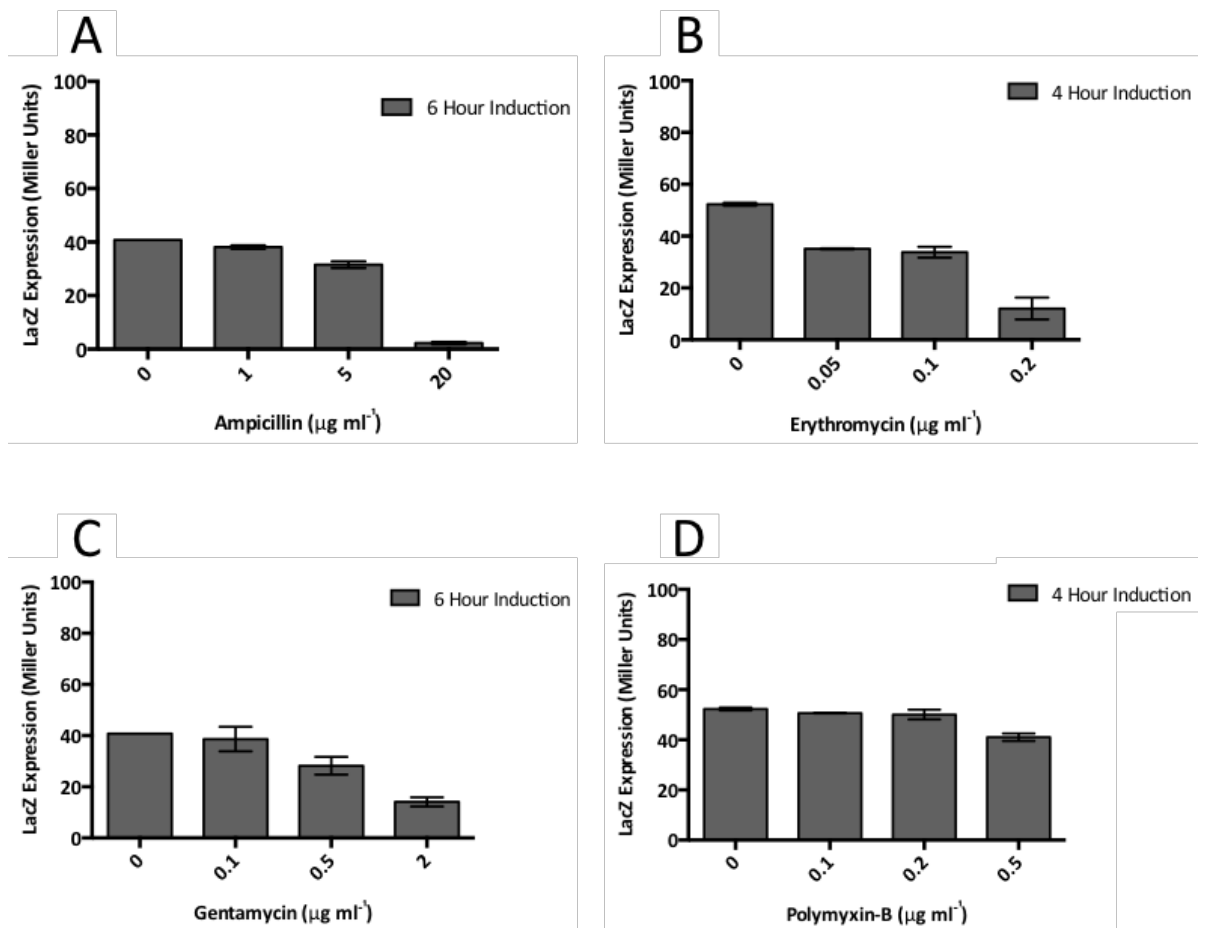


Figure 58: Expression of the *lacZ* reporter when challenged with antibiotics. The *lacZ* reporter strain was grown to a starting $\text{OD}_{600_{nm}}$ of 0.5 and the antibiotics added. The cultures were incubated for 6 hours with ampicillin and gentamycin (A and C respectively) or 4 hours with erythromycin and polymyxin-B (B and D respectively). The concentration ranges are shown on the individual graphs. The 0 concentrations were used as negative controls. The error bars are the standard deviation from 2 biological replicates.

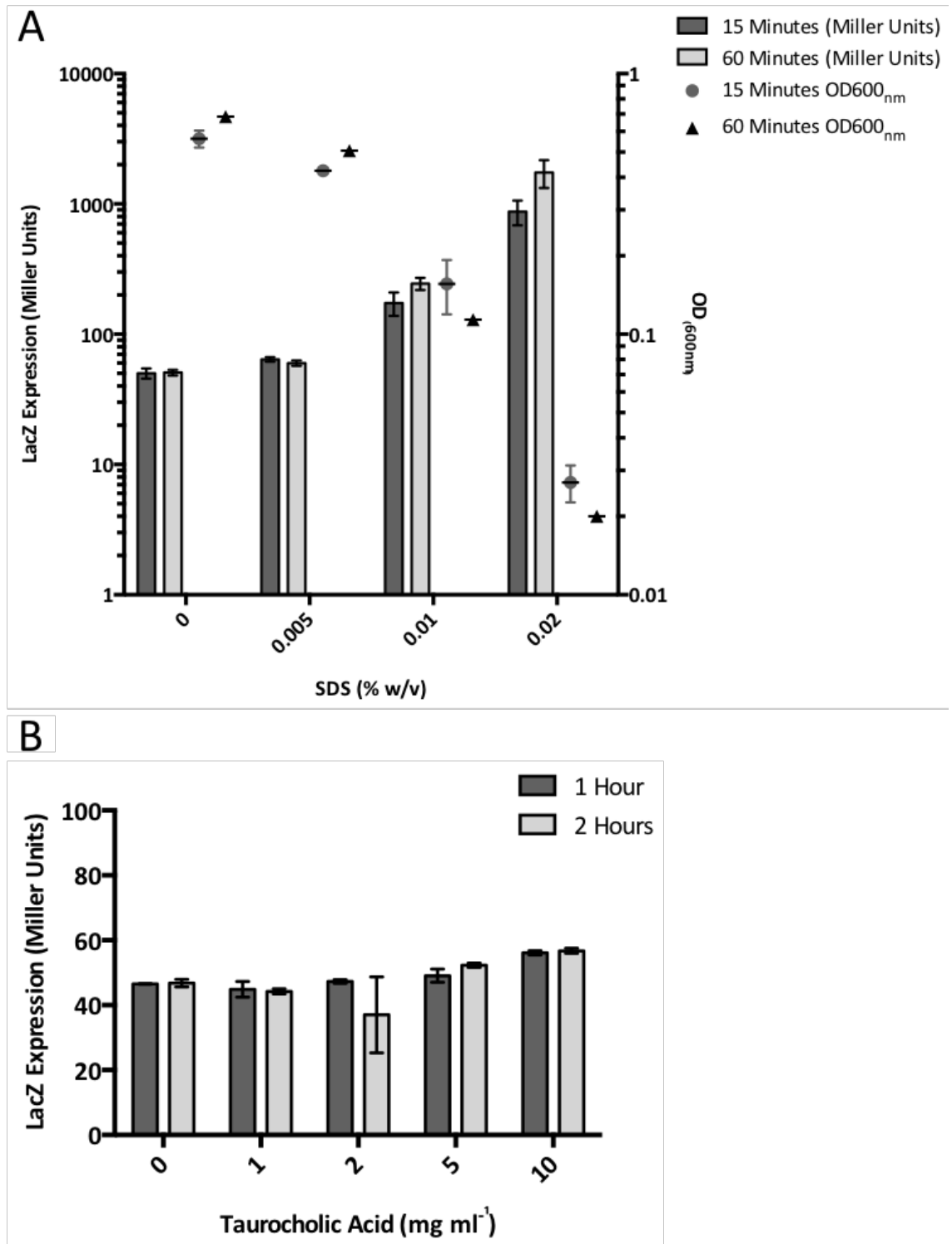


Figure 59: Expression of the *lacZ* reporter when challenged with SDS and bile acid. The *lacZ* reporter strain was grown to a starting OD_{600nm} of 0.5 and the SDS and Taurocholic acid added. (A) shows both the calculated Miller units and the OD_{600nm} values for the reporter strain when challenged with SDS. The error bars show the standard deviations from 3 biological replicates. (B) shows the gene expression in response to the bile acid taurocholic acid. The error bars show the standard deviations from 2 biological replicates.

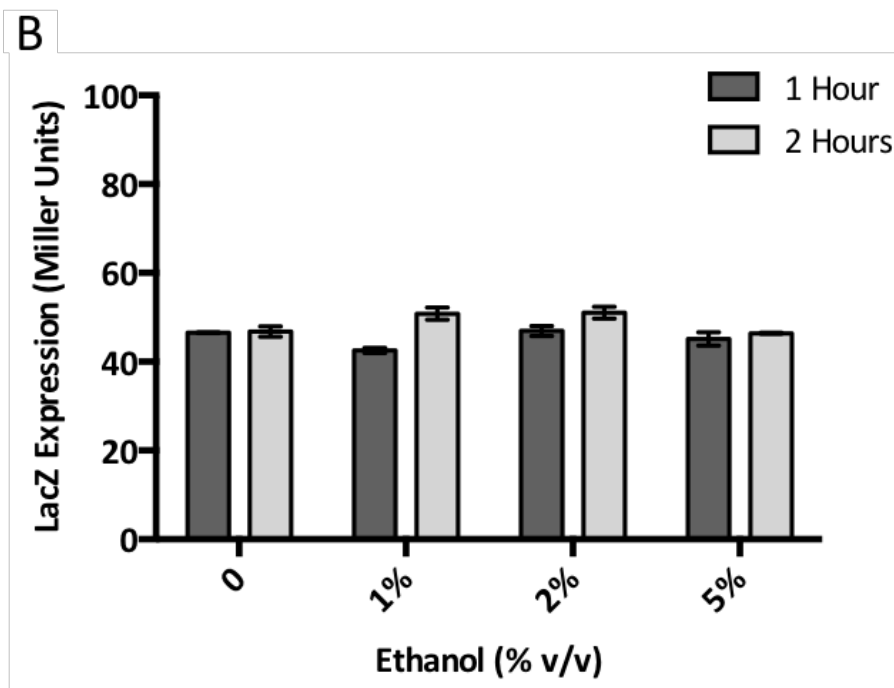
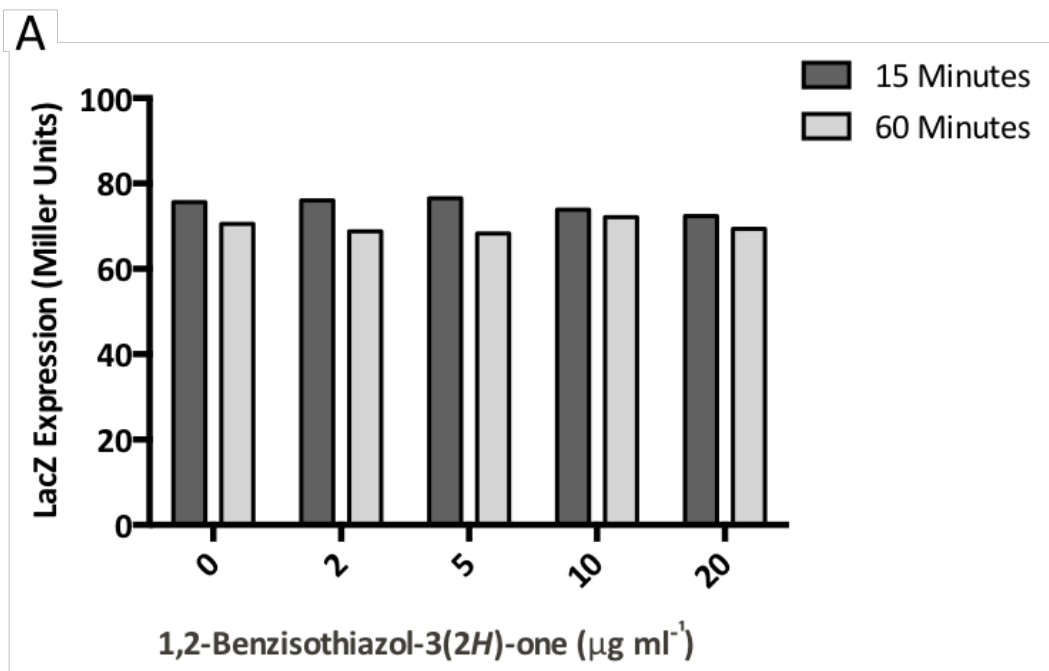


Figure 60: Expression of the *lacZ* reporter when challenged with BIT and ethanol. The *lacZ* reporter strain was grown to a starting OD_{600nm} of 0.5 and the 1,2-Benzisothiazole-3(2H)-one (BIT) and Ethanol added. **(A)** shows the expression in Miller units at 15 and 60 minutes post challenge with BIT. The data is from single replicates of at each concentration. **(B)** shows the expression in Miller units at 1 hour and 2 hours post challenge with ethanol. The error bars show the standard deviations form 2 biological replicates.

5.2.4 Assaying sera and peptidoglycan fragments for induction of the *cj0423-5* operon

Since none of the antimicrobials tested for induction have produced a detectable up-regulation I decided to test some other compounds and conditions which *C. jejuni* may encounter during chicken colonisation or during the human infection cycle. *C. jejuni* has been shown to be sensitive to human serum *in-vitro* (Pennie *et al.*, 1986) and it was thought the *cj0423-5* operon may help provide resistance. Both human and chicken sera were purchased from Sigma-Aldrich and tested as potential inducers of the operon. Since sera is quite opaque and may interfere with the OD_{600nm} readings the cultures were incubated with sera and at the appropriate time points 1 ml of culture was quickly centrifuged and re-suspended in an equal volume of MHS broth prior to the OD_{600nm} reading being taken. The data is shown in (Figure 61) and shows no significant change in LacZ expression.

As discussed in the previous chapter (Section 4.2.14) Cj0425 may act as an inhibitor of peptidoglycan degrading or modification enzymes. In order to test whether degradation of peptidoglycan induces the *cj0423-5* operon, 3 peptidoglycan specific non proteinogenic amino acids D-Alanine, D-Glutamic acid and diaminopimelic acid (mDAP) were tested as potential inducers of the operon. The data is shown in (Figure 61) and while there is a slight increase in LacZ expression, it is not large enough to be considered biologically significant.

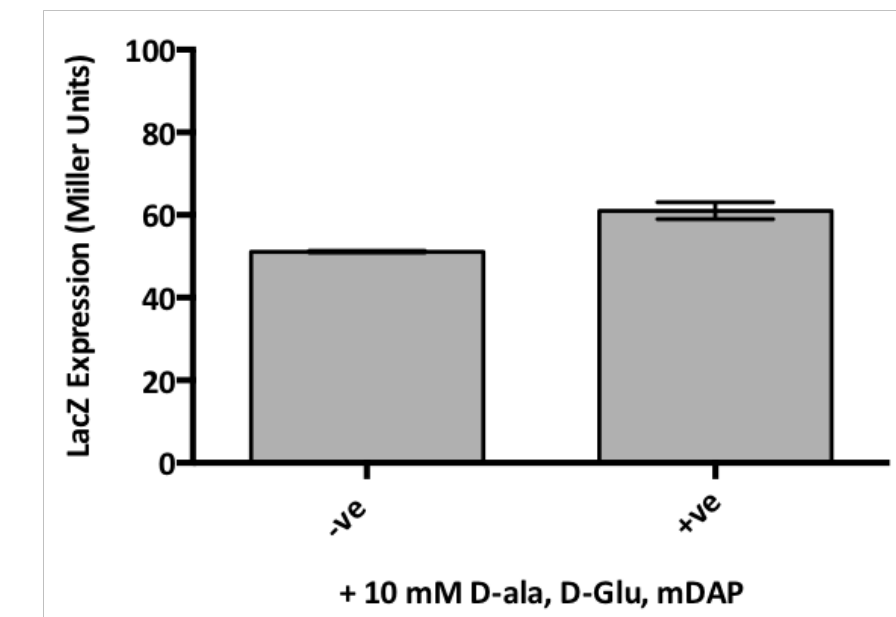
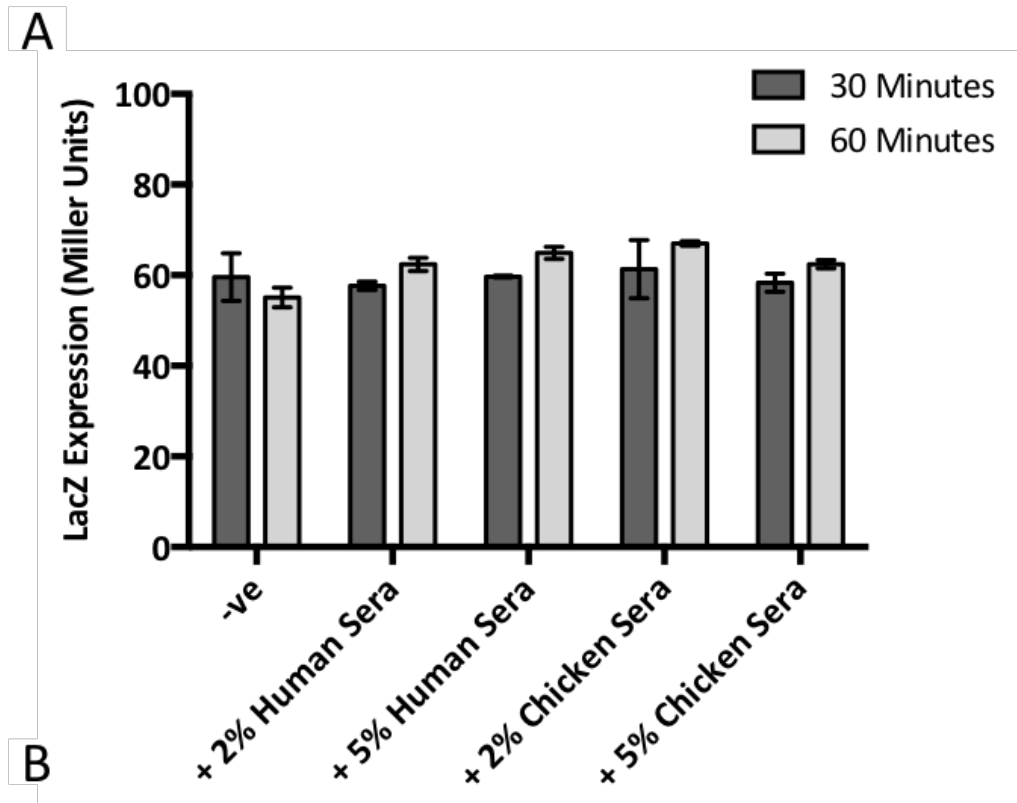


Figure 61: Expression of the *lacZ* reporter when challenged with sera and peptidoglycan derived amino acids. The *lacZ* reporter strain was grown to a starting OD_{600nm} of 0.5 and the sera and peptidoglycan fragments added. (A) shows the expression in Miller units at 30 and 60 minutes' post challenge with both human and chicken sera. The error bars show the standard deviation from 2 biological replicates. (B) shows the expression in Miller units at 2 hours post incubation with 10 mM of D-alanine, D-glutamic acid and diaminopimelic acid (mDAP) mixed together. The error bars show the standard deviations from 3 biological replicates.

5.2.5 Assaying environmental stress conditions for induction of the *cj0423-5* operon

As well as antimicrobial compounds *Campylobacter* will likely encounter non-specific stress conditions such as oxidative stress, osmotic stress, variations in pH and temperature changes. Oxidative stress was tested as a potential inducer by mixing the reporter strain with hydrogen peroxide and by transferring the reporter strain to increasing atmospheric oxygen concentrations (substituted with nitrogen), the data is shown in (Figure 62). No biologically significant increases in LacZ expression was observed when the reporter strain was incubated with hydrogen peroxide and only minor changes were observed when incubated under different atmospheric oxygen conditions.

Both positive and negative osmotic shock were tested as potential inducers for the *cj0423-5* operon. For positive osmotic shock the reporter strain was cultured under normal conditions in MHS broth with increasing concentrations of NaCl. To test for potential induction under negative osmotic stress the reporter strain was centrifuged and re-suspended in pre-equilibrated sterile distilled water (SDW) with increasing NaCl concentrations, the data is shown in (Figure 63). Neither positive nor negative osmotic shock produced a biologically significant increase in LacZ expression.

Changes in pH were tested as a potential inducer of the *cj0423-5* operon, the reporter strain was centrifuged and re-suspended in MHS broth containing either 100 mM MES or TRIS buffers which had been adjusted to a range of acidic and basic pH. The data is shown in (Figure 64) and shows no biologically significant increase in LacZ expression between the pH values. The pH of each media was also tested after the experiment to ensure the pH had not altered during the experiment.

Temperature shock was tested as a potential inducer of the *cj0423-5* operon. This was tested because the Cj0422c protein is unstable when chilled to below 20°C, this is discussed further in Chapter 6. Because the Cj0422c regulatory protein is unstable at low temperatures it was thought that a sudden drop in temperature may cause the protein to become unbound from the *cj0423* promoter region and therefore allow for increased expression of the *cj0423-5* operon. The reporter strain was grown under normal conditions and then transferred to a range of temperature incubators, the data is shown in (Figure 65) and shows no biologically significant difference in LacZ expression at different temperatures.

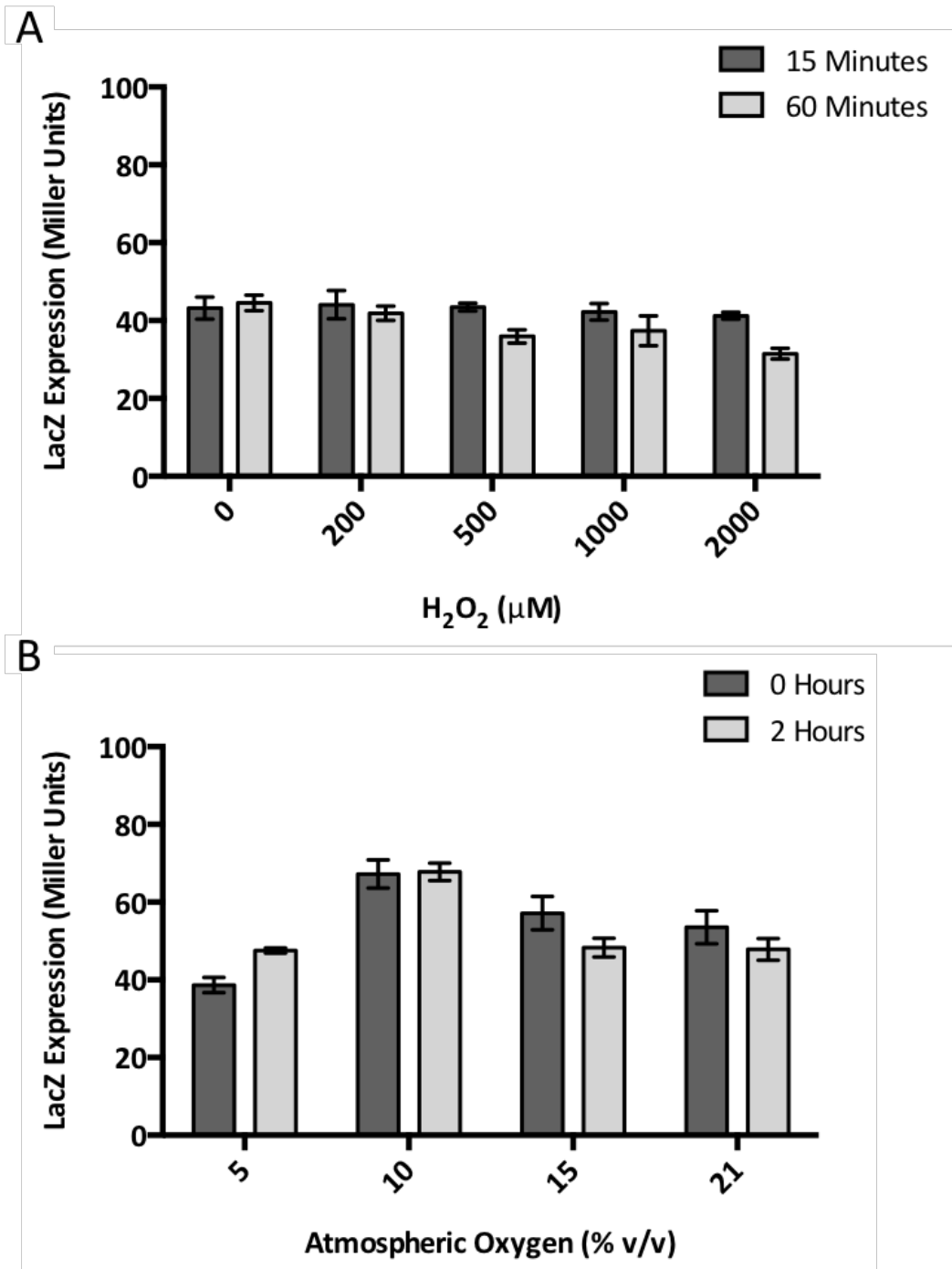


Figure 62: Expression of the *lacZ* reporter when challenged with H₂O₂ and atmospheric oxygen. The *lacZ* reporter strain was grown to a starting OD_{600nm} of 0.5 and mixed with hydrogen peroxide or incubated in varying atmospheric conditions. **(A)** shows the expression in Miller units at 15 and 60 minutes' post challenge with hydrogen peroxide. The error bars show the standard deviation from 3 biological replicates. **(B)** shows the expression in Miller units at 0 and 2 hours post incubation at different oxygen concentrations. The error bars show the standard deviations from 3 biological replicates.

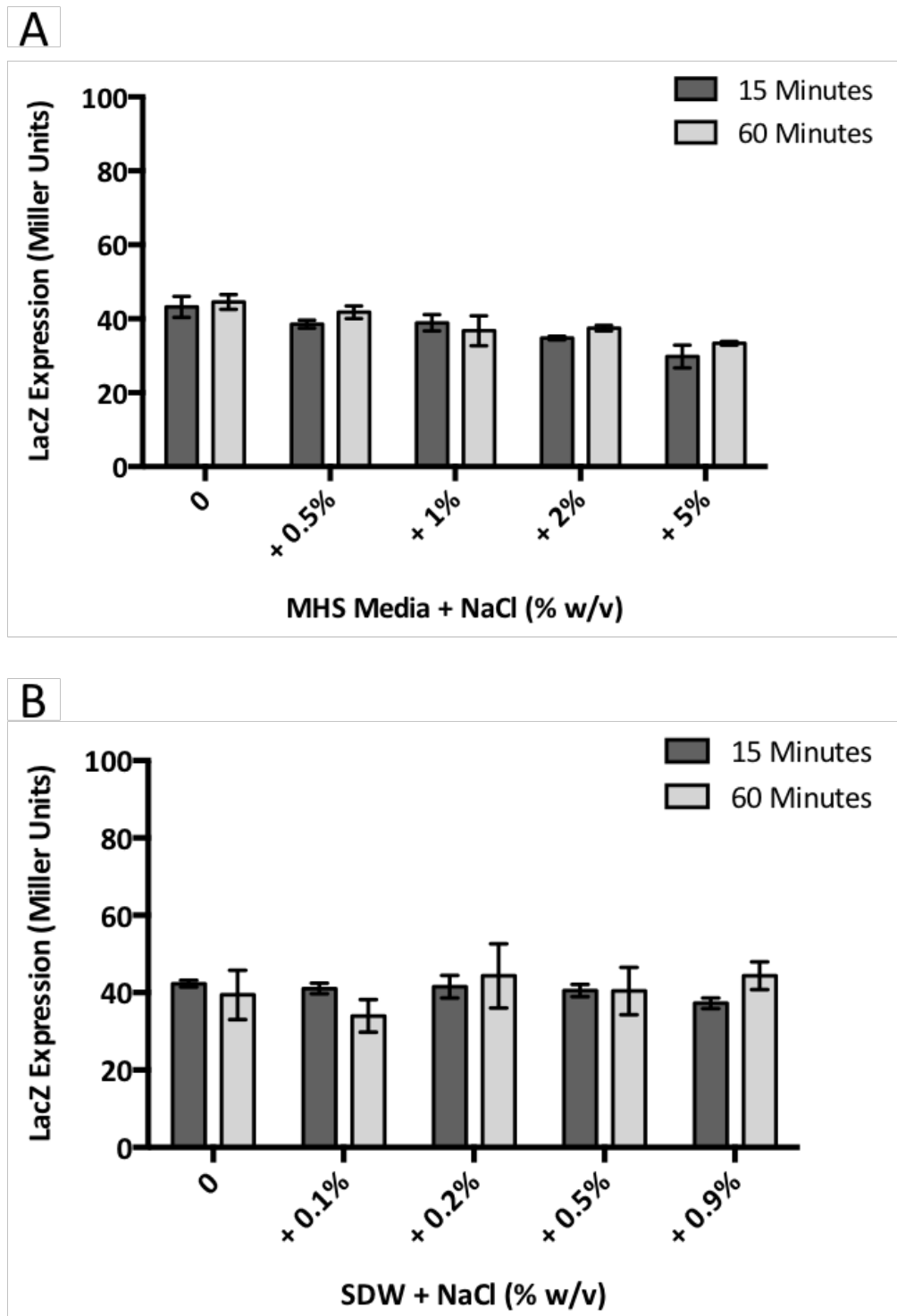


Figure 63: Expression of the *lacZ* reporter when challenged by positive and negative osmotic shock. The *lacZ* reporter strain was grown to a starting $OD_{600_{nm}}$ of 0.5 and mixed with varying salt concentrations. (A) shows the expression in Miller units at 15 and 60 minutes' post challenge with increasing salt concentrations. The error bars show the standard deviation from 3 biological replicates. (B) shows the expression in Miller units at 15 and 60 minutes' post challenge with decreasing salt concentrations. The cells were cultured in MHS media and briefly centrifuged and re-suspended in sterile distilled water that had been pre-equilibrated to normal growth conditions. The error bars show the standard deviations from 3 biological replicates.

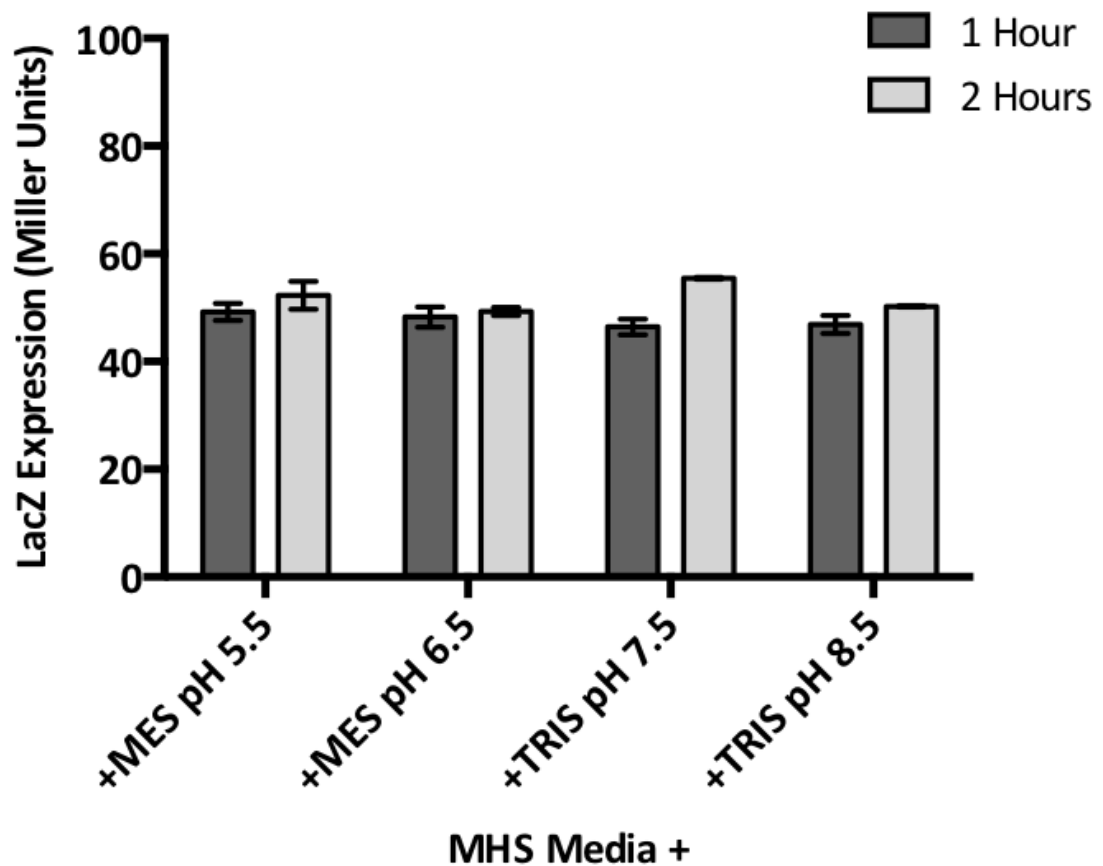


Figure 64: Expression of the *lacZ* reporter when challenged by acidic and basic pH. The *lacZ* reporter strain was grown to a starting OD_{600nm} of 0.5 and briefly centrifuged and re-suspended in fresh MHS media with either 100 mM MES (2-(*N*-morpholino)ethanesulfonic acid) for acidic pH adjustment or 100 mM TRIS (Tris(hydroxymethyl)aminomethane) for basic pH adjustment. The medias were adjusted to the correct pH with 1 M of HCl or NaOH. The data shows the expression in Miller units at 1 hour and 2 hours' post incubation over a range of pH conditions. The error bars show the standard deviation from 2 biological replicates.

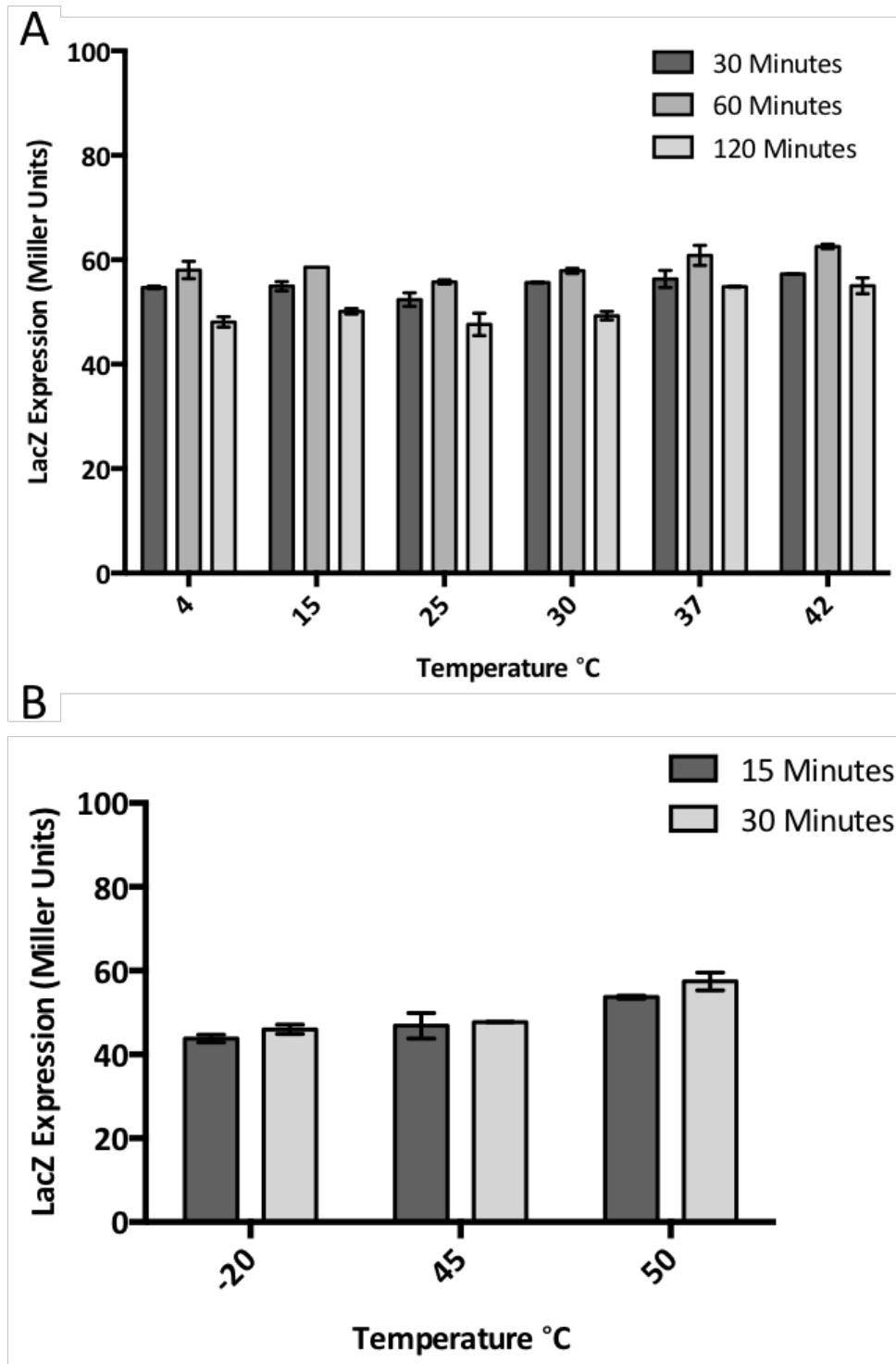


Figure 65: Expression of the *lacZ* reporter when challenged by temperature change. The *lacZ* reporter strain was grown to a starting OD_{600nm} of 0.5 and incubated at various temperatures. (A) shows the expression in Miller units at 30, 60 and 120 minutes' post incubation at varying temperatures. The error bars show the standard deviation from 2 biological replicates. (B) shows the expression in Miller units at 15 and 30 minutes' post incubation at -20°C, 45°C and 50°C which would likely lead to quick cell death. The error bars show the standard deviations from 2 biological replicates.

5.2.6 High throughput screening of the *lacZ* reporter strain using the Biolog Phenotype Microarray system

The induction assays up to this point have failed to identify a condition or compound that causes the up-regulation of the *cj0423* operon. So far the Miller assays used to screen for potential inducers have focused on one individual compound or condition at a time. In order to screen multiple compounds at once it was decided to utilise the phenotype microarray system from Biolog™ to screen for potential inducers of the *cj0423* operon. The phenotype microarray system is based on a series of commercially available 96 well plates where each well contains a different compound such as different Carbon, Nitrogen or Sulphur sources. Typically, the phenotype microarray plates are used to screen strains of bacteria for changes in metabolism, an example of this in *Campylobacter* is a 2010 publication where the authors used the carbon source phenotype microarray plates to look for changes in amino acid utilization in response to temperature variation (Line *et al.*, 2010).

10 phenotype microarray plates (PM1-PM10) were used to screen up to 950 different compounds (some plates contain duplications) for induction of the *cj0423* promoter. The reporter strain was cultured in the modified MCLMAN minimal media system (Section 2.6.1), this was done to ensure that any up-regulation is the result of the individual compound being tested. All the phenotype microarray assays were performed using the methods described in (Section 2.20.1). The compounds in each of the phenotype microarray plates are listed in the appendix (Section 8.2), the data is also available at (http://www.biolog.com/pdf/pm_lit/PM1-PM10.pdf), at the time of writing. The data is shown in (Figure 66-69) and shows the expression (in Miller units) for each individual well. The data shows a reasonably large degree of variation in the expression of each well. None of the individual compounds produced a strong (>5 fold) up-regulation of LacZ so the assay has not definitively shown any single compound to be the 'inducer' for the *cj0423-5* operon.

In order to calculate a fold change in expression, the average expression of all the wells (excluding the blank well) for each individual plate was calculated. The difference between each individual well and the plate average was then calculated and expressed as a fold change in expression. This method of determining the fold change is reasonably conservative but the Biolog plates only contain a single negative well which must be used as a blank for measuring the OD600_{nm} and OD420_{nm}. This means that there are no reference values to use as a negative control, so it is assumed that the total average value for each individual plate is close enough to the theoretical un-induced control to act as a reference, a >2-fold cutoff was considered

significant enough to warrant further analysis. The average Miller unit values for each plate are listed in the figure legends.

In total 14 individual wells out of 950 showed a >2-fold change in expression compared to the individual plate average, these represented with black stars on the individual bars in (Figure 66-69) and are listed in (Table 16). It should be noted that the largest increase in expression is 3.94-fold (plate PM4 well C10) which is not a large increase and is considerably less than the 50-fold increase in LacZ expression seen in the *cj0422c* mutant (Figure 57). Out of the 14 individual wells which showed as >2-fold increase, 6 contained compounds which are duplicated in other wells and did not produce a >2- fold increase in expression (the fold changes in the duplicated wells are listed in (Table 16). These 6 wells were discounted as they did not produce a repeatable induction. The remaining 8 compounds are discussed in (Section 5.3.6).

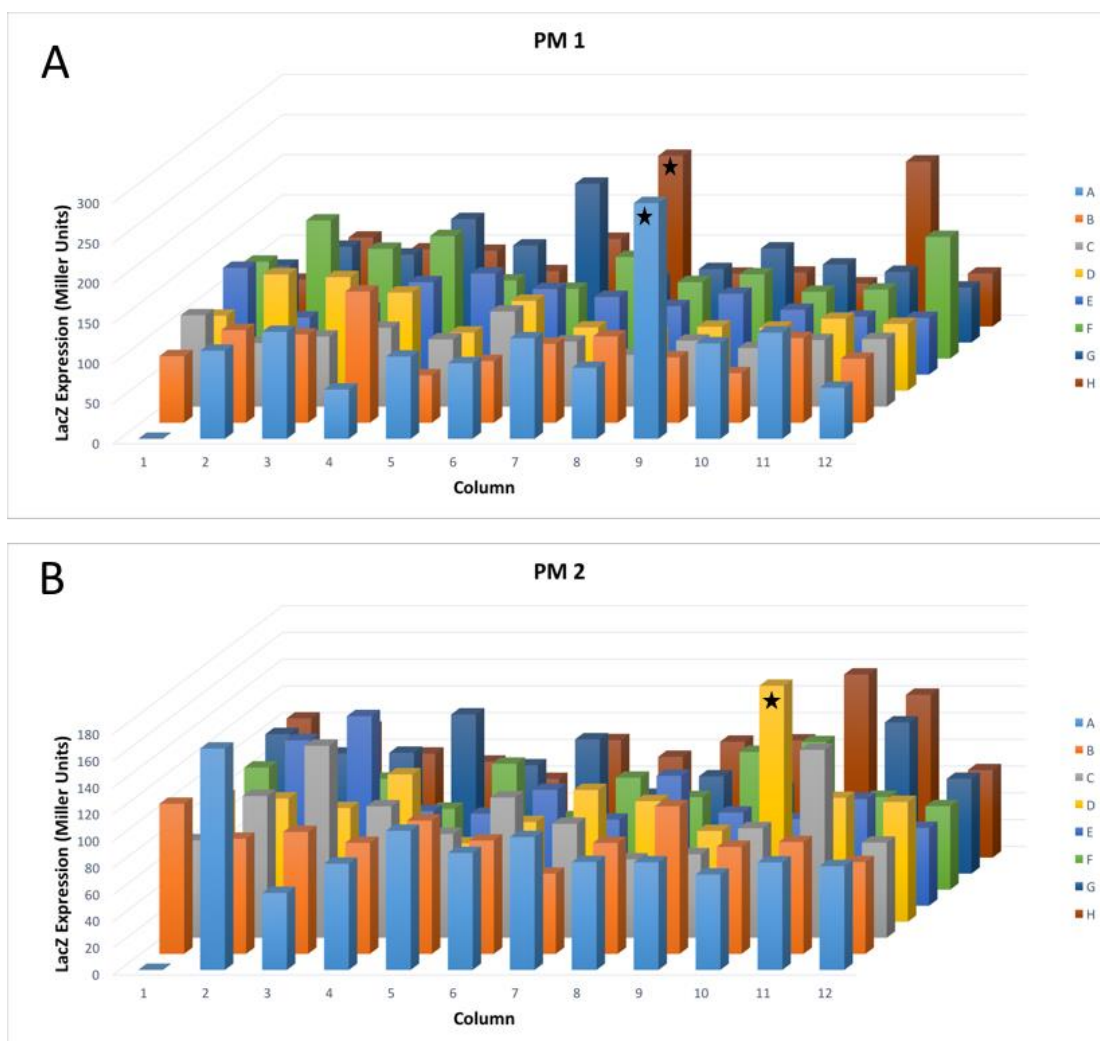


Figure 66: Expression of the *lacZ* reporter when cultured on different carbon sources. The *lacZ* reporter strain was grown to a starting OD_{600nm} of 0.9 and re-suspended in the MCLMAN minimal media to an OD_{600nm} of 0.4 and incubated for 2 hours under normal conditions. The cultures were then transferred to the individual wells of the phenotype microarray plates and incubated for 2 hours under standard conditions with gentle shaking. (**A** and **B**) show the expression in Miller units for the wells in the PM1 and PM2 respectively which both contain various carbon sources (the PM1 plate average is 102.93 Miller units) (the PM2A plate average is 86.82 Miller units). Stars represent individual wells with a >2-fold increase in LacZ expression.

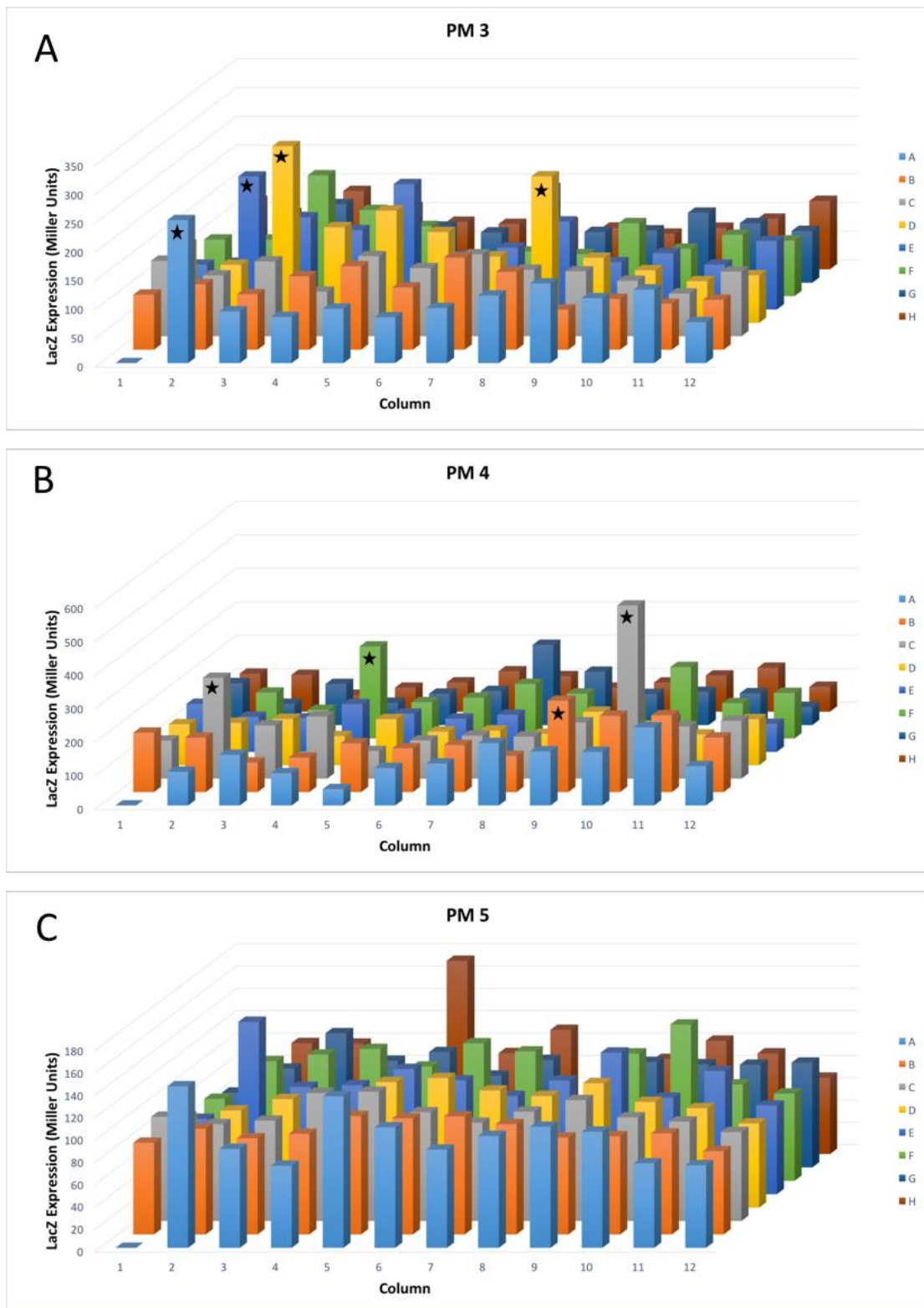


Figure 67: Expression of the *lacZ* reporter when cultured on nitrogen, phosphorus and sulphur sources. The *lacZ* reporter strain was grown to a starting OD_{600nm} of 0.9 and re-suspended in the MCLMAN minimal media to an OD_{600nm} of 0.4 and incubated for 2 hours under normal conditions. The cultures were then transferred to the individual wells of the phenotype microarray plates and incubated for 2 hours under standard conditions with gentle shaking. (A) shows the expression in Miller units for the wells in the PM3 plate which contains various nitrogen sources (the PM3 plate average is 114.89 Miller units). (B) shows the expression in Miller units for the wells in the PM4 plate which contains phosphorus and sulphur sources (the PM4 plate average is 130.98 Miller units). (C) shows the expression in Miller Units for the wells in the PM5 plate which contains a range of standard nutritional supplements (the PM5 plate average is 97.39 Miller units). Stars represent individual wells with a >2-fold increase in LacZ expression.

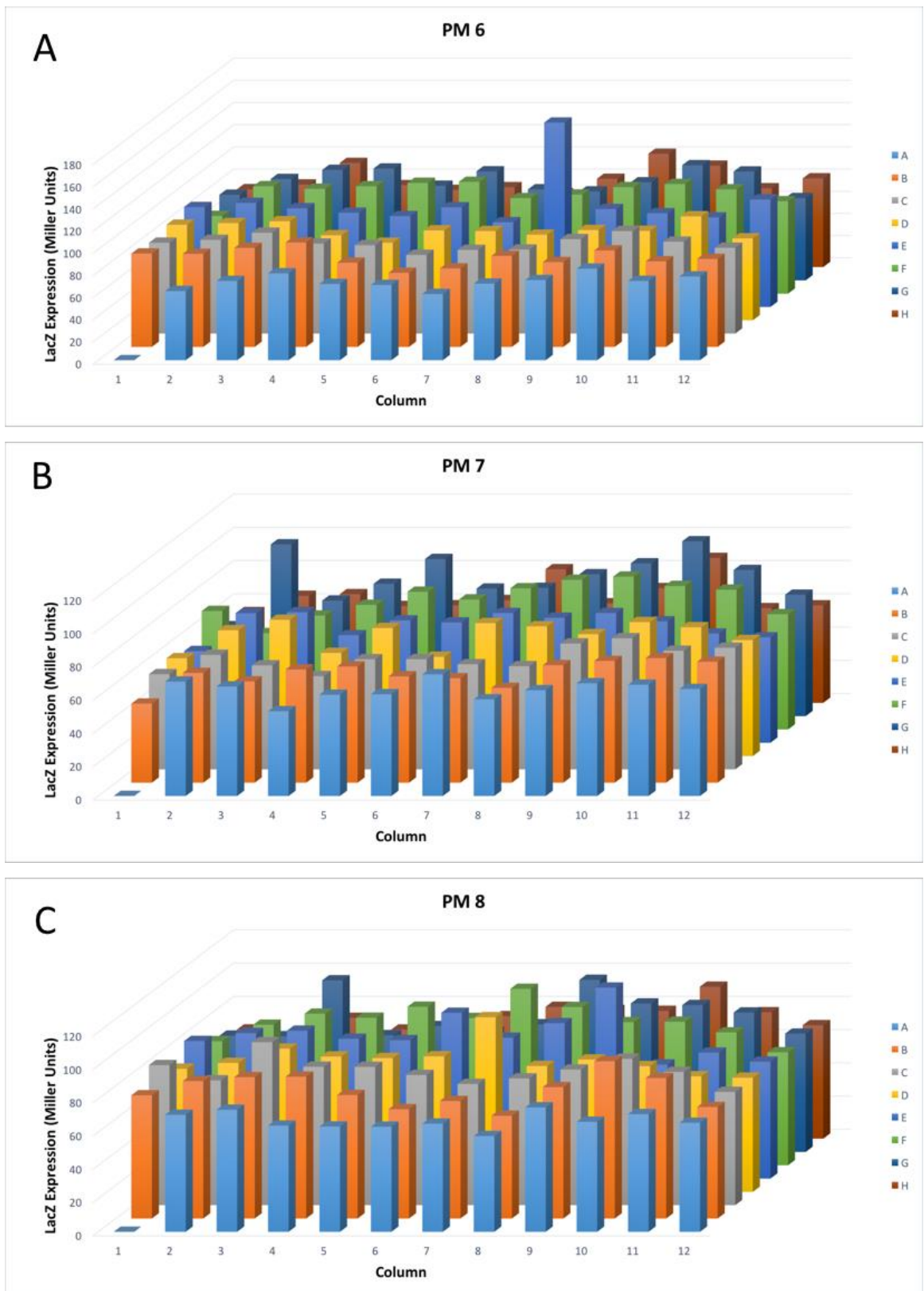


Figure 68: Expression of the *lacZ* reporter when cultured on di/tri peptides. The *lacZ* reporter strain was grown to a starting OD_{600nm} of 0.9 and re-suspended in the MCLMAN minimal media to an OD_{600nm} of 0.4 and incubated for 2 hours under normal conditions. The cultures were then transferred to the individual wells of the phenotype microarray plates and incubated for 2 hours under standard conditions with gentle shaking. (A, B and C) all show the expression in Miller units for the wells in the PM6, 7 and 8 plates respectively, all of which contain various di and tri peptides (the PM6 plate average is 83.72 Miller units) (the PM7 plate average is 70.73 Miller units) (the PM8 plate average is 78.95 Miller units).

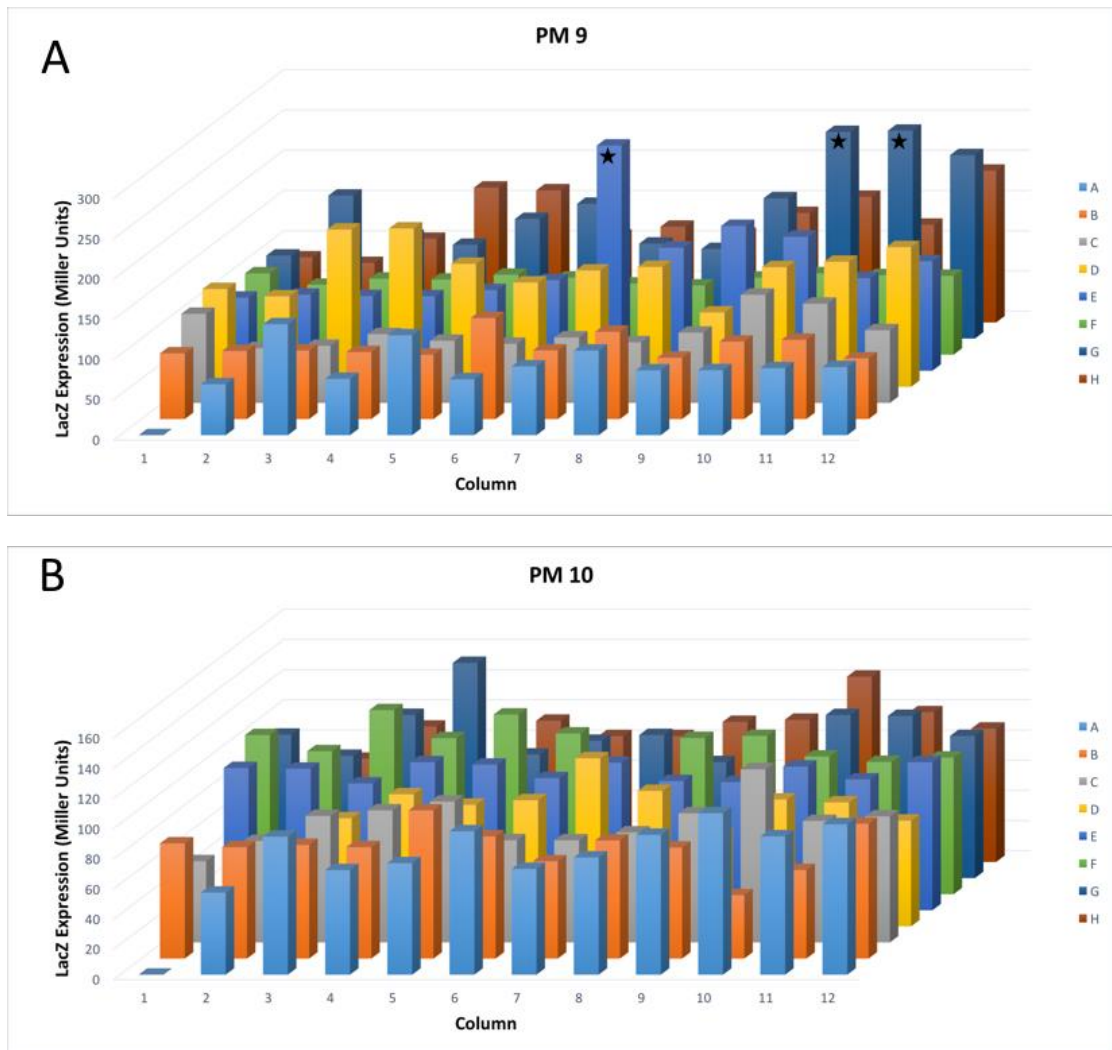


Figure 69: Expression of the *lacZ* reporter when cultured on different osmolytes and pH sources. The *lacZ* reporter strain was grown to a starting OD_{600nm} of 0.9 and re-suspended in the MCLMAN minimal media to an OD_{600nm} of 0.4 and incubated for 2 hours under normal conditions. The cultures were then transferred to the individual wells of the phenotype microarray plates and incubated for 2 hours under standard conditions with gentle shaking. **(A)** shows the expression in Miller units for the wells in the PM9 plate which contains various osmolytes (the PM9 plate average is 117.5 Miller units). **(B)** shows the expression in Miller units for the wells in the PM10 plate which contains different buffering systems set to a variety of pH values (the PM10 plate average is 83.96 Miller units). Stars represent individual wells with a >2-fold increase in LacZ expression.

5.2.7 Fold change in LacZ expression from the phenotype microarray assays

Table 16

Plate / Well	Fold Change (>2)	Compound	Duplications
PM1 / A9	2.85	D-Alanine	Also found in PM3-C3 (1.13 fold) and PM5-D6 (1.19 fold)
PM1 / H7	2.07	Glucuronamide	Also found in PM3-E6 (0.81 fold)
PM2 / D10	2.03	γ -Amino Butyric Acid	
PM3 / A2	2.17	Ammonia	
PM3 / D3	2.68	L-Pyroglutamic Acid	Also found in PM2-H3 (0.9 fold)
PM3 / D8	2.22	Ethylamine	
PM3 / E2	2.01	β -Phenylethyl-amine	
PM4 / B9	2.08	Guanosine 3'-monophosphate	
PM4 / C2	2.30	Phospho-Glycolic Acid	
PM4 / C10	3.94	Cytidine-5'-monophosphate	
PM4 / F4	2.10	Tetrathionate	
PM9 / E7	2.38	Urea (2%)	Also found in PM3-A5 (0.82 fold) and in PM9 wells E8-E12 (3%, 4%, 5%, 6%, 7% respectively) (1.3, 1.53, 1.42, 0.98, 1.2 fold respectively).
PM9 G10	2.18	Ammonium Sulfate pH8 (20 mM)	Found in PM9 wells G9-G12 (10, 20, 50, 100 mM respectively) (1.48, 2.18, 2.2, 1.94 fold respectively)
PM9 G11	2.20	Ammonium Sulfate pH8 (50 mM)	Found in PM9 wells G9-G12 (10, 20, 50, 100 mM respectively) (1.48, 2.18, 2.2, 1.94 fold respectively)

Table 16: Individual compounds producing a >2-fold increase in LacZ expression. 14 separate wells from the Biolog phenotype microarray plates showed a greater than >2-fold increase in LacZ expression. The Individual wells are highlighted by black stars in (Figures 66-69) and the fold changes are listed here. The table shows the plate and well numbers as well as the fold change in Miller units and the individual compounds. The table also shows the compounds which are duplicated in other wells and did not produce a >2-fold increase in expression.

In total 8 of the compounds from the phenotype microarray plate produced a >2-fold increase in LacZ expression (after discounting those which were duplicated elsewhere). These 8 compounds (γ -Amino Butyric Acid, Ammonia, Ethylamine, β -Phenylethyl-amine, Guanosine 3'-monophosphate, Phospho-Glycolic Acid, Cytidine-5'-monophosphate and Tetrathionate) are discussed further individually in the discussion.

5.2.8 Screening for the up-regulation of the *cj0423-5* operon when *cj0423* is artificially up-regulated

The phenotype microarray screening system failed to identify a particular compound or condition that would 'activate' the *cj0423-5* operon. Since so many external compounds and conditions have been assayed as potential inducers of the operon I decided to examine the possibility that the induction signal may be the presence of the Cj0423 protein itself. The inner membrane spanning Cj0423 is potentially a holin like protein and it may be that up-regulation of Cj0423 may be detrimental to the cell. While the previous chapter has established there are no growth defects in the *cj0422c* mutant strain (where *cj0423* is up-regulated) it may still be that up-regulation of Cj0423 is detrimental to the cell in non-laboratory conditions. As discussed in (Section 3.3.2) the holing-like proteins are also the only family of proteins found in all *C. jejuni* strains that have this operon structure thereby indicating that their role may be essential to the role of the operon as a whole.

In order to test this hypothesis a complementation construct was produced where *cj0423* was under the control of the iron inducible *fdxA* promoter. This construct was produced using the same methods as a normal complementation as described in (Section 4.2.6). This construct was transformed into wild type *C. jejuni* 11168 and the gene induced with 50 μ M ammonium Iron (II) sulphate. As a negative control the expression of the *fdxA* promoter was repressed by the addition of 20 μ M desferrioxamine-B (DES). The expression of both *cj0423* and *cj0424* was measured by qRT-PCR, the data is shown in (Figure 71). Unfortunately, the expression of *cj0423* was not significantly different between the iron-limited (DES) and iron-induced (Fe(II)) conditions. This may be due to the high levels of iron in the MHS media or some other compound interfering with DES and it would be worth repeating the experiment using an iron-limited minimal media. Because there was no significant increase in *cj0423* expression the expression of *cj0424* is not relevant.

5.2.9 Construction of the iron inducible *cj0423::fdxA* construct in 11168

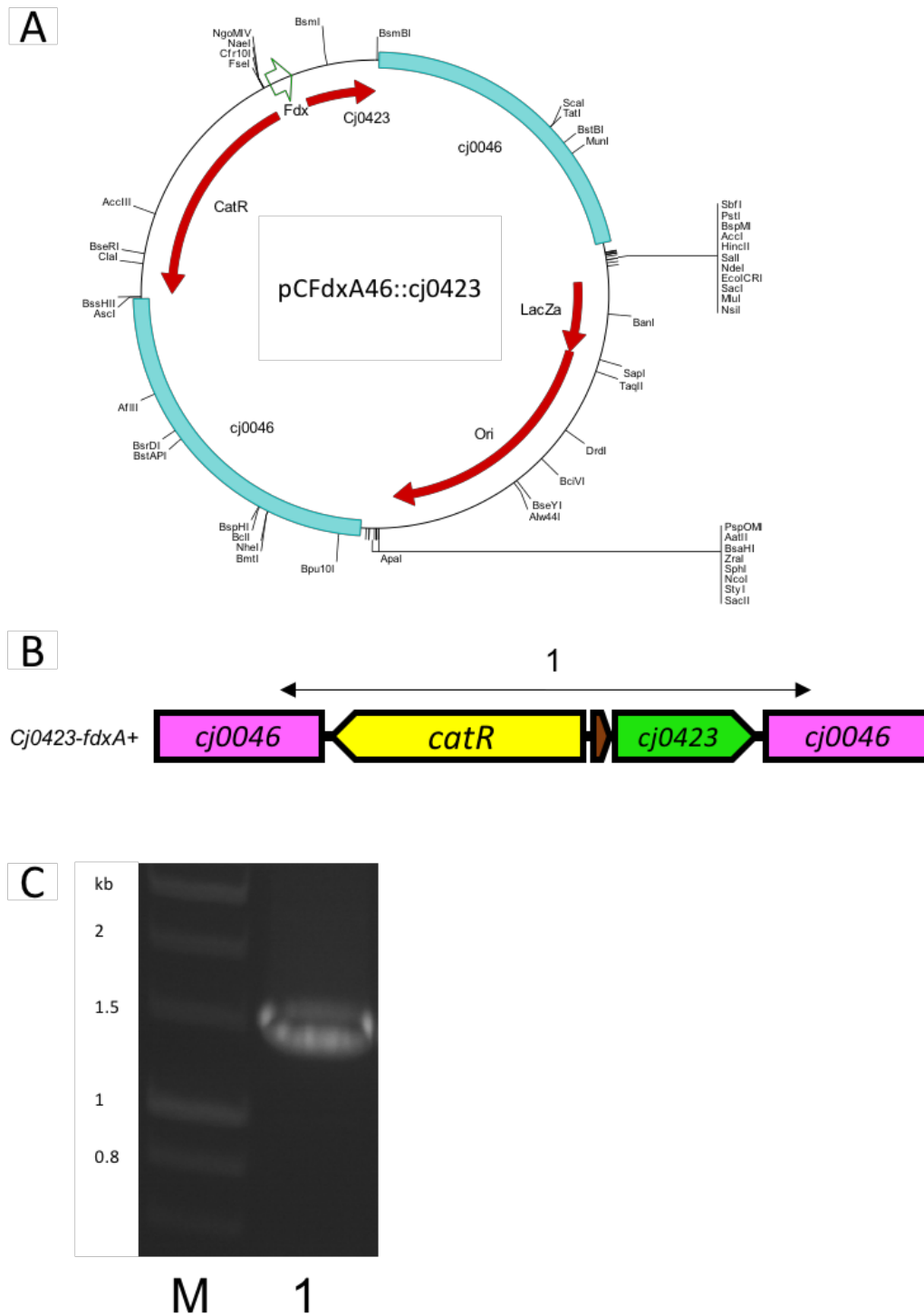


Figure 70: Construction and screening of the iron-inducible *cj0423+* strain. (A) the plasmid map of the pCFdxA46::*cj0423* construct generated by ISA cloning. The FdxA promoter is represented by the green arrow upstream of the *cj0423* ORF. (B) The gene arrangement in the ISA construct prior to transformation into wild type *C. jejuni* 11168-DJK. (C) following transformation the strain was screened by PCR using the *cj0046* screening primers, which are represented by the arrow in (B). The expected band size is 1491 bp.

5.2.10 qRT-PCR analysis of the *cj0423FdxA* strain

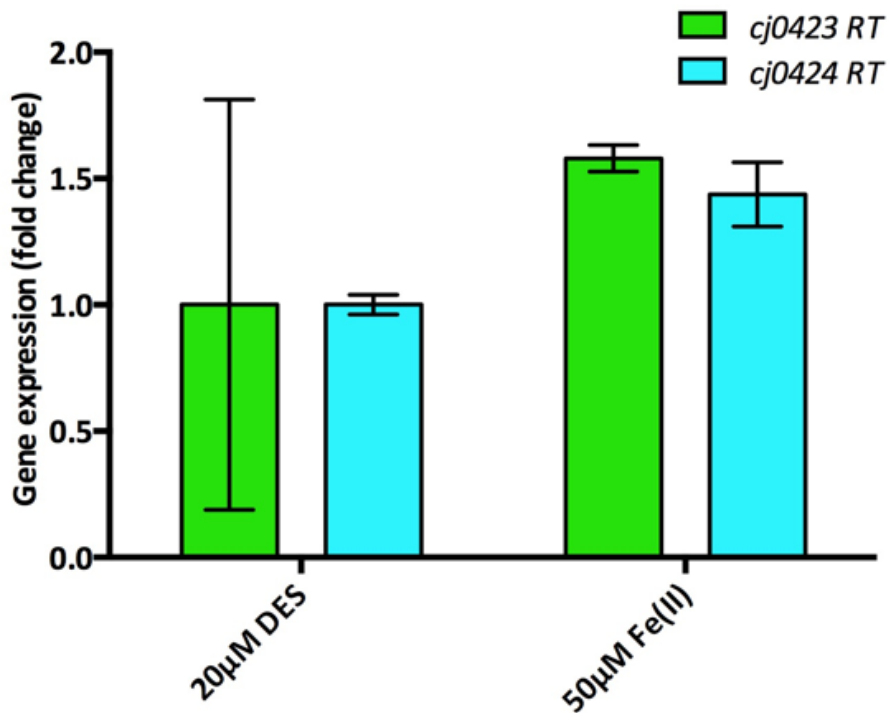


Figure 71: qRT-PCR analysis of *cj0423* and *cj0424* gene expression in the *cj0423-fdxA* construct. 6 biological replicates of the *cj0423-fdxA*⁺ strain were grown to an OD_{600nm} of 0.4, 20 µM desferrioxamine-B (DES) was added to 3 and 50 µM ammonium iron (II) sulphate (Fe(II)) was added to 3. The cultures were incubated under normal conditions for 1 hour prior to RNA extractions. Whole cell RNA was extracted and matched to 10 ng µl⁻¹ in nuclease free water (Section 2.15). qRT-PCR reactions were performed according to the methods described in (Section 2.15.1), the *gyrA* gene was used as an internal control. The data is expressed as a fold change in *cj0423* and *cj0424* gene expression between the two conditions. The data shows no significant changes in expression between the two conditions. The error bars represent the standard deviations from 9 replicates.

5.3 Chapter 5 Discussion

The aim of this chapter was to produce a reporter strain of *C. jejuni* to screen for potential inducers of the *cj0423-5* operon using a *lacZ* reporter strain. Unfortunately, no such potential inducer was found to strongly up-regulate the *cj0423* promoter. The *lacZ* reporter strain was shown to be a viable method for screening different conditions as the *cj0422c* mutant control strain showed strong up-regulation and to the best of the authors knowledge this is the first time the Biolog phenotype microarray system has been used as a high throughput screening method using a reporter strain in this way.

5.3.1 Construction of the *lacZ* reporter strain using the *cj0046* complementation system

There are numerous examples in the literature of *lacZ* reporter strains being used in bacteria to test for changes in gene regulation, there are also some examples of using the system in *Campylobacter* species (Van Vliet *et al.*, 2001, Bayliss *et al.*, 2012). The data shown in (Figure 57) shows that when the reporter construct is transformed into wild type 11168 the expression is relatively low which is consistent with the qRT-PCR data from Chapter 4. The transformation of the reporter strain into the *cj0422c* mutant acted as a positive control to show that the reporter strain is able to successfully mimic the regulation of the *cj0423* promoter. The very high level of *lacZ* expression seen in the *cj0422c* mutant strain (3000-4000 Miller units) does imply that the *cj0423* promoter sequence is a strong promoter when not repressed, which may have some use to overexpress other genes in *C. jejuni* should a very high expression be required. As an example the expression of the T7 promoter used for recombinant protein expression in *E. coli* can go up to 50,000 Miller units when expressed using the pET vector system (though that is when expressed from multiple plasmid promoters) (Chao *et al.*, 2001). The qRT-PCR data shown in the previous chapter showed the expression of *cj0423* is up-regulated around 100-fold at the RNA level in the *cj0422c* mutant (Figure 39). The data presented here shows that translates to an approximately 50-fold increase at the protein level.

5.3.2 Screening therapeutic antimicrobial compounds using the *lacZ* reporter system

A series of commonly used antimicrobials were screened as potential inducers of the *cj0423-5* operon. The data shown in (Figure 58) screened a range of standard antibiotics as inducers. These included the model CAMP polymyxin-B and erythromycin which is commonly used to treat *Campylobacter* infections (Anders *et al.*, 1982). Polymyxin-B was tested as it is a cationic antimicrobial peptide and though it has been tested for induction before in Chapter 3 (Figures

22-23), it was decided to re-test it as part of this chapter. The macrolide antibiotic erythromycin was tested as there is some evidence in the literature that erythromycin may cause the up-regulation of Cj0425. A study from 2013 showed that the expression of *cj0425* may be up-regulated in response to erythromycin (Xia *et al.*, 2013). These results should be treated with some caution as the increased expression was only detected by microarray analysis and could not be replicated with qRT-PCR. The data presented in (Figure 58) shows that there is no up-regulation of the *cj0423-5* operon in response to erythromycin, though it is worth noting that the paper only mentioned *cj0425* as being up-regulated not the whole operon.

5.3.3 Screening non-therapeutic antimicrobial compounds using the *lacZ* reporter system

In addition to screening antibiotics which can be used as treatments for induction I decided to screen a series of non-therapeutic antimicrobials for potential induction of the *cj0423-5* operon. The membrane targeting anionic surfactant compound sodium dodecyl sulfate was tested as a potential inducer as it non-specifically disrupts the outer membrane at low concentrations. The data shown in (Figure 59) does show an apparent up-regulation of LacZ in response to higher concentrations of SDS, however this is because the SDS is rapidly lysing the cells and due to the way the Miller units are calculated this artificially increases the apparent level of expression when in fact the expression of LacZ has not changed.

The bile acid (taurocholic acid) was also tested as *C. jejuni* is likely to encounter bile acids following ingestion. The bacteriostatic antimicrobial 1,2-Benzisothiazole-3(2H)-one (BIT) and ethanol were also tested as potential inducers. BIT is an isothiazole based antimicrobial which can transverse the membrane layers of Gram-negative bacteria and targets free thiol groups thereby inhibiting growth (Diehl and Chapman, 1999). Ethanol and other organic solvents non-specifically permeable the membranes of Gram-negative bacteria thereby causing cell death (Heipieper and De Bont, 1994). The data presented in (Figure 59-60) shows no significant change in gene regulation in the *lacZ* reporter strain when challenged with SDS, taurocholic acid, BIT or ethanol.

5.3.4 Screening Human and Chicken sera and peptidoglycan fragments using the *lacZ* reporter system

Blood sera contains components of the innate and adaptive immune system in higher organisms, as part of an infection cycle *C. jejuni* may encounter blood sera and potentially

need to resist components of the immune system. Human serum has been shown to be bactericidal *in-vitro* at 10% final concentration (Pennie *et al.*, 1986) and since *C. jejuni* is known as a coloniser of chickens, chicken serum was also tested. The data is shown in (Figure 61) and does not show any significant change in LacZ expression.

As discussed in Chapter 4 the crystal structure of Cj0425 has revealed it to share structural homology with a class of cysteine protease inhibitors known as cystatins. Since cysteine protease enzymes are structurally similar to some peptidoglycan hydrolase enzymes (Section 4.1). I decided to use a mixture of peptidoglycan fragments as potential inducers of the *cj0423-5* operon, only the non-proteinogenic amino acids found in gram negative peptidoglycan were used for this assay (Park and Uehara, 2008). D-Alanine, D-Glutamic acid and diaminopimelic acid (mDAP) were mixed together and mixed with the LacZ reporter strain to a final concentration of 10 mM each. The data is shown in (Figure 61) and shows a very slight increase in expression but since it is less than 2-fold it is not considered biologically significant.

5.3.5 Screening oxidative stress, osmotic stress, pH and temperature changes using the *lacZ* reporter system

The chicken colonisation data presented in Chapter 4 strongly suggests that the *cj0423-5* operon is not required for survival in the chicken digestive tract (Figure 47). Because *C. jejuni* will at some point have to survive outside the chicken gut in order to re-colonise another bird or cause infection it will probably need to cope with atmospheric oxygen levels, osmotic stress and sudden changes in pH and temperature. The response of *C. jejuni* to all of these environmental stress conditions has been previously studied in a range of publications, some of which have focused on the transcriptomic response of *C. jejuni* to these conditions (Palyada *et al.*, 2009, Cameron *et al.*, 2012, Reid *et al.*, 2008, Stintzi, 2002). None of these publications showed any notable change in the expression of *cj0421c-cj0425* in response to the stress conditions tested. The data presented in (Figures 62-65) agrees with this as no significant change in LacZ expression could be detected in response to any of these conditions.

5.3.6 High throughput screening of compounds using phenotype microarray plates with the *lacZ* reporter system

The phenotype microarray™ (Biolog) system is a screening system designed to screen for changes in metabolic profiles between strains. The system uses 96 well plates containing a variety of potential metabolites. When used for analysing microbial strains the cells are cultured with a buffer containing a tetrazolium dye which when reduced absorbs at 590_{nm} and can be quantified. The production of NADH during normal cellular metabolism causes the irreversible reduction of the tetrazolium dye, so a signal can only be detected when the cell is respiring. Various metabolites can be screened using the phenotype microarray plates to generate a metabolic profile of an organism (Bochner *et al.*, 2001). For this study the process was adapted so that the plates could be used to screen up to 950 different compounds for induction of the *lacZ* reporter strain. To the best of our knowledge this is the first time the phenotype microarray system has been used in this way. The lists of phenotype microarray plates used are listed in (Section 8.2). The data for all 10 plates used is shown in (Figures 66-69), unfortunately there does not appear to be any particular compound that strongly up-regulates the operon. Some of the individual wells did show a slight increase in LacZ expression however upon closer examination many of these compounds produced at most only a 2-3-fold increase in LacZ expression. Since the 'activated' operon has been shown to be up-regulated 50-fold (Figure 57), a 2-3-fold increase is not considered biologically significant, especially since this is a high throughput screen with only one replicate per well. Many of the wells also contained compounds which produced a colour change in the media and as such produced anomalous results. These wells were listed during the experiment and this was taken into account when analysing the data. The well which showed the highest increase in LacZ expression is shown in (Figure 67), plate PM4, well C-10 which contains cytidine-5'-monophosphate, was measured at 517 Miller units compared to the plate average of 130. This approximate 4-fold increase is still far short of the 50-fold increase seen in the *cj0422c* mutant strain though it may be worth re-evaluating this compound in the future. The full list of the compounds tested in each individual plate can be found at (http://www.biolog.com/pdf/pm_lit/PM1-PM10.pdf) and in the appendix (Section 8.2).

5.3.7 Attempted artificial overexpression of *cj0423*

Because no apparent chemical or physical inducer of the *cj0423-5* operon has yet been found I decided to examine the possibility that the inducer may in fact be the inner membrane spanning Cj0423 protein itself. As discussed in (Section 3.3.2) Cj0423 may act as a holin like protein, though overexpression of *cj0423* in the *cj0422c* mutant does not cause any apparent growth defect (Figure 40,) it may still be detrimental to the cell outside of laboratory conditions. My hypothesis was that the expression of *cj0423* is tightly regulated by Cj0422c and that the operon is either repressed or de-repressed to maintain some kind of equilibrium of Cj0423 in the inner membrane. In order to test this, I constructed a vector which placed *cj0423* under the control of the iron inducible *fdxA* promoter. Unfortunately as the data in (Figure 71) shows this construct did not successfully up-regulate the expression of *cj0423* and so I can draw no firm conclusions about the hypothesis either way. It may be worth re-producing the vector where *cj0423* is under a stronger promoter region or possibly repeating the experiment in a minimal media setting where the concentration of iron can be better controlled.

This chapter aimed to elucidate the inducing compound or condition which causes an up-regulation of the *cj0423-5* operon. Unfortunately, despite extensive testing no compound or condition has been found. Since there is still no assigned function to the operon as a whole It was decided to continue with biochemical and structural analysis of the individual proteins within the operon. It was hoped that by assigning functions to some of the proteins within the Cj0421c-Cj0425 gene cluster we may be able to assign a role to the operon as a whole.

6 [Chapter 6 – Biochemical and structural characterisation of Cj0421c, Cj0422c and Cj0425](#)

6.1 [Chapter 6 Introduction](#)

Thus far the role of the *cj0421c-cj0425* gene cluster has remained elusive. The data presented in chapters 4 and 5 has not revealed any potential role for the cluster even after extensive screening of potential inducer compounds and conditions in chapter 5. While there is no coherent hypothesis about the role of the gene cluster as a whole, the individual proteins do have some characterised functions. It is assumed that the roles of Cj0421c and Cj0422c are linked as they appear in an operon together in strain NCTC 11168 and are nearly always found together in other strains (Figure 11). The role of Cj0422c as a master regulator has been well characterised by both previous work and by the data presented in chapters 3, 4 and 5. The role of Cj0421c is assumed to be as a sensor protein, though deletion of the gene produces no detectable change in expression of the operon, the current hypothesis is that Cj0421c interacts with Cj0422c to de-repress the operon upon receiving a currently unknown stimulus.

The crystal structure of Cj0425 has been solved by Halah Al-Haideri in collaboration with Dr John Rafferty. The Cj0425 protein is exported to the *C. jejuni* periplasm and contains a single disulfide bond. The structure revealed that Cj0425 is similar at the structural level to a class of proteins known as cystatins. These proteins act as cysteine protease inhibitors and are widely distributed in eukaryotes but are not well studied in bacteria, largely due to a lack of sequence homology between bacterial cystatins and their eukaryotic counterparts (Kordiš *et al.*, 2009). Phylogenetic analysis of *cj0425* distribution has not revealed any potential binding partners within the *C. jejuni* 11168 genome. This analysis was performed by Dr Roy Chaudhuri where 4699 publicly available *C. jejuni* genomes were examined to see if any other *c. jejuni* genes correlate with the presence or absence of *cj0425* (Data not shown). Cj0425 has been shown by a previous student (Al-Haideri, 2015) to inhibit the cysteine protease papain *in-vitro* but the data was inconclusive about how strong this effect was.

The aim of this chapter was to clone, overexpress and purify Cj0421c, Cj0422c and Cj0425 to try and assign specific roles to the proteins. Attempts were made to crystallise both Cj0421c and Cj0422c to try and determine the structure of both proteins. The role of Cj0421c as a sensor protein was tested by screening potential binding ligands for Cj0421c using the high throughput thermal shift (thermofluor) assay. The potential for Cj0421c and Cj0422c to

interact with each other was also tested by protein crosslinking experiments. While previous work has shown that Cj0425 inhibits the cysteine protease papain, the inhibition is weak and the data is inconclusive about how effectively Cj0425 is able to inhibit papain. These experiments were repeated and since Cj0425 only weakly inhibits papain another cysteine protease cathepsin-B was also tested. Cathepsin-B is a commercially available cysteine protease that is structurally similar to papain and is found in humans, so it may be a more likely target for Cj0425.

6.2 Chapter 6 Results

6.2.1 Overexpression of Cj0421c, Cj0422c and Cj0425 in *E. coli* BL21-DE3

The amino acid sequence of Cj0421c shows 6 predicted transmembrane regions and a cytoplasmic C-terminal domain (Section 4.2.6). The C-terminal cytoplasmic domain of the protein was amplified by Phusion PCR. The product was cloned into the pET28a vector using the *Nde*I and *Xho*I restriction sites. The pET28a vector (Addgene) contains an N-terminal 6-His sequence followed by a thrombin digestion site (Figure 72). The same process was used for overexpression of Cj0422c in pET28a. The complete Cj0422c ORF was cloned into pET28a using the *Nhe*I and *Xho*I restriction sites. The Cj0425 ORF contains a periplasmic signal sequence (SignalP 4.1 Server). Work by a previous student (Hitchcock, 2011) has shown that Cj0425 is insoluble when expressed in the *E. coli* cytoplasm and the crystal structure has revealed that Cj0425 contains a single disulfide bond. The Cj0425 ORF (without the native signal sequence) was amplified by Phusion PCR and cloned into the pET22b vector using the *Nco*I and *Xho*I restriction sites. The pET22b vector contains the *E. coli pelB* signal sequence which allows for expression in the *E. coli* periplasm. The arrangement of the genes within the pET vectors is shown in (Figure 72).

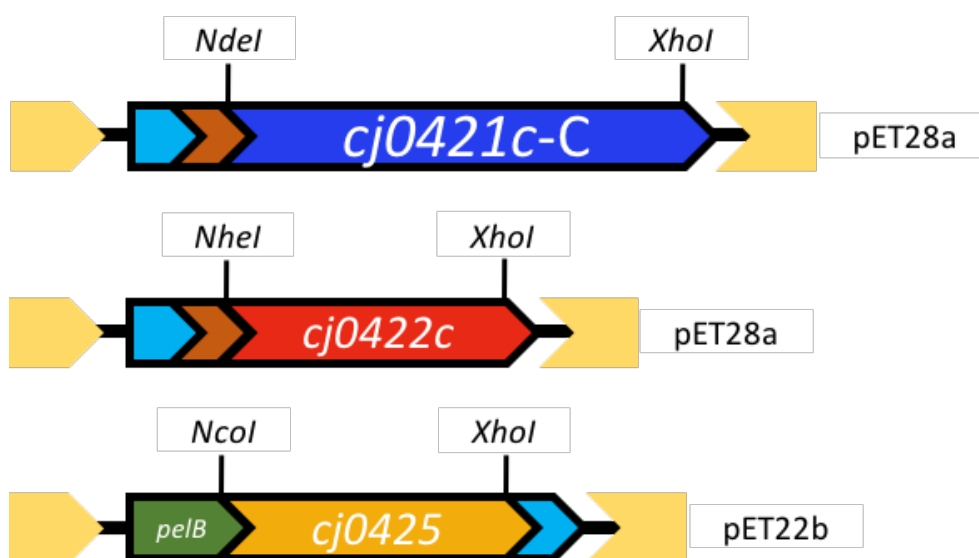


Figure 72: Overexpression constructs for Cj0421c, Cj0422c and Cj0425. The genes of interest were cloned into pET vector using standard cloning techniques. The *cj0421c* and *cj0422c* genes were cloned into pET28a downstream of a 6His tag (light blue) and thrombin cut site (brown). The *cj0425* gene was cloned into pET22b downstream of the *pelB* periplasmic localisation sequence (green). All constructs were under the control of the T7 promoter (yellow arrow).

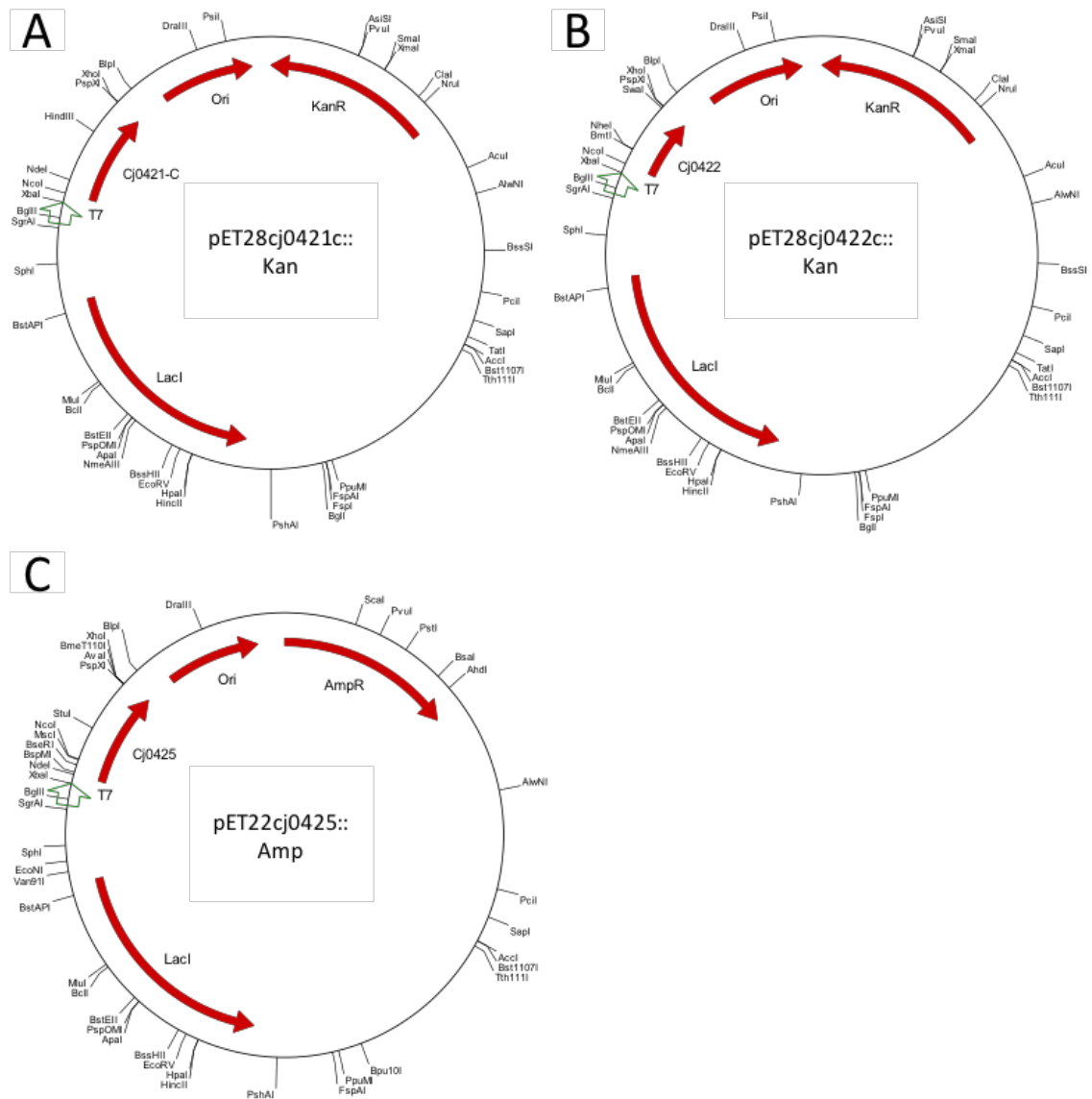


Figure 73: Plasmid maps of the *cj0421c*, *cj0422c* and *cj0425* overexpression plasmids. All plasmids shown were produced using restriction enzyme cloning methods described in (Section 2.10.6). (A) and (B) show the overexpression constructs for the C-terminal of *cj0421c* and *cj0422c* respectively. Both were cloned into pET28a which contains a kanamycin resistance marker. (C) shows the overexpression construct for *cj0425* in pET22b which contains the *pelB* leader sequence and an ampicillin resistance marker. The T7 promoter is represented by the green arrow in all 3 maps. All constructs were confirmed by DNA sequencing of the inserted fragments.

6.2.2 Overexpression and purification of the C-terminal of Cj0421c

The pET28cj0421c::Kan plasmid was transformed into the *E. coli* strain BL21-(DE3), a series of overexpression trials were performed to determine the best condition to use for high protein expression (data not shown). The Cj0421c overexpression strain was grown to an OD_{600nm} of 0.6 in LB broth containing 50 µg ml⁻¹ kanamycin and induced with 0.5 mM IPTG. The cultures were incubated at 37°C for 3 hours and harvested by centrifugation. The cell free extract was extracted from the pellets using methods described in (Section 2.26.3). The resuspension buffer contained 20 mM sodium Phosphate buffer pH 7.4 with 20 mM imidazole and 500 mM sodium chloride. The protein was separated from the cell free extract using a His-Trap chromatography column where the imidazole concentration was steadily increased from 20-500 mM. The overexpression and His-trap purification of Cj0421c is shown in (Figure 74). The gel filtration and mass spectrometry analysis of Cj0421 is shown in (Figure 75). The gel filtration was initially performed by Dr Dr Svetlana Sedelnikova and the protein elutes from the column as a monomer (data not shown). All chromatography steps were performed using an AKTA Prime Plus chromatography system with the associated columns and buffering systems. The protein was then concentrated using 10 kDa cutoff concentration columns (GE Life Sciences). The purified protein was analysed by mass spectrometry and was shown to have a molecular weight of 17136.84 Da which is consistent with the predicted molecular weight of the protein without the starting methionine (17136.6 Da). The protein has a predicted isoelectric point of pH 9.3 and a predicted extinction coefficient of 8480 M⁻¹ cm⁻¹.

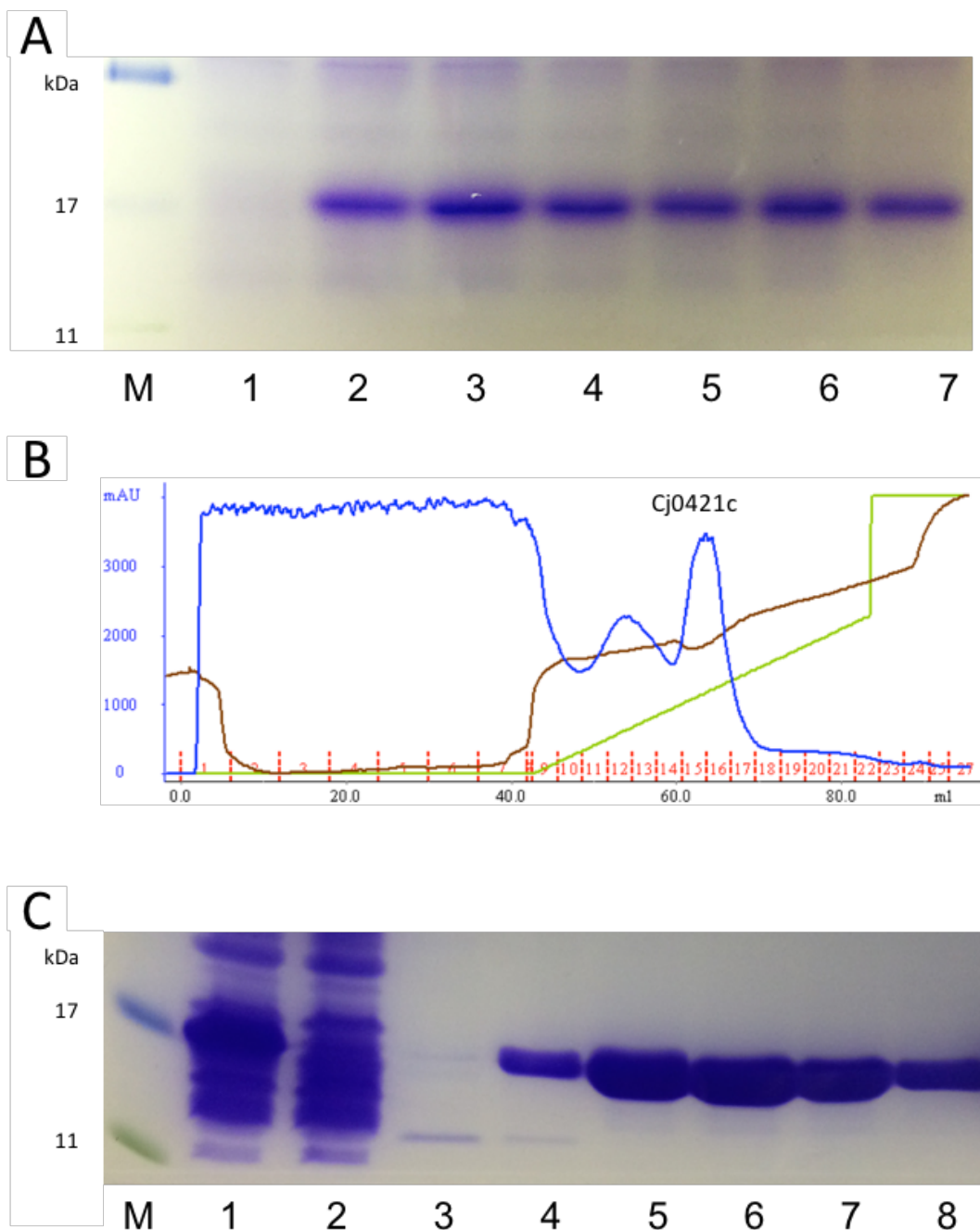


Figure 74: Overexpression and His-trap purification of Cj0421c. (A) shows a 14% SDS-PAGE gel loaded with the whole cell soluble extracts of the overexpression of Cj0421c in a 100 ml culture when induced with 0.5 mM IPTG. Lane 1 shows the cell proteins before induction with IPTG and lanes 2-7 show the cell proteins at 1, 2, 3, 4, 6 and 24 hours after induction. The expected band size for the C-terminal of Cj0421c is 17.267 kDa. (B) shows the UV spectroscopy traces from the His-Trap purification of Cj0421c. The blue line shows the Abs 280_{nm} trace, the green line shows the relative buffer concentrations where the increase corresponds to an increase in imidazole concentration. The brown line shows the conductivity of the sample which indicated the salt concentration in the sample. The Cj0421c-C terminal peak is labelled and the elutions are shown by the red numbers. (C) shows a 14% SDS-PAGE gel, lane 1 is the whole cell free extract (CFE) prior to loading on the AKTA column, lane 2 shows the CFE after passing through the column. Lanes 3-8 show elution numbers 13-18 respectively from (B).

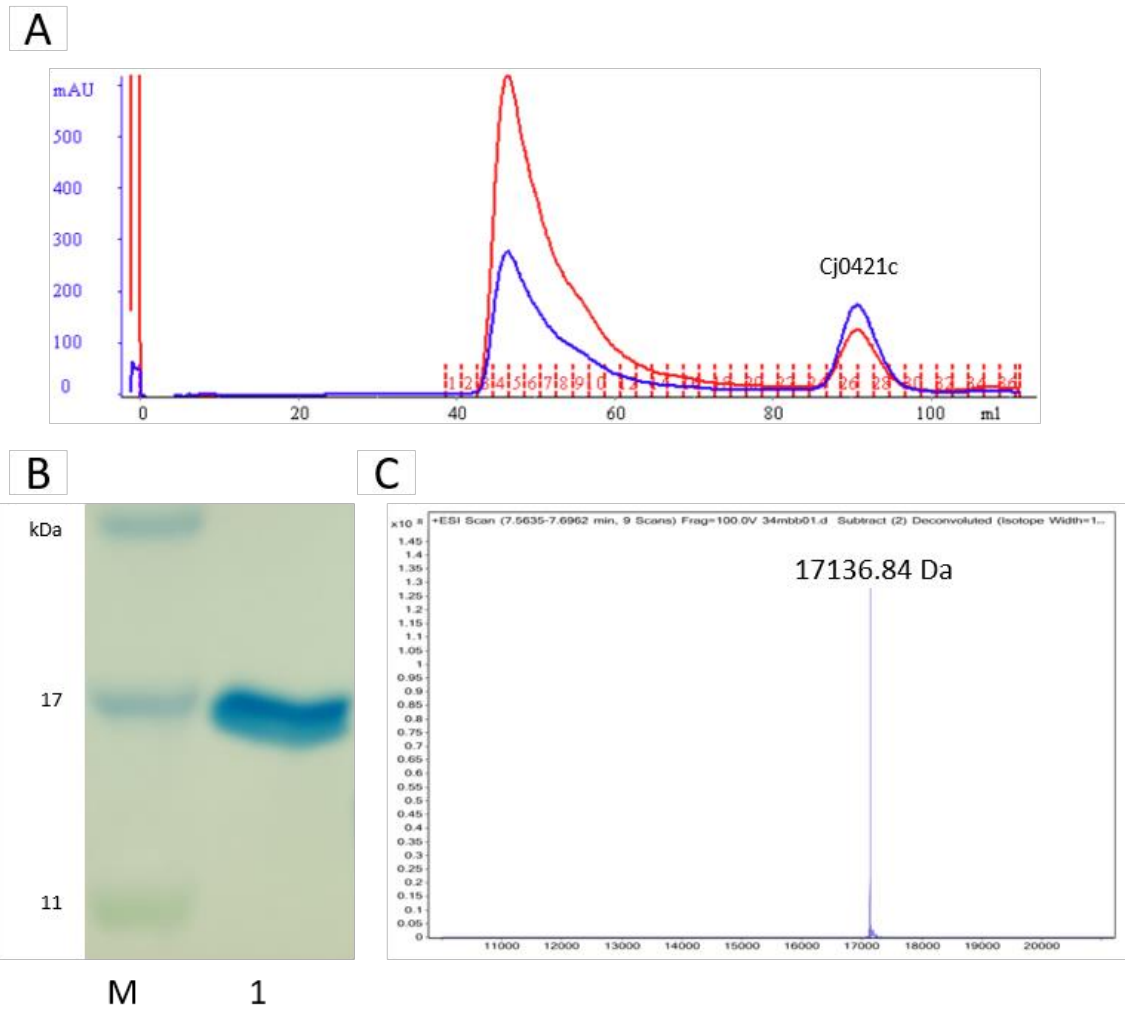


Figure 75: Gel filtration and mass spectrometry analysis of Cj0421c. (A) shows UV spectroscopy traces from the gel filtration of the C-terminal of Cj0421c. The blue line represents the Abs_{280nm} and the red line shows the conductivity. The Cj0421c peak is labelled, the fractions containing the protein were collected and mixed. (B) shows a 14% SDS-PAGE gel loaded with the mixed fractions from (A). (C) shows the mass spectrometry trace of the purified Cj0421c, 17136.84 Da (predicted MW is 17136.6 Da).

6.2.3 Screening Cj0421c for potential ligands using thermofluor

Since no information about the role of Cj0421c is available I decided to screen for potential ligand binding partners. The C-terminal of Cj0421c shows no strong homology to any known family of proteins (there is some homology to diguanylate cyclase proteins but as discussed in (Section 4.1) Cj0421c is probably not one of these). As such there are no obvious ligands to screen for so a range of metal ions were tested as well as polymyxin-B, EDTA and cyclic-di-GMP. Polymyxin-B was tested as this experiment was performed when it was thought that Cj0421c was involved in resistance to cationic antimicrobial peptides. EDTA was tested as it was thought that the protein may already be bound to an unknown metal ion. Cyclic-di-GMP was tested to show that Cj0421c is probably not a c-di-GMP diguanylate cyclase. The thermofluor screen is a method of comparing the thermal denaturation profile of proteins when bound or unbound to ligands (Niesen *et al.*, 2007). The theory is that if a protein is bound to a ligand then it is more stable and thus will denature at a higher temperature. The thermofluor method allows for high throughput screening of potential ligands and binding partners for proteins. The full method is described in (Section 2.28). The thermofluor data was analysed using publicly available Microsoft excel and graphpad files produced to analyse the raw data, which are available at (<ftp://ftp.sgc.ox.ac.uk/pub/biophysics>). The data is shown in (Figure 76) and shows no increase in the thermal stability of Cj0421c when assayed with any of the compounds. The thermal melt curve for Zinc, and to a lesser extent Copper and Cobalt ions caused a negative shift in thermal stability, possibly due these metals denaturing the protein which would be non-specific toxicity rather than binding.

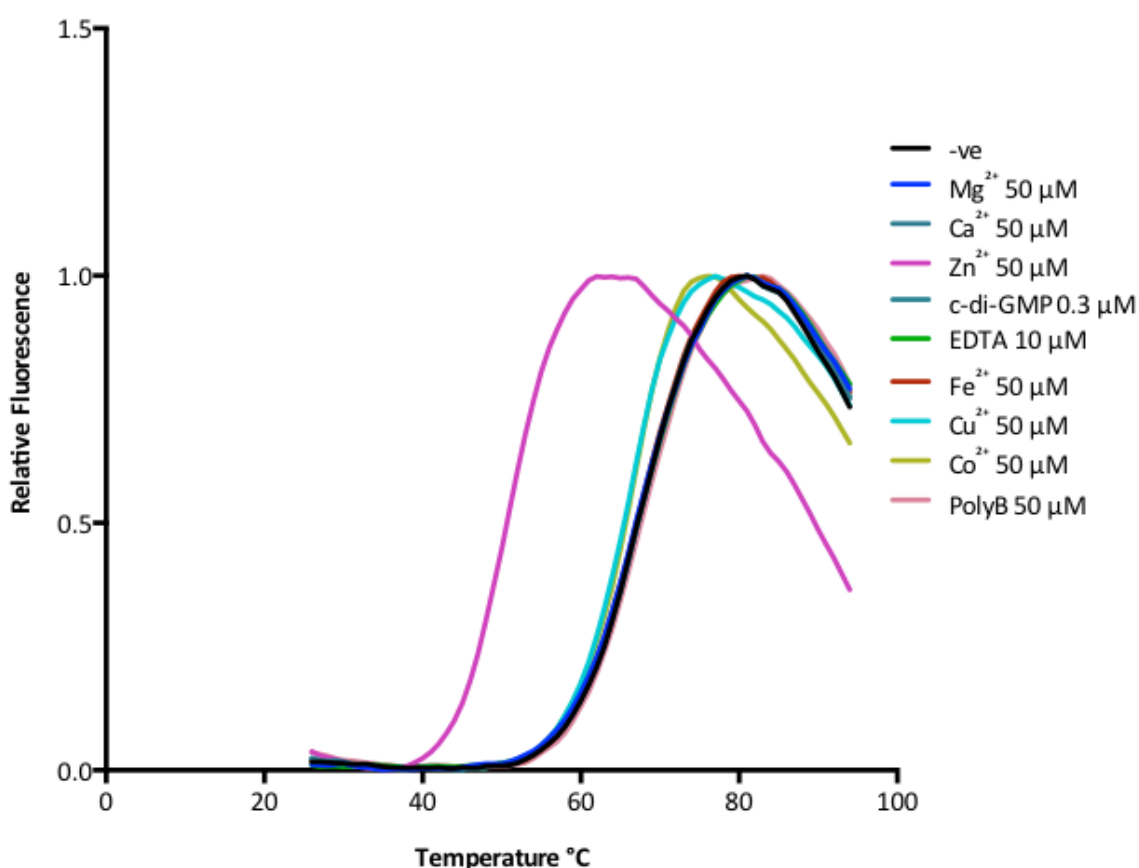


Figure 76: Thermal denaturation profile of the C-terminal of Cj0421c with added ligands. Each 50 μ l well contained 50 μ M purified Cj0421c in 20 mM sodium phosphate buffer with 500 mM NaCl pH7.4 and 5 μ l of the 10X SYPRO orange dye (Invitrogen). The colours correspond to the different compounds tested. Each data set is the mean result of 3 technical replicates. The data was processed using the Boltzmann equation to calculate the relative thermal denaturation profile. The data was normalized to the maximum fluorescence signal which is given a value of 1.

6.2.4 Attempted crystallisation of Cj0421c

Because no role could be assigned to Cj0421c attempts were made to crystallise the protein. The protein was concentrated to approximately 10 mg ml⁻¹ and was screened for crystallisation in the PACT, JCSG+, Ammonium Sulphate, Proplex, MPD and classic crystal screens (Qiagen). Microdrops of 200 nl protein and 200 nl precipitant were set up in sitting drop vapour diffusion trials using a Matrix Hydra II Plus One crystallisation robot in collaboration with Dr John Rafferty and Rachel Plumb. Unfortunately, no crystals grew in any of the conditions tested, it may be that the C-terminal domain of Cj0421c cannot be crystallised or it may require further optimization of the conditions to produce successful crystals.

6.2.5 Overexpression and purification of Cj0422c

When purifying proteins, it is usual to keep the protein chilled at all times to inhibit contaminating proteases from degrading the protein of interest, or to prevent the growth of any contaminating microorganisms. When purified, the Cj0422c protein was found to precipitate out of solution when chilled below 18-20°C. This precipitation means that the Cj0422c protein had to be kept at room temperature or higher at all times. To accomplish this the protein was never chilled below 25°C when being purified or concentrated. The pET28cj0422c::Kan plasmid was transformed into the *E. coli* strain BI21-(DE3), a series of overexpression trials were performed to determine the best condition to use for high protein expression (data not shown). The Cj0422c overexpression strain was grown to an OD_{600nm} of 0.7 in LB broth containing 50 µg ml⁻¹ kanamycin and induced with 1 mM IPTG. The cultures were incubated at 37°C for 3 hours and harvested by centrifugation. The cell free extract was extracted from the pellets using methods described in (Section 2.26.3). The resuspension buffer contained 50 mM Tris-HCl buffer pH 7.4 with 20 mM imidazole and 500 mM sodium chloride. The protein was separated from the cell free extract using a His-Trap chromatography column. The Cj0422c protein binds unusually strongly to the His-trap column, initial attempts to purify the protein using a 20-500 mM imidazole gradient did not produce any purified protein despite the protein being visible on SDS-PAGE gels. The protein could only be purified using up to 700 mM imidazole and this was achieved in a single step. After loading the His-trap column with the cell free extract the column was washed with buffer containing 300mM imidazole and then the protein eluted by running 700 mM imidazole through and the fractions collected. This 2-step purification method means the protein was already highly pure after only a single purification step. (Figure 77) shows the 2 step purification method being performed on an AKTA prime plus.

To remove the imidazole, the Cj0422c protein sample was dialysed using a 5 kDa cutoff dialysis tubing (Sigma). The protein was dialysed overnight in 50 mM Tris-HCl pH7.4, 500 mM NaCl buffer containing 10 mM EDTA and 0.2% sodium azide. The EDTA was added because the protein binds so tightly to the His-trap column it may pull some nickel out from the column. The sodium azide was added to prevent the growth of microorganisms in the buffer as the dialysis was performed at 30°C (because the protein precipitates below 20°C). The protein was then re-dialysed in 50 mM TRIS-HCl pH7.4 and 500 mM NaCl to remove the EDTA and sodium azide. The protein was then concentrated using 10 kDa cutoff concentration columns (GE Life Sciences)

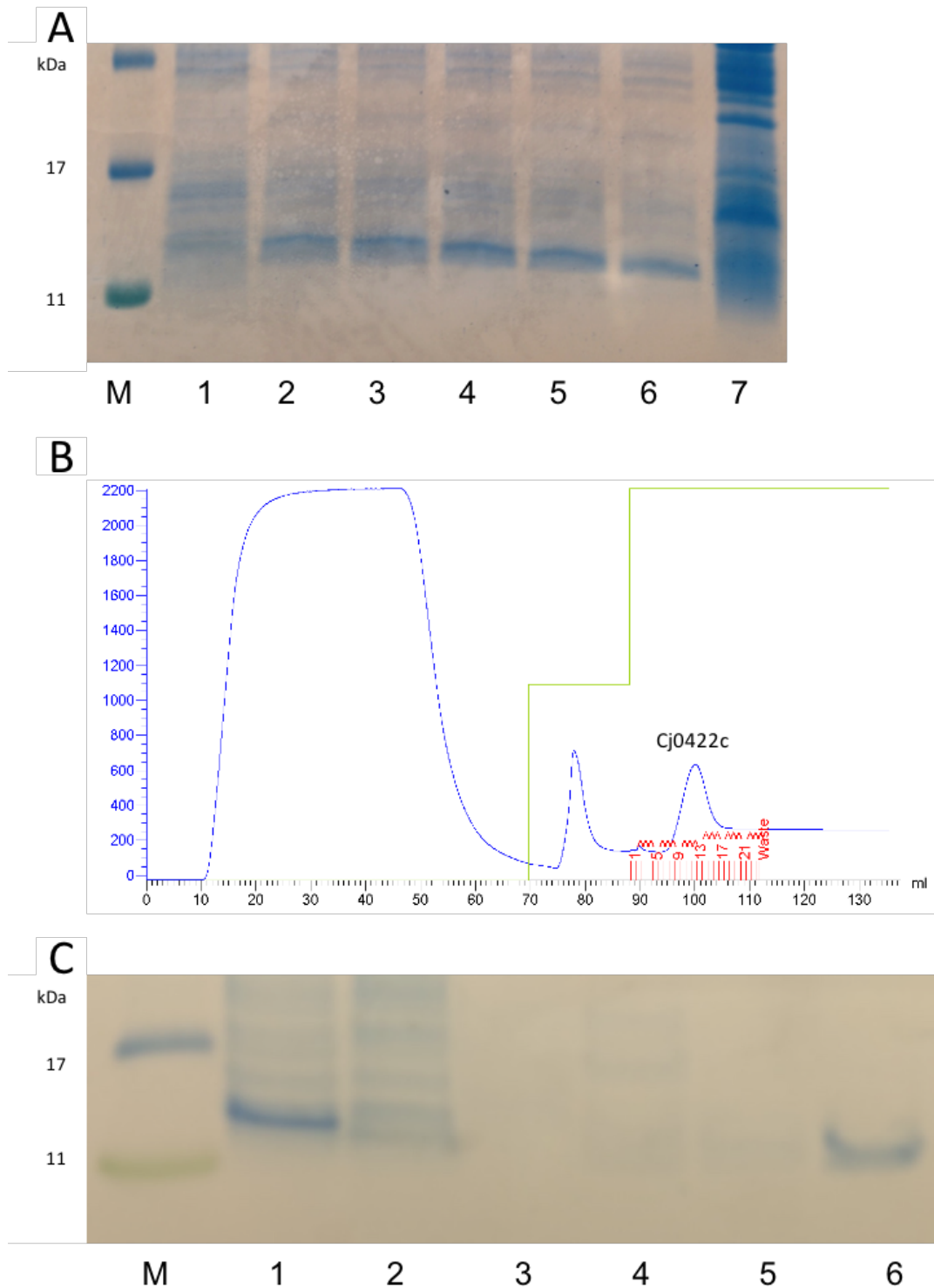


Figure 77: Overexpression and His-trap purification of Cj0422c. (A) shows a 14% SDS-PAGE gel loaded with the whole cell soluble extracts of the overexpression of Cj0422c in a 100 ml culture when induced with 1 mM IPTG. Lane 1 shows the cell proteins before induction with IPTG and lanes 2-7 show the cell proteins at 1, 2, 3, 4, 6 and 24 hours after induction. The expected band size for Cj0422c is 10.73 kDa. (B) shows the UV spectroscopy traces from the His-Trap purification of Cj0422c. The blue line shows the Abs_{280nm} trace, the green line shows the relative buffer concentrations, which jumps from 0% to 40% and then to 100%. The Cj0422c peak is labelled and the elutions are shown by the red numbers. (C) shows a 14% SDS-PAGE gel, lane 1 is the whole cell free extract (CFE) prior to loading on the the AKTA column, lane 2 shows the CFE after passing through the column. Lanes 3-6 shows the material collected after washing the column through with 20%, 40%, 60% and 80% 700 mM imidazole. The Cj0422c band is shown in lane 6 after mixing the collected fractions.

6.2.6 Do Cj0421c and Cj0422c interact

Both Cj0421c and Cj0422c are encoded in the same operon and are nearly always encoded as linked genes in the same strains of *C. jejuni* (Figure 11). The role of Cj0422c as a DNA binding repressor is well established from a previous student (Hitchcock, 2011) however the role of Cj0421c is elusive. Protein-protein crosslinking reactions were performed with purified Cj0421c and Cj0422c to test if the C-terminal domain of Cj0421c interacts with Cj0422c. Initially both Cj0421c and Cj0422c were crosslinked individually to determine if they form dimers or multimers, Cj0422c is predicted to form a dimer as this is typical of helix-turn-helix proteins. The protein samples were mixed with the crosslinking reagent dithiobis(succinimidyl) propionate (DSP) (Thermo-Fisher) at either 0.5 or 2 mM and incubated for 30 minutes at 25°C. The samples were then separated on 16% SDS-PAGE tricine gels. The experiment was repeated using Cj0421c and Cj0422c mixed together to assess if they bind to each other. Cj0421c was concentrated to 100 µM while Cj0422c was concentrated to 60 µM. The concentration of Cj0421c was kept constant and the concentration of Cj0422c was increased. The crosslinking reaction SDS-PAGE gel shown in (Figure 78) shows that Cj0422c does indeed form a dimer and may form higher oligomers, though this may be a by-product of the crosslinking reaction. Cj0421c did show some higher band sizes after crosslinking but the majority of the protein remained in monomeric form, implying that the protein does not dimerise. This is backed up by gel filtration purification of Cj0421c (Figure 75) where Cj0421c elutes as a single peak at the expected molecular weight (Data not shown). The crosslinking reaction SDS-PAGE gel shown in (Figure 79) shows that Cj0421c and Cj0422c may interact at the protein level, the data shows that the monomeric Cj0422c band completely disappears when crosslinked with Cj0421c, and a larger band appears at a size consistent with the combined molecular weights of Cj0421c and Cj0422c (about 27.7 kDa). Unfortunately, the assay did not go as expected as after adding the DSP crosslinking reagent to the mixed protein a precipitant formed (most likely Cj0422c) which is visible at the top of the gel as an insoluble protein band. The Cj0421c band intensity is seen decreasing as the concentration of Cj0422c is increased across the gel. This may be because the precipitated Cj0422c is non-specifically binding to Cj0421c, which means no firm conclusions can be drawn about whether Cj0421c and Cj0422c interact at the protein level.

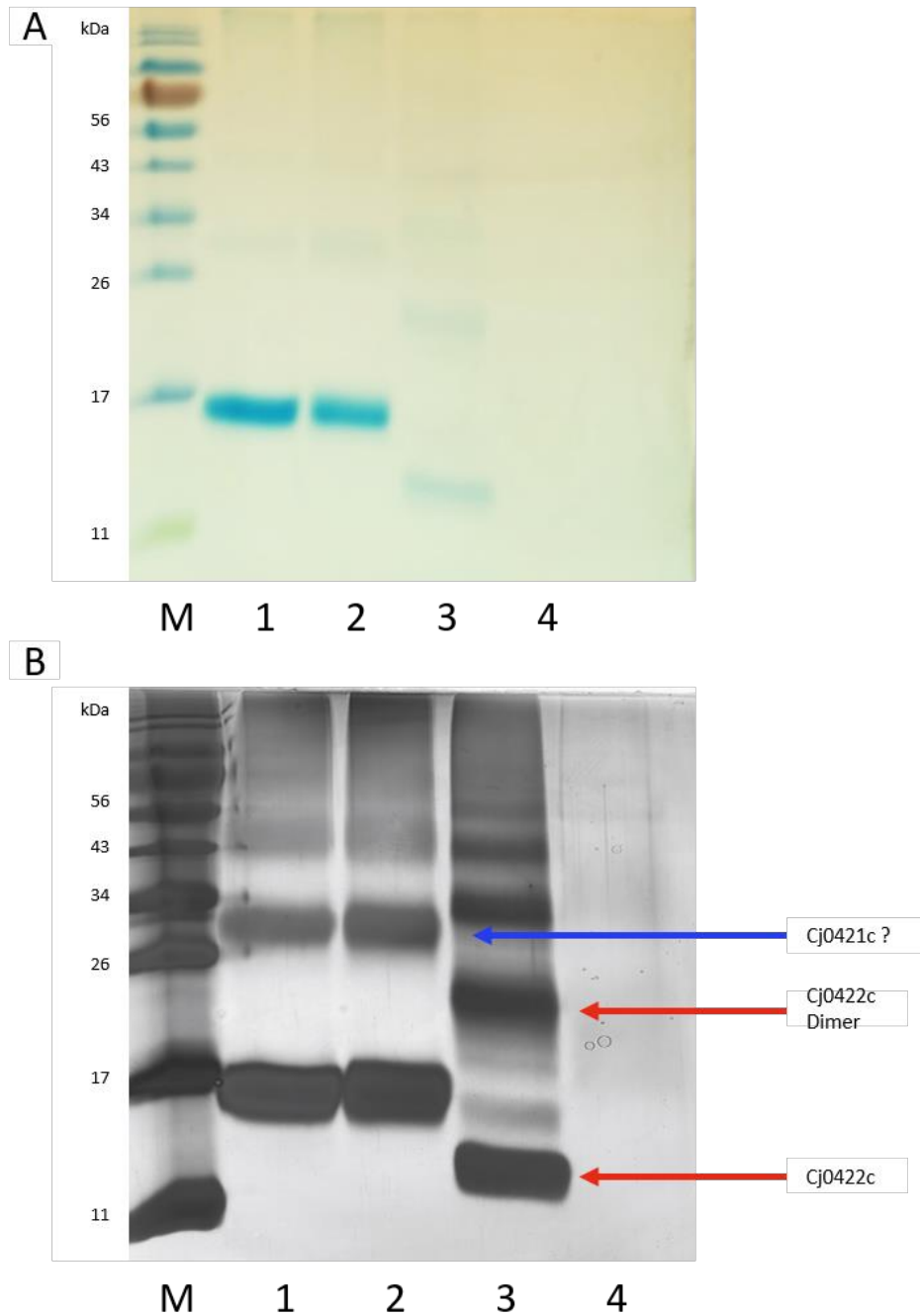


Figure 78: Chemical crosslinking of Cj0421c and Cj0422c. (A) 16% SDS-PAGE tricine gel loaded with 100 μ M Cj0421c and 60 μ M Cj0422c after crosslinking with DSP. Lane 1 is Cj0421c with 0.5 mM DSP, lane 2 is Cj0421c with 2 mM DSP. Lane 3 is Cj0422c with 0.5 mM DSP and lane 4 is Cj0422c with 2 mM DSP). (B) is the same SDS-PAGE gel but silver stained. The blue arrow shows the potential dimerization of Cj0421c and the red arrows show the potential dimerization of Cj0422c.

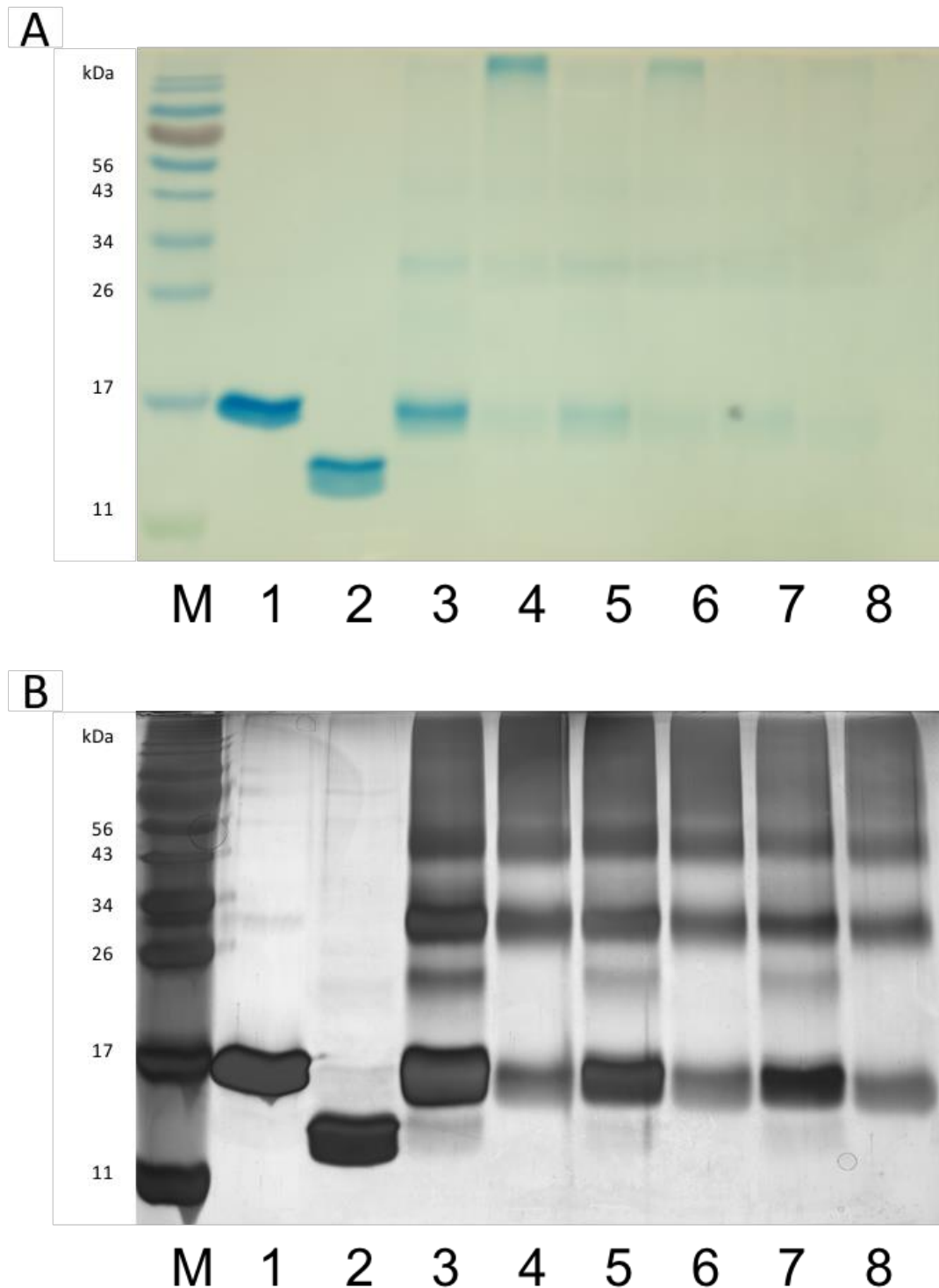


Figure 79: Chemical crosslinking of Cj0421c and Cj0422c together. (A) 16% SDS-PAGE tricine gel loaded with 100 μ M Cj0421c alone (lane1) and 60 μ M Cj0422c alone (lane2). The following list is the Cj0421c:Cj0422c proteins at increasing ratios. Lanes 3 and 4 are at a 1:1 with 0.5 and 2 mM DSP respectively. Lanes 5 and 6 are at a 1:2 ratio with 0.5 and 2 mM DSP respectively. Lanes 7 and 8 are at a 1:4 ratio with 0.5 and 2 mM DSP respectively. (B) is the same SDS-PAGE gel but silver stained.

6.2.7 *Crystallisation of Cj0422c*

6.2.7.1 *Crystallisation of the native C-terminal His tagged Cj0422c protein*

Initially work on the Cj0422c protein involved using the C-terminal His tagged construct which was produced by Dr Ed Guccione. This construct was generated in pET21a where the protein contains a 6-histidine tag at the C-terminal end of Cj0422c (data not shown). This protein was overexpressed and purified using similar methods to those described in (Section 6.2.5) with the exception that the buffer used was PBS buffer with 500 mM NaCl at pH7.4. The protein could be purified but the yield was low (typically around 1 mg of pure protein could be obtained from 1 litre of culture). The protein could not be concentrated above around 5 mg ml⁻¹ as precipitate formed at higher concentrations and the protein could not be chilled. The purified protein was screened for crystallisation using microdrops of 200 nl protein and 200 nl precipitant which were set up in sitting drop vapour diffusion trials using a Matrix Hydra II Plus One crystallisation robot in collaboration with Dr John Rafferty. Crystals formed in the PACT crystal screen (Qiagen) well C2 which contained 0.1 M PCB, pH5, 25% PEG1500. The protein was re-purified and crystals were generated using hanging drop crystal trials where 3 µl of protein and 3 µl of precipitant were mixed onto siliconized coverslips and allowed to vapour diffuse with 1 ml of the crystallisation buffer. The crystals typically formed after 1 week at 17°C and were stored in cryoprotectant (the crystallisation buffer with 2% more PEG 1500 and 20% ethylene glycol) and sent to the Diamond Light Source (Oxfordshire) for X-ray diffraction analysis, the crystals are shown in (Figure 80). The data was collected from 7 individual crystals on beamline I03 with a beam size of 50 X 35 µm, the analysis was performed by Dr John Rafferty. The crystals produced good diffraction patterns but the structure could not be solved due to the phase problem. The crystal unit cell dimensions are a = 38 Å, b = 67 Å, c = 72 Å, $\alpha = \gamma = 90^\circ$, $\beta = 95^\circ$ with each unit composed of 2 copies of the monomer. Which implies that Cj0422c may form crystals in its dimeric form.

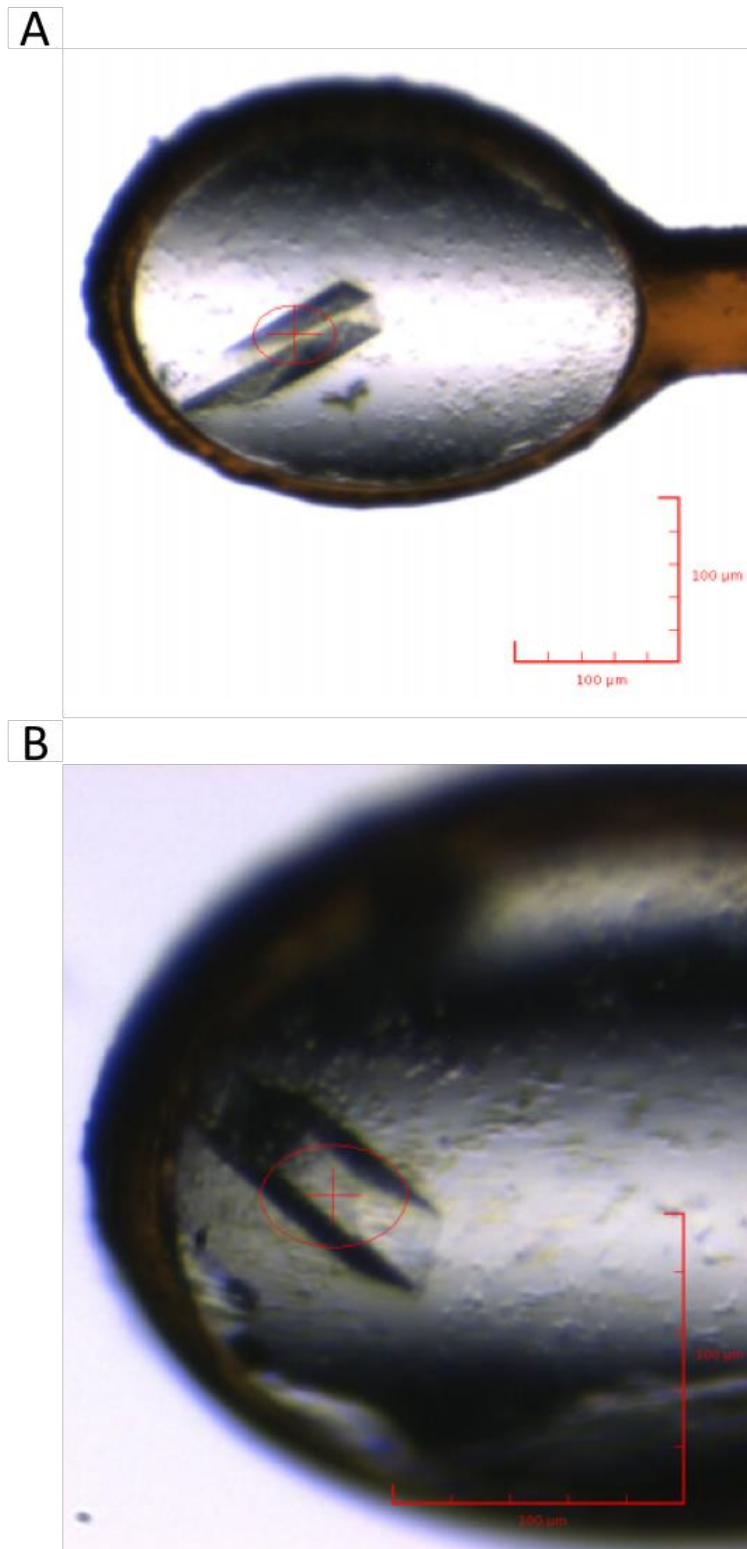


Figure 80: Looped crystal of the C-terminal His tagged Cj0422c protein. Image taken from the I03 beamline at Diamond light source. The crosshair highlights the exact position of the X-ray beam (beam size 50 X 35 μm). (A) and (B) shown different magnifications of the same crystal in different orientations.

6.2.7.2 *Overexpression and purification of selenomethionine incorporated Cj0422c*

When producing protein samples for X-ray crystallographic analysis heavy elements can be incorporated into the protein to solve the phase problem. There are several ways of doing this but one of the most popular is producing protein samples where selenomethionine has been incorporated into the protein. The method for production of selenomethionine incorporated protein is described in (Section 2.26.2). Despite numerous attempts high concentrations of selenomethionine incorporated Cj0422c could not be produced. This was attempted using the C-terminally tagged Cj0422c construct produced by Dr Ed Guccione. Because of this I decided to move the His tag to the N-terminal end of the protein and to re-attempt the crystallisation process. The construction of the N-terminally tagged Cj0422c protein and its purification are described in (Section 6.2.5). The N-terminal protein tag proved to be more stable and could be produced in higher concentrations than the C-terminal tag (typically 3-4 mg of protein produced per liter).

The native Cj0422c-N protein was purified and screened for crystallisation using the same methods described in (Section 2.33). Crystals formed after 1 week in the Proplex B7 (0.2 M ammonium acetate, 0.1 M sodium acetate, pH4, 15% PEG4000) and the PACT D1 (0.1 M MMT, pH5, 25% PEG1500) wells. The crystals were re-generated using hanging drop trials in both of these conditions with the crystals in the PACT D1 conditions growing faster and producing better quality crystals.

The N-terminally tagged Cj0422c protein was then produced with selenomethionine incorporation, the purification method is the same as described in (Section 6.2.5). Both the regular protein and selenomethionine incorporated protein were checked by mass spectrometry analysis. Because the N-terminal methionine is often cleaved off the protein the predicted molecular weight for both the non-incorporated and selenomethionine incorporated Cj0422c without the starting methionine is 10601.97 Da and 10742.67 Da respectively. The mass spectrometry data shown in (Figure 81) confirms this and suggest that the selenomethionine has been successfully incorporated into the protein. The native Cj0422c protein has a predicted isoelectric point of pH 8.9 and a predicted extinction coefficient of $11460 \text{ M}^{-1} \text{ cm}^{-1}$.

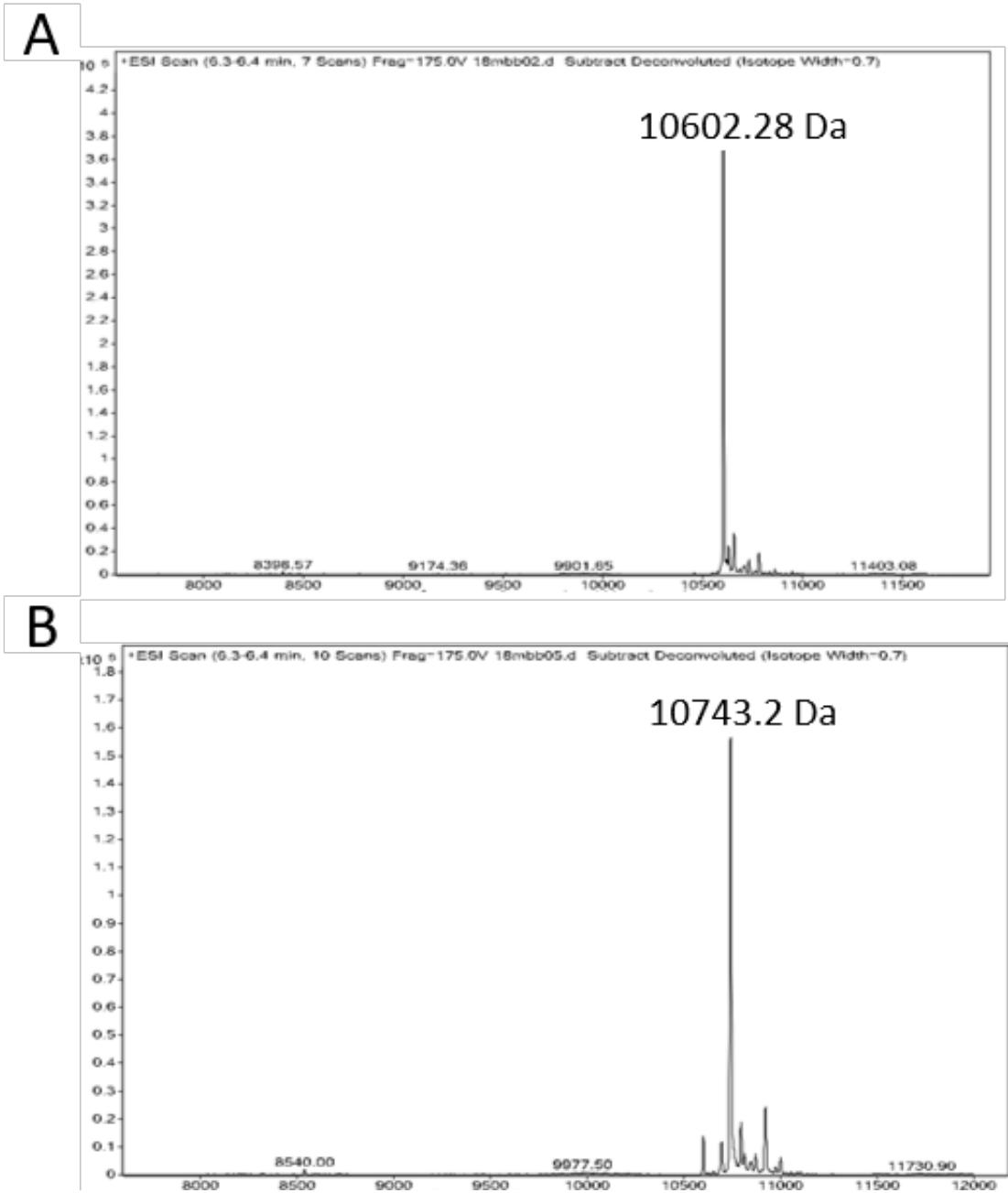


Figure 81: Mass spectrometry analysis of Cj0422c and selenomethionine-incorporated Cj0422c. (A) shows the molecular weight of the purified Cj0422c protein 10602.28 Da (predicted MW is 10601.97 Da). (B) shows the molecular weight of purified selenomethionine incorporated Cj0422c 10743.20 Da (predicted MW is 10742.67 Da).

6.2.7.3 *Crystallisation of selenomethionine incorporated Cj0422-N*

Part of the problem with crystallising Cj0422c (a problem with both the C and N terminally tagged proteins) is that the protein is difficult to concentrate past 5 mg ml^{-1} and cannot be chilled to lower than 20°C without the protein precipitating out of solution. To prevent this the protein was kept above 25°C at all times and the siliconized cover slips were warmed up using the underside of a standard lab metallic heating block when the protein solution and crystallisation buffer were mixed together. The crystallisation trays were then stored at 37°C for 24 hours, then at 30°C for 24 hours, then at 25°C for 24 hours before being stored at 17°C until crystals formed. This was designed to keep the protein in solution while the nascent crystals form around a nucleation site. These hanging drop trials of the selenomethionine incorporated Cj0422c-N protein produced many small crystals, which were too small to provide reliable diffraction data. Because of this I decided to use the small crystals as a seed stock to produce larger crystals. The crystals were broken up by vortexing with small glass beads and were serially diluted 10-fold in cryoprotectant (the same buffer as the crystallisation buffer with 4% more PEG1500). The 10^{-3} and 10^{-5} dilutions were mixed with the next crystallisation buffer before adding the Cj0422c protein solution. Unfortunately, this did not result in any change in the size of the crystals. Another method for generating bigger crystals is to use a whole or partial crystal as a 'macro seed', which involves looping a fully formed crystal and transferring it to a new hanging drop where the protein in solution should form around the existing crystal in preference to forming new crystals. This method was attempted and did produce bigger crystals, but these did not produce diffractions pattern to a low enough resolution to produce a structural model from.

6.2.8 Overexpression and purification of Cj0425

The Cj0425 protein had already been purified by a previous student Halah Al-Haideri so the overexpression and purification procedure was already established. The pET22cj0425::Amp plasmid was transformed into the *E. coli* strain BL21-(DE3). The Cj0425 overexpression strain was grown to an OD_{600nm} of 0.6 in LB broth containing 50 µg ml⁻¹ ampicillin and induced with 0.5 mM IPTG. The cultures were incubated at 25°C overnight and harvested by centrifugation. The cell free extract was extracted from the pellets using methods described in (Section 2.26.3). The resuspension buffer contained 20 mM sodium phosphate buffer pH 7.4 with 20 mM imidazole and 500 mM sodium chloride. The protein was separated from the cell free extract using a His-Trap chromatography column where the imidazole concentration was steadily increased from 20-300 mM. The Cj0425 protein was not initially pure and so was further purified by hydrophobic interaction chromatography and then by gel filtration chromatography, all of which are shown in (Figure 83). The protein was then concentrated using 10 kDa cutoff concentration columns (GE Life Sciences). All chromatography steps were performed using an AKTA Prime Plus chromatography system with the associated columns and buffering systems. The protein has a predicted molecular weight of 14790 Da, a predicted isoelectric point of pH 5.6 and a predicted extinction coefficient of 14565 M⁻¹ cm⁻¹ assuming the disulfide bond is correctly formed.

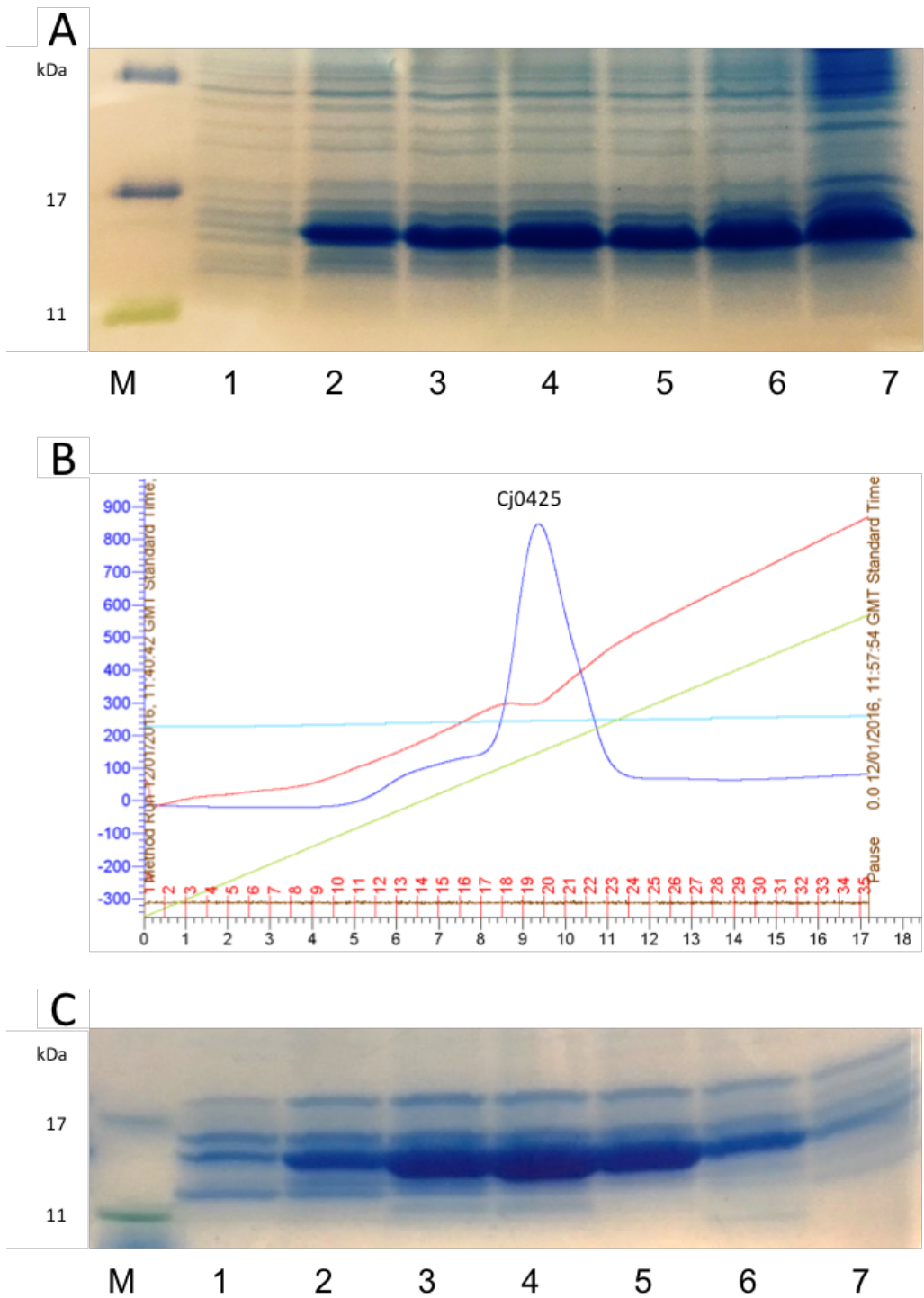


Figure 82: Overexpression and His-trap purification of Cj0425. (A) shows a 14% SDS-PAGE gel loaded with the whole cell soluble extracts of the overexpression of Cj0425 in a 100 ml culture when induced with 0.5 mM IPTG. Lane 1 shows the cell proteins before induction with IPTG and lanes 2-7 show the cell proteins at 1, 2, 3, 4, 6 and 24 hours after induction. The expected band size for the Cj0425 is 14.79 kDa. (B) shows the UV spectroscopy traces from the His-Trap purification of Cj0425. The blue line shows the Abs 280_{nm} trace, the green line shows the relative buffer concentrations where the increase corresponds to an increase in imidazole concentration. The red line shows the conductivity of the sample which indicated the salt concentration in the sample. The Cj0425 terminal peak is labelled and the elutions are shown by the red numbers below. (C) shows a 14% SDS-PAGE gel, lanes 1-7 correspond to elutions 17-23 from (B).

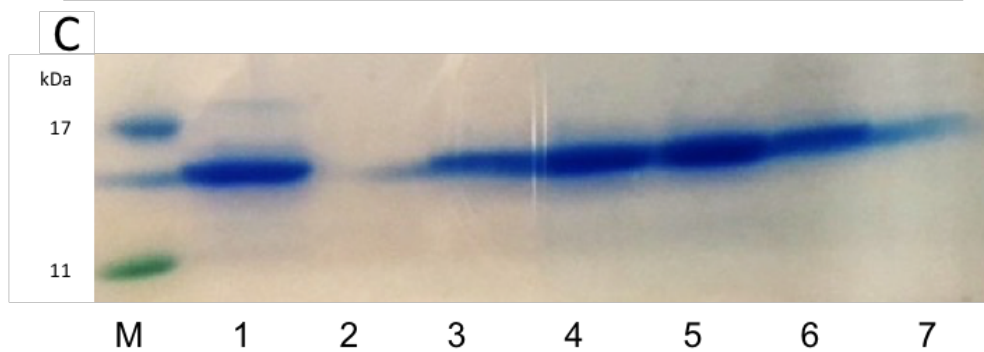
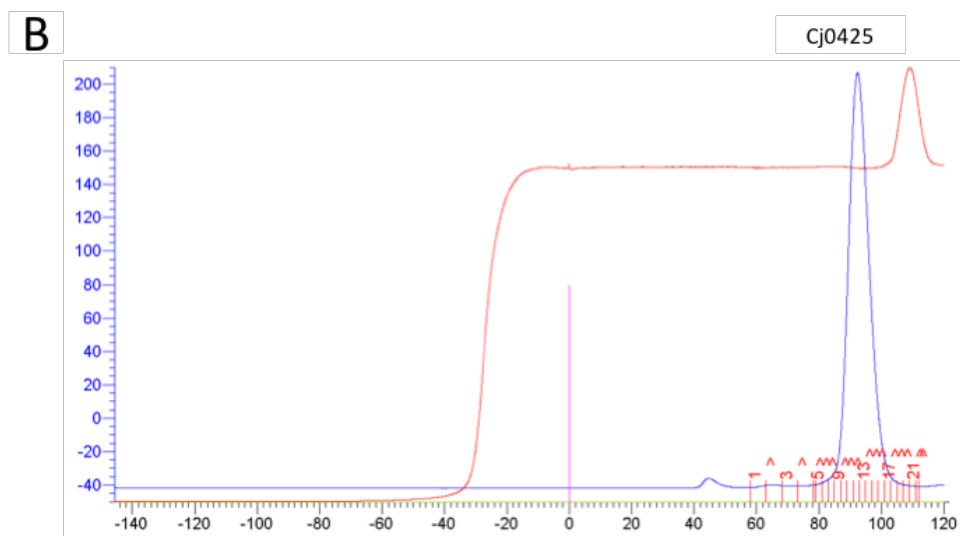
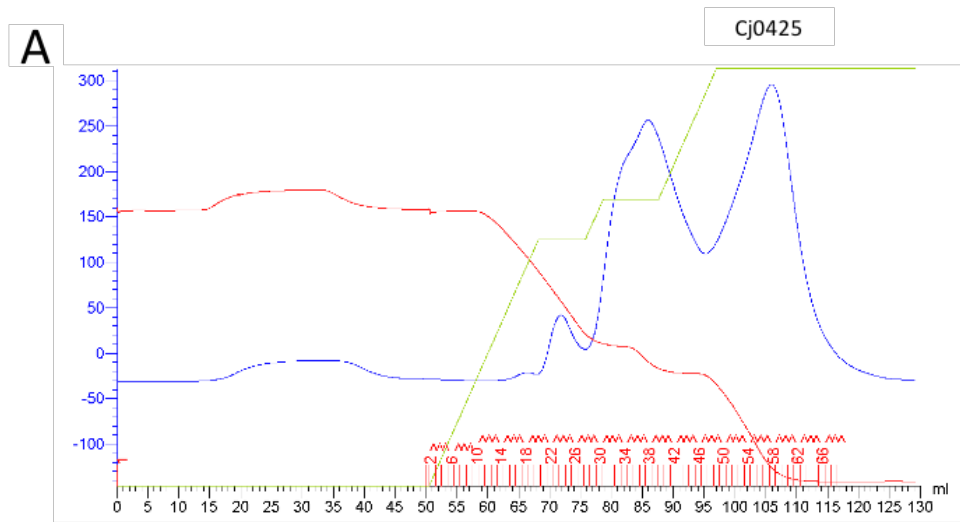


Figure 83: Hydrophobic interaction and gel filtration of Cj0425. (A) shows UV spectroscopy traces from hydrophobic interaction of Cj0425. The blue line represents the Abs_{280nm} and the red line shows the conductivity. The green line shows the relative concentration of NaCl used to separate the protein, the Cj0425 peak is labelled. The fractions containing the protein were collected and mixed. (B) shows the UV trace from the gel filtration of Cj0425 with the lines corresponding to the same as (A). The pink line shows the sample injection time. (C) shows a 14% SDS-PAGE gel loaded with the fractions from (B) where lane 1 shows the samples prior to loading onto the hydrophobic interaction column and lanes 2-7 correspond to elutions 10-15 from (B).

6.2.9 Checking purified Cj0425 for the formation of a disulfide bond

The Cj0425 protein contains a single disulfide bond, the protein is expressed in the periplasm of *E. coli* to allow to bond to form and the protein to fold correctly. To test that the disulfide bond is formed the molar concentration of free thiol groups was assayed using the DTNB assay or (Ellman's reagent) as described in (Section 2.29), this reagent reacts with free thiol groups and then absorbs at 412_{nm}. A standard curve of free thiols was generated using acetylcysteine with the results shown in (Figure 84). The molar concentration of free thiols in the purified Cj0425 sample was calculated using the standard curve. BSA was used as a control as purified BSA should contain 1 free thiol group (it contains other cysteine residues but these form disulfide bonds). The calculated free thiol concentration in Cj0425 was calculated as 0.85 μM from a 15 μM protein samples which indicates that the majority of the protein contains disulfide bonds.

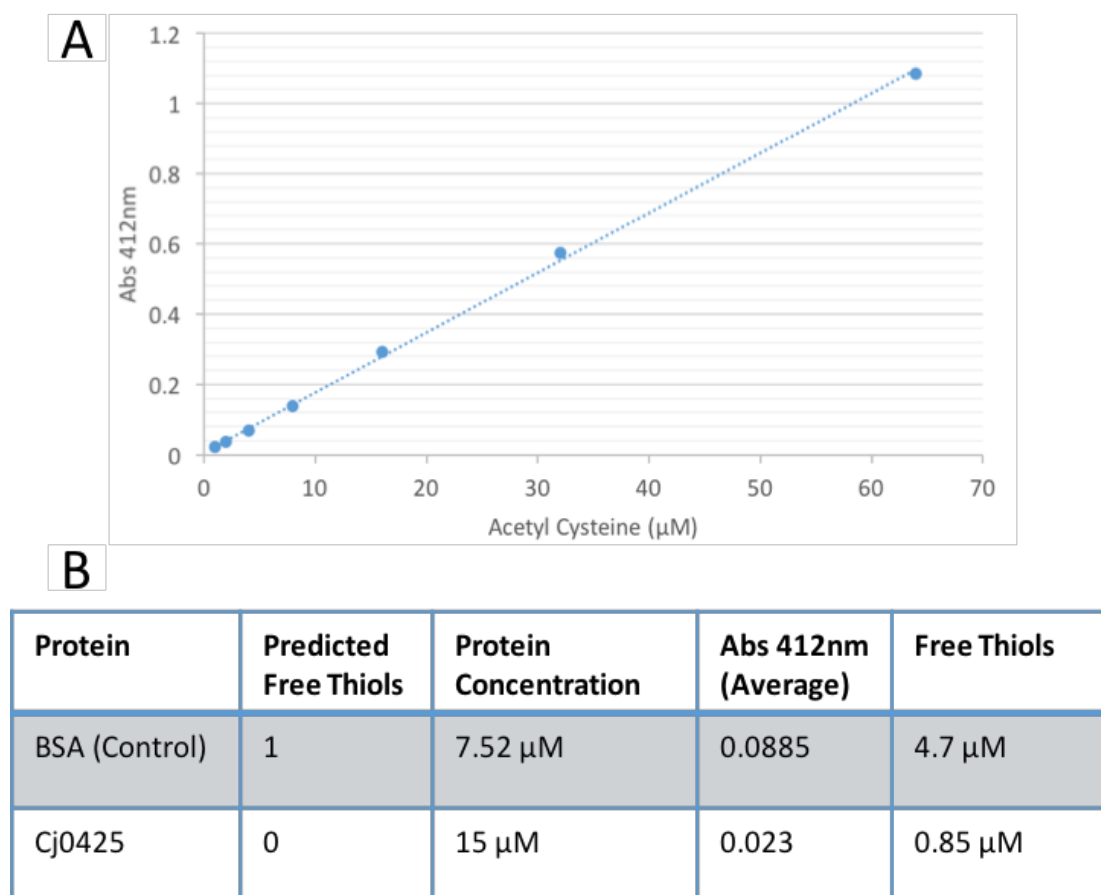


Figure 84: The concentration of free thiols in purified Cj0425. (A) the standard curve showing the Abs 412_{nm} of increasing concentration of acetylcysteine. The equation of the line was calculated as $Abs_{412nm} = 0.017 X + 0.0086$. (B) shows the molar concentration of free thiols in Cj0425 and the BSA positive control. The BSA control showed 53% free thiols and the Cj0425 protein showed 5.6% free thiols.

6.2.10 Cysteine protease inhibitory activity of Cj0425

Previous work on Cj0425 had shown it to inhibit the cysteine protease papain, though the inhibition was small and attempts to titrate the binding of Cj0425 to papain were unsuccessful. The hydrolytic activity of papain can be assayed using BAEE-coumarin (Sigma) which is cleaved by papain and releases the fluorescent substrate 7-amino-4-methyl coumarin, the assay is described in (Section 2.30). As part of this assay the concentration of active papain (Sigma) was determined by titrating with a cysteine protease inhibitor E64 [1-[N-[(L-3-trans-carboxyoxirane-2-carbonyl)-L-leucyl]amino]-4-guanidinobutane]. This inhibitor irreversibly binds to the active thiol residue in cysteine proteases thereby permanently inhibiting protease activity (Kim *et al.*, 1992). The rate of reaction is measured in moles of 7-amino-4-methyl coumarin liberated per minute where one unit of papain will hydrolyse 1 μmol BAEE per minute at 25°C pH 6.2. The temperature of the reaction was increased to 37°C to try and ensure the Cj0425 protein is active as *C. jejuni* is adapted to this temperature. The titration of papain with E64 is shown in (Figure 85) and shows a linear decrease in the rate of reaction with increasing concentration of E64. Because E64 irreversibly binds to papain in a 1:1 ratio the concentration of E64 that results in a reaction rate of 0 is equimolar to the concentration of active papain. This was calculated as 177.36 nM papain. This concentration was used for all experiments using papain.

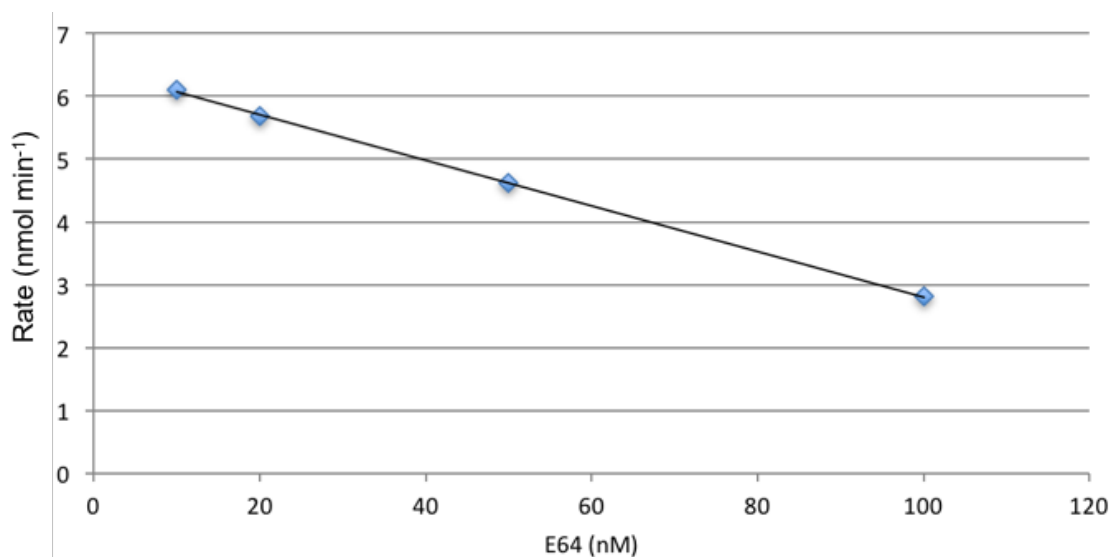


Figure 85: Titration of papain with E64. The rate of reaction was calculated as the nmoles of coumarin liberated per minute. Increasing the concentration of E64 generates a linear decrease in the rate of reaction. The concentration of papain in the final reaction is calculated at the point the line of best fit crosses the X axis. The equation of the line is $Y = -0.0363x + 6.4381$. Each data point is the result of 2 replicates.

The same experimental procedure was repeated using purified Cj0425 and E64 as a control. The experiment was performed initially using a high concentration of Cj0425 relative to papain (initially using 1 μ M Cj0425 final concentration. The experiment failed to show any decrease in the rate of reaction. The data shown in (Figure 86) shows only a very small change in the rate of reaction of papain when compared to the reaction with no inhibitor present. Given that the concentration of Cj0425 in the reaction is around 5 times that of the active papain this implies that Cj0425 is not inhibiting the reaction. Cysteine proteases need to be 'activated' prior to use by reducing agents such as cysteine, β -mercaptoethanol. It was thought that this may break the disulfide bond in Cj0425 thereby inactivating it, so the reaction was repeated where the papain was 'activated' in a reducing buffer and then transferred to a non-reducing buffer for the assay. This also showed no difference in the rate of reaction (data not shown).

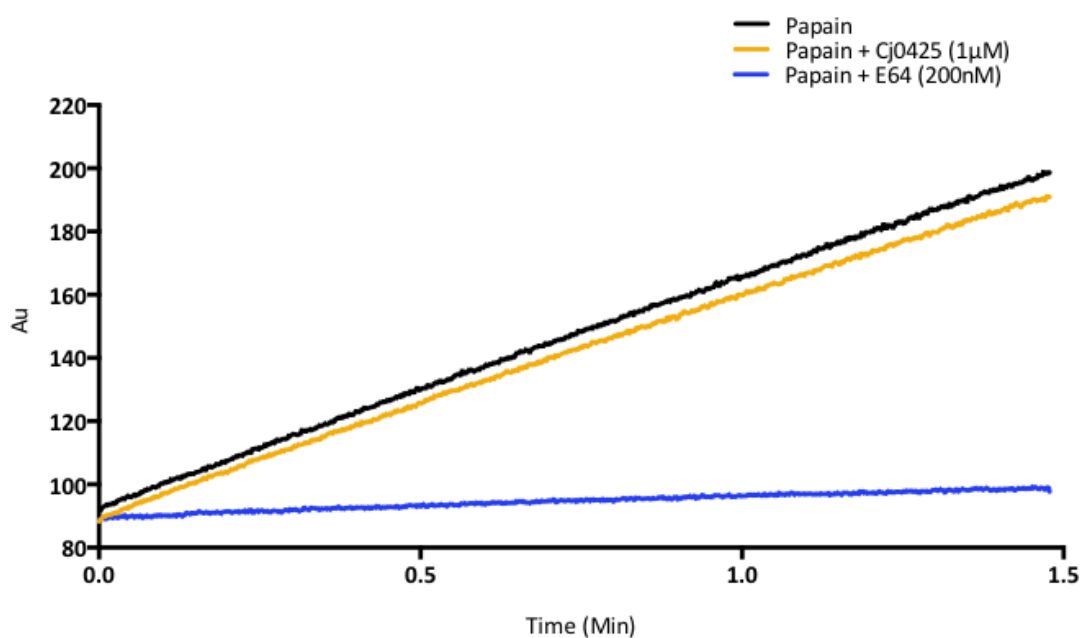


Figure 86: Fluorescence spectroscopy of the hydrolysis of BAEE-coumarin by papain with Cj0425 and E64. The cysteine protease activity of papain alone is shown by the black line and clearly shows the hydrolysis of BAEE-coumarin. The blue line shows the lack of any rate when inhibited with near equimolar E64. The yellow line shows the rate when mixed with a near 5-fold excess of Cj0425. The concentration of papain was calculated previously as 177 nM. Each data point is the result of 2 replicates. The fluorescence is measured in relative units.

Because the data in (Figure 86) shows almost no inhibition of papain by Cj0425, it was decided to repeat the experiment using a different cysteine protease. Because papain is a plant cysteine protease it was decided to use the human cysteine protease cathepsin-B (Sigma) as it is commercially available and *C. jejuni* is more likely to encounter an animal derived cysteine protease than a plant enzyme. The assay for measuring the protease activity of cathepsin-B is similar to papain but uses a different substrate ZAA-Coumarin. The assay is described in (Section 2.31) and is based on (Barrett, 1980). The Cj0425 protein was re-purified and re-assayed for formation of the disulfide bond. The assay was initially performed again using a high concentration of Cj0425 and E64 (15 μ M each) to look for any inhibition of cathepsin-B. The data shown in (Figure 87) again shows a complete inhibition of cathepsin-B when mixed with E64 and no discernible difference in the rate of reaction when mixed with Cj0425. The concentration of cathepsin-B was not calculated by titration as no inhibition could be observed when assayed in the presence of Cj0425. The rate of ZAA-coumarin hydrolysis was found to be considerably slower with cathepsin-B than with papain, so the assays were performed over a longer time period.

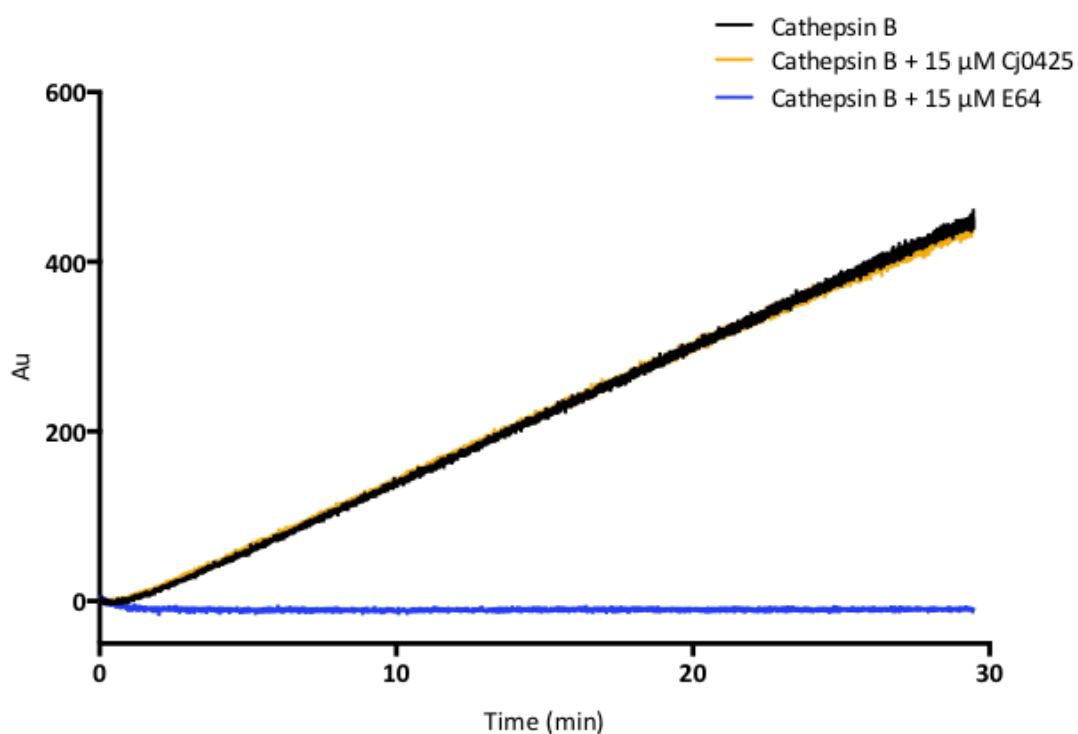


Figure 87: Fluorescence spectroscopy of the hydrolysis of ZAA-coumarin by cathepsin-B with Cj0425 and E64. The cysteine protease activity of cathepsin-B alone is shown by the black line and clearly shows the hydrolysis of ZAA-coumarin. The blue line shows the lack of any rate when inhibited with 15 μ M E64. The yellow line shows the rate when mixed with 15 μ M of Cj0425. Each data point is the result of 2 replicates. The fluorescence is measured in relative units.

6.2.11 Does Cj0425 have any binding partners in *C. jejuni*

Because Cj0425 shows no inhibitory activity against the cysteine protease enzymes papain or cathepsin-B, it may be that Cj0425 is not a cysteine protease inhibitor. Though it shows structural similarity to cystatins it may act as an inhibitor of a different kind of enzyme or potentially has a completely different role. It was decided to examine the *C. jejuni* genome for potential binding partners. A sample of 4699 publicly available *C. jejuni* genomes was analysed to look for potential Cj0425 binding partners. The data was collected and analysed by Dr Roy Chaudhuri and shows no apparent positive or negative correlation between the presence of *cj0425* and any other genes (apart from *cj0423* and *cj0424*) (data not shown).

I decided to screen for potential interaction partners using pull down assays, using both purified Cj0425 and natively expressed Cj0425 in *C. jejuni* 11168. To screen for potential interaction partners using recombinant Cj0425, 2 litres of wild type *C. jejuni* were cultured under normal conditions and the total soluble protein extracted into 20 mM sodium phosphate buffer and 100 mM NaCl at pH 7.4. The total soluble protein was passed through a His trap column and washed with the loading buffer with 20 mM imidazole and 300 mM imidazole. All the elutions were collected as a single fraction. The column was then washed with loading buffer and the purified recombinant Cj0425 protein was loaded onto the column. The total *C. jejuni* cell free extract was then re-loaded onto the column and the process repeated. All fractions were collected and separated on SDS-PAGE gels to look for any differences. Any proteins which bind to Cj0425 should, in theory, be visible in lane 9 but not in lane 4. The SDS-PAGE gel shown in (Figure 88) shows no immediately obvious binding partner for Cj0425 as no additional bands are seen eluting off the His trap column with Cj0425.

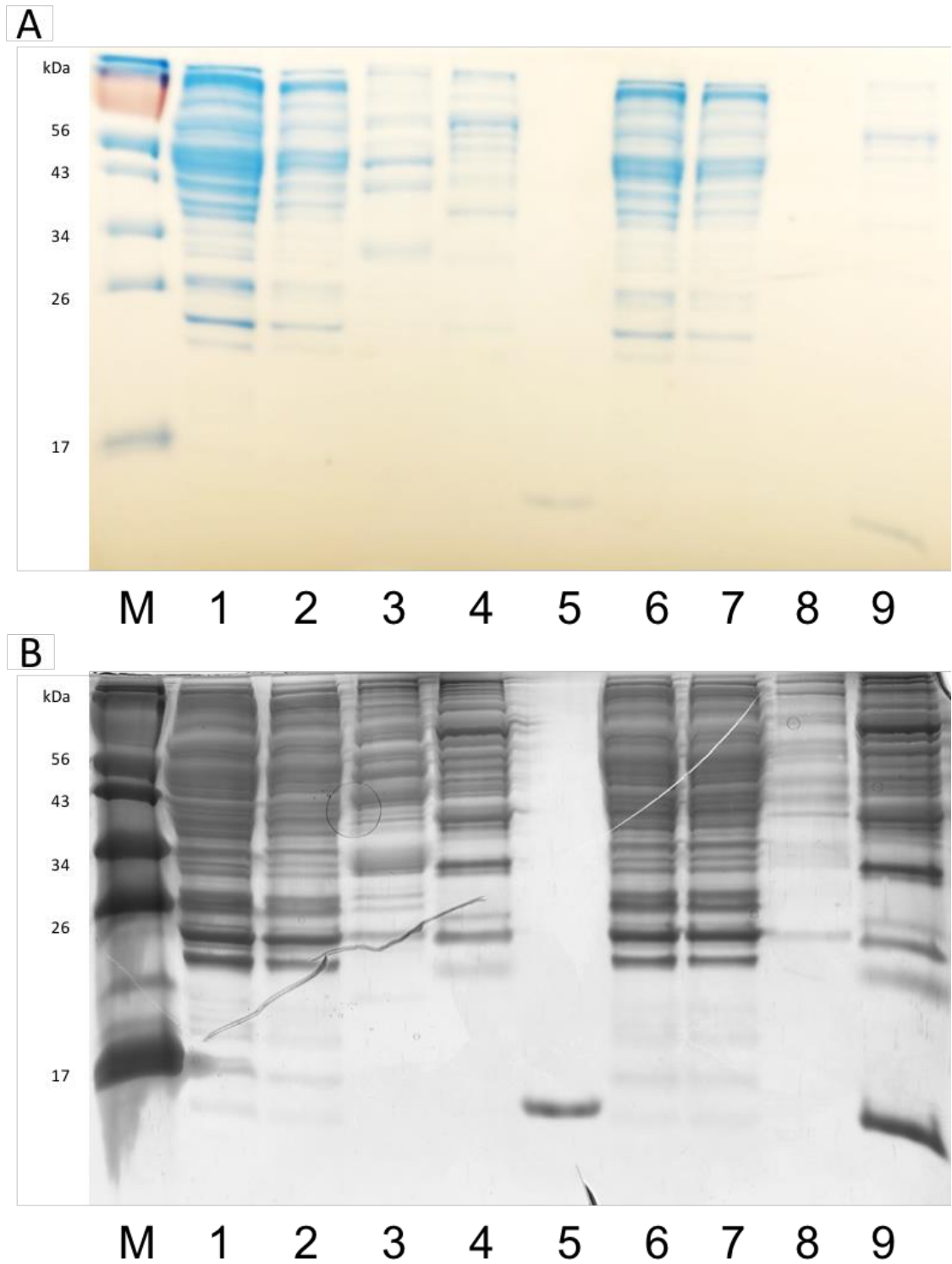


Figure 88: His trap pulldown of recombinant Cj0425 with *C. jejuni* soluble proteins. (A) 14% SDS-PAGE gel showing the elution fractions from the pulldown of Cj0425 with soluble *C. jejuni* proteins. Lane 1 is the *C. jejuni* CFE prior to loading, lane 2 is after washing with loading buffer (no imidazole), lane 3 is after washing with 20 mM imidazole, lane 4 after washing with 300 mM imidazole. Lane 5 is the recombinant Cj0425 protein (14.7 kDa), lane 6 is the re-mixed soluble *C. jejuni* proteins. Lane 7 is re-washing with loading buffer, lane 8 with 20 mM imidazole and lane 9 with 300 mM imidazole. (B) is the same SDS-PAGE gel after silver staining.

Because the pulldown assay shown in (Figure 88) shows no potential binding partner for recombinant Cj0425 it was decided to repeat the experiment using native Cj0425 under the iron inducible *fdxA* promoter. The complete *cj0425* ORF was cloned into the pCFdxA vector where 6 Histidine residues were attached to the C-terminal end of the protein by designing the codons into the primer sequence (Table 7). The construct was produced using methods described previously (Section 4.2.6), (Figure 89) shows the construction and screening of the pCFdxA46::cj0425-His plasmid after transformation into *C. jejuni* 11168.

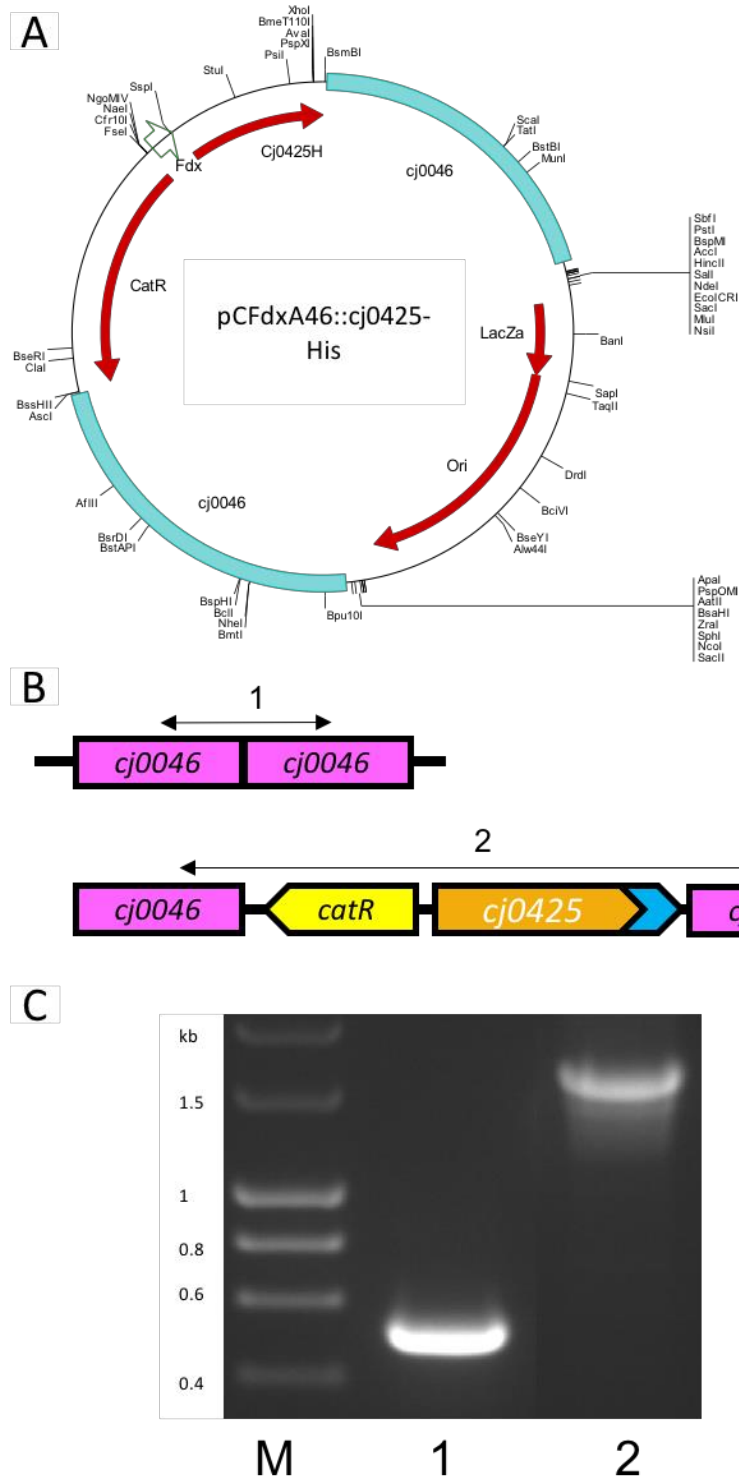


Figure 89: Construction and screening of the iron inducible *cj0425+* strain. (A) the plasmid map of the pCFdxA46::*cj0425*-His construct generated by ISA cloning. The FdxA promoter is represented by the green arrow upstream of the *cj0425* ORF. (B) The gene arrangement in the ISA construct prior to transformation into wild type *C. jejuni* 11168-DJK. (C) following transformation the strain was screened by PCR using the *cj0046* screening primers, which are represented by the arrow in (B). The expected band size is 455 bp for lane 1 and 1704 bp for lane 2.

The pull down assay using the *fdxA* expressed Cj0425 protein was performed in a similar way to the pulldown using the recombinant protein. The cell free extract was loaded onto the His trap column and steadily increasing concentrations of imidazole were passed through the column. Unfortunately, there was no detectable peak from the UV trace of the assay and upon loading onto an SDS-PAGE gel there was no visible Cj0425 protein band (data not shown).

6.3 Chapter 6 Discussion

The aim of this chapter was to overexpress and purify Cj0421c, Cj0422c and Cj0425 and to biochemically characterize them. Unfortunately, the roles of Cj0421c and Cj0425 have not been determined by biochemical methods, since there is currently no hypothesis about what the role of the *cj0421c-cj0425* gene cluster is, the role of Cj0421c as a regulatory protein is difficult to test. Previous structural studies on Cj0425 have showed that it is structurally similar to the cystatin family of cysteine protease inhibitors. The data presented here shows that Cj0425 does not inhibit either papain or cathepsin-B and so it may not actually be a classical cysteine protease inhibitor.

6.3.1 Metal binding analysis of *cj0421c*

The melt curve thermofluor analysis of Cj0421c shown in (Figure 76) did not identify any potential ligands or binding partners. The analysis of Cj0421c was performed when it was thought that the role of the gene cluster was as an antimicrobial peptide defense mechanism. The antimicrobial peptide defence mechanism in *Salmonella typhimurium* (the PhoP/Q sensor regulator system) is activated by both acidic pH and CAMPs displacing divalent metal ions from the outer membrane which is sensed by PhoQ (Prost *et al.*, 2007). The protein was tested for binding to a range of divalent metal cations as well as the model CAMP polymyxin-B which produced no detectable increase in protein stability. Cj0421c shows no strong homology to any proteins in the NCBI genomes database outside of *Campylobacter* species (as of September 2016). The closest match is to the cyclic-di-GMP diguanylate cyclase enzymes which produce the second messenger cyclic-di-GMP (Romling *et al.*, 2013). As discussed in (Section 4.1) *C. jejuni* does not possess any other cyclic-di-GMP related proteins which implies that Cj0421c does not bind to cyclic-di-GMP. The thermofluor data supports this as there was no change in the thermal stability of Cj0421c when mixed with cyclic-di-GMP which implies that it does not bind the second messenger (Figure 76). Attempts to crystallise Cj0421c using both the C- and N-terminal His-tagged protein produced no viable crystals despite testing numerous conditions. The Cj0421c protein is relatively easy to overexpress and purify and protein yields are generally high (>10 mg per litre), the protein is also stable during medium term storage and does not degrade easily or precipitate. The purification procedures for this protein are available for any future work that may be undertaken.

6.3.2 Interaction between Cj0421c and Cj0422c

The Cj0422c protein is challenging to work with as it cannot be concentrated to $>5 \text{ mg ml}^{-1}$ and will precipitate out of solution when chilled below 20°C . The protein can be kept in solution by re-heating however attempts to crystallise the protein after precipitation and re-solubilising have not been successful so it is assumed that the conformation of the protein is altered after precipitation has occurred. Because of this there is only a short window of opportunity to study the protein after purification. Prokaryotic helix-turn-helix transcriptional regulators like Cj0422c often form dimers and typically bind to palindromic repeat sequences, some are soluble as monomers and only form dimers when bound to DNA. Other H-T-H proteins bind to DNA as single monomers or sometimes tetramers but dimers appear the most common (Huffman and Brennan, 2002). Chemical crosslinking reactions have shown that Cj0422c forms a dimer in solution and previous work has shown that it binds to an 18 bp palindromic repeat sequence upstream of the *cj0423* ORF. It is likely then that 2 copies of the protein bind to each other in the cytoplasm and then bind to the palindromic repeat sequence in opposing orientations. This shows that Cj0422c is a typical prokaryotic transcriptional regulator but does not explain how the *cj0423-5* operon is controlled. Chemical crosslinking of Cj0421c alone did show some higher bands that may indicate dimerization, however the bands were very faint and were only visible after silver staining (Figure 78), and since Cj0421c is membrane bound and not normally free in solution the band may just be non-specific binding. The crosslinking reaction between Cj0421c and Cj0422c is harder to interpret as the Cj0422c protein appeared to precipitate out of solution and a large amount of insoluble protein is visible at the top of the SDS-PAGE gel (Figure 79). The data suggests that the two proteins may not interact with each other directly, however because of the Cj0422c precipitation and because the Cj0421c globular domain is not membrane bound *in-vitro* it may not be functioning or folding correctly so further work, possibly using *in-vivo* methods such as two hybrid analysis may be needed to thoroughly analyse any interactions between the two proteins.

6.3.3 Crystallisation of Cj0422c

The N-terminally His tagged Cj0422c protein can be crystallised with relative ease, however the difficulty in producing highly concentrated protein means that producing large enough crystals is difficult. Initial crystallization trials using the C-terminally tagged Cj0422c protein were relatively successful in that high resolution diffraction patterns were produced. However, selenomethionine derivatives of this protein were unstable and could not be purified in large enough quantities to produce crystals. Switching the His tag to the N-terminal end of the

protein did produce more stable selenomethionine crystals which could be grown to a reasonable size for X-ray diffraction analysis. Unfortunately, despite numerous attempts these crystals did not generate good enough diffraction patterns to construct a structural model of Cj0422c. Future work on the Cj0422c protein should involve trying to find a way to increase the yield and concentration of the protein and maybe attempting to find a buffer condition where the protein does not precipitate when chilled.

6.3.4 *Cj0425 does not inhibit the cysteine proteases papain or cathepsin-B*

The Cj0425 protein had already been purified and crystallised by a previous student, the crystal structure was solved using selenomethionine incorporated Cj0425 to a 2 Å resolution by Dr John Rafferty. The structure of the protein shows strong homology to cysteine protease inhibitor proteins known as cystatins. Cystatins are well studied in humans as they can often play a crucial role in disease progression, the role of cystatins in higher eukaryotes appears to be as a way to post translationally regulate the action of cysteine proteases (Turk *et al.*, 2008). Eukaryotic cystatins appear to be reasonably non-specific inhibitors and do not differentiate between different cysteine protease enzymes (though they can differentiate between endo and exo peptidase enzymes), typically cystatins inhibit proteases in a 1:1 ratio (Jenko *et al.*, 2003). The role of cystatins in prokaryotic systems is less well studied, this may be because cystatins are classed by their structure rather than by specific residues or domains, therefore they are difficult to predict bioinformatically. It may be that cystatins are very widespread in bacteria but with highly divergent protein sequences. The Cj0425 protein sequence showed that it is periplasmic but showed no sequence homology to other cystatins (either microbial or eukaryotic). This chapter aimed to elucidate how effective Cj0425 is as a cysteine protease inhibitor by titrating it against the cysteine protease papain. Unfortunately, when tested for inhibitory activity against papain, no detectable decrease in activity could be measured. Steps were taken to ensure that the Cj0425 protein was correctly folded and still no inhibitory activity could be observed. The same experiment was repeated using the human cysteine protease cathepsin-B. Again, no decrease in activity was observed even with a very large increase in the concentration of Cj0425 relative to the cathepsin-B. While it is feasible that the purified protein was not folded correctly or may have been damaged in some way, the data suggests that Cj0425 may not be a cysteine protease inhibitor. Part of the previous hypothesis about the role of Cj0425 as a peptidoglycan amidase inhibitor was based on the similarity between the active site of cysteine proteases and some types of peptidoglycan amidases, namely the presence of a reactive thiol group (Sanz-Gaitero *et al.*, 2014). As part of a future study on Cj0425 it may be worth testing for inhibitory activity against peptidoglycan specific

cysteine proteases rather than more generic ones like papain. Unfortunately, I was unable to find any commercially available peptidoglycan specific cysteine protease enzymes so each one being tested would need to be purified individually and a suitable assay developed to look for inhibition.

6.3.5 *Cj0425 pulldown assays could not find any potential binding partners*

The Cj0425c pulldown assay shown in (Figure 88) did not reveal any immediately obvious binding partners for Cj0425. As shown in (Figures 86-87) Cj0425 does not appear to inhibit cysteine protease enzymes *in-vitro* and as such it is difficult to predict what kind of proteins Cj0425 may bind to. Bioinformatic analysis of 4699 publically available *C. jejuni* genomes by Dr Roy Chaudhuri could not find any likely binding partners for Cj0425, the analysis looked at correlations between the presence of *cj0425* and other genes within the 11168 genome. No likely candidate genes were strongly correlated (either positively or negatively) with the presence of *cj0425* (data not shown). Attempts to pulldown Cj0425 binding partners may have been more successfully using natively expressed protein rather than recombinant Cj0425. However, attempts to overexpress His tagged Cj0425 using the *fdxA* promoter (Figure 89) in wild type *C. jejuni* were unsuccessful. As a side note, the same technique was used to overexpress the Cj0423 protein in Chapter 5, which also did not produce strong up-regulation. The lack of strong expression under the *fdxA* promoter highlights the need for a system of high protein expression in the *C. jejuni* background. Work being continued by another student Aidan Taylor on the *C. jejuni metK* and *fdxA* promoters shows that the *fdxA* promoter is expressed to around 700-800 Miller units when induced with iron which is probably too low to overexpress enough protein for native pulldown assays.

The role of Cj0425 was thought to be as cysteine protease inhibitor based on the structure of the protein. However, the lack of any inhibitory activity and the lack of any characterised binding partners mean the true role of Cj0425 remains elusive. The Cj0425 protein may still act as a type of protease inhibitor, possibly acting on peptidoglycan specific cysteine proteases. The data shown in (Figure 12) in Chapter 3 shows that the *cj0421c-cj0425* gene cluster varies between *C. jejuni* strains, the 3 structural genes within the *C. jejuni* 81116 operon include 2 genes which are similar in domain architecture to *cj0423* (*c8j_0398* and *c8j_0400*). The other gene in the 81116 operon (*c8j_0399*) is annotated as hypothetical periplasmic protein. The mature protein sequence of *C8j_0399* has a similar length to Cj0425 (97 to 118 residues respectively) and also contains 2 internal cysteine residues. Both *cj0425* and *c8j_0399* are

under the regulatory control of the Cj0422c repressor so it may be that C8j_0399 is also an un-annotated cystatin. This will need to be tested biochemically but if an un-related cystatin like protein is found in the same operon from 81116 then it strongly suggests separate evolutionary origins for these proteins.

7 [Chapter 7 general discussion and future work](#)

7.1 [Unravelling the rid system](#)

The initial aim of this project was to examine the regulatory roles of Cj0421c and Cj0422c in relation to the resistance to innate defences (*rid*) operon. The *rid* operon was thought to be involved in resistance to cationic antimicrobial peptides (CAMPs), partly because of the high sensitivity of the *cj0422c* mutant strain to the model CAMP polymyxin-B. The microarray data shown in chapter 1 (Figure 7) appeared to imply that several genes throughout the NCTC 11168 genome could be up or down-regulated by Cj0422c. During the course of the data presented in chapter 3 it became apparent that the high level of CAMP sensitivity seen in the *cj0422c* mutant strain was not found in mutants of other genes within the same operon and that there is no apparent regulatory response within the operon to the presence of polymyxin-B in wild type *C. jejuni*. Initially it was thought that the high level of sensitivity seen in the *cj0422c* mutant was due to an un-intentional recombination event within the *cj0423* promoter region (Figure 25), although this turned out to be unrelated to the polymyxin-B sensitive phenotype. Further work showed that the the polymyxin-B sensitivity seen in the mutant strain was actually un-related to the *cj0421c-cj0425* operon. The complete genome sequences of two variants of the *cj0422c* mutant strain revealed that the likely cause of the polymyxin-B sensitivity seen in the *cj0422c* mutant was due to a single frame shift SNP within the *cj0256* ORF. Cj0425 is an ethanolaminephosphotransferase protein responsible for attaching phosphoethanolamine to both lipid-A and the flagellar rod protein FlgG. Another study has shown that deletion of *cj0256* results in much higher sensitivity to polymyxin-B, which has been supported (albeit unintentionally) here (Cullen and Trent, 2010).

The wild type strain of *C. jejuni* 11168 used in our laboratory was also genome sequenced which revealed multiple small variations from the original NCTC 11168 sequence (Parkhill *et al.*, 2000). The strain was re-named as *C. jejuni* 11168-DJK for the purposes of this study. In total the laboratory strain genome contained 49 differences to the reference strain, of which 7 were in intergenic regions, 21 resulted in in-frame codon changes, 12 resulted in a likely loss of gene product and 9 were other changes which are categorised in chapter 3 (Section 3.2.15). Many of the changes appeared to be adaptations to continued growth under laboratory conditions. Many of the genes responsible for motility and chemotaxis contained frame shift SNPs. Several genes responsible for the uptake of nutrients such as lactate also contained frame shift SNPs. Since the laboratory strain of *C. jejuni* is routinely cultured in rich broth, the strain has no need for motility or the uptake of alternative metabolites. The lack of Cj0076c (L-lactate permease) is likely responsible for the inability of the lab strain to use lactate as a

primary carbon source, this was discovered when attempting to culture the strain in the MCLMAN minimal media which uses lactate as the primary carbon source, as discussed in the materials and methods. The carbon source used for the media was subsequently altered to L-serine.

The genome sequence of the *cj0422c* mutant strains also showed a number of changes either nearby or within the genes which were differentially expressed in the *cj0422c* mutant microarray, such as *cj0204*, *cj0653c* and *cj0864*. Initially it was thought that these differences may be due to the genes being differentially regulated in the mutant strain and that SNPs have accumulated to cope with the altered expression. However, after further analysis of the expression of these genes by qRT-PCR, which is a considerably more accurate measure of individual gene expression, it seems apparent that the differences seen in the microarray data may be because of the SNPs, rather than causing them. As discussed in (Section 4.2.8) this may be due to the inherent unreliability of microarray data concerning individual genes, where the probes are designed from a reference strain genome rather than the genome of the strain being tested.

As a side project the genome sequence of a hypermotile variant of *C. jejuni*, known as NCTC 11168-H was also genome sequenced. This variant was originally described by (Karlyshev *et al.*, 2002) who was looking at phase variable motility variants, to the best of our knowledge this variant has not been completely genome sequenced before. The genome sequence of this strain revealed only 6 SNP variants between this strain and the reference strain (Parkhill *et al.*, 2000). This implies that what is known as the hypermotile variant of *C. jejuni* may actually just be a closer relative to the original reference strain than other laboratory strains, which may have acquired SNPs or contain altered phase variable genes making them less motile.

7.2 Bioinformatic analysis of the *cj0421c-cj0425* operon

As shown in Chapter 1 (Section 11), the proposed regulatory genes *cj0421c* and *cj0422c* are found in around 90% of *C. jejuni* strains. The genes being regulated are however highly variable between strains. Since the promoter region is conserved it appears that different *C. jejuni* strains contain a different set of genes to respond to the same hypothetical stimulus. Bioinformatic analysis shows that all the sub-strains contain at least one small inner membrane protein such as *cj0423*. This is the only conserved feature between the sub strains and may act as a holin like protein due to structural similarity to phage derived holins.

7.3 *The cj0421c-cj0425 mutant strains show no obvious phenotype*

For chapter 4 a series of new mutant and complementation strains were produced in the 11168-DJK background strain. Initially the *cj0421c* and *cj0422c* mutant strains were assayed for changes in gene expression by qRT-PCR. This showed that *Cj0422c* alone appears to be responsible for repression of the *cj0423-5* operon and that deletion of *cj0421c* produces no detectable change in gene expression. Following on from this the set of mutant strains were assayed for growth defects and for any changes in sensitivity to various antimicrobials, none were observed. Because the *cj0423-5* operon is repressed by *Cj0422c* under normal conditions, mutations within these genes may not show any observable phenotype. The *cj0422c* mutant strain thus acts as a convenient overexpression strain and will be more likely to show a phenotypic difference compared to wild type *C. jejuni*. The *cj0422c* mutant strain was assayed for differences in membrane order and integrity and showed no biologically significant difference to wild type. Work performed in collaboration with Cosmin Chintoan-Uta in the laboratory of Professor Mark Stevens showed that the *cj0423-4* double mutant strain showed no attenuation of chicken colonisation compared to wild type. This is arguably the most relevant negative result from this chapter, as it suggests that the role of the *cj0423-5* operon is un-related to survival in chickens. The fact that not all strain of *C. jejuni* contain these genes also backs up this hypothesis.

7.4 *Cj0425 and the type VI secretion system*

The crystal structure of *Cj0425* was solved by Dr John Rafferty and was shown to be structurally similar to a family of cysteine protease inhibitors known as cystatins. For reasons discussed in Chapter 4 (Section 4.2.14) it was thought that *Cj0425* may act to inhibit periplasmically localised peptidoglycan hydrolase enzymes. Because both bioinformatic analysis and pull-down assays could not locate a native binding partner for *Cj0425* (though this does not conclusively disprove this), it was thought that *Cj0425* may act to inhibit foreign peptidoglycan hydrolases or proteases. One possible source for foreign peptidoglycan hydrolases being in the *C. jejuni* periplasm are from other bacteria via the type VI secretion system (T6SS). In collaboration with Dr Sarah Coulthurst at the University of Dundee, various *C. jejuni* mutant strains were assayed for sensitivity to the *Serratia marcescens* T6SS. While many laboratories have performed interbacterial T6SS killing assays, to the best of the authors knowledge this is the first time *C. jejuni* has been shown to be sensitive to the T6SS, and is also the first time an ϵ -proteobacterium has been shown to be sensitive to the T6SS. The data shown in chapter 4 shows that *C. jejuni* is sensitive to *S. marcescens* and the killing appears to be dependent on the T6SS. Unfortunately, the *cj0422c* mutant did not appear to be any more

resistant to the T6SS as would be expected if the *cj0423-5* operon was designed to defend against the T6SS.

7.5 Screening for potential inducers of the *cj0423* promoter

Because the *cj0423* promoter is repressed by Cj0422c during normal growth, it seems logical that the operon should be up-regulated in response to a certain stimulus. A *lacZ* reporter construct was generated to report on the regulation of the *cj0423* promoter in response to various potential stimuli. Despite testing nearly 1000 different compounds and conditions the reporter strain could not identify any particular condition that up-regulated the operon. While this does not dis-prove that an external compound or condition may up-regulate the operon, it does suggest that whatever the induction signal is it may be internal rather than external. I attempted to test the hypothesis that the signal may be the presence of the Cj0423 membrane protein itself, however due to difficulties in artificially up-regulating Cj0423 this hypothesis could not be tested thoroughly.

7.6 Purification of Cj0421c, Cj0422c and Cj0425

The work detailed in chapter 6 focuses on the expression and purification of Cj0421c, Cj0422c and Cj0425. Cj0421c can be purified with relative ease and remains stable during storage. Cj0422c is harder to purify and readily precipitates out of solution, the protein can be readily crystallised but attempts to generate high resolution X-ray diffraction data have so far been unsuccessful. Protein crosslinking assays between Cj0421c and Cj0422c show that the cytoplasmic domain of Cj0421c is probably monomeric and that Cj0422c forms a dimer in solution. No evidence suggesting that Cj0421c and Cj0422c interact at the protein level could be found, though this may have been due to Cj0422c readily precipitating out of solution during the assays.

Cj0425 can be readily purified, with the disulfide bond formed, from the periplasm of *E. coli*. Despite work by a previous student to the contrary Cj0425 does not appear to inhibit the activity of the cysteine protease enzymes papain or human cathepsin-B *in-vitro*.

7.7 Future work

To thoroughly examine the role of Cj0425 as a cystatin. Since there is no evidence that Cj0425 inhibits archetypal cysteine protease enzymes such as papain, it would be useful to determine if Cj0425 is able to inhibit periplasmically acting peptidoglycan hydrolase enzymes. Since these

enzymes are not commercially available they would need to be purified and a suitable assay developed to look for inhibition.

To examine the role of Cj0423 as a holin-like protein. Holins typically contain two Met start sites within a single ORF, which Cj0423 also does. In phage-derived holins these two produce form a holin-antiholin system which inhibits the formation of inner membrane pores until the phage is ready to lyse the cell. This equilibrium can be upset in phage infected *E. coli* by energy inhibition toxins such as cyanide or dinitrophenol (Žiedaite *et al.*, 2005). This could in theory be tested in the *cj0422c* mutant where the *cj0423* operon is strongly up-regulated and as such may be in a holin-antiholin equilibrium state. Artificial up-regulation of *cj0423* with a site directed alteration of the internal start codon may also allow this hypothesis to be tested.

To continue with structural studies of the Cj0421c and Cj0422c proteins, potentially by attempting to produce native crystals of Cj0422c and to use other methods to generate X-ray diffraction data, such as iodine soaking to allow the phase of the diffraction to be solved. Cj0421c was unable to be crystallised in this study, so producing alternative protein constructs or by removing the His tag after purification may allow the protein to be crystallised.

To examine the role of the *cj0421c-cj0425* operon in phage defense. With the role of Cj0425 hypothesised to be as a foreign peptidoglycan hydrolase inhibitor, and Cj0423 thought to be a mimic of a phage derived holin, it may be that the gene cluster is involved in phage defence. The high level of variability seen in the operon between different *C. jejuni* sub strains implies that the role of the genes is related to a variable condition. A recent publication on the transcriptomic response of *C. jejuni* to phage infection showed no change in the expression of the *cj0423-5* operon compared to un-infected *C. jejuni* (Brathwaite *et al.*, 2015). However, this study was primarily looking at the response to phage in a carrier state and so not committed to lysis. In order to thoroughly test the holin-cystatin hypothesis a *Campylobacter* specific phage with both holin genes and peptidoglycan hydrolase genes will need to be found before any *in-vivo* work can be performed.

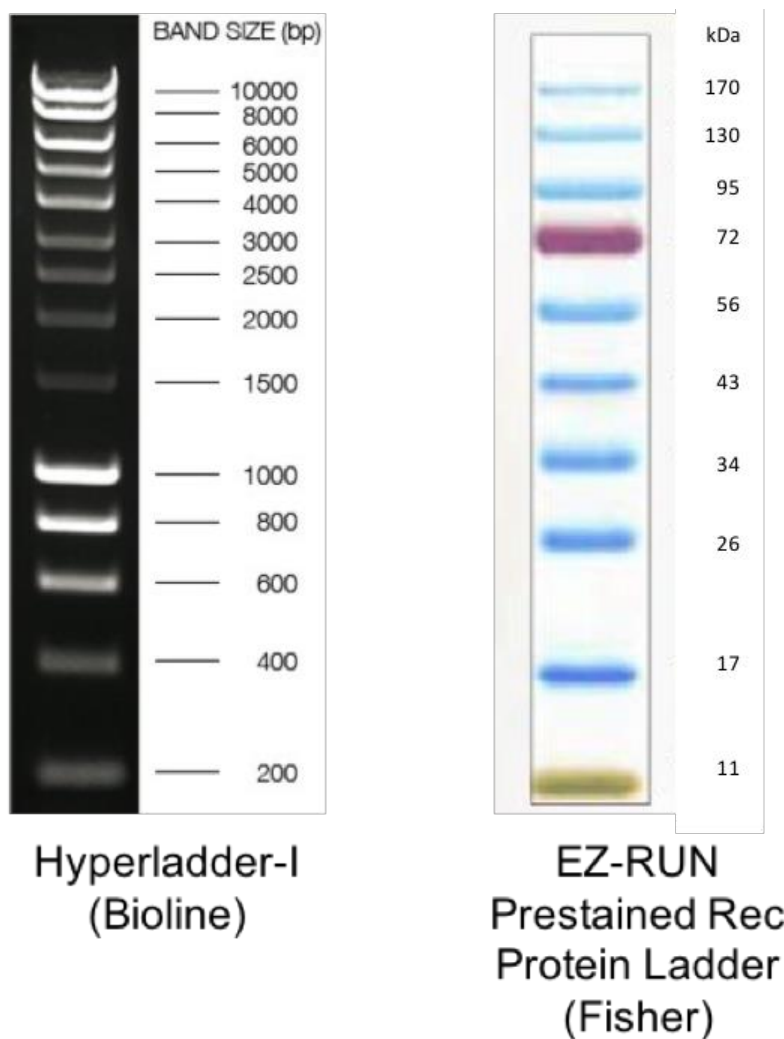
To examine the role of the MORN protein Cj0424 as a membrane binding protein. Previous data has shown that the presence of recombinant Cj0424 protects liposomes from lysis by polymyxin-B (unpublished data). Neither the *cj0422c* or *cj0424* mutant strains show any apparent difference in polymyxin-B sensitivity and the rigidity of the *C. jejuni* membrane is apparently not altered in either mutant. Currently work on the Cj0424 protein is focused on NMR analysis of protein interactions with model membranes to assess which residues of the

protein are involved in lipid binding. Preliminary data suggests that the MORN motifs are not actively involved in binding and are more likely involved in maintaining the β -sheet structure. This work is ongoing.

8 Appendix

8.1 Gel electrophoresis size markers

The band size markers for agarose gel electrophoresis and SDS-PAGE from Bioline and Fisher scientific respectively are shown.



8.2 Phenotype microarray plates

The compounds from the individual wells from the phenotype microarray plates (Biolog) are listed below. The plate wells correspond to the data shown in (Figures 66-69). The list can also be found at (http://www.biolog.com/pdf/pm_lit/PM1-PM10.pdf).

PM1 MicroPlate™ Carbon Sources

A1 Negative Control	A2 L-Arabinose	A3 N-Acetyl-D-Glucosamine	A4 D-Saccharic Acid	A5 Succinic Acid	A6 D-Galactose	A7 L-Aspartic Acid	A8 L-Proline	A9 D-Alanine	A10 D-Trehalose	A11 D-Mannose	A12 Dulcitol
B1 D-Serine	B2 D-Sorbitol	B3 Glycerol	B4 L-Fucose	B5 D-Glucuronic Acid	B6 D-Gluconic Acid	B7 D,L- α -Glycerol-Phosphate	B8 D-Xylose	B9 L-Lactic Acid	B10 Formic Acid	B11 D-Mannitol	B12 L-Glutamic Acid
C1 D-Glucose-6-Phosphate	C2 D-Galactonic Acid- γ -Lactone	C3 D,L-Malic Acid	C4 D-Ribose	C5 Tween 20	C6 L-Rhamnose	C7 D-Fructose	C8 Acetic Acid	C9 α -D-Glucose	C10 Maltose	C11 D-Melibiose	C12 Thymidine
D-1 L-Asparagine	D2 D-Aspartic Acid	D3 D-Glucosaminic Acid	D4 1,2-Propanediol	D5 Tween 40	D6 α -Keto-Glutaric Acid	D7 α -Keto-Butyric Acid	D8 α -Methyl-D-Galactoside	D9 α -D-Lactose	D10 Lactulose	D11 Sucrose	D12 Uridine
E1 L-Glutamine	E2 m-Tartaric Acid	E3 D-Glucose-1-Phosphate	E4 D-Fructose-6-Phosphate	E5 Tween 80	E6 α -Hydroxy Glutaric Acid- γ -Lactone	E7 α -Hydroxy Butyric Acid	E8 β -Methyl-D-Glucoside	E9 Adonitol	E10 Maltotriose	E11 2-Deoxy Adenosine	E12 Adenosine
F1 Glycyl-L-Aspartic Acid	F2 Citric Acid	F3 m-Inositol	F4 D-Threonine	F5 Fumaric Acid	F6 Bromo Succinic Acid	F7 Propionic Acid	F8 Mucic Acid	F9 Glycolic Acid	F10 Glyoxylic Acid	F11 D-Cellobiose	F12 Inosine
G1 Glycyl-L-Glutamic Acid	G2 Tricarballic Acid	G3 L-Serine	G4 L-Threonine	G5 L-Alanine	G6 L-Alanyl-Glycine	G7 Acetoacetic Acid	G8 N-Acetyl- β -D-Mannosamine	G9 Mono Methyl Succinate	G10 Methyl Pyruvate	G11 D-Malic Acid	G12 L-Malic Acid
H1 Glycyl-L-Proline	H2 m-Hydroxy Phenyl Acetic Acid	H3 m-Hydroxy Phenyl Acetic Acid	H4 Tyramine	H5 D- Psicose	H6 L-Lyxose	H7 Glucuronamide	H8 Pyruvic Acid	H9 L-Galactonic Acid- γ -Lactone	H10 D-Galacturonic Acid	H11 Phenylethylamine	H12 2-Aminoethanol

PM2A MicroPlate™ Carbon Sources

A1 Negative Control	A2 Chondroitin Sulfate C	A3 α -Cyclodextrin	A4 β -Cyclodextrin	A5 γ -Cyclodextrin	A6 Dextrin	A7 Gelatin	A8 Glycogen	A9 Inulin	A10 Laminarin	A11 Mannan	A12 Pectin
B1 N-Acetyl-D-Galactosamine	B2 N-Acetyl-Neuraminic Acid	B3 β -D-Allose	B4 Amygdalin	B5 D-Arabinose	B6 D-Arabitol	B7 L-Arabitol	B8 Arbutin	B9 2-Deoxy-D-Ribose	B10 α -Erythritol	B11 D-Fucose	B12 3-O- β -D-Galactopyranosyl-D-Arabinose
C1 Gentiobiose	C2 L-Glucose	C3 Lactitol	C4 D-Melezitose	C5 Maltitol	C6 α -Methyl-D-Glucoside	C7 β -Methyl-D-Galactoside	C8 3-Methyl Glucose	C9 β -Methyl-D-Glucuronic Acid	C10 α -Methyl-D-Mannoside	C11 β -Methyl-D-Xyloside	C12 Palatinose
D1 D-Raffinose	D2 Salicin	D3 Sedoheptulosan	D4 L-Sorbose	D5 Stachyose	D6 D-Tagatose	D7 Turannose	D8 Xylitol	D9 N-Acetyl-D-Glucosaminitol	D10 γ -Amino Butyric Acid	D11 β -Amino Valeric Acid	D12 Butyric Acid
E1 Capric Acid	E2 Caproic Acid	E3 Citraconic Acid	E4 Citramalic Acid	E5 D-Glucosamine	E6 2-Hydroxy Benzoic Acid	E7 4-Hydroxy Benzoic Acid	E8 β -Hydroxy Butyric Acid	E9 γ -Hydroxy Butyric Acid	E10 α -Keto-Valeric Acid	E11 Itaconic Acid	E12 3-Keto-D-Gluconic Acid
F1 D-Lactic Acid Methyl Ester	F2 Malonic Acid	F3 Melibionc Acid	F4 Oxalic Acid	F5 Oxalomalic Acid	F6 Quinic Acid	F7 D-Ribono-1,4-Lactone	F8 Sebaic Acid	F9 Sorbic Acid	F10 Succinamic Acid	F11 D-Tartaric Acid	F12 L-Tartaric Acid
G1 Acetamide	G2 L-Alaninamide	G3 N-Acetyl-L-Glutamic Acid	G4 L-Arginine	G5 Glycine	G6 L-Histidine	G7 L-Homoserine	G8 Hydroxy-L-Proline	G9 L-Isoleucine	G10 L-Leucine	G11 L-Lysine	G12 L-Methionine
H1 L-Ornithine	H2 L-Phenylalanine	H3 L-Pyroglutamic Acid	H4 L-Valine	H5 D,L-Carnitine	H6 Sec-Butylamine	H7 D,L-Octopamine	H8 Putrescine	H9 Dihydroxy Acetone	H10 2,3-Butanediol	H11 2,3-Butanone	H12 3-Hydroxy 2-Butanone

PM3B MicroPlate™ Nitrogen Sources

A1 Negative Control	A2 Ammonia	A3 Nitrite	A4 Nitrate	A5 Urea	A6 Biuret	A7 L-Alanine	A8 L-Arginine	A9 L-Asparagine	A10 L-Aspartic Acid	A11 L-Cysteine	A12 L-Glutamic Acid
B1 L-Glutamine	B2 Glycine	B3 L-Histidine	B4 L-Isoleucine	B5 L-Leucine	B6 L-Lysine	B7 L-Methionine	B8 L-Phenylalanine	B9 L-Proline	B10 L-Serine	B11 L-Threonine	B12 L-Tryptophan
C1 L-Tyrosine	C2 L-Valine	C3 D-Alanine	C4 D-Asparagine	C5 D-Aspartic Acid	C6 D-Glutamic Acid	C7 D-Lysine	C8 D-Serine	C9 D-Valine	C10 L-Citrulline	C11 L-Homoserine	C12 L-Ornithine
D-1 N-Acetyl-L-Glutamic Acid	D2 N-Phthaloyl-L-Glutamic Acid	D3 L-Pyroglutamic Acid	D4 Hydroxylamine	D5 Methylamine	D6 N-Amylamine	D7 N-Butylamine	D8 Ethylamine	D9 Ethanolamine	D10 Ethylenediamine	D11 Putrescine	D12 Agmatine
E1 Histamine	E2 β -Phenylethylamine	E3 Tyramine	E4 Acetamide	E5 Formamide	E6 Glucuronamide	E7 D,L-Lactamide	E8 D-Glucosamine	E9 D-Galactosamine	E10 D-Mannosamine	E11 N-Acetyl-D-Glucosamine	E12 N-Acetyl-D-Galactosamine
F1 N-Acetyl-D-Mannosamine	F2 Adenine	F3 Adenosine	F4 Cytidine	F5 Cytosine	F6 Guanine	F7 Guanosine	F8 Thymine	F9 Thymidine	F10 Uracil	F11 Uridine	F12 Inosine
G1 Xanthine	G2 Xanthosine	G3 Uric Acid	G4 Alloxan	G5 Allantoin	G6 Parabanic Acid	G7 D,L- α -Amino-N-Butyric Acid	G8 γ -Amino-N-Butyric Acid	G9 ϵ -Amino-N-Caproic Acid	G10 D,L- α -Amino-Caprylic Acid	G11 δ -Amino-N-Valeric Acid	G12 α -Amino-N-Valeric Acid
H1 Ala-Asp	H2 Ala-Gln	H3 Ala-Glu	H4 Ala-Gly	H5 Ala-His	H6 Ala-Leu	H7 Ala-Thr	H8 Gly-Asn	H9 Gly-Gln	H10 Gly-Glu	H11 Gly-Met	H12 Met-Ala

PM4A MicroPlate™ Phosphorus and Sulfur Sources

A1 Negative Control	A2 Phosphate	A3 Pyrophosphate	A4 Trimeta-phosphate	A5 Tripoly-phosphate	A6 Triethyl Phosphate	A7 Hypophosphite	A8 Adenosine-2'-monophosphate	A9 Adenosine-3'-monophosphate	A10 Adenosine-5'-monophosphate	A11 Adenosine-2',3'-cyclic monophosphate	A12 Adenosine-3',5'-cyclic monophosphate
B1 Thiophosphate	B2 Dithiophosphate	B3 D,L-α-Glycerol Phosphate	B4 β-Glycerol Phosphate	B5 Carbamyl Phosphate	B6 D-2-Phospho-Glyceric Acid	B7 D-3-Phospho-Glyceric Acid	B8 Guanosine-2'-monophosphate	B9 Guanosine-3'-monophosphate	B10 Guanosine-5'-monophosphate	B11 Guanosine-2',3'-cyclic monophosphate	B12 Guanosine-3',5'-cyclic monophosphate
C1 Phosphoenol Pyruvate	C2 Phospho-Glycolic Acid	C3 D-Glucose-1-Phosphate	C4 D-Glucose-6-Phosphate	C5 2-Deoxy-D-Glucose 6-Phosphate	C6 D-Glucosamine-6-Phosphate	C7 6-Phospho-Gluconic Acid	C8 Cytidine-2'-monophosphate	C9 Cytidine-3'-monophosphate	C10 Cytidine-5'-monophosphate	C11 Cytidine-2',3'-cyclic monophosphate	C12 Cytidine-3',5'-cyclic monophosphate
D1 D-Mannose-1-Phosphate	D2 D-Mannose-6-Phosphate	D3 Cysteamine-S-Phosphate	D4 Phospho-L-Arginine	D5 O-Phospho-D-Serine	D6 O-Phospho-L-Serine	D7 O-Phospho-L-Threonine	D8 Uridine-2'-monophosphate	D9 Uridine-3'-monophosphate	D10 Uridine-5'-monophosphate	D11 Uridine-2',3'-cyclic monophosphate	D12 Uridine-3',5'-cyclic monophosphate
E1 O-Phospho-D-Tyrosine	E2 O-Phospho-L-Tyrosine	E3 Phosphocreatine	E4 Phosphoryl Choline	E5 O-Phosphoryl-Ethanolamine	E6 Phosphono Acetic Acid	E7 2-Aminoethyl Phosphonic Acid	E8 Methylene Diphosphonic Acid	E9 Thymidine-3'-monophosphate	E10 Thymidine-5'-monophosphate	E11 Inositol Hexaphosphate	E12 Thymidine 3',5'-cyclic monophosphate
F1 Negative Control	F2 Sulfate	F3 Thiosulfate	F4 Tetrathionate	F5 Thiophosphate	F6 Dithiophosphate	F7 L-Cysteine	F8 D-Cysteine	F9 L-Cysteinyl-Glycine	F10 L-Cysteic Acid	F11 Cysteamine	F12 L-Cysteine Sulfonic Acid
G1 N-Acetyl-L-Cysteine	G2 S-Methyl-L-Cysteine	G3 Cystathionine	G4 Lanthionine	G5 Glutathione	G6 D,L-Ethionine	G7 L-Methionine	G8 D-Methionine	G9 Glycyl-L-Methionine	G10 N-Acetyl-D,L-Methionine	G11 L-Methionine Sulfoxide	G12 L-Methionine Sulfone
H1 L-Djenkolic Acid	H2 Thiourea	H3 1-Thio-β-D-Glucose	H4 D,L-Lipoamide	H5 Taurocholic Acid	H6 Taurine	H7 Hypotaurine	H8 p-Amino Benzene Sulfonic Acid	H9 Butane Sulfonic Acid	H10 2-Hydroxyethane Sulfonic Acid	H11 Methane Sulfonic Acid	H12 Tetramethylene Sulfone

PM5 MicroPlate™ Nutrient Supplements

A1 Negative Control	A2 Positive Control	A3 L-Alanine	A4 L-Arginine	A5 L-Asparagine	A6 L-Aspartic Acid	A7 L-Cysteine	A8 L-Glutamic Acid	A9 Adenosine-3',5'-cyclic monophosphate	A10 Adenine	A11 Adenosine	A12 2'-Deoxy Adenosine
B1 L-Glutamine	B2 Glycine	B3 L-Histidine	B4 L-Isoleucine	B5 L-Leucine	B6 L-Lysine	B7 L-Methionine	B8 L-Phenylalanine	B9 Guanosine-3',5'-cyclic monophosphate	B10 Guanine	B11 Guanosine	B12 2'-Deoxy Guanosine
C1 L-Proline	C2 L-Serine	C3 L-Threonine	C4 L-Tryptophan	C5 L-Tyrosine	C6 L-Valine	C7 L-Isoleucine + L-Valine	C8 trans-4-Hydroxy L-Proline	C9 (S) 4-Amino-Imidazole-4(5)-Carboxamide	C10 Hypoxanthine	C11 Inosine	C12 2'-Deoxy Inosine
D1 L-Ornithine	D2 L-Citrulline	D3 Chorismic Acid	D4 (-)Shikimic Acid	D5 L-Homoserine Lactone	D6 D-Alanine	D7 D-Aspartic Acid	D8 D-Glutamic Acid	D9 D,L-α,ε-Diaminopimelic Acid	D10 Cytosine	D11 Cytidine	D12 2'-Deoxy Cytidine
E1 Putrescine	E2 Spermidine	E3 Spermine	E4 Pyridoxine	E5 Pyridoxal	E6 Pyridoxamine	E7 β-Alanine	E8 D-Pantothenic Acid	E9 Orotic Acid	E10 Uracil	E11 Uridine	E12 2'-Deoxy Uridine
F1 Quinolnic Acid	F2 Nicotinic Acid	F3 Nicotinamide	F4 β-Nicotinamide Adenine Dinucleotide	F5 β-Amino-Levulinic Acid	F6 Hematin	F7 Deferoxamine Mesylate	F8 D-(+)-Glucose	F9 N-Acetyl D-Glucosamine	F10 Thymine	F11 Glutathione (reduced form)	F12 Thymidine
G1 Oxaloacetic Acid	G2 D-Biotin	G3 Cyano-Cobalamin	G4 p-Amino-Benzic Acid	G5 Folic Acid	G6 Inosine + Thiamine	G7 Thiamine	G8 Thiamine Pyrophosphate	G9 Riboflavin	G10 Pyrolo-Quinoline Quinone	G11 Menadione	G12 m-Inositol
H1 Butyric Acid	H2 D,L-α-Hydroxy-Butyric Acid	H3 α-Keto-Butyric Acid	H4 Caprylic Acid	H5 D,L-α-Lipoic Acid (oxidized form)	H6 D,L-Mevalonic Acid	H7 D,L-Carnitine	H8 Choline	H9 Tween 20	H10 Tween 40	H11 Tween 60	H12 Tween 80

PM6 MicroPlate™ Peptide Nitrogen sources

A1 Negative Control	A2 Positive Control: L-Glutamine	A3 Ala-Ala	A4 Ala-Arg	A5 Ala-Asn	A6 Ala-Glu	A7 Ala-Gly	A8 Ala-His	A9 Ala-Leu	A10 Ala-Lys	A11 Ala-Phe	A12 Ala-Pro
B1 Ala-Ser	B2 Ala-Thr	B3 Ala-Trp	B4 Ala-Tyr	B5 Arg-Ala	B6 Arg-Arg	B7 Arg-Asp	B8 Arg-Gln	B9 Arg-Glu	B10 Arg-Ile	B11 Arg-Leu	B12 Arg-Lys
C1 Arg-Met	C2 Arg-Phe	C3 Arg-Ser	C4 Arg-Trp	C5 Arg-Tyr	C6 Arg-Val	C7 Asn-Glu	C8 Asn-Val	C9 Asp-Asp	C10 Asp-Glu	C11 Asp-Leu	C12 Asp-Lys
D1 Asp-Phe	D2 Asp-Trp	D3 Asp-Val	D4 Cys-Gly	D5 Gln-Gln	D6 Gln-Gly	D7 Glu-Asp	D8 Glu-Glu	D9 Glu-Gly	D10 Glu-Ser	D11 Glu-Trp	D12 Glu-Tyr
E1 Glu-Val	E2 Gly-Ala	E3 Gly-Arg	E4 Gly-Cys	E5 Gly-Gly	E6 Gly-His	E7 Gly-Leu	E8 Gly-Lys	E9 Gly-Met	E10 Gly-Phe	E11 Gly-Pro	E12 Gly-Ser
F1 Gly-Thr	F2 Gly-Trp	F3 Gly-Tyr	F4 Gly-Val	F5 His-Asp	F6 His-Gly	F7 His-Leu	F8 His-Lys	F9 His-Met	F10 His-Pro	F11 His-Ser	F12 His-Trp
G1 His-Tyr	G2 Ile-Val	G3 Ile-Ala	G4 Ile-Arg	G5 Ile-Gln	G6 Ile-Gly	G7 Ile-His	G8 Ile-Ile	G9 Ile-Met	G10 Ile-Phe	G11 Ile-Pro	G12 Ile-Ser
H1 Ile-Trp	H2 Ile-Tyr	H3 Ile-Val	H4 Leu-Ala	H5 Leu-Arg	H6 Leu-Asp	H7 Leu-Glu	H8 Leu-Gly	H9 Leu-Ile	H10 Leu-Leu	H11 Leu-Met	H12 Leu-Phe

PM7 MicroPlate™ Peptide Nitrogen sources

A1 Negative Control	A2 Positive Control: L-Glutamine	A3 Leu-Ser	A4 Leu-Trp	A5 Leu-Val	A6 Lys-Ala	A7 Lys-Arg	A8 Lys-Glu	A9 Lys-Ile	A10 Lys-Leu	A11 Lys-Lys	A12 Lys-Phe
B1 Lys-Pro	B2 Lys-Ser	B3 Lys-Thr	B4 Lys-Trp	B5 Lys-Tyr	B6 Lys-Val	B7 Met-Arg	B8 Met-Asp	B9 Met-Gln	B10 Met-Glu	B11 Met-Gly	B12 Met-His
C1 Met-Ile	C2 Met-Leu	C3 Met-Lys	C4 Met-Met	C5 Met-Phe	C6 Met-Pro	C7 Met-Trp	C8 Met-Val	C9 Phe-Ala	C10 Phe-Gly	C11 Phe-Ile	C12 Phe-Phe
D1 Phe-Pro	D2 Phe-Ser	D3 Phe-Trp	D4 Pro-Ala	D5 Pro-Asp	D6 Pro-Gln	D7 Pro-Gly	D8 Pro-Hyp	D9 Pro-Leu	D10 Pro-Phe	D11 Pro-Pro	D12 Pro-Tyr
E1 Ser-Ala	E2 Ser-Gly	E3 Ser-His	E4 Ser-Leu	E5 Ser-Met	E6 Ser-Phe	E7 Ser-Pro	E8 Ser-Ser	E9 Ser-Tyr	E10 Ser-Val	E11 Thr-Ala	E12 Thr-Arg
F1 Thr-Glu	F2 Thr-Gly	F3 Thr-Leu	F4 Thr-Met	F5 Thr-Pro	F6 Trp-Ala	F7 Trp-Arg	F8 Trp-Asp	F9 Trp-Glu	F10 Trp-Gly	F11 Trp-Leu	F12 Trp-Lys
G1 Trp-Phe	G2 Trp-Ser	G3 Trp-Trp	G4 Trp-Tyr	G5 Tyr-Ala	G6 Tyr-Gln	G7 Tyr-Glu	G8 Tyr-Gly	G9 Tyr-His	G10 Tyr-Leu	G11 Tyr-Lys	G12 Tyr-Phe
H1 Tyr-Trp	H2 Tyr-Tyr	H3 Val-Arg	H4 Val-Asn	H5 Val-Asp	H6 Val-Gly	H7 Val-His	H8 Val-Ile	H9 Val-Leu	H10 Val-Tyr	H11 Val-Val	H12 Y-Glu-Gly

PM8 MicroPlate™ Peptide Nitrogen sources

A1 Negative Control	A2 Positive Control: L-Glutamine	A3 Ala-Asp	A4 Ala-Gln	A5 Ala-Ile	A6 Ala-Met	A7 Ala-Val	A8 Asp-Ala	A9 Asp-Gln	A10 Asp-Gly	A11 Glu-Ala	A12 Gly-Asn
B1 Gly-Asp	B2 Gly-Ile	B3 His-Ala	B4 His-Glu	B5 His-His	B6 Ile-Asn	B7 Ile-Leu	B8 Leu-Asn	B9 Leu-His	B10 Leu-Pro	B11 Leu-Tyr	B12 Lys-Asp
C1 Lys-Gly	C2 Lys-Met	C3 Met-Thr	C4 Met-Tyr	C5 Phe-Asp	C6 Phe-Glu	C7 Gln-Glu	C8 Phe-Met	C9 Phe-Tyr	C10 Phe-Val	C11 Pro-Arg	C12 Pro-Asn
D1 Pro-Glu	D2 Pro-Ile	D3 Pro-Lys	D4 Pro-Ser	D5 Pro-Trp	D6 Pro-Val	D7 Ser-Asn	D8 Ser-Asp	D9 Ser-Gln	D10 Ser-Glu	D11 Thr-Asp	D12 Thr-Gln
E1 Thr-Phe	E2 Thr-Ser	E3 Trp-Val	E4 Tyr-Ile	E5 Tyr-Val	E6 Val-Ala	E7 Val-Gln	E8 Val-Glu	E9 Val-Lys	E10 Val-Met	E11 Val-Phe	E12 Val-Pro
F1 Val-Ser	F2 β -Ala-Ala	F3 β -Ala-Gly	F4 β -Ala-His	F5 Met- β -Ala	F6 β -Ala-Phe	F7 D-Ala-D-Ala	F8 D-Ala-Gly	F9 D-Ala-Leu	F10 D-Leu-D-Leu	F11 D-Leu-Gly	F12 D-Leu-Tyr
G1 Y-Glu-Gly	G2 Y-D-Glu-Gly	G3 Gly-D-Ala	G4 Gly-D-Asp	G5 Gly-D-Ser	G6 Gly-D-Thr	G7 Gly-D-Val	G8 Leu- β -Ala	G9 Leu-D-Leu	G10 Phe- β -Ala	G11 Ala-Ala-Ala	G12 D-Ala-Gly-Gly
H1 Gly-Gly-Ala	H2 Gly-Gly-D-Leu	H3 Gly-Gly-Gly	H4 Gly-Gly-Ile	H5 Gly-Gly-Leu	H6 Gly-Gly-Phe	H7 Val-Tyr-Val	H8 Gly-Phe-Phe	H9 Leu-Gly-Gly	H10 Leu-Leu-Leu	H11 Phe-Gly-Gly	H12 Tyr-Gly-Gly

PM9 MicroPlate™ Osmolytes

A1 NaCl 1%	A2 NaCl 2%	A3 NaCl 3%	A4 NaCl 4%	A5 NaCl 5%	A6 NaCl 5.5%	A7 NaCl 6%	A8 NaCl 6.5%	A9 NaCl 7%	A10 NaCl 8%	A11 NaCl 9%	A12 NaCl 10%
B1 NaCl 6%	B2 NaCl 6% + Betaine	B3 NaCl 6% + N,N Dimethyl Glycine	B4 NaCl 6% + Sarcosine	B5 NaCl 6% + Dimethyl sulphonyl propionate	B6 NaCl 6% + MOPS	B7 NaCl 6% + Ectoine	B8 NaCl 8% + Choline	B9 NaCl 6% + Phosphoryl Choline	B10 NaCl 8% + Creatine	B11 NaCl 6% + Creatinine	B12 NaCl 6% + L-Carnitine
C1 NaCl 6% + KCl	C2 NaCl 6% + L-Proline	C3 NaCl 6% + N-Acetyl L-Glutamine	C4 NaCl 6% + β-Glutamic Acid	C5 NaCl 6% + γ-Amino-N-Butyric Acid	C6 NaCl 6% + Glutathione	C7 NaCl 6% + Glycerol	C8 NaCl 6% + Trehalose	C9 NaCl 6% + Trimethylamine-N-oxide	C10 NaCl 6% + Trimethylamine	C11 NaCl 6% + Octopine	C12 NaCl 6% + Trigonelline
D1 Potassium chloride 3%	D2 Potassium chloride 4%	D3 Potassium chloride 5%	D4 Potassium chloride 6%	D5 Sodium sulfate 2%	D6 Sodium sulfate 3%	D7 Sodium sulfate 4%	D8 Sodium sulfate 5%	D9 Ethylene glycol 5%	D10 Ethylene glycol 10%	D11 Ethylene glycol 15%	D12 Ethylene glycol 20%
E1 Sodium formate 1%	E2 Sodium formate 2%	E3 Sodium formate 3%	E4 Sodium formate 4%	E5 Sodium formate 5%	E6 Sodium formate 6%	E7 Urea 2%	E8 Urea 3%	E9 Urea 4%	E10 Urea 5%	E11 Urea 6%	E12 Urea 7%
F1 Sodium Lactate 1%	F2 Sodium Lactate 2%	F3 Sodium Lactate 3%	F4 Sodium Lactate 4%	F5 Sodium Lactate 5%	F6 Sodium Lactate 6%	F7 Sodium Lactate 7%	F8 Sodium Lactate 8%	F9 Sodium Lactate 9%	F10 Sodium Lactate 10%	F11 Sodium Lactate 11%	F12 Sodium Lactate 12%
G1 Sodium Phosphate pH 7 20mM	G2 Sodium Phosphate pH 7 50mM	G3 Sodium Phosphate pH 7 100mM	G4 Sodium Phosphate pH 7 200mM	G5 Sodium Benzoate pH 5.2 20mM	G6 Sodium Benzoate pH 5.2 50mM	G7 Sodium Benzoate pH 5.2 100mM	G8 Sodium Benzoate pH 5.2 200mM	G9 Ammonium sulfate pH 8 10mM	G10 Ammonium sulfate pH 8 20mM	G11 Ammonium sulfate pH 8 50mM	G12 Ammonium sulfate pH 8 100mM
H1 Sodium Nitrate 10mM	H2 Sodium Nitrate 20mM	H3 Sodium Nitrate 40mM	H4 Sodium Nitrate 60mM	H5 Sodium Nitrate 80mM	H6 Sodium Nitrate 100mM	H7 Sodium Nitrate 10mM	H8 Sodium Nitrate 20mM	H9 Sodium Nitrate 40mM	H10 Sodium Nitrate 60mM	H11 Sodium Nitrate 80mM	H12 Sodium Nitrate 100mM

PM10 MicroPlate™ pH

A1 pH 3.5	A2 pH 4	A3 pH 4.5	A4 pH 5	A5 pH 5.5	A6 pH 6	A7 pH 7	A8 pH 8	A9 pH 8.5	A10 pH 9	A11 pH 9.5	A12 pH 10
B1 pH 4.5	B2 pH 4.5 + L-Alanine	B3 pH 4.5 + L-Arginine	B4 pH 4.5 + L-Asparagine	B5 pH 4.5 + L-Aspartic Acid	B6 pH 4.5 + L-Glutamic Acid	B7 pH 4.5 + L-Glutamine	B8 pH 4.5 + Glycine	B9 pH 4.5 + L-Histidine	B10 pH 4.5 + L-Isoleucine	B11 pH 4.5 + L-Leucine	B12 pH 4.5 + L-Lysine
C1 pH 4.5 + L-Methionine	C2 pH 4.5 + L-Phenylalanine	C3 pH 4.5 + L-Proline	C4 pH 4.5 + L-Serine	C5 pH 4.5 + L-Threonine	C6 pH 4.5 + L-Tryptophan	C7 pH 4.5 + L-Citrulline	C8 pH 4.5 + L-Valine	C9 pH 4.5 + Hydroxy-L-Proline	C10 pH 4.5 + L-Ornithine	C11 pH 4.5 + L-Homoarginine	C12 pH 4.5 + L-Homoserine
D-1 pH 4.5 + Anthranilic Acid	D2 pH 4.5 + L-Norleucine	D3 pH 4.5 + L-Norvaline	D4 pH 4.5 + α-Amino-N-Butyric Acid	D5 pH 4.5 + p-Amino-Benzoic Acid	D6 pH 4.5 + L-Cysteic Acid	D7 pH 4.5 + D-Lysine	D8 pH 4.5 + 5-Hydroxy Lysine	D9 pH 4.5 + 5-Hydroxy Tryptophan	D10 pH 4.5 + D,L-Diamino pimelic Acid	D11 pH 4.5 + Trimethylamine-N-oxide	D12 pH 4.5 + Urea
E1 pH 9.5	E2 pH 9.5 + L-Alanine	E3 pH 9.5 + L-Arginine	E4 pH 9.5 + L-Asparagine	E5 pH 9.5 + L-Aspartic Acid	E6 pH 9.5 + L-Glutamic Acid	E7 pH 9.5 + L-Glutamine	E8 pH 9.5 + Glycine	E9 pH 9.5 + L-Histidine	E10 pH 9.5 + L-Isoleucine	E11 pH 9.5 + L-Leucine	E12 pH 9.5 + L-Lysine
F1 pH 9.5 + L-Methionine	F2 pH 9.5 + L-Phenylalanine	F3 pH 9.5 + L-Proline	F4 pH 9.5 + L-Serine	F5 pH 9.5 + L-Threonine	F6 pH 9.5 + L-Tryptophan	F7 pH 9.5 + L-Tyrosine	F8 pH 9.5 + L-Valine	F9 pH 9.5 + Hydroxy-L-Proline	F10 pH 9.5 + L-Ornithine	F11 pH 9.5 + L-Homoarginine	F12 pH 9.5 + L-Homoserine
G1 pH 9.5 + Anthranilic acid	G2 pH 9.5 + L-Norleucine	G3 pH 9.5 + L-Norvaline	G4 pH 9.5 + Agmatine	G5 pH 9.5 + Cadaverine	G6 pH 9.5 + Putrescine	G7 pH 9.5 + Histamine	G8 pH 9.5 + Phenylethylamine	G9 pH 9.5 + Tyramine	G10 pH 9.5 + Creatine	G11 pH 9.5 + Trimethylamine-N-oxide	G12 pH 9.5 + Urea
H1 X-Caprylate	H2 X-β-D-Glucoside	H3 X-β-D-Glucoside	H4 X-α-D-Galactoside	H5 X-β-D-Galactoside	H6 X-α-D-Glucuronide	H7 X-β-D-Glucuronide	H8 X-β-D-Glucosaminide	H9 X-β-D-Galactosaminide	H10 X-α-D-Mannoside	H11 X-PO4	H12 X-SO4

9 [References](#)

- Alazzam, B., Bonnassie-Rouxin, S., Dufour, V., and Ermel, G. (2011). MCLMAN, a new minimal medium for *Campylobacter jejuni* NCTC 11168. *Res. Microbiol.* *162*, 173–179.
- Hitchcock, A. (2011). The role of the twin arginine translocase in the assembly and function of electron transport chains in *Campylobacter jejuni*.
- Al-Haideri, H. (2015). Characterization of novel proteins in the cell envelope of *Campylobacter jejuni*.
- Al-Haideri, H., White, M.A., and Kelly, D.J. (2016). Major contribution of the type II beta carbonic anhydrase CanB (Cj0237) to the capnophilic growth phenotype of *Campylobacter jejuni*. *Environ. Microbiol.* *18*, 721–735.
- Allos, B.M., and Blaser, M.J. (1995). *Campylobacter jejuni* and the expanding spectrum of related infections. *Clin. Infect. Dis.* *20*, 1092–1101.
- Anders, B., Paisley, J., Lauer, B., and Barth Reller, L. (1982). Double-Blind Placebo Controlled Trial of Erythromycin for Treatment of *Campylobacter* Enteritis. *Lancet* *319*, 131–132.
- Arnett, E., Lehrer, R.I., Pratikhya, P., Lu, W., and Seveau, S. (2011). Defensins enable macrophages to inhibit the intracellular proliferation of *Listeria monocytogenes*. *Cell. Microbiol.* *13*, 635–651.
- Ashgar, S.S.A., Oldfield, N.J., Wooldridge, K.G., Jones, M.A., Irving, G.J., Turner, D.P.J., and Ala'Aldeen, D.A.A. (2007). CapA, an autotransporter protein of *Campylobacter jejuni*, mediates association with human epithelial cells and colonization of the chicken gut. *J. Bacteriol.* *189*, 1856–1865.
- Atack, J.M., and Kelly, D.J. (2008). Contribution of the stereospecific methionine sulphoxide reductases MsrA and MsrB to oxidative and nitrosative stress resistance in the food-borne pathogen *Campylobacter jejuni*. *Microbiology* *154*, 2219–2230.
- Baar, C., Eppinger, M., Raddatz, G., Simon, J., Lanz, C., Klimmek, O., Nandakumar, R., Gross, R., Rosinus, A., Keller, H., *et al.* (2003). Complete genome sequence and analysis of *Wolinella succinogenes*. *Proc. Natl. Acad. Sci. U. S. A.* *100*, 11690–11695.
- Bader, M.W., Sanowar, S., Daley, M.E., Schneider, A.R., Cho, U., Xu, W., Klevit, R.E., Le Moual, H., and Miller, S.I. (2005). Recognition of antimicrobial peptides by a bacterial sensor kinase. *Cell* *122*, 461–472.
- Barrett, A.J. (1980). Fluorimetric assays for cathepsin B and cathepsin H with methylcoumarylamide substrates. *Biochem. J.* *187*, 909–912.
- Batchelor, R.A., Pearson, B.M., Friis, L.M., Guerry, P., and Wells, J.M. (2004). Nucleotide sequences and comparison of two large conjugative plasmids from different *Campylobacter* species. *Microbiology* *150*, 3507–3517.
- Bateman, A., and Rawlings, N.D. (2003). The CHAP domain: a large family of amidases including GSP amidase and peptidoglycan hydrolases. *Trends Biochem. Sci.* *28*, 234–237.
- Bayliss, C.D., Bidmos, F.A., Anjum, A., Manchev, V.T., Richards, R.L., Grossier, J.P., Wooldridge, K.G., Ketley, J.M., Barrow, P.A., Jones, M.A., *et al.* (2012). Phase variable genes of *Campylobacter jejuni* exhibit high mutation rates and specific mutational patterns but mutability is not the major determinant of population structure during host colonization. *Nucleic Acids Res.* *40*, 5876–5889.
- Blaser, M.J. (1997). Epidemiologic and Clinical Features of *Campylobacter jejuni* Infections. *176*, 103–105.
- Bochner, B.R., Gadzinski, P., and Panomitros, E. (2001). Phenotype Microarrays for high-throughput phenotypic testing and assay of gene function. *Genome Res.* *11*, 1246–1255.
- Bolton, F.J., and Coates, D. (1983). A study of the oxygen and carbon dioxide requirements of thermophilic campylobacters. *J. Clin. Pathol.* *36*, 829–834.
- Boman, H.G. (2003). Antibacterial peptides: basic facts and emerging concepts. *J. Intern. Med.* *254*, 197–215.
- Brathwaite, K.J., Siringan, P., Connerton, P.L., and Connerton, I.F. (2015). Host adaption to the

- bacteriophage carrier state of *Campylobacter jejuni*. *Res. Microbiol.* *166*, 504–515.
- Braun, V. (1975). Covalent lipoprotein from the outer membrane of *Escherichia coli*. *Biochim. Biophys. Acta - Rev. Biomembr.* *415*, 335–377.
- Brooks, T.M., Unterweger, D., Bachmann, V., Kostiuk, B., and Pukatzki, S. (2013). Lytic activity of the *Vibrio cholerae* type VI secretion toxin VgrG-3 is inhibited by the antitoxin TsaB. *J. Biol. Chem.* *288*, 7618–7625.
- Burnens, A., Stucki, U., Nicolet, J., and Frey, J. (1995). Identification and characterization of an immunogenic outer membrane protein of *Campylobacter jejuni*. *J. Clin. Microbiol.* *33*, 2826–2832.
- Burns, B.P., Hazell, S.L., and Mendz, G.L. (1995). Acetyl-CoA carboxylase activity in *Helicobacter pylori* and the requirement of increased CO₂ for growth. *Microbiology* *141*, 3113–3118.
- Butzler, J.P., Dekeyser, P., Detrain, M., and Dehaen, F. (1973). Related vibrio in stools. *J. Pediatr.* *82*, 493–495.
- Cameron, A., Frirdich, E., Huynh, S., Parker, C.T., and Gaynor, E.C. (2012). Hyperosmotic Stress Response of *Campylobacter jejuni*. *J. Bacteriol.* *194*, 6116–6130.
- Campbell, B.J., Engel, A.S., Porter, M.L., and Takai, K. (2006). The versatile ϵ -proteobacteria: key players in sulphidic habitats. *Nat. Rev. Microbiol.* *4*, 458–468.
- Campos, M. a, Vargas, M. a, Regueiro, V., Llompart, C.M., Albertí, S., and José, A. (2004). Capsule Polysaccharide Mediates Bacterial Resistance to Antimicrobial Peptides. *Infect. Immun.* *72*, 7107–7114.
- Carlsson, A., Engstrom, P., Palva, E.T., and Bennich, H. (1991). Attacin, an antibacterial protein from *Hyalophora cecropia*, inhibits synthesis of outer membrane proteins in *Escherichia coli* by interfering with *omp* gene transcription. *Infect. Immun.* *59*, 3040–3045.
- Chang, W.K., Wimley, W.C., Searson, P.C., Hristova, K., and Merzlyakov, M. (2008). Characterization of antimicrobial peptide activity by electrochemical impedance spectroscopy. *Biochim. Biophys. Acta* *1778*, 2430–2436.
- Chantarapanont, W., Berrang, M.E., and Frank, J.F. (2004). Direct microscopic observation of viability of *Campylobacter jejuni* on chicken skin treated with selected chemical sanitizing agents. *J. Food Prot.* *67*, 1146–1152.
- Chao, Y.P., Chern, J.T., and Wen, C.S. (2001). Coupling the T7 A1 promoter to the runaway-replication vector as an efficient method for stringent control and high-level expression of *lacZ*. *Biotechnol. Prog.* *17*, 203–207.
- Chen, F.-Y., Lee, M.-T., and Huang, H.W. (2003). Evidence for membrane thinning effect as the mechanism for peptide-induced pore formation. *Biophys. J.* *84*, 3751–3758.
- Chou, S., Bui, N.K., Russell, A.B., Lexa, K.W., Gardiner, T.E., Leroux, M., Vollmer, W., and Mougous, J.D. (2012). Report Structure of a Peptidoglycan Amidase Effector Targeted to Gram-Negative Bacteria by the Type VI Secretion System. *CellReports* *1*, 656–664.
- Clausell, A., Pujol, M., Alsina, M.A., and Cajal, Y. (2003). Influence of polymyxins on the structural dynamics of *Escherichia coli* lipid membranes. *Talanta* *60*, 225–234.
- Cullen, T.W., and Trent, M.S. (2010). A link between the assembly of flagella and lipooligosaccharide of the Gram-negative bacterium *Campylobacter jejuni*. *Proc. Natl. Acad. Sci. U. S. A.* *107*, 5160–5165.
- Dasti, J.I., Tareen, A.M., Lugert, R., Zautner, A.E., and Groß, U. (2010). *Campylobacter jejuni*: A brief overview on pathogenicity-associated factors and disease-mediating mechanisms. *Int. J. Med. Microbiol.* *300*, 205–211.
- Deaton, J., Savva, C.G., Sun, J., Holzenburg, A., Berry, J., and Young, R. (2004). Solubilization and delivery by GroEL of megadalton complexes of the lambda holin. *Protein Sci* *13*, 1778–1786.
- Diehl, M.A., and Chapman, J.S. (1999). Association of the biocide 5-chloro-2-methyl-isothiazol-3-one with *Pseudomonas aeruginosa* and *Pseudomonas fluorescens*. *Int. Biodeterior. Biodegrad.* *44*, 191–199.

- van Dijk, A., Veldhuizen, E.J.A., and Haagsman, H.P. (2008). Avian defensins. *Vet. Immunol. Immunopathol.* *124*, 1–18.
- Ding, J., Wang, W., Feng, H., Zhang, Y., and Wang, D.C. (2012). Structural insights into the *Pseudomonas aeruginosa* type VI virulence effector tse1 bacteriolysis and self-protection mechanisms. *J. Biol. Chem.* *287*, 26911–26920.
- Domingues, M.M., Inacio, R.G., Raimundo, J.M., Martins, M., Castanho, M.A.R.B., and Santos, N.C. (2012). Biophysical characterization of polymyxin B interaction with LPS aggregates and membrane model systems. *Biopolymers* *98*, 338–344.
- Dramsi, S., and Cossart, P. (1998). Intracellular Pathogens and the Actin Cytoskeleton. *Annu. Rev. Cell Dev. Biol.* *14*, 137–166.
- Dugar, G., Herbig, A., Förstner, K.U., Heidrich, N., Reinhardt, R., Nieselt, K., and Sharma, C.M. (2013). High-Resolution Transcriptome Maps Reveal Strain-Specific Regulatory Features of Multiple *Campylobacter jejuni* Isolates. *PLoS Genet.* *9*.
- Elliott, K.T., and DiRita, V.J. (2008). Characterization of CetA and CetB, a bipartite energy taxis system in *Campylobacter jejuni*. *Mol. Microbiol.* *69*, 1091–1103.
- English, G., Trunk, K., Rao, V.A., Srikannathasan, V., Hunter, W.N., and Coulthurst, S.J. (2012). New secreted toxins and immunity proteins encoded within the type VI secretion system gene cluster of *Serratia marcescens*. *Mol. Microbiol.* *86*, 921–936.
- Evans, S.J., and Sayers, A.R. (2000). A longitudinal study of campylobacter infection of broiler flocks in Great Britain. *Prev. Vet. Med.* *46*, 209–223.
- Fouts, D.E., Mongodin, E.F., Mandrell, R.E., Miller, W.G., Rasko, D.A., Ravel, J., Brinkac, L.M., Deboy, R.T., Parker, C.T., Daugherty, S.C., *et al.* (2005). Major structural differences and novel potential virulence mechanisms from the genomes of multiple campylobacter species. *PLoS Biol.* *3*.
- Fridrich, E., Biboy, J., Adams, C., Lee, J., Ellermeier, J., Giolda, L.D., DiRita, V.J., Girardin, S.E., Vollmer, W., and Gaynor, E.C. (2012). Peptidoglycan-modifying enzyme Pgp1 is required for helical cell shape and pathogenicity traits in campylobacter jejuni. *PLoS Pathog.* *8*.
- Fridrich, E., Vermeulen, J., Biboy, J., Soares, F., Taveirne, M.E., Johnson, J.G., DiRita, V.J., Girardin, S.E., Vollmer, W., and Gaynor, E.C. (2014). Peptidoglycan LD-carboxypeptidase Pgp2 influences *Campylobacter jejuni* helical cell shape and pathogenic properties and provides the substrate for the DL-carboxypeptidase Pgp1. *J. Biol. Chem.* *289*, 8007–8018.
- Fritsch, M.J., Trunk, K., Diniz, J.A., Guo, M., Trost, M., and Coulthurst, S.J. (2013). Proteomic Identification of Novel Secreted Antibacterial Toxins of the *Serratia marcescens* Type VI Secretion System. *Mol. Cell. Proteomics* *12*, 2735–2749.
- Gaasbeek, E.J., Wagenaar, J.A., Guilhabert, M.R., Van Putten, J.P.M., Parker, C.T., and Van Der Wal, F.J. (2010). Nucleases encoded by the integrated elements CJIE2 and CJIE4 inhibit natural transformation of *Campylobacter jejuni*. *J. Bacteriol.* *192*, 936–941.
- Gaynor, E.C., Cawthraw, S., Manning, G., MacKichan, J.K., Falkow, S., and Newell, D.G. (2004). The Genome-Sequenced Variant of *Campylobacter jejuni* NCTC 11168 and the Original Clonal Clinical Isolate Differ Markedly in Colonization, Gene Expression, and Virulence-Associated Phenotypes. *J. Bacteriol.* *186*, 503–517.
- Gérard, F., Brooks, M.A., Barreteau, H., Touzé, T., Graille, M., Bouhss, A., Blanot, D., Van Tilbeurgh, H., and Mengin-Lecreulx, D. (2011). X-ray structure and site-directed mutagenesis analysis of the *Escherichia coli* colicin M immunity protein. *J. Bacteriol.* *193*, 205–214.
- Gibson, D.G., Young, L., Chuang, R., Venter, J.C., Hutchison, C. a, Smith, H.O., Iii, C.A.H., and America, N. (2009). Enzymatic assembly of DNA molecules up to several hundred kilobases. *Nat. Methods* *6*, 343–345.
- Gilbert, M., Karwaski, M.F., Bernatchez, S., Young, N.M., Taboada, E., Michniewicz, J., Cunningham, A.M., and Wakarchuk, W.W. (2002). The genetic bases for the variation in the lipo-oligosaccharide of the mucosal pathogen, *Campylobacter jejuni*. Biosynthesis of sialylated ganglioside mimics in the core

- oligosaccharide. *J. Biol. Chem.* 277, 327–337.
- Gilbreath, J.J., Cody, W.L., Merrell, D.S., and Hendrixson, D.R. (2011). Change is good: variations in common biological mechanisms in the epsilonproteobacterial genera *Campylobacter* and *Helicobacter*. *Microbiol. Mol. Biol. Rev.* 75, 84–132.
- Glauner, B. (1988). Separation and quantification of mucopeptides with high-performance liquid chromatography. *Anal. Biochem.* 172, 451–464.
- Golden, N.J., and Acheson, D.W.K. (2002). Identification of motility and autoagglutination *Campylobacter jejuni* mutants by random transposon mutagenesis. *Infect. Immun.* 70, 1761–1771.
- Goodell, E.W. (1985). Recycling of murein by *Escherichia coli*. *J. Bacteriol.* 163, 305–310.
- Goodhead, I., and Darby, A.C. (2015). Taking the pseudo out of pseudogenes. *Curr. Opin. Microbiol.* 23, 102–109.
- Grant, C.C.R., Konkel, M.E., Cieplak, W., and Tompkins, L.S. (1993). Role of flagella in adherence, internalization, and translocation of *Campylobacter jejuni* in nonpolarized and polarized epithelial cell cultures. *Infect. Immun.* 61, 1764–1771.
- Gresock, M.G., Savenkova, M.I., Larsen, R.A., Ollis, A.A., and Postle, K. (2011). Death of the tonB shuttle hypothesis. *Front. Microbiol.* 2, 1–8.
- Groisman, E. a, and Mouslim, C. (2006). Sensing by bacterial regulatory systems in host and non-host environments. *Nat. Rev. Microbiol.* 4, 705–709.
- Gruenheid, S., and Le Moual, H. (2012). Resistance to antimicrobial peptides in Gram-negative bacteria. *FEMS Microbiol. Lett.* 330, 81–89.
- Gubbels, M., Vaishnav, S., Boot, N., Dubremetz, J., and Striepen, B. (2006). A MORN-repeat protein is a dynamic component of the *Toxoplasma gondii* cell division apparatus. *J. Cell Sci.* 119, 2236–2245.
- Guerry, P., Alm, R.A., Power, M.E., Logan, S.M., and Trust, T.J. (1991). Role of Two Flagellin Genes in *Campylobacter* Motility. 173, 4757–4764.
- Guinane, C.M., Cotter, P.D., Hill, C., and Ross, R.P. (2005). Microbial solutions to microbial problems; lactococcal bacteriocins for the control of undesirable biota in food. *J. Appl. Microbiol.* 98, 1316–1325.
- Gundogdu, O., Bentley, S.D., Holden, M.T., Parkhill, J., Dorrell, N., and Wren, B.W. (2007). NCTC11168 genome sequence. 8, 1–8.
- Gundogdu, O., Mills, D.C., Elmi, A., Martin, M.J., Wren, B.W., and Dorrell, N. (2011). The *Campylobacter jejuni* transcriptional regulator Cj1556 plays a role in the oxidative and aerobic stress response and is important for bacterial survival in vivo. *J. Bacteriol.* 193, 4238–4249.
- Gundogdu, O., da Silva, D.T., Mohammad, B., Elmi, A., Mills, D.C., Wren, B.W., and Dorrell, N. (2015). The *Campylobacter jejuni* MarR-like transcriptional regulators RrpA and RrpB both influence bacterial responses to oxidative and aerobic stresses. *Front. Microbiol.* 6, 1–12.
- Guo, L., Lim, K.B., Poduje, C.M., Daniel, M., Gunn, J.S., Hackett, M., and Miller, S.I. (1998). Lipid A acylation and bacterial resistance against vertebrate antimicrobial peptides. *Cell* 95, 189–198.
- Ha, R., Frirdich, E., Sychantha, D., Biboy, J., Taveirne, M.E., Johnson, J.G., DiRita, V.J., Vollmer, W., Clarke, A.J., and Gaynor, E.C. (2016). Accumulation of Peptidoglycan O-Acetylation Leads to Altered Cell Wall Biochemistry and Negatively Impacts Pathogenesis Factors of *Campylobacter jejuni*. *J. Biol. Chem.* jbc.M116.746404.
- Habicht, J., Woehle, C., and Gould, S.B. (2015). *Tetrahymena* expresses more than a hundred proteins with lipid-binding MORN motifs that can differ in their subcellular localisations. *J. Eukaryot. Microbiol.* 62, 694–700.
- Hanahan, D. (1983). Studies on transformation of *Escherichia coli* with plasmids. *J. Mol. Biol.* 166, 557–580.
- Hancock, R.E.W. (1997). Peptide antibiotics. *Lancet* 349, 418–422.

- Hancock, R.E.W., and Sahl, H.G. (2006). Antimicrobial and host-defense peptides as new anti-infective therapeutic strategies. *Nat. Biotechnol.* *24*, 1551–1557.
- Heilborn, J.D., Frohm Nilsson, M., Kratz, G., Weber, G., Sørensen, O., Borregaard, N., and Ståhle-Bäckdahl, M. (2003). The cathelicidin anti-microbial peptide LL-37 is involved in re-epithelialization of human skin wounds and is lacking in chronic ulcer epithelium. *J. Invest. Dermatol.* *120*, 379–389.
- Heipieper, H.J., and De Bont, J.A.M. (1994). Adaptation of *Pseudomonas putida* S12 to ethanol and toluene at the level of fatty acid composition of membranes. *Appl. Environ. Microbiol.* *60*, 4440–4444.
- Hendrixson, D.R., and DiRita, V.J. (2004). Identification of *Campylobacter jejuni* genes involved in commensal colonization of the chick gastrointestinal tract. *Mol. Microbiol.* *52*, 471–484.
- Hermans, D., Van Deun, K., Martel, A., Van Immerseel, F., Messens, W., Heyndrickx, M., Haesebrouck, F., and Pasmans, F. (2011). Colonization factors of *Campylobacter jejuni* in the chicken gut. *Vet. Res.* *42*, 82.
- Heywood, W., Henderson, B., and Nair, S.P. (2005). Cytolethal distending toxin: Creating a gap in the cell cycle. *J. Med. Microbiol.* *54*, 207–216.
- Hitchcock, A. (2011). The role of the twin arginine translocase in the assembly and function of electron transport chains in *Campylobacter jejuni*.
- Ho, B.T., Dong, T.G., and Mekalanos, J.J. (2014). A View to a Kill: The Bacterial Type VI Secretion System. *Cell Host Microbe* *15*, 9–21.
- Hofreuter, D., Tsai, J., Watson, R.O., Novik, V., Altman, B., Benitez, M., Clark, C., Perbost, C., Jarvie, T., Du, L., *et al.* (2006). Unique features of a highly pathogenic *Campylobacter jejuni* strain. *Infect. Immun.* *74*, 4694–4707.
- Huffman, J.L., and Brennan, R.G. (2002). Prokaryotic transcription regulators: More than just the helix-turn-helix motif. *Curr. Opin. Struct. Biol.* *12*, 98–106.
- Hugdahl, M.B., Beery, J.T., and Doyle, M.P. (1988). Chemotactic behavior of *Campylobacter jejuni*. *Infect. Immun.* *56*, 1560–1566.
- Hughes, N.J., Chalk, P.A., Clayton, C.L., Kelly, D.J., and Acteriol, J.B. (1995). Identification of Carboxylation Enzymes and Characterization of a Novel Four-Subunit Pyruvate : Flavodoxin Oxidoreductase from *Helicobacter pylori*. *J. Biol. Chem.* *270*, 3953–3959.
- Jacobs, C., Huang, L.J., Bartowsky, E., Normark, S., and Park, J.T. (1994). Bacterial cell wall recycling provides cytosolic muropeptides as effectors for beta-lactamase induction. *EMBO J.* *13*, 4684–4694.
- Jagannathan, A., Constantinidou, C., and Penn, C.W. (2001). Roles of *rpoN*, *fliA*, and *flgR* in expression of flagella in *Campylobacter jejuni*. *J. Bacteriol.* *183*, 2937–2942.
- Jenko, S., Dolenc, I., Gunčar, G., Doberšek, A., Podobnik, M., and Turk, D. (2003). Crystal structure of stefin A in complex with cathepsin H: N-terminal residues of inhibitors can adapt to the active sites of endo- and exopeptidases. *J. Mol. Biol.* *326*, 875–885.
- Jeon, B., Muraoka, W., Scupham, A., and Zhang, Q. (2009). Roles of lipooligosaccharide and capsular polysaccharide in antimicrobial resistance and natural transformation of *Campylobacter jejuni*. *J. Antimicrob. Chemother.* *63*, 462–468.
- Jin, S., Joe, A., Lynett, J., Hani, E.K., Sherman, P., and Chan, V.L. (2001). JlpA, a novel surface-exposed lipoprotein specific to *Campylobacter jejuni*, mediates adherence to host epithelial cells. *Mol. Microbiol.* *39*, 1225–1236.
- Jones, F.S., Orcutt, M., and Little, R.B. (1931). Vibrios (*Vibrio jejuni*, n. sp.) associated with intestinal disorders of cows and calves. *J. Exp. Med.* *53*, 853–864.
- Joslin, S.N., and Hendrixson, D.R. (2009). Activation of the *Campylobacter jejuni* FlgSR two-component system is linked to the flagellar export apparatus. *J. Bacteriol.* *191*, 2656–2667.
- Karlyshev, A. V., Linton, D., Gregson, N.A., and Wren, B.W. (2002). A novel paralogous gene family involved in phase-variable flagella-mediated motility in *Campylobacter jejuni*. *Microbiology* *148*, 473–480.

- Karlyshev, A. V., Everest, P., Linton, D., Cawthraw, S., Newell, D.G., and Wren, B.W. (2004). The *Campylobacter jejuni* general glycosylation system is important for attachment to human epithelial cells and in the colonization of chicks. *Microbiology* *150*, 1957–1964.
- Kendall, J.J., Barrero-Tobon, A.M., Hendrixson, D.R., and Kelly, D.J. (2014). Hemerythrins in the microaerophilic bacterium *Campylobacter jejuni* help protect key iron-sulphur cluster enzymes from oxidative damage. *Environ. Microbiol.* *16*, 1105–1121.
- Key, S., Technology, M., and Sciences, L. (2012). Structural insight into how *Pseudomonas aeruginosa* peptidoglycan- hydrolase Tse1 and its immunity protein Tsi1 function. *211*, 201–211.
- Kim, H.S., Kim, J., Im, H.N., An, D.R., Lee, M., Heseck, D., Mobashery, S., Kim, J.Y., Cho, K., Yoon, H.J., *et al.* (2014). Structural basis for the recognition of muramyltripeptide by *Helicobacter pylori* Csd4, a d,l-carboxypeptidase controlling the helical cell shape. *Acta Crystallogr. Sect. D Biol. Crystallogr.* *70*, 2800–2812.
- Kim, M.J., Yamamoto, D., Matsumoto, K., Inoue, M., Ishida, T., Mizuno, H., Sumiya, S., and Kitamura, K. (1992). Crystal structure of papain-E64-c complex. Binding diversity of E64-c to papain S2 and S3 subsites. *Biochem. J.* *287*, 797–803.
- Kim, S.Y., Park, S.Y., Choi, S.K., and Park, S.H. (2015). Biosynthesis of polymyxins B, E, and P using genetically engineered polymyxin synthetases in the surrogate Host *Bacillus subtilis*. *J. Microbiol. Biotechnol.* *25*, 1015–1025.
- King, E.O. (1957). Human infections with vibrio fetus and a closely related vibrio. *J. Infect. Dis.* *101*, 119–128.
- King, E.O. (1962). The laboratory recognition of *Vibrio fetus* and a closely related *Vibrio* isolated from cases of human vibriosis. *Ann. N. Y. Acad. Sci.* *98*, 700–711.
- Konkel, M.E., Mead, D.J., and Cieplak, W. (1996). Cloning, sequencing, and expression of a gene from *Campylobacter jejuni* encoding a protein (Omp18) with similarity to peptidoglycan-associated lipoproteins. *Infect. Immun.* *64*, 1850–1853.
- Konkel, M.E., Garvis, S.G., Tipton, S.L., Anderson Jr., D.E., and Cieplak Jr., W. (1997). Identification and molecular cloning of a gene encoding a fibronectin-binding protein (CadF) from *Campylobacter jejuni*. *Mol. Microbiol.* *24*, 953–963.
- Konkel, M.E., Klena, J.D., Rivera-Amill, V., Monteville, M.R., Biswas, D., Raphael, B., and Mickelson, J. (2004). Secretion of virulence proteins from *Campylobacter jejuni* is dependent on a functional flagellar export apparatus. *J. Bacteriol.* *186*, 3296–3303.
- Kordiš, D., Turk, V., Barrett, A., Rawlings, N., Davies, M., Machleidt, W., Salvesen, G., Turk, V., Alvarez-Fernandez, M., Barrett, A., *et al.* (2009). Phylogenomic analysis of the cystatin superfamily in eukaryotes and prokaryotes. *BMC Evol. Biol.* *9*, 266.
- Kowarik, M., Numao, S., Feldman, M.F., Schulz, B.L., Callewaert, N., Kiermaier, E., Catrein, I., and Aebi, M. (2006). N-linked glycosylation of folded proteins by the bacterial oligosaccharyltransferase. *Science* *314*, 1148–1150.
- Kröger, A., Biel, S., Simon, J., Gross, R., Unden, G., and Lancaster, C.R.D. (2002). Fumarate respiration of *Wolinella succinogenes*: Enzymology, energetics and coupling mechanism. *Biochim. Biophys. Acta - Bioenerg.* *1553*, 23–38.
- Kusters, J.G., Van Vliet, A.H.M., and Kuipers, E.J. (2006). Pathogenesis of *Helicobacter pylori* infection. *Clin. Microbiol. Rev.* *19*, 449–490.
- Lara-Tejero, M., and Galán, J.E. (2001). CdtA , CdtB , and CdtC Form a Tripartite Complex That Is Required for Cytolethal Distending Toxin Activity CdtA , CdtB , and CdtC Form a Tripartite Complex That Is Required for Cytolethal Distending Toxin Activity. *Infect. Immun.* *69*, 4358–4365.
- Lee, H.S., Park, C.B., Kim, J.M., Jang, S.A., Park, I.Y., Kim, M.S., Cho, J.H., and Kim, S.C. (2008). Mechanism of anticancer activity of buforin IIb, a histone H2A-derived peptide. *Cancer Lett.* *271*, 47–55.
- Lerat, E., and Ochman, H. (2005). Recognizing the pseudogenes in bacterial genomes. *Nucleic Acids Res.*

33, 3125–3132.

Lertpiriyapong, K., Gamazon, E.R., Feng, Y., Park, D.S., Pang, J., Botka, G., Graffam, M.E., Ge, Z., and Fox, J.G. (2012). *Campylobacter jejuni* type VI secretion system: Roles in adaptation to deoxycholic acid, host cell adherence, invasion, and in vivo colonization. *PLoS One* 7.

Levy, A.J. (1946). A gastro-enteritis outbreak probably due to a bovine strain of vibrio. *Yale J. Biol. Med.* 18, 243–258.

Lin, J., Wang, Y., and Hoang, K. Van (2009). Systematic identification of genetic loci required for polymyxin resistance in *Campylobacter jejuni* using an efficient in vivo transposon mutagenesis system. *Foodborne Pathog. Dis.* 6, 173–185.

Line, J.E., Hiett, K.L., Guard-Bouldin, J., and Seal, B.S. (2010). Differential carbon source utilization by *Campylobacter jejuni* 11168 in response to growth temperature variation. *J. Microbiol. Methods* 80, 198–202.

Llobet, E., Tomás, J.M., and Bengoechea, J.A. (2008). Capsule polysaccharide is a bacterial decoy for antimicrobial peptides. *Microbiology* 154, 3877–3886.

Llobet, E., Campos, M.A., Giménez, P., Moranta, D., and Bengoechea, J.A. (2011). Analysis of the networks controlling the antimicrobial-peptide-dependent induction of *Klebsiella pneumoniae* virulence factors. *Infect. Immun.* 79, 3718–3732.

Logan, S.M., and Trust, T.J. (1982). Outer membrane characteristics of *Campylobacter jejuni*. *Infect. Immun.* 38, 898–906.

Lu, M., and Henning, U. (1989). The immunity (imm) gene of *Escherichia coli* bacteriophage T4. *J. Virol.* 63, 3472–3478.

Ludtke, S.J., He, K., Heller, W.T., Harroun, T.A., Yang, L., and Huang, H.W. (1996). Membrane pores induced by magainin. *Biochemistry* 35, 13723–13728.

Manning, G., Duim, B., Wassenaar, T., Wagenaar, J.A., Ridley, A., and Newell, D.G. (2001). Evidence for a Genetically Stable Strain of *Campylobacter jejuni*. *Appl. Environ. Microbiol.* 67, 1185–1189.

Marchant, J., Wren, B., and Ketley, J. (2002). Exploiting genome sequence: Predictions for mechanisms of *Campylobacter* chemotaxis. *Trends Microbiol.* 10, 155–159.

Marshall, B., Warren, J.R., Blincow, E., Phillips, M., Goodwin, C.S., Murray, R., Blackbourn, S., Waters, T., and Sanderson, C. (1988). PROSPECTIVE DOUBLE-BLIND TRIAL OF DUODENAL ULCER RELAPSE AFTER ERADICATION OF *CAMPYLOBACTER PYLORI*. *Lancet* 332, 1437–1442.

Matsuzaki, K. (1999). Why and how are peptide-lipid interactions utilized for self-defense? Magainins and tachyplesins as archetypes. *Biochim. Biophys. Acta - Biomembr.* 1462, 1–10.

McGuire, A.M., Cochrane, K., Griggs, A.D., Haas, B.J., Abeel, T., Zeng, Q., Nice, J.B., Macdonald, H., Birren, B.W., Berger, B.W., *et al.* (2014). Evolution of invasion in a diverse set of *Fusobacterium* species. *MBio* 5, e01864.

McNally, D.J., Hui, J.P.M., Aubry, A.J., Mui, K.K.K., Guerry, P., Brisson, J.R., Logan, S.M., and Soo, E.C. (2006). Functional characterization of the flagellar glycosylation locus in *Campylobacter jejuni* 81-176 using a focused metabolomics approach. *J. Biol. Chem.* 281, 18489–18498.

Meinersmann, R.J., Patton, C.M., Evins, G.M., Wachsmuth, I.K., and Fields, P.I. (2002). Genetic diversity and relationships of *Campylobacter* species and subspecies. *Int. J. Syst. Evol. Microbiol.* 52, 1789–1797.

Moskowitz, S.M., Ernst, R.K., and Miller, S.I. (2004). PmrAB, a Two-Component Regulatory System of *Pseudomonas aeruginosa* that Modulates Resistance to Cationic Antimicrobial Peptides and Addition of Aminoarabinose to Lipid A. *J. Bacteriol.* 186, 575–579.

Mougous, J.D., Cuff, M.E., Raunser, S., Shen, A., Zhou, M., Gifford, C.A., Goodman, A.L., Joachimiak, G., Ordoñez, C.L., Lory, S., *et al.* (2006). A virulence locus of *Pseudomonas aeruginosa* encodes a protein secretion apparatus. *Science* 312, 1526–1530.

Van Mourik, A., Steeghs, L., Van Laar, J., Meiring, H.D., Hamstra, H.J., Van Putten, J.P.M., and Wösten,

- M.M.S.M. (2010). Altered linkage of hydroxyacyl chains in lipid a of *Campylobacter jejuni* reduces TLR4 activation and antimicrobial resistance. *J. Biol. Chem.* *285*, 15828–15836.
- Mukhopadhyaya, C.S., Kumar, R., and Brahc, G.S. (2010). Gallinacin and Fowlicidin : Two Promising Antimicrobial Peptides in Chickens — A Review. *Vet. World* *3*, 297–300.
- Müllner, P., Collins-Emerson, J.M., Midwinter, A.C., Carter, P., Spencer, S.E.F., Van Der Logt, P., Hathaway, S., and French, N.P. (2010). Molecular epidemiology of *campylobacter jejuni* in a geographically isolated country with a uniquely structured poultry industry. *Appl. Environ. Microbiol.* *76*, 2145–2154.
- Murdoch, S.L., Trunk, K., English, G., Fritsch, M.J., Pourkarimi, E., and Coulthurst, S.J. (2011). The opportunistic pathogen *Serratia marcescens* utilizes type VI secretion to target bacterial competitors. *J. Bacteriol.* *193*, 6057–6069.
- Naikare, H., Palyada, K., Panciera, R., Marlow, D., and Stintzi, A. (2006). Major role for FeoB in *Campylobacter jejuni* ferrous iron acquisition, gut colonization, and intracellular survival. *Infect. Immun.* *74*, 5433–5444.
- Naikare, H., Butcher, J., Flint, A., Xu, J., Raymond, K.N., and Stintzi, A. (2013). *Campylobacter jejuni* ferric-enterobactin receptor CfrA is TonB3 dependent and mediates iron acquisition from structurally different catechol siderophores. *Metallomics* *5*, 988–996.
- Naito, M., Frirdich, E., Fields, J.A., Pryjma, M., Li, J., Cameron, A., Gilbert, M., Thompson, S.A., and Gaynor, E.C. (2010). Effects of sequential *Campylobacter jejuni* 81-176 lipooligosaccharide core truncations on biofilm formation, stress survival, and pathogenesis. *J. Bacteriol.* *192*, 2182–2192.
- Nakagawa, S., and Takai, K. (2008). Deep-sea vent chemoautotrophs: Diversity, biochemistry and ecological significance. *FEMS Microbiol. Ecol.* *65*, 1–14.
- Nakagawa, S., Takaki, Y., Shimamura, S., Reysenbach, A., Takai, K., and Horikoshi, K. (2007). Deep-sea vent epsilon-proteobacterial genomes provide insights into emergence of pathogens. *Proc. Natl. Acad. Sci. U. S. A.* *104*, 12146–12150.
- Neely, M.N., and Friedman, D.I. (1998). Functional and genetic analysis of regulatory regions of coliphage H- 19B: Location of shiga-like toxin and lysis genes suggest a role for phage functions in toxin release. *Mol. Microbiol.* *28*, 1255–1267.
- Niesen, F.H., Berglund, H., and Vedadi, M. (2007). The use of differential scanning fluorimetry to detect ligand interactions that promote protein stability. *Nat. Protoc.* *2*, 2212–2221.
- Niyonsaba, F., Iwabuchi, K., Someya, A., Hirata, M., Matsuda, H., Ogawa, H., and Nagaoka, I. (2002). A cathelicidin family of human antibacterial peptide LL-37 induces mast cell chemotaxis. *Immunology* *106*, 20–26.
- Nothaft, H., and Szymanski, C.M. (2010). Protein glycosylation in bacteria: sweeter than ever. *Nat. Rev. Microbiol.* *8*, 765–778.
- Oelschlaeger, T.A., Guerry, P., and Kopecko, D.J. (1993). Unusual microtubule-dependent endocytosis mechanisms triggered by *Campylobacter jejuni* and *Citrobacter freundii*. *Proc. Natl. Acad. Sci. U. S. A.* *90*, 6884–6888.
- Okoli, A.S., Wadstrom, T., and Mendz, G.L. (2007). MiniReview: Bioinformatic study of bile responses in *Campylobacterales*. *FEMS Immunol. Med. Microbiol.* *49*, 101–123.
- Olson, J.W., and Maier, R.J. (2002). Molecular hydrogen as an energy source for *Helicobacter pylori*. *Science* *298*, 1788–1790.
- Otto, M. (2009). Bacterial sensing of antimicrobial peptides. *Contrib. Microbiol.* *16*, 136–149.
- Palyada, K., Sun, Y., Flint, A., Butcher, J., Naikare, H., and Stintzi, A. (2009). Characterization of the oxidative stress stimulon and PerR regulon of *Campylobacter jejuni*. *BMC Genomics* *10*, 481.
- Parisien, A., Allain, B., Zhang, J., Mandeville, R., and Lan, C.Q. (2008). Novel alternatives to antibiotics: Bacteriophages, bacterial cell wall hydrolases, and antimicrobial peptides. *J. Appl. Microbiol.* *104*, 1–13.

- Park, J.T., and Uehara, T. (2008). How Bacteria Consume Their Own Exoskeletons (Turnover and Recycling of Cell Wall Peptidoglycan). *Microbiol. Mol. Biol. Rev.* **72**, 211–227.
- Park, C.B., Kim, H.S., and Kim, S.C. (1998). Mechanism of action of the antimicrobial peptide buforin II: buforin II kills microorganisms by penetrating the cell membrane and inhibiting cellular functions. *Biochem. Biophys. Res. Commun.* **244**, 253–257.
- Parkhill, J., Wren, B.W., Mungall, K., Ketley, J.M., Churcher, C., Basham, D., Chillingworth, T., Davies, R.M., Feltwell, T., Holroyd, S., *et al.* (2000). The genome sequence of the food-borne pathogen *Campylobacter jejuni* reveals hypervariable sequences. *Nature* **403**, 665–668.
- Parra-Lopez, C., Baer, M.T., and Groisman, E.A. (1993). Molecular genetic analysis of a locus required for resistance to antimicrobial peptides in *Salmonella typhimurium*. *EMBO J.* **12**, 4053–4062.
- Pasupuleti, M., Schmidtchen, A., and Malmsten, M. (2012). Antimicrobial peptides: key components of the innate immune system. *Crit. Rev. Biotechnol.* **32**, 143–171.
- Paulus, H., and Gray, E. (1964). The Biosynthesis of Polymyxin B by Growing Cultures of *Bacillus Polymyxa*. *J. Biol. Chem.* **239**, 865–871.
- Pearson, B.M., Gaskin, D.J.H., Segers, R.P.A.M., Wells, J.M., Nuijten, P.J.M., and Van Vliet, A.H.M. (2007). The complete genome sequence of *Campylobacter jejuni* strain 81116 (NCTC11828). *J. Bacteriol.* **189**, 8402–8403.
- Peleteiro, B., Bastos, A., Ferro, A., and Lunet, N. (2014). Prevalence of *Helicobacter pylori* infection worldwide: A systematic review of studies with national coverage. *Dig. Dis. Sci.* **59**, 1698–1709.
- Pennie, R.A., Pearson, R.D., Barrett, L.J., Lior, H., and Guerrant, R.L. (1986). Susceptibility of *Campylobacter jejuni* to strain-specific bactericidal activity in sera of infected patients. *Infect. Immun.* **52**, 702–706.
- Petersen, L., Larsen, T.S., Ussery, D.W., On, S.L.W., and Krogh, A. (2003). Rpo D promoters in *Campylobacter jejuni* exhibit a strong periodic signal instead of a -35 box. *J. Mol. Biol.* **326**, 1361–1372.
- Pinho, M.G., Kjos, M., and Veening, J. (2013). How to get (a)round: mechanisms controlling growth and division of coccoid bacteria. *Nat. Rev. Microbiol.* **11**, 601–614.
- Polgár, L. (1973). On the mode of activation of the catalytically essential sulfhydryl group of papain. *Eur. J. Biochem.* **33**, 104–109.
- Prehna, G., Zhang, G., Gong, X., Duszyk, M., Okon, M., McIntosh, L.P., Weiner, J.H., and Strynadka, N.C.J. (2012). A protein export pathway involving *Escherichia coli* porins. *Structure* **20**, 1154–1166.
- Prost, L.R., Daley, M.E., Le Sage, V., Bader, M.W., Le Moual, H., Klevit, R.E., and Miller, S.I. (2007). Activation of the Bacterial Sensor Kinase PhoQ by Acidic pH. *Mol. Cell* **26**, 165–174.
- Pukatzki, S., Ma, A.T., Sturtevant, D., Krastins, B., Sarracino, D., Nelson, W.C., Heidelberg, J.F., and Mekalanos, J.J. (2006). Identification of a conserved bacterial protein secretion system in *Vibrio cholerae* using the *Dictyostelium* host model system. *Proc. Natl. Acad. Sci.* **103**, 1528–1533.
- Pukatzki, S., Ma, A.T., Revel, A.T., Sturtevant, D., and Mekalanos, J.J. (2007). Type VI secretion system translocates a phage tail spike-like protein into target cells where it cross-links actin. *Proc. Natl. Acad. Sci. U. S. A.* **104**, 15508–15513.
- Reddy, B.L., and Saier, M.H. (2013). Topological and phylogenetic analyses of bacterial holin families and superfamilies. *Biochim. Biophys. Acta - Biomembr.* **1828**, 2654–2671.
- Reid, A.N., Pandey, R., Palyada, K., Naikare, H., and Stintzi, A. (2008). Identification of *Campylobacter jejuni* genes involved in the response to acidic pH and stomach transit. *Appl. Environ. Microbiol.* **74**, 1583–1597.
- Rigden, D.J., Mosolov, V. V., and Galperin, M.Y. (2002). Sequence conservation in the chagasin family suggests a common trend in cysteine proteinase binding by unrelated protein inhibitors. *Protein Sci.* **11**, 1971–1977.
- Rivera-Amill, V., Kim, B.J., Seshu, J., and Konkol, M.E. (2001). Secretion of the Virulence-Associated

- Campylobacter Invasion Antigens from Campylobacter jejuni Requires a Stimulatory Signal. *J. Infect. Dis.* **183**, 1607–1616.
- Robinson, D.A. (1981). Infective dose of Campylobacter jejuni in milk. *Br. Med. J.* **282**, 1584.
- Romling, U., Galperin, M.Y., and Gomelsky, M. (2013). Cyclic di-GMP: the first 25 years of a universal bacterial second messenger. *Microbiol. Mol. Biol. Rev.* **77**, 1–52.
- Rosado, C.J., Kondos, S., Bull, T.E., Kuiper, M.J., Law, R.H.P., Buckle, A.M., Voskoboinik, I., Bird, P.I., Trapani, J.A., Whisstock, J.C., *et al.* (2008). The MACPF/CDC family of pore-forming toxins. *Cell. Microbiol.* **10**, 1765–1774.
- Russell, A.B., Hood, R.D., Bui, N.K., LeRoux, M., Vollmer, W., and Mougous, J.D. (2011). Type VI secretion delivers bacteriolytic effectors to target cells. *Nature* **475**, 343–347.
- Russell, A.B., Peterson, S.B., and Mougous, J.D. (2014). Type VI secretion system effectors: poisons with a purpose. *Nat. Rev. Microbiol.* **12**, 137–148.
- Sařamaszyńska-Guz, A., and Klimuszko, D. (2008). Functional analysis of the Campylobacter jejuni cj0183 and cj0588 genes. *Curr. Microbiol.* **56**, 592–596.
- Salzman, N.H., Chou, M.M., De Jong, H., Liu, L., Porter, E.M., and Paterson, Y. (2003). Enteric Salmonella infection inhibits paneth cell antimicrobial peptide expression. *Infect. Immun.* **71**, 1109–1115.
- Sambrook, J., Fritsch, E.F., and Maniatis, T. (1989). *Molecular Cloning: A Laboratory Manual* (Akademie-Verlag).
- Sanz-Gaitero, M., Keary, R., Garcia-Doval, C., Coffey, A., and van Raaij, M.J. (2014). Crystal structure of the lytic CHAP(K) domain of the endolysin LysK from Staphylococcus aureus bacteriophage K. *Virology* **11**, 133.
- Savva, C.G., Dewey, J.S., Moussa, S.H., To, K.H., Holzenburg, A., and Young, R. (2014). Stable micron-scale holes are a general feature of canonical holins. *Mol. Microbiol.* **91**, 57–65.
- Schell, M.A., Ulrich, R.L., Ribot, W.J., Brueggemann, E.E., Hines, H.B., Chen, D., Lipscomb, L., Kim, H.S., Mrázek, J., Nierman, W.C., *et al.* (2007). Type VI secretion is a major virulence determinant in Burkholderia mallei. *Mol. Microbiol.* **64**, 1466–1485.
- Schmidtchen, A., Frick, I.M., Andersson, E., Tapper, H., and Björck, L. (2002). Proteinases of common pathogenic bacteria degrade and inactivate the antibacterial peptide LL-37. *Mol. Microbiol.* **46**, 157–168.
- Schroeder, B.O., Wu, Z., Nuding, S., Groscurth, S., Marcinowski, M., Beisner, J., Buchner, J., Schaller, M., Stange, E.F., and Wehkamp, J. (2011). Reduction of disulphide bonds unmasks potent antimicrobial activity of human β -defensin 1. *Nature* **469**, 419–423.
- Sebald, M., and Veron, M. (1963). Teneur en Bases de l'ADN et Classification des Vibrions. *Ann. l'Institut Pasteur* **105**, 897–910.
- Sellars, M.J., Hall, S.J., and Kelly, D.J. (2002). Growth of Campylobacter jejuni supported by respiration of fumarate, nitrate, nitrite, trimethylamine-N-oxide, or dimethyl sulfoxide requires oxygen. *J. Bacteriol.* **184**, 4187–4196.
- Semchenko, E.A., Day, C.J., Wilson, J.C., Grice, I.D., Moran, A.P., and Korolik, V. (2010). Temperature-dependent phenotypic variation of Campylobacter jejuni lipooligosaccharides. *BMC Microbiol.* **10**, 305.
- Shafer, W.M., Qu, X., Waring, a J., and Lehrer, R.I. (1998). Modulation of Neisseria gonorrhoeae susceptibility to vertebrate antibacterial peptides due to a member of the resistance/nodulation/division efflux pump family. *Proc. Natl. Acad. Sci. U. S. A.* **95**, 1829–1833.
- Shen, Z., Patil, R.D., Sahin, O., Wu, Z., Pu, X., Dai, L., Plummer, P.J., Yaeger, M.J., and Zhang, Q. (2016). Identification and functional analysis of two toxin-antitoxin systems in Campylobacter jejuni. *Mol. Microbiol.* **101**, 909–923.
- Sheppard, S.K., Colles, F., Richardson, J., Cody, A.J., Elson, R., Lawson, A., Brick, G., Meldrum, R., Little, C.L., Owen, R.J., *et al.* (2010). Host association of campylobacter genotypes transcends geographic variations. *Appl. Environ. Microbiol.* **76**, 5269–5277.

- Shimada, H., Koizumi, M., Kuroki, K., Mochizuki, M., Fujimoto, H., Ohta, H., Masuda, T., and Takamiya, K. (2004). ARC3, a chloroplast division factor, is a chimera of prokaryotic FtsZ and part of eukaryotic phosphatidylinositol-4-phosphate 5-kinase. *Plant Cell Physiol.* *45*, 960–967.
- Simons, R.W., Hoopes, B.C., McClure, W.F.L., and Kleckner, N. (1983). Three Promoters near the *l* & mini PIN, POUT, and pill of ISIO: *Cell* *34*, 673–682.
- Skirrow, M.B. (1977). Campylobacter enteritis: a 'new' disease. *Br. Med. J.* *2*, 9–11.
- Skirrow, M.B. (1982). Campylobacter enteritis - the first five years. *J. Hyg. (Lond).* *89*, 175–184.
- Smith, T. (1918). SPIRILLA ASSOCIATED WITH DISEASE OF THE FETAL MEMBRANES IN CATTLE (INFECTIOUS ABORTION). *J. Exp. Med.* *28*, 701–719.
- Smith, K.S., and Ferry, J.G. (2000). Prokaryotic carbonic anhydrases. *FEMS Microbiol. Rev.* *24*, 335–366.
- Spratt, B.G., and Cromie, K.D. (1988). Penicillin-binding proteins of gram-negative bacteria. *Rev Infect Dis* *10*, 699–711.
- Srikannathasan, V., English, G., Bui, N.K., Trunk, K., O'Rourke, P.E.F., Rao, V.A., Vollmer, W., Coulthurst, S.J., and Hunter, W.N. (2013). Structural basis for type VI secreted peptidoglycan di-endopeptidase function, specificity and neutralization in *Serratia marcescens*. *Acta Crystallogr. Sect. D Biol. Crystallogr.* *69*, 2468–2482.
- Stintzi, A. (2002). Gene Expression Profile of Campylobacter jejuni in Response to Growth Temperature Variation. *J. Bacteriol.* *185*, 2009–2016.
- Storz, G., and Imlay, J.A. (1999). Oxidative stress. *Curr. Opin. Microbiol.* *2*, 188–194.
- Szymanski, C.M., King, M., Haardt, M., and Armstrong, G.D. (1995). Campylobacter-Jejuni Motility and Invasion of Caco-2 Cells. *Infect. Immun.* *63*, 4295–4300.
- Szymanski, C.M., Yao, R., Ewing, C.P., Trust, T.J., and Guerry, P. (1999). Evidence for a system of general protein glycosylation in Campylobacter jejuni. *Mol. Microbiol.* *32*, 1022–1030.
- Takai, K., Inagaki, F., Nakagawa, S., Hirayama, H., Nunoura, T., Sako, Y., Nealson, K.H., and Horikoshi, K. (2003). Isolation and phylogenetic diversity of members of previously uncultivated epsilon-Proteobacteria in deep-sea hydrothermal fields. *FEMS Microbiol. Lett.* *218*, 167–174.
- Takeshima, H., Komazaki, S., Nishi, M., Iino, M., and Kangawa, K. (2000). Junctophilins: A Novel Family of Junctional Membrane Complex Proteins. *Mol. Cell* *6*, 11–22.
- Tang, Y.Q., Yuan, J.U.N., Miller, C.J., and Selsted, M.E. (1999). Isolation, characterization, cDNA cloning, and antimicrobial properties of two distinct subfamilies of alpha-defensins from rhesus macaque leukocytes. *Infect. Immun.* *67*, 6139–6144.
- Thomas, M.T., Shepherd, M., Poole, R.K., Van Vliet, A.H.M., Kelly, D.J., and Pearson, B.M. (2011). Two respiratory enzyme systems in Campylobacter jejuni NCTC 11168 contribute to growth on l-lactate. *Environ. Microbiol.* *13*, 48–61.
- Tran, T.A.T., Struck, D.K., and Young, R. (2005). Periplasmic domains define holin-antiholin interactions in T4 lysis inhibition. *J. Bacteriol.* *187*, 6631–6640.
- Turk, V., and Bode, W. (1991). The cystatins: Protein inhibitors of cysteine proteinases. *FEBS Lett.* *285*, 213–219.
- Turk, V., Stoka, V., and Turk, D. (2008). Cystatins: Biochemical and structural properties, and medical relevance. *Bioscience* *13*, 5406–5420.
- Unterweger, D., Miyata, S.T., Bachmann, V., Brooks, T.M., Mullins, T., Kostiuk, B., Provenzano, D., and Pukatzki, S. (2014). The Vibrio cholerae type VI secretion system employs diverse effector modules for intraspecific competition. *Nat. Commun.* *5*, 3549.
- Velayudhan, J., Jones, M.A., Barrow, P.A., and Kelly, D.J. (2004). L-Serine Catabolism via an Oxygen-Labile L-Serine Dehydratase Is Essential for Colonization of the Avian Gut by Campylobacter jejuni. *Infect. Immun.* *72*, 260–268.

- Van Vliet, A.H.M., Baillon, M.L.A., Penn, C.W., and Ketley, J.M. (1999). *Campylobacter jejuni* contains two fur homologs: Characterization of iron-responsive regulation of peroxide stress defense genes by the PerR repressor. *J. Bacteriol.* *181*, 6371–6376.
- Van Vliet, A.H.M., Baillon, M.L.A., Penn, C.W., and Ketley, J.M. (2001). The iron-induced ferredoxin FdxA of *Campylobacter jejuni* is involved in aerotolerance. *FEMS Microbiol. Lett.* *196*, 189–193.
- Van Vliet, A.H.M., Ketley, J.M., Park, S.F., and Penn, C.W. (2002). The role of iron in *Campylobacter* gene regulation, metabolism and oxidative stress defense. *FEMS Microbiol. Rev.* *26*, 173–186.
- Vollmer, W., Hölte, J., and Ho, J. (2004). The Architecture of the Murein (Peptidoglycan) in Gram-Negative Bacteria : Vertical Scaffold or Horizontal Layer (s)? MINIREVIEW The Architecture of the Murein (Peptidoglycan) in Gram-Negative Bacteria : Vertical Scaffold or Horizontal Layer (s)?†. *186*, 5978–5987.
- Wai, S.N., Takata, T., Takade, A., Hamasaki, N., and Amako, K. (1995). Purification and characterization of ferritin from *Campylobacter jejuni*. *Arch. Microbiol.* *164*, 1–6.
- Wang, I.-N., Smith, D.L., and Young, R. (2000). Holins: The Protein Clocks of Bacteriophage Infections. *Annu. Rev. Microbiol.* *54*, 799–825.
- Wassenaar, T.M. (2011). Following an imaginary *Campylobacter* population from farm to fork and beyond: A bacterial perspective. *Lett. Appl. Microbiol.* *53*, 253–263.
- Wassenaar, T.M., Van Der Zeijst, B.A., Ayling, R., and Newell, D.G. (1993). Colonization of chicks by motility mutants of *Campylobacter jejuni* demonstrates the importance of flagellin A expression. *J. Gen. Microbiol.* *139*, 1171–1175.
- Watson, R.O., and Galán, J.E. (2008). *Campylobacter jejuni* survives within epithelial cells by avoiding delivery to lysosomes. *PLoS Pathog.* *4*, 0069–0083.
- Wiesner, J., and Vilcinskas, A. (2010). Antimicrobial peptides: the ancient arm of the human immune system. *Virulence* *1*, 440–464.
- Wooldridge, K.G., and Ketley, J.M. (1997). *Campylobacter*-host cell interactions. *Trends Microbiol.* *5*, 96–102.
- Wösten, M.M.S.M., Wagenaar, J.A., and Van Putten, J.P.M. (2004). The FlgS/FlgR Two-component Signal Transduction System Regulates the fla Regulon in *Campylobacter jejuni*. *J. Biol. Chem.* *279*, 16214–16222.
- Wu, C.H., Bialecka-Fornal, M., and Newman, D.K. (2015). Methylation at the C-2 position of hopanoids increases rigidity in native bacterial membranes. *Elife* *2015*, 1–18.
- Xia, Q., Muraoka, W.T., Shen, Z., Sahin, O., Wang, H., Wu, Z., Liu, P., and Zhang, Q. (2013). Adaptive mechanisms of *Campylobacter jejuni* to erythromycin treatment. *BMC Microbiol.* *13*, 133.
- Yasin, B., Wang, W., Pang, M., Cheshenko, N., Hong, T., Waring, A.J., Herold, B.C., Wagar, E.A., and Lehrer, R.I. (2004). Theta defensins protect cells from infection by herpes simplex virus by inhibiting viral adhesion and entry. *J. Virol.* *78*, 5147–5156.
- Yin, N., Marshall, R.L., Matheson, S., and Savage, P.B. (2003). Synthesis of lipid A derivatives and their interactions with polymyxin B and polymyxin B nonapeptide. *J. Am. Chem. Soc.* *125*, 2426–2435.
- Young, R. (2014). Phage lysis: Three steps, three choices, one outcome. *J. Microbiol.* *52*, 243–258.
- Young, K.T., Davis, L.M., and Dirita, V.J. (2007). *Campylobacter jejuni*: molecular biology and pathogenesis. *Nat. Rev. Microbiol.* *5*, 665–679.
- Young, N.M., Brisson, J.R., Kelly, J., Watson, D.C., Tessier, L., Lanthier, P.H., Jarrell, H.C., Cadotte, N., St. Michael, F., Aberg, E., *et al.* (2002). Structure of the N-linked glycan present on multiple glycoproteins in the gram-negative bacterium, *Campylobacter jejuni*. *J. Biol. Chem.* *277*, 42530–42539.
- Young, R., Wang, I.N., and Roof, W.D. (2000). Phages will out: Strategies of host cell lysis. *Trends Microbiol.* *8*, 120–128.

Zhang, X., and Bremer, H. (1995). Control of the *Escherichia coli* *rrnB* P1 promoter strength by ppGpp. *J. Biol. Chem.* *270*, 11181–11189.

Zhang, Y., Cougnon, F.B.L., Wanniarachchi, Y.A., Hayden, J.A., and Nolan, E.M. (2013). Reduction of human defensin 5 affords a high-affinity zinc-chelating peptide. *ACS Chem. Biol.* *8*, 1907–1911.

Žiedaite, G., Daugelavičius, R., Bamford, J.K.H., and Bamford, D.H. (2005). The holin protein of bacteriophage PRD1 forms a pore for small-molecule and endolysin translocation. *J. Bacteriol.* *187*, 5397–5405.

Ziprin, R.L., Young, C.R., Byrd, J.A., Stanker, L.H., Hume, M.E., Gray, S.A., Kim, B.J., and Konkel, M.E. (2014). Role of *Campylobacter jejuni* potential virulence genes in cecal colonization. *Avian Dis.* *45*, 549–557.